Naval Research Laboratory

Monterey, CA 93943-5502

NRL/MR/7534--05-8899

A Summary of First Year Activities of the United Arab Emirates Unified Aerosol Experiment: UAE^2

Edited by

JEFFREY S. REID
Atmospheric Dynamics and Prediction Branch
Marine Meteorology Divison

STUART J. PIKETH
University of the Witwatersrand
Johannesburg, South Africa

RALPH KAHN
Jet Propulsion Laboratory
Pasadena, CA

ROELOF T. BRUINTJES
National Center for Atmospheric Research
Boulder, CO

BRENT N. HOLBEN
Goddard Space Flight Center
Greenbelt, MD

September 26, 2005

A Summary of First Year Activities of the United Arab Emirates Unified Aerosol Experiment: UAE^2

August 1, 2005

Edited by: Jeffrey S. Reid(NRL), Stuart J. Piketh(Wits), Ralph Kahn(JPL), Roelof T. Bruintjes(NCAR), and Brent N. Holben(GSFC)

With Contributions from: Sundar Christopher(UAH), Gerrit de Leeuw(TNO), Rebecca Eager (NC State), Thomas Eck(UMBC), Jack Ji(UMBC), Piotr Flatau (SIO), Christina Hsu(GSFC), Ralph Kahn(JPL), Michel Legrand (Univ. of Lille), Steve Miller(NRL), John Porter(UofH), Sethu Raman(NC State), Elizabeth Reid(NRL), Kristy Ross(Wits), Benjamin Ruston(NRL), Alexander Smirnov(UMBC), and Ellsworth Judd Welton (GSFC)

NCAR

REPORT DOCUMENTATION PAGE

Form Approved
OMB No. 0704-0188

1. REPORT DATE *(DD-MM-YYYY)*	2. REPORT TYPE	3. DATES COVERED *(From - To)*
26-09-2005	Memorandum Report	

4. TITLE AND SUBTITLE

A Summary of First Year Activities of the United Arab Emirates Unified Aerosol Experiment: UAE^2

5a. CONTRACT NUMBER

5b. GRANT NUMBER

5c. PROGRAM ELEMENT NUMBER

6. AUTHOR(S)

Jeffrey S. Reid, Stuart J. Piketh,* Ralph Kahn,† Roelof T. Bruintjes,‡ and Brent N. Holben§

5d. PROJECT NUMBER

5e. TASK NUMBER

5f. WORK UNIT NUMBER

7. PERFORMING ORGANIZATION NAME(S) AND ADDRESS(ES)

Naval Research Laboratory, Code 7534
Marine Meteorology Division
Monterey, CA 93943-5502

8. PERFORMING ORGANIZATION REPORT NUMBER

NRL/MR/7534--05-8899

9. SPONSORING / MONITORING AGENCY NAME(S) AND ADDRESS(ES)

Office of Naval Research
800 North Quincy Street
Arlington, VA 22217

10. SPONSOR / MONITOR'S ACRONYM(S)

11. SPONSOR / MONITOR'S REPORT NUMBER(S)

12. DISTRIBUTION / AVAILABILITY STATEMENT

Approved for public release; distribution is unlimited.

13. SUPPLEMENTARY NOTES *Climatology Research Group, University of the Witwatersrand, Private bag 3, Johannesburg, South Africa
†Jet Propulsion Laboratory, MS 169-237, 4800 Oak Grove Drive, Pasadena CA, 91109
‡National Center for Atmospheric Research, 3450 Mitchel Lane, Boulder, CO 80301
§Goddard Space Flight Center, Code 923, Greenbelt, MD 20771

14. ABSTRACT

In August and September of 2004, scientists from two dozen international research organizations converged in the Arabian Gulf region to participate in the United Arab Emirates Unified Aerosol Experiment (UAE^2). The four primary goals of the mission were to (a) provide the first ground truth of a variety of environmental satellite and model products in this extremely complicated region of the world, (b) perform the first assessment of the nature of aerosol particles in the Arabian Gulf, (c) determine the role of aerosol particles on the radiative balance of desert regions, and (d) understand how perturbations in the earth's radiative balance can influence atmospheric flow patterns from local to regional scales. This progress report is compiled for mission sponsors and other interested parties. Given, is an overview of the program and individual reports from key investigators. Specific areas of intense interest include understanding the atmospheric flow patterns of Southwest Asia using a suite of mesoscale and global models. The calibration/validation of satellite sensors such as the Multi-angle Imaging Spectro-radiometer (MISR), the MODerate resolution Imaging Spectro-radiometer (MODIS), the Advanced Along Tract Scanning Radiometer (AATSR), and the Advanced Very High Resolution Radiometer (AVHRR) was also very successful. Lastly, this mission has provided the very first complete study of the chemical, physical, and optical properties of pollution and dust particles in the Arabian Gulf.

15. SUBJECT TERMS

Airborne dust; Pollution: Coastal meteorology; Visibility; Southwest Asia; Arabian Gulf

16. SECURITY CLASSIFICATION OF:			17. LIMITATION OF ABSTRACT	18. NUMBER OF PAGES	19a. NAME OF RESPONSIBLE PERSON
a. REPORT	b. ABSTRACT	c. THIS PAGE			Jeffrey S. Reid
Unclassified	Unclassified	Unclassified	UL	150	19b. TELEPHONE NUMBER *(include area code)* (831) 656-4725

Standard Form 298 (Rev. 8-98)
Prescribed by ANSI Std. Z39.18

A Summary of First Year Activities of the United Arab Emirates Unified Aerosol Experiment: UAE^2

Prepared for the following funding agencies:

Maj. Abdulla Al Mandoos, Dept. of Water Resource Studies, UAE
Dr. Eric Hartwig, Naval Research Laboratory
Dr. Ronald Ferek, Office of Naval Research Code 32
Dr. Hal Maring, NASA Radiation Sciences Program
Dr. Wim Pelt, Ministry of Defense/WCS, Netherlands
Dr. Quentin Saulter, Office of Naval Research Code 35

Compiled and Edited on Behalf of the UAE^2 Science Team by

Jeffrey S. Reid
Marine Meteorology Division
Naval Research Laboratory
7 Grcae Hopper St., Stop 2
Monterey, CA 93943
Phone: 831-656-4725
Fax: 831-656-4769
e-mail: reidj@nrlmry.navy.mil

Stuart J. Piketh
Climatology Research Group
University of the Witwatersrand
Private bag 3
Johannesburg, South Africa
Phone: +271 1 717 6532
Fax: +271 1 717 6535
e-mail: stuart@crg.bpb.wits.ac.za

Roelof T. Bruintjes
National Center for Atmospheric Research
3450 Mitchel Ln
Boulder, CO 80301
Phone: 303-497-8909
Fax: 303-497-8401
e-mail: roelof@ucar.edu

Ralph Kahn
Jet Propulsion Laboratory
MS 169-237
4800 Oak Grove Dr.
Pasadena CA 91109
Phone: 818-354-9024
FAX: 818-393-4619
e-mail: ralph.kahn@jpl.nasa.gov

Brent N. Holben
Goddard Space Flight Center Code 923
Greenbelt, MD 20771
Phone: 301-614-6658
Fax 301-614-6695
e-mail: brent@ltpmail.gsfc.nasa.gov

-

**This report is prepared for the exclusive use of the above listed sponsors. It is not intended for public release or distribution. The views expressed are those of the UAE^2 science team and are not necessarily those of the United States National Aeronautics and Space Administration, National Center for Atmospheric Research, Department of Defense or South African University of the Witwatersrand. Please contact J.S. Reid for additional release information*

Primary Contributors to this Report

Gerrit de Leeuw
TNO-Fysisch en Electronisch Lab
P.O. Box 96864
2509 JG The Hague
The Netherlands
Phone: +31 70 374 0462
Fax: +31 70 374 0654
e-mail: deleeuw@fel.tno.nl

Tom F. Eck
Goddard Space Flight Center/GEST
Code 923
Greenbelt, MD 20771
Phone: 301-614-6625
Fax 301-614-6695
e-mail: teck@ltpmail.gsfc.nasa.gov

Rebecca Eager
NC State University
4219-2 Avent Ferry Rd
Raleigh, NC 27606
e-mail: reeager@ncsu.edu

Piotr Flatau
Scripps Institution of Oceanography
Visiting Scientist Naval Research Laboratory
7 Grace Hopper St., Stop 2
Monterey, CA 93907
Phone: 831-656-4759
Fax: 831-656-4769
e-mail: flataup.ucar@nrlmry.navy.mil

Brent Holben
Goddard Space Flight Center
Code 923
Greenbelt, MD 20771
Phone: 301-614-6658
Fax 301-614-6695
e-mail: brent@ltpmail.gsfc.nasa.gov

Christina Hsu
NASA GSFC
Code 916
Greenbelt, MD 20771
Phone: 301-614-5554
Fax 301-614-5903
e-mail: hsu@climate.gsfc.nasa.gov

Jack Ji
NASA GSFC Code 913
Greenbelt, MD 20771
Phone: (301) 614-6231
Fax 301-286-1759
e-mail: ji@climate.gsfc.nasa.gov

Ralph Kahn
MS 169-237
Jet Propulsion Laboratory
4800 Oak Grove Drive
Pasadena, CA 91109 USA
Phone: 818-354-9024
Fax 818-393-4619
e-mail: ralph.kahn@jpl.nasa.gov

Michel Legrand
Laboratoire d'Optique
Atmosphérique, Université de Lille-1
59655 Villeneuve d'Ascq cedex
France
e-mail: *legrand@loa.univ-lille1.fr*

Steve Miller
Naval Research Laboratory
7 Grace Hopper St., Stop 2
Monterey, CA 93907
Phone: 831-656-5149
Fax: 831-656-4769
email: miller@nrlmry.navy.mil

Stuart Piketh
Climatology Research Group
University of the Witwatersrand
Johannesburg, South Africa
Phone: +2711 717 6532
Fax: +2711 717 6535
e-mail: stuart@crg.bpb.wits.ac.za

John Porter
University of Hawaii
Hawaii Institute of Geophysics
2525 Correa Rd.
Honolulu, HI 96822
Phone: 808 956-6483
fax 808 956-3189
e-mail johnport@hawaii.edu

Elizabeth A Reid
Naval Research Laboratory
7 Grace Hopper St., Stop 2
Monterey, CA 93907
Phone: 831-656-4712
Fax: 831-656-4769
email: reidb@nrlmry.navy.mil

Jeffrey S. Reid
Naval Research Laboratory
7 Grace Hopper St., Stop 2
Monterey, CA 93907
Phone: 831-656-4725
Fax: 831-656-4769
email: reidj@nrlmry.navy.mil

Sethu Raman
1005 Capability Dr., Suite 213
Campus Box 7236
North Carolina State University
Raleigh NC 27695-7236
Tel: 919-515-1440
Fax: 919-515 -1441
e-mail: sethu_raman@ncsu.edu

Kristy Ross
Climatology Research Group
University of the Witwatersrand
Private bag 3
Wits, South Africa
2050
Tel: +27 11 717-6534
Fax: +27 11 717-6535
e-mail:Kristy@crg.bpb.wits.ac.za

Ben Ruston
Naval Research Laboratory
7 Grace Hopper St., Stop 2
Monterey, CA 93907
Phone: 831-656-4725
Fax: 831-656-4769
email: ruston@nrlmry.navy.mil

Alexander Smirnov
Goddard Space Flight Center/GEST
Code 923
Greenbelt, MD 20771
Phone: 301-614-6626
Fax 301-614-6695
e-mail:
asmirnov@aeronet.gsfc.nasa.gov

Ellseworth Judd Welton
NASA GSFC
Greenbelt, MD 20771
Phone: 301-614-6279
Fax: 301-614-5492
e-mail:Ellsworth.J.Welton@nasa.gov

Table of Contents

Acknowledgements: The United Arab Emirates Unified Aerosol Experiment (UAE^2) was funded by a number of international sponsoring agencies. Each investigator solicited funds from their own sponsoring agencies for this research, and no general proposal call was in place. Key sponsoring agencies for this mission include the Office of his Highness the President-Department of Water Resource Studies (DWRS)-United Arab Emirates, NASA Radiation Sciences Program, NASA Earth Observing System Program Office, the Naval Research Laboratory base program (Code 7000), Office of Naval Research Code 32, Office of Naval Research Code 35, and the Ministry of Defense/WCS-Netherlands. We are most grateful to staff of DWRS and the University of Witwatersrand South Africa Climatology Research Group for their extensive logistical support of the UAE^2 mission.

Part I: Mission Summary

1.0 Executive Summary:

In August and September of 2004 scientists from two dozen international research organizations converged in the Arabian Gulf region to participate in the United Arab Emirates Unified Aerosol Experiment (UAE^2). The four primary goals of the mission were to a) provide the first ground truth of a variety of environmental satellite and model products in this extremely complicated region of the world, b) Perform the first assessment of the nature of aerosol particles in the Arabian Gulf c) Determine the role of aerosol particles on the radiative balance of desert regions, and d) Understand how perturbations in the earth's radiative balance can influence atmospheric flow patterns from local to regional scales. In summary:

- Over 60 scientists from 8 countries and 24 institutions were involved.
- Fifteen satellite sensors, five models, two aircraft, and a multitude of ground stations were used.
- Twenty-one flights for over 80 hours were used to monitor the atmosphere and vertical distribution of pollution and dust.

Based on these measurements applied science research topics of importance to the United Arab Emirates have been advanced. The scientific community is now to the point where the UAE region can be evaluated and monitored with confidence, and approach significant fundamental research topics of significance to the region and world as a whole. This document presents a series of research topics that the UAE^2 science team is currently analyzing. Research has essentially followed the primary goals above. Specific areas of intense interest include understanding the atmospheric flow patters of Southwest Asia using a suite of mesoscale and global models. The calibration/validation of specific satellite sensors such as the Multi-angle Imaging Spectro-radiometer (MISR) and the MODerate resolution Imaging Spectro-radiometer (MODIS), and the Advanced Very High Resolution Radiometer (AVHRR) was also very successful. Lastly, this mission has provided the very first complete study of the chemical, physical, and optical properties of pollution and dust particles in the United Arab Emirates.

This first year progress report is compiled for the UAE Ministry of Presidential Affairs, Department of Water Resource Studies (DWRS), NASA Radiation Sciences Program, the Office of Naval Research (ONR) Codes 32 and 35, and the Naval Research Laboratory (NRL) Base Program. Given is an overview of the program and individual reports from key investigators. Included are recommendations for the DWRS for further research.

Manuscript approved August 8, 2005.

2.0 Background and Rationale for the UAE^2 Mission:

The Arabian Gulf has one of the largest aerosol burdens in the world with frequent dust storms, smoke advection from the Indian subcontinent, and its own high emission rates of pollution from the petroleum industry and local construction. Particle size distributions and chemistries are highly variable. In addition, the Arabian Gulf exhibits extremely complicated meteorology, with variable sea surface temperatures, enormous latent heat fluxes, abrupt topography and strong mesoscale circulations. This combination of factors makes both modeling and remote sensing in the region extremely difficult. Consequently, although there have been large numbers of papers discussing atmospheric properties in the Arabian Sea and Indian Ocean, the meteorology and nature of aerosol particles in the Arabian Gulf region were until very recently mostly unstudied. The one exception is the international field measurements surrounding the 1991 Gulf War/Kuwaiti oil fires incident. These circumstances are certainly an anomaly and are problematic to apply to more typical conditions. There are a few studies that can be used to understand the regions fundamental meteorological properties.

The absence of environmental studies on the Arabian Peninsula is a direct result of its harsh environmental conditions. While the latest generation of remote sensing algorithms has greatly expanded the utility of space-based sensors to cover desert areas, they are still in a prototype form. Aerosol Optical Thickness (AOT), ocean color, temperature profiles, and cloud properties should be retrievable at unprecedented accuracy. But in hot desert regions and shallow coastal areas, this is not fully proven.

In response to the need for fundamental measurements in the Southwest Asian sub-continent a field campaign was necessary. The United Arab Emirates was chosen as the base area for this study, for a number of reasons. These include:

- The atmospheric environment of the Arabian Gulf is mostly unstudied. Hence, new science can be performed simultaneously with calibration/validation studies.

- Bright desert surfaces and shallow water disrupt satellite sensors on a number of levels. This region is also difficult for meteorology models to simulate. Thus, this is one of the few regions of the world that can be used to fully stress aerosol algorithms and assumptions.

- The infrastructure and available support in the UAE is much greater than other possible study locations. The resources of the DWRS are unsurpassed compared to other Arabian Gulf counties. This makes the UAE an ideal location to work to improve such satellite and meteorological systems.

- The DWRS was already funding an extensive cloud seeding program with the University of Witwatersrand and the National Center for Atmospheric Research. Consequently, necessary airborne assets were already in place for further research.

- Nowhere else in the world can the desert atmosphere be studied in such extensive detail. Dust and the desert atmosphere are important unresolved aspects of global climate change science.

- Several spatial scales of the atmosphere can be studied simultaneously: From the afternoon sea breeze to large-scale patters that cover all of Southwest Asia.

For all of these reasons, the scientific community grew quickly excited when the United Arab Emirates Unified Aerosol Experiment (UAE^2) mission was initiated. External sponsors included the UAE Dept. of Water Resource Studies, the United States National Aeronautics and Space Administration (NASA) Radiation Sciences Program, the United States Office of Naval Research (ONR), the United States Naval Research Laboratory (NRL), and several other international agencies. All involved agencies had similar goals that would benefit the UAE and the world.

3.0 Mission Philosophy and the "Unified" in the United Arab Emirates Unified Aerosol Experiment (UAE^2)

While many elements of the UAE^2 program can be categorized in the areas of aerosol microphysics, radiative transfer, satellite/model calibration/validation, and general meteorology, most are interdisciplinary. The ultimate goal of the program is to develop as complete an understanding as possible of aerosol-radiation-meteorology feedbacks in Southwest Asian region. In order to succeed, the principal areas of atmospheric research need to be "unified" into a coherent data assimilation and product system. This is summarized in Figure 3.1.

There are three principal areas of atmospheric investigation: Field Fundamental understanding through measurements and theory; monitoring through remote sensing; and extrapolation through modeling. The most fundamental research is in the direct observation of the environment, and its subsequent description through theory. However, localized observations rarely capture the full complexity of the global environment. To monitor on the global scales, one must ultimately resort to remote sensing systems where large spatial domains can be monitored frequently. From such data, field measurements and theory can be applied to produce additional products. Conversely, findings from remote sensing studies can be used to refine additional field measurement campaigns. But, remote sensing systems by nature are underdetermined. Somewhere fundamental assumptions on the atmosphere microphysics are made and the boundary conditions are in part assumed. For example, how does one monitor the existence of aerosol particles in heavily clouded regions or in

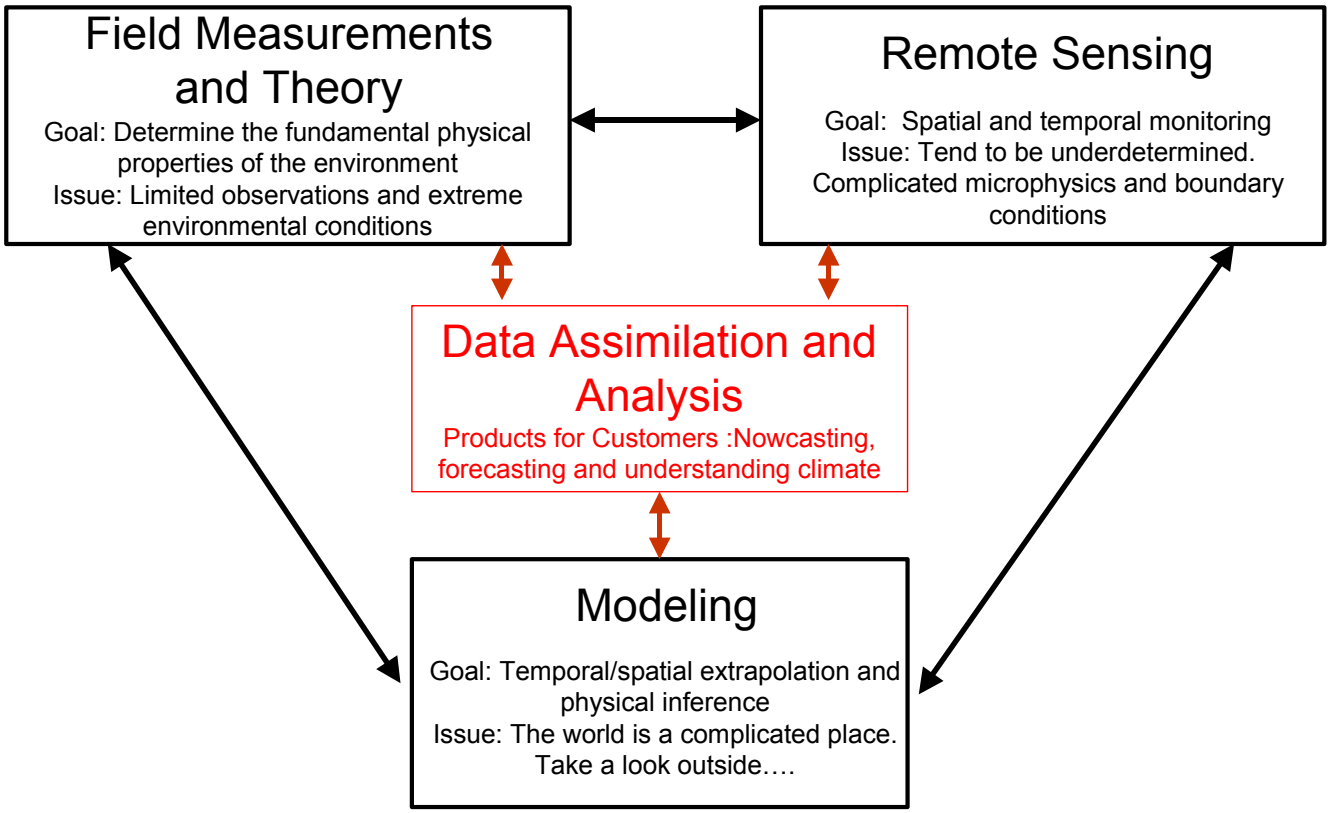

Figure 3.1 Description of the four primary components of research in UAE^2

complicated regions? To address this, extrapolation is made via numerical models. Models can reproduce the 4-dimensional nature of the environment. But their own boundary conditions must come from theory and field measurement derived parameterizations as well as remote sensing observations. Also, verification of model output can only come from these observing systems. But at present, the full complexity of the environment cannot be represented numerically.

Traditionally, theory, field measurements, remote sensing, and modeling studies have been relatively independent. But recent studies have begun to integrate these areas of research. The goal of the UAE^2 campaign is to fully unify these research areas into a coherent data assimilation and analysis system. This will yield products for all of the mission's customers from meteorological nowcasting and forecasting to understanding the region and globe's climate.

4.0 Summary Results from the 2004 UAE^2 Field Campaign

From August 1st – through October 5th, 2004, the Intensive Operations Period (IOP) of the United Arab Emirates Unified Aerosol Experiment (UAE^2) officially took place. During this groundbreaking mission, the southern Arabian Gulf atmospheric environment was examined in unprecedented detail. Using satellites coupled with comprehensive ground and airborne monitoring, this experiment characterized the clouds, airborne dust and pollution of the UAE and surrounding region. This mission will allow scientists to understand how the complicated meteorology of this region fits into the global climate picture, as well as provide NASA with data to build better satellite sensors and algorithms to help UAE institutions monitor the local atmospheric and ocean environment.

There were a number of scientifically sound and pragmatic reasons for many scientists of the world to converge on the region for the UAE^2. First and foremost, the atmospheric environment of southwest Asia is mostly unstudied. Dust and the desert atmosphere remain important unresolved aspects of global change science, and the Southwest Asian region defies assessment. This is partly because the region is so challenging to space based sensors: bright desert surfaces and shallow water disrupt satellite sensors. The hot desert, sharp mountains and seas also make the application of meteorological models difficult. Because the infrastructure and available support in the UAE is much greater than other potential study locations, the UAE is a logical location from which to study the region. In particular, because of its varying terrain and extensive mesonet of weather stations the UAE is an ideal location to work to improve such satellite and meteorology systems. Indeed, this is one of the best places in the world to study the desert and coastal atmosphere in extensive detail. Several spatial and temporal scales of the atmosphere can also be studied simultaneously. From the afternoon sea breeze to large-scale patterns that cover all of Southwest Asia, few places offer such interplay of varying meteorological phenomenon.

In this DWRS, NASA, NRL, and University of Witwatersrand led experiment, over 60 scientists from 8 countries and 18 research institutions were involved. A summary list presented in Table 4.1 Fifteen satellite sensors, five atmospheric models, two aircraft, and a multitude of ground stations were utilized. Much use was made of the South African Weather Service/University of Witwatersrand Aerocommander and Cheyenne research aircraft already on station as part of a DWRS funded cloud seeding program. For UAE^2, these aircraft performed twenty-one flights totaling over 80 hours, to monitor the atmosphere, including the vertical distribution of pollution and dust. The end result of all of this work is that the latest state-of-the-art satellite and atmospheric products are being transitioned to the Office of H.H. the President, Department of Water Resource Studies (Currently in the Ministry of Presidential Affairs).

4.1 *The Atmospheric Environment During the UAE^2 Mission*

As would be expected, the aerosol particle loadings in the UAE are dominated by airborne dust, with an important admixture of pollution aerosols. Typically, Total Suspended Particulate matter (TSP) was on the order of 100-300 $\mu g\ m^{-3}$. We estimate Particulate Matter less than 10 microns diameter (PM10)

levels to be roughly two-thirds this value. The year 2004 showed higher dust concentrations than in the previous 5 years. The exact reason for this is unclear but is currently an area of study by mission scientists. Dust from the UAE, Iraq, Iran, Saudi Arabia, Qatar, and Afghanistan were all observed in the region during the mission.

Dust in general is composed of clays, alumina-silicates and various evaporates. However, the Arabian Peninsula is enriched with shallow oceanic deposits, with oceanic carbonate deposits underlying most of the region. This

Table 4.1 List of Primary UAE^2 Organizations

Funding Agencies:
Dept. of Water Resources, Office of the President, United Arab Emirates (Mangoosh)
NASA HQ, Washington DC (Maring)
Naval Research Laboratory Base Funding, 6.1 Platform Support (Hartwig)
Office of Naval Research Code 32 (Ferek)
Office of Naval Research Code 35/NAVSEA PMS 405 (Saulter/Nolting)

Steering Committee:
Roelof Bruintjes (NCAR): Joint hygroscopiccloud seeding mission scientist
Pior Flatau (Scripps): Radiation sciences leader
Charles Gatebe (GEST/GSFC) US mission deputy
Brent Holben, (NASA GSFC): Ground team leader
Christina Hsu,(NASA GSFC): Remote sensing co-leader
Ralph Kahn, (Jet Propulsion Laboratory): Remote sensing co-leader
Michael King, (NASA GSFC): Radiation sciences
Hal Maring (NASA HQ): Lead program manager
Abdulla Al Mandoos, (DWRS): UAE mission scientist
Stuart Piketh (Univ. of Witts): South Africa mission scientist, cloud physics
Jeffrey Reid (NRL): US mission scientist, microphysics & chemistry
Douglas Westphal (NRL): Meteorology team leader, Aerosol transport

Participating Institutions
Dept. of Water Resources, Office of the President, United Arab Emirates
Jet Propulsion Laboratory, Pasadena, CA.
National Center for Atmospheric Research, Boulder CO.
NASA Goddard Space Flight Center, Greenbelt MD.
Naval Postgraduate School, Monterey CA.
Naval Research Laboratory, Monterey, CA
North Carolina State University, Raleigh, NC
Scripps Institution of Oceanography
TNO Physics and Electronics Laboratory, The Hague, Netherlands
Universite de Shebrooke, Sherbrooke, Quebec, Canada
Universite Lille, Lille, France
University of Alabama, Huntsville, AL
University of California, Davis, CA
University Corporation for Atmospheric Research
University of Hawaii, Honolulu HI
University of Maryland, Baltimore County, Baltimore MD
University of Maryland, Collage Park, MD
University of Witwatersrand, South Africa
Warsaw University, Warsaw, Poland

was well demonstrated in the aerosol data, with extremely high carbonate concentrations found during some of the dustiest days. These elemental signatures are enabling the team to estimate the exact source region of most dust. Dust sources also varied a bit more than expected. During the mission we observed a number of haboobs-dust storms that form in the outflow from thunderstorms. Clear regional air quality episodes can be linked to three such events.

The most significant dust event during the emission occurred on Sept 12, 2004. In the preceding days, a strong frontal boundary formed north of Iraq generating extremely high winds in the Tigris-Euphrates valley. Dust from that event was transported into the Southern Arabian Gulf causing extremely heavy air quality degradation and poor visibility throughout the UAE.

Regional air quality and pollution was also monitored successfully throughout the mission at the coastal MAARCO site (Figure 4.2). The sampling area around Taweela should be considered indicative of regional values and was not impacted by any significant local sources. Particulate Matter with diameters less than 2.5 μm ($PM_{2.5}$), a key air quality index, averaged 35 μg m^{-3} during the study with a maximum value of up to 80 μg m^{-3}. (on August 31st, 2004). Other significant pollution days were September 6th and Sept 12th (coexisting with the dust event), both at 65 . During most of the study period, however, pollution

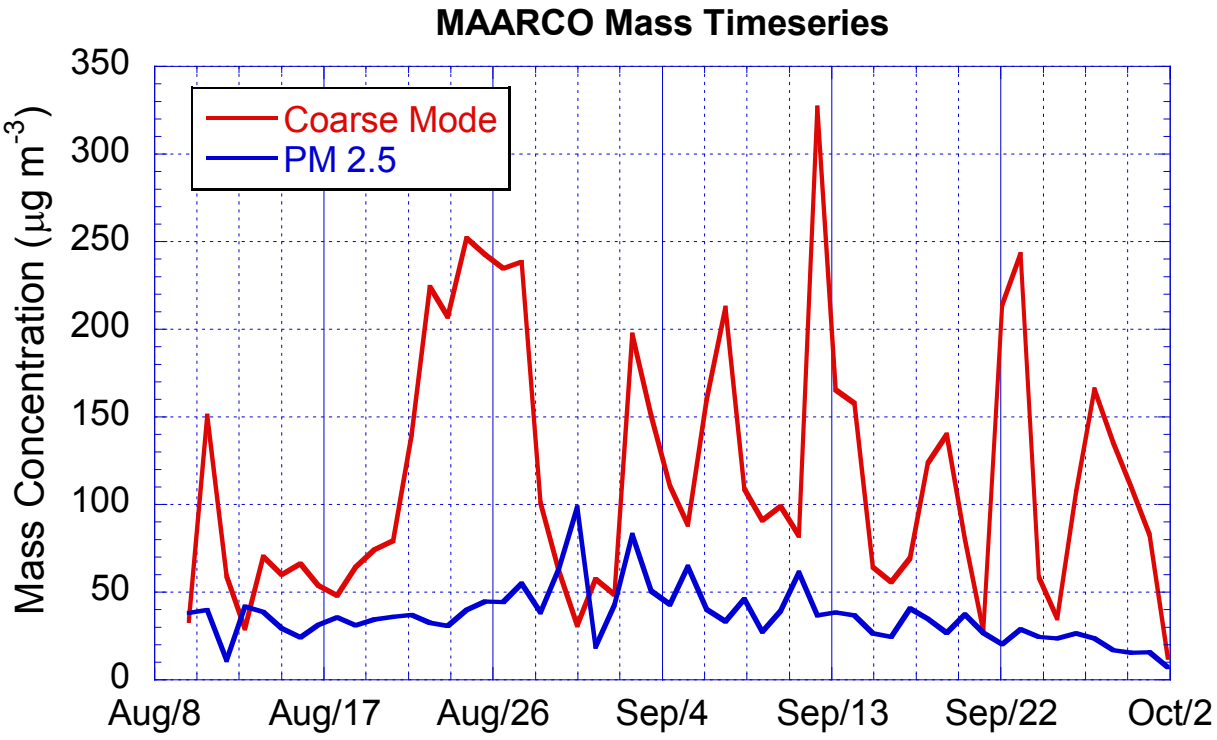

Figure 4.1. Time series of daily average coarse mode (particles larger than 2.5 microns in diameter, and fine mode particulate matter less than 2.5 microns in diameter (PM2.5) during the UAE^2 mission,

loadings were relatively constant.

Pollution composition was surprisingly organic free. On a whole, simple ammonium sulfate accounted for nearly 60% of $PM_{2.5}$ dry mass, followed by ~25% from intrusions from coarse mode dust. Only ~20% of mass can be contributed to black carbon (soot) or particulate organic matter. This mass separation is consistent with the bulk of the pollution coming from the petroleum industry and in particular flares and power plants. Samples near the city centers will most likely have increased contributions of black carbon and organic matter and higher mass concentrations.

The measured values for $PM_{2.5}$ pollution are considered high by most western standards, but are considered typical or better than most of the world. For example, the regional "background" level is considered significantly higher by comparison to Canada, the EU, or the United States. However, loadings are half the regional values of Southeast Asia, East Asia, India and most of Africa.

In evaluating UAE air quality there are a number of issues that need to be considered. First, sampling was performed during the worst air quality months of the year. Further, most of the significant pollution events were easily identifiable as being a result of transport from northern and central gulf countries. Lastly, the presence of so much dust in the atmosphere of Southwest Asia makes any comparison to more industrialized parts of the world somewhat problematic.

Modulating the regional aerosol loadings was the complicated flow patterns of the region. It was clear during the study that on a daily basis the complicated land-sea breeze significantly influenced the relative vertical distribution of dust

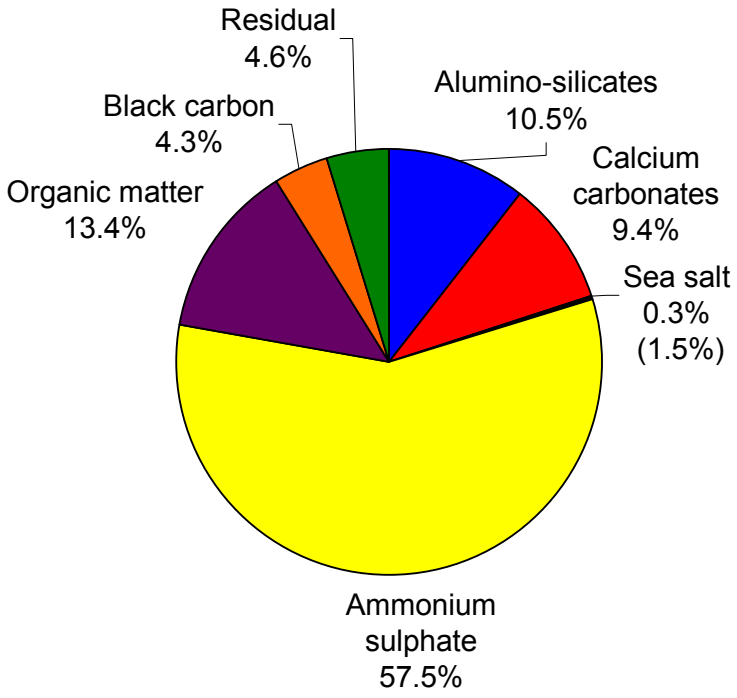

Figure 4.2. Average apportionment of $PM_{2.5}$ pollution at the MAARCO site.

and pollution. While strong shallow stable layers form over the ocean effectively partitioning the near surface and mid level atmosphere, the steady oscillation of the sea/land breeze can vertically mix the atmosphere. The development of internal boundary layers during onshore flow was particularly interesting. Currently, the modeling team members are analyzing the data and will present first results in December.

4.2 Efficacy of remote sensing products in the region

One of the primary goals of the UAE^2 mission is the calibration and validation of remote sensing systems that have traditionally had difficulty monitoring this part of the world. Science team members have focused on three principle areas: 1) The retrieval of aerosol particle properties from satellite over bright deserts and shallow water 2) the retrieval of land and water temperatures by satellite in the presence of absorbing dust and varying surface types, and 3) the inversion of aerosol particle optical properties from ground based AERONET systems. In each of these categories the UAE^2 mission met its primary goals.

Most satellite systems determine the aerosol loading in the atmosphere by comparing the "brightness" of the planet from space to some theoretical clear sky result. Like clouds, aerosol particles such as dust and pollution "lighten" the image and reflect more light to space than an otherwise clear sky. Over dark water, it is very easy to see the lightening effect of aerosol particles. If the ground is bright, such as in deserts or in shallow water, it becomes much more difficult. Another difficulty is if there is dust in the atmosphere. Dust particles have irregular shapes and their optical properties are difficult to model. A key purpose of this mission is to develop systems that can overcome this issue. The UAE environment is perfect for performing these valuations.

Overall, the standard MODIS algorithm for monitoring aerosol particle loadings over water worked reasonably well. It tracked the relative changes in atmospheric loading of dust and pollution and even showed some skill in partitioning the relative amounts of dust and pollution. Typically, the MODIS over water algorithm was good to within 15% (Figure 4.3).

What we were most interested in, however, was the next generation of over desert algorithms, such as "Deep blue." This algorithm, takes advantage of the fact that deserts are fairly bright in red wavelengths, but are dark in the blue. So the hypothesis is that by using traditional over water methods but in shorter wavelengths, satellites can get a dark enough background to see the change in scene brightness due to dust and pollution. Preliminary results from the study are quite positive. Typically, the Deep Blue algorithm correctly determined the amount of dust and pollution over desert to within 30%.

A second satellite system utilized during the mission was the Multi-Image SpectroRadiometer (MISR), which determines the properties of the atmosphere by viewing the scene at nine angles, some as steep as 70 degrees. By looking at a progressively steeper slant paths through the atmosphere, the relative contributions of surface and skylight to the scene systematically increase. Early results from the mission show that in addition to optical depth, MISR is also sensitive to aerosol properties over bright surfaces.

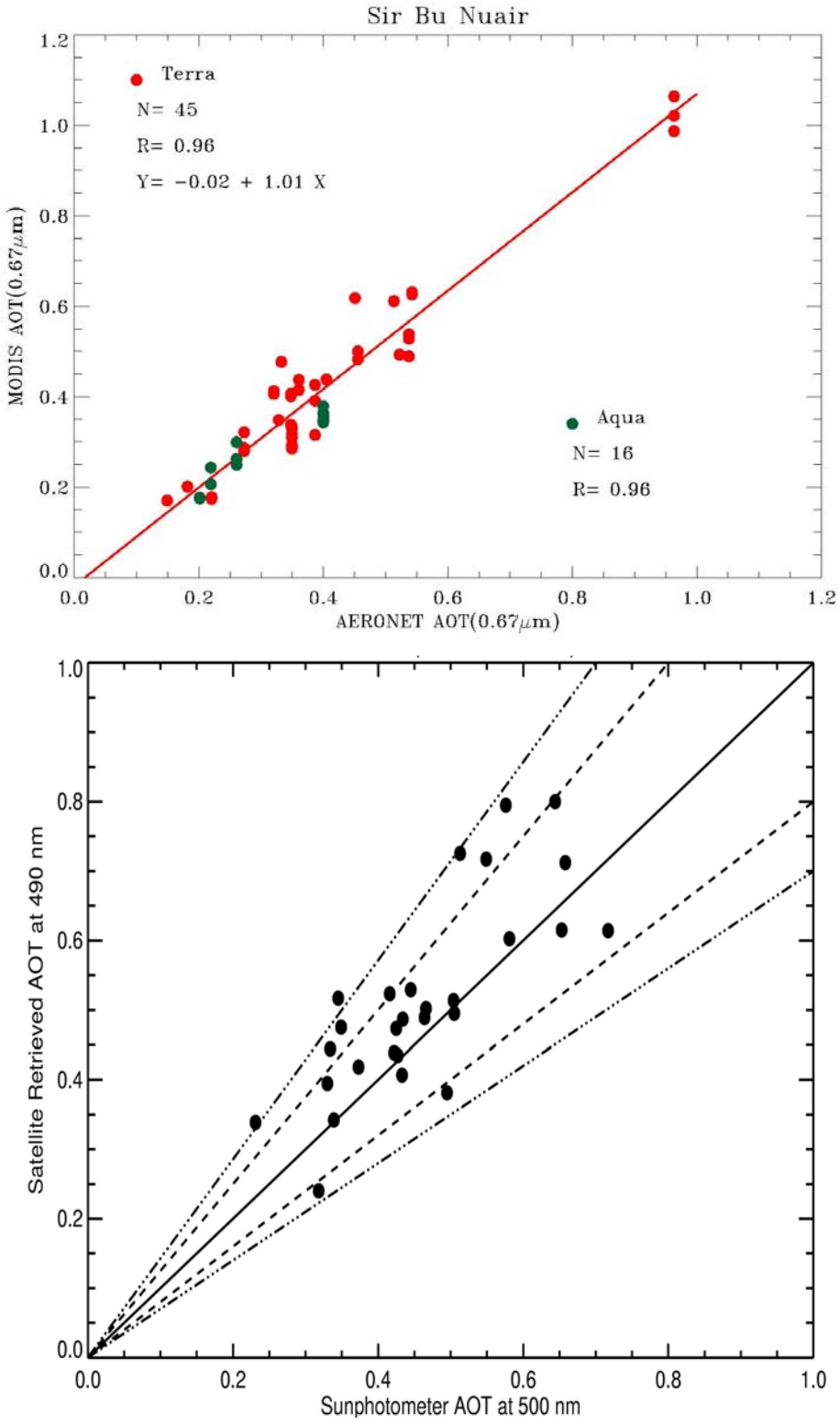

Figure 4.3. Scatter plots of the MODIS standard optical depth product compared to the Sir Bu Nair island site (upper-over water) and the new Deep Blue algorithm (lower over desert) over the Hamim site. *Plot courtesy of Jianglong Zhang, NRL*

A second priority of the mission was to examine how satellites can determine the land and sea temperature (Figure 4.4). By using this information, meteorology models can much more accurately improve wind and cloud forecasting. Typically, temperature retrievals are performed at infrared or microwave wavelengths. The direct measurement of temperature from the infrared is straight forward with regard to land surface type, but is complicated by large airborne dust particles. The higher the dust is in the atmosphere, the colder it is and the more it affects the retrieval. Conversely, microwave retrievals of temperature are not affected by dust, but are more sensitive to the land surface underneath. During the mission we examined land and sea temperatures from space and are comparing them with field measurements.

Lastly, during the UAE^2 mission we wanted to know how well ground based AERONET systems characterize the atmosphere. Just as a satellite system looks down and determines atmospheric properties by apparent changes in ground brightness, the AERONET sun photometer looks up at the sun and sky; based on variations in sun and sky brightness, it determines the loading and properties of aerosol particles above. The UAE environment is very challenging for such measurements because again the atmosphere is heavily loaded with complicated dust particles. Other issues include the bright desert surfaces that reflect more light into the sky, and the variable amount of pollution.

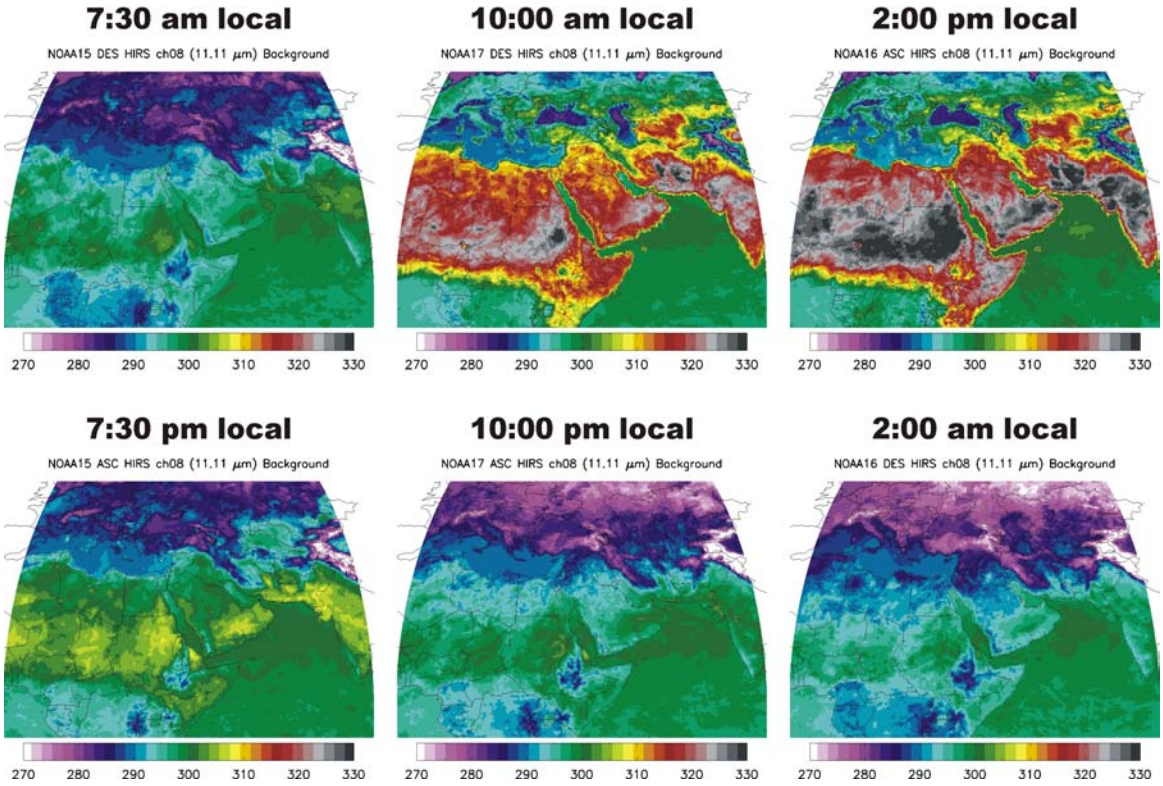

Figure 4.4. Examples of the diurnal cycle of regional temperature over the Middle East area.

5.0 Recommendations for DWRS

The science teams operating with DWRS have five primary recommendations for future transformations and research. These are listed below from the most broad to the specific.

a) With its computer and hardware infrastructure the DWRS is in a unique position in the Southwest Asian region. The earth science research projects it has hosted far exceed those of neighboring countries. DWRS is the logical host organization for developing the UAE's applied earth science corporate laboratory. Its mission and goals should expand to cover all the UAE's earth sciences needs. This should include not only precipitation and hydrology, but also oceanography, pollution and applied science engineering.

b) A high priority for DWRS studies is the evaluation of the impact of pollution and dust particles on cloud microphysics and precipitation. This should include not only periods of intensive operations but also longer-term monitoring. As part of this program the DWRS should become a member of the AERONET network with three instruments (and preferably four). These should be located at an island site in the Arabian Gulf, at a coastal location, and a third in the interior in an inflow region for mountain convection. A fourth instrument (perhaps jointly with Oman) should be placed on the Omani side of the Jebel Muqaylit to monitor inflow from the Arabian Sea.

c) DWRS is in a position to begin state-of-the-art monitoring of UAE pollution emissions and transport from neighboring countries. Although there already exist air quality programs in individual emirates, such data needs to be unified into a common database and standardized auditing procedure need to be developed. This will not only help the emirates understand their own environment, but will also allow for informed negotiations on other climate related issues such as the Kyoto Protocol on greenhouse gas emissions.

d) Effort should be made to develop updated forecasting tools to improve precipitation forecasting. The geography and flow patterns are rigid enough that a series of observations can go into conditional empirical analysis for the next days forecast.

DWRS should start systematically collecting remote sensing earth science data, including regional level 1b and 2 MODIS and MISR data. Such data is freely available at the DAACS via website and efforts should be made to regularly gather and process the products.

Part II: Individual Reports and Summaries

A.1 AERONET Advances and UAE^2

Principal Investigator: Brent Holben, NASA Goddard Space Flight Center

Co-Investigators: Tom Eck, Alexander Smirnov, David Giles, and Ilya Slutsker

A.1 Nature of the problem

The sun and sky scanning spectral radiometers that make up the AERONET network automatically measure the intensity of the sunlight and directional sky brightness in the UV (340 nm) through the near infrared (1,640 nm) in 9 spectral band passes throughout the day. These data are relayed by satellite to NASA's Goddard Space Flight Center where they are processed in near real time to retrieve aerosol optical depth, particle size distribution and complex index of refraction available through the public access website: http://aeronet.gsfc.nasa.gov.

Given the nearly continuous daylight observations, AERONET has provided a significant contribution to the aerosol research community since the first observations in 1993 of biomass burning in Brazil's Amazon basin. The program has grown from a few instruments making local observations to approximately 300 globally distributed sites in 2005 (Fig. A.1). The UAE^2 campaign of 2004 ushered in a new era in research from ground-based aerosol characterization that has here-to-fore not been attempted, that is mesoscale aerosol observations with a sufficient dense network of instruments to provide a new understanding of aerosol transport processes, evaluate aerosol properties with respect to local and regional sources and characterize aerosol distributions in time space (Fig. A.2). The UAE2 AERONET data while providing regional and local aerosol characterization (see Eck case study in this report), also allowed opportunities to research new measurements unique to the program including polarization (see Smirnov summary this report), ocean leaving radiances and evaluation of new processing algorithms to be implemented on the entire AERONET database. Finally the mesoscale AERONET network in concert with the DWRS mesoscale meteorology network is providing the opportunity to understand and improve mesoscale aerosol transport models (see Reid and Westphal this report), validation of new and/or improved satellite aerosol algorithms (see Kahn and Hsu, this report).

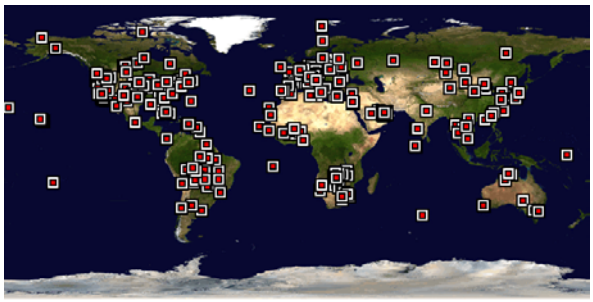

Figure A.1 The global distribution of AERONET sites covers all major aerosol types however the sites are widely spaced resulting in relational connectivity between station observations.

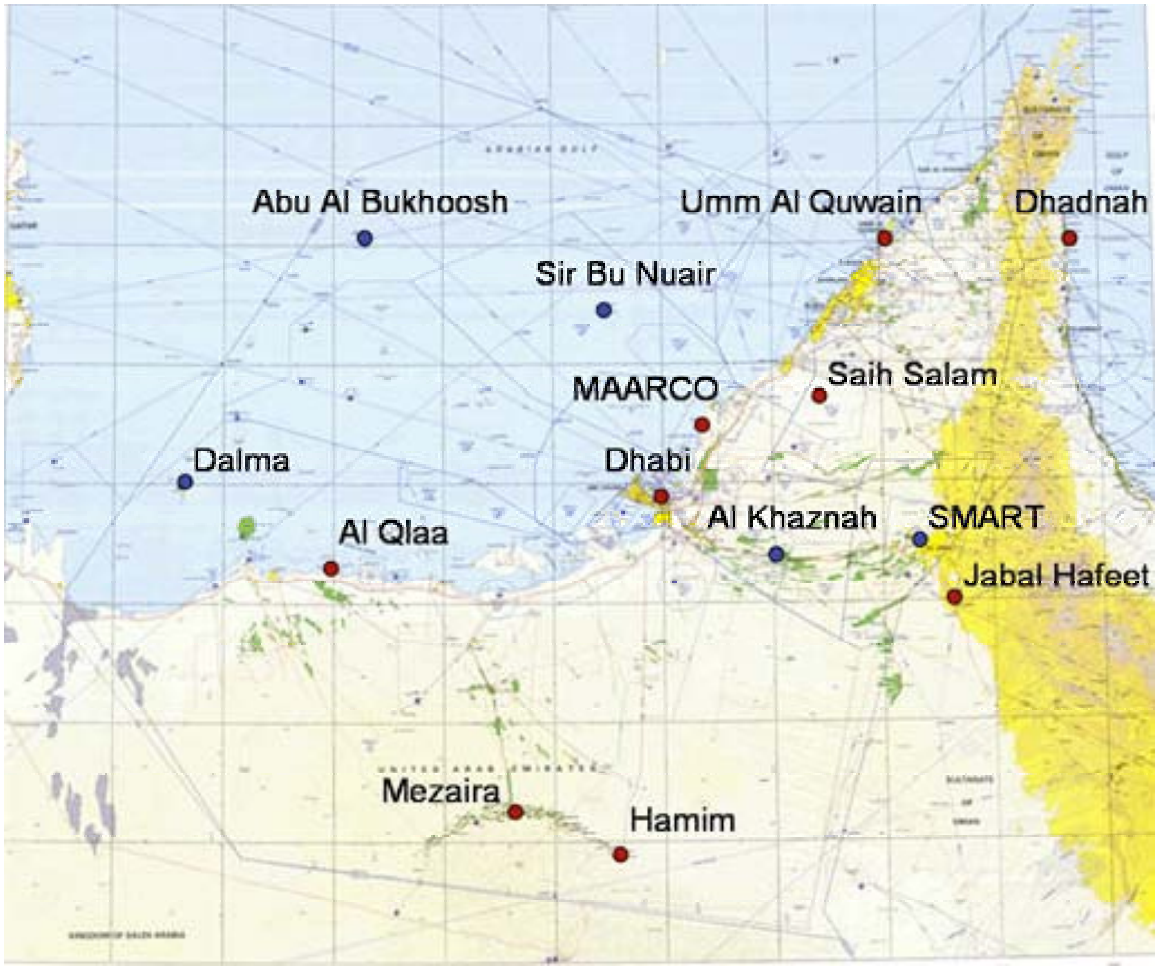

Figure A.2 shows the mesoscale spatial distribution between the AERONET sites during the UAE^2 campaign.

A.2 AERONET Version 2 summary and implications for UAE^2

AERONET Version 2 (**V2**) for the sun measurements (**V2S**) was released in July 2005. This will be followed in September with **V2** for the inversion retrievals (**V2R**). Our philosophy towards the processing algorithms has not changed, that is we are using published community accepted algorithms and data sets to process the direct sun and sky radiance data…, but with a caveat as described later. If you, the users, prefer to make your own corrections, we also provide the total optical depth as well as the component optical depths for each spectral measurement in **V2S**. If you find an error or discrepancy in the **V2S** database, please contact me immediately so that I can alert the community using the data and we can solve the problem quickly.

A.3 V2S Application to the Database:

All **V2** processing will be retroactive for the entire AERONET database dating back to 1993. The old 'AERONET Version 1' (**V1**) processing will continue in parallel through at least December 2005 to insure continuity for those wishing to complete data sets or investigations. Access, availability and website appearance will remain exactly as in the past. The **V2** data are available from the same website (http://aeronet.gsfc.nasa.gov) as are the complete and updated **V1** database. Both data sets are clearly labeled. Until **V2R** products are operational, the only retrievals that will be available are the legacy products based on **V1** inputs. All climatologies have been recomputed thus providing a **V1** and **V2** AOD and water vapor climatology. Although the direct sun **V2S** products are inputs to the retrievals there will be no mixing **V2S** with **V1R** products. Quality controlled data, levels 1, 1.5 and 2.0, are available in **V2S**.

A.4 V2S Summary-what is the net effect?

Please refer to Table A.1 and A.2 for a **V1** and **V2S** comparison and the discussion below. Table A.3 with references is the complete description of the changes implemented in **V2S**.

Ozone: We replaced London's global average O_3 climatology with TOMS 30 year climatology. In all but extreme cases this is a difference of less than 0.003 AOT at 675 nm. Other affected bands are less.

Table A.1 Algorithm modifications from Version 1: Rayleigh, Solar flux, NO_2, O_3, CH_4, H_20, CO_2

Parameter	Version 1	Version 2
Rayleigh optical thickness	Edlen 1966	Bodhaine et al. 1999
Air Pressure	1013.25 mb & height eq.	NCEP interpolated pressure ht
Solar Flux	Neckel and Labs 1981; and Frohlich and Wehrli 1981	Woods et al. 1996
Ozone	London et al. 1976	TOMS O_3 1979-2004
NO_2	None	Schiamachy monthly climatology
Water Vapor Content	Bruegge et al. 1992; Reagan et al. 1992	Michalsky et al. 1995; Schmid et al. 1996
Water vapor correction for AOD (1020 nm)	None	LBLRTM

NO_2: Caveat-NO_2 is optically present in very small quantities in the stratosphere but is highly variable in the lower troposphere being highest in urban/industrial regions due to fossil fuel combustion. We ignored this absorption in **V1** due to lack of widespread observations. **V2S** uses a 2 to 3 year climatology by month from SCIAMACHY. Although the SCIAMACHY data are not fully independent observations, comparisons to GOME and ground-based observations indicate the SCIAMACHY data are relatively accurate (but we feel slightly underestimate the measured concentration) and thus merits inclusion in our correction scheme. Net effect ~ 0.01 at 380 nm in urban areas but globally is <0.003 depending on wavelengths between 340 nm through 500 nm.

Rayleigh: The algorithms are only slightly improved to account for polarization effects. The overall difference between **V1** and **V2** is insignificant, maximum of 0.003 at 340 nm at sea level.

Air Pressure: This input to the Rayleigh algorithms is extremely important especially for the UV and blue bands. In **V1** we used a constant pressure of 1013.25 adjusted by elevation of the station. For high elevation sites and moderate elevation continental sites, the calculated 'station pressure' was sometimes off by more than 20 hPa resulting in miss-correcting AOD at 340 nm by more than 0.015.

The NCEP/NCAR Reanalysis 6-hourly data access base provides global mean sea-level pressure and standard pressure level heights (1000, 925, 850,

Table A.2: Spectral Corrections/components

Standard Wavelengths (nm)	Version 1	Version 2
340 (2nm)	Rayleigh, O_3	Rayleigh, NO_2, O_3
380 (4 nm)	Rayleigh	Rayleigh, NO_2
440 (10 nm)	Rayleigh	Rayleigh, NO_2
500 (10 nm)	Rayleigh, O_3	Rayleigh, NO_2, O_3
675 (10 nm)	Rayleigh, O_3	Rayleigh, O_3
870 (10 nm)	Rayleigh	Rayleigh
940 (10 nm)	Aerosol: Interpolate 870 to 1020	Aerosol: Extrapolate 440 thru 870 to 940
1020 (10 nm)	Rayleigh	Rayleigh, H_2O
1640 (25 nm)	Rayleigh	Rayleigh, H_20, $C0_2$, CH_4
Sea-Prism Wavelengths (nm)	**Version 1**	**Version 2**
412 (10 nm)	Rayleigh	Rayleigh, NO_2
555 (10 nm)	Rayleigh, O_3	Rayleigh, NO_2, O_3

700, 600 hPa). These pressure level data are used to interpolate and fit the pressure at the station elevation. Our analysis shows that 95% of all observations are within 1 hPa of measured station pressure and difficult sites such as Mauna Loa, owing to it's high elevation, had 95% of all observations within 2 hPa of recorded station pressure. NCEP air pressure inputs for Rayleigh corrections represents the most significant improvement in **V2S** processing and, because of ready access to the data, is highly recommended for sun photometry in the absence of measured station pressure.

The NCEP/NCAR Reanalysis 6-hourly data has a 2.5 by 2.5 degree spatial resolution and are normally available after a four to five week delay. Thus we compiled a monthly climatology (from a 50 year record) to use for the real time level 1 and 1.5 data. Histograms of the climatology to measured station pressure show 95% of observations less than 2 hPa deviation for Goddard and 4 hPa at MLO. The 6-hourly will replace 1, and 1.5 as it becomes available and will always be used for level 2.0 data.

H_20: LBLRTM was used to compute the A and B coefficients for all 940 filters where the filter function was available to more accurately account for water vapor absorption. The resulting water vapor retrievals showed a decrease of approximately 13 to 19% from **V1** retrievals. This is in agreement with published biases of Schmid and comparisons to ~7000 GPS retrievals at GSFC showed a bias of ~2% thus suggesting great improvement over **V1**. We will now support a quality assured product (level 2.0) for water vapor.

Measured filter functions for each filter in the network, including the 940 water vapor absorption band, were consistently available back to 1997 and only about 50% of the 940's prior to that. Because we require the filter function to determine the A and B coefficients, only water vapor retrievals from those instruments with measured filter functions will be raised to level 2. Prior to 1997, depending on circumstances, batch filter function was determined from a measured subset and was applied to each instrument's 940 filter to compute coefficients A and B, calibration coefficients and finally the column integrated water vapor. This effort will only result in level 1.5 data. As we continue to uncover more spectral curves from the past or measure the filter function (we have most of the filters in the AERONET museum), we will be able to promote more of the early data to level 2.

Due to temperature dependence and water vapor absorption in 1020 nm filters the resulting AOD is slightly more uncertain compared to other channels. Thus we decided to extrapolate from 440 through 870 nm to 940 nm to estimate the AOD component rather than interpolate between 870 and 1020 nm as in **V1**.

Water vapor absorption is removed from the 1020 nm and 1640 nm filters based on the improved H_20 algorithm.

Trace Gasses: CH_4 and CO_2 optical depths are computed for each filter function using profiles from US 1976 standard atmospheric model. Absorptions are removed from the 1640 nm filter according to the NCEP height-pressure relationship. This replaces the standard air pressure vs height algorithm of **V1**.

Table A.3: AERONET Version 2 Direct Sun Algorithm

Ancillary Data Set Corrections	Data Product	Spatial Resolution	Temporal Resolution	Source
NO_2 *[Reference 1]*	Total column concentration [molec/cm^2]	Global: 0.25 x 0.25 degrees resolution	Monthly climatology (2003-2005)	ESA SCanning Imaging Absorption SpectroMeter for Atmospheric CHartographY (SCIAMACHY)
O_3 *[Reference 2]*	Total column concentration [Dobson Units]	Global: 1 x 1.25 degrees resolution	Monthly climatology (1978-2004)	NASA Total Ozone Mapping Spectrometer (TOMS): Earth Probe and Nimbus
Pressure *[Reference 3]*	Station pressure [hPa] derived from standard pressure level heights [m] and sea-level pressure by using quadratic fit in logarithmic space	Global 2.5 x 2.5 degrees resolution Six pressure level heights: sea-level, 1000, 925, 850, 700 600 hPa	Use 6-hourly when available and default to monthly climatology (1993-2004)	NCEP/NCAR Reanalysis

Corrections	Explanation	Implication
O_3 Absorption *[Reference 4]*	Integration of ozone spectroscopy and fitted to filter function for each wavelengths to obtain ozone absorption coefficients.	Improved ozone wavelength-dependent absorption correction
NO_2 Absorption *[Reference 5]*	Integration of NO_2 spectroscopy and fitted to filter function for each wavelength to obtain NO_2 absorption coefficients.	Improved NO_2 wavelength-dependent absorption correction
CO_2 *[Reference 6]*	Constant value of 0.0089 at standard atmospheric pressure and temperature; adjusted by P/P_o.	Affects extended wavelength instruments (e.g., channel 1640nm)
CH_4 *[Reference 7]*	Constant value of 0.0036 at standard atmospheric pressure and temperature; adjusted by P/P_o.	Affects extended wavelength instruments (e.g., channel 1640nm)
Filter Functions *[Reference 8]*	Filter functions have been updated for instruments after 1997.	Improved data quality.
Rayleigh Optical Air Mass Formula *[Reference 9]*	Updated Kasten 1965 to Kasten and Young 1989.	Very small differences in air mass calculations at high solar zenith angles.
Ozone Optical Air Mass Formula *[Reference 10]*	Updated to Komhyr et. al. 1989.	The ozone layer is no longer fixed at 22km. The ozone layer height is adjusted by latitude to provide a more accurate representation of the ozone height layer.
Water Vapor Optical Air Mass [Reference 11]	Implement Kasten 1965.	Account for the water vapor optical air mass.
Water Vapor A and B Coefficients Recalculated *[Reference 12]*	Water vapor transmission (T_w) was modeled as $T_w = \exp[-A(mw)^B]$ using the radiative transfer code from Alexei Lyapustin. Constants A and B are unique to the particular filter and w is the vertical column water vapor content.	Improved water vapor calculations by up to 20%.
Rayleigh *[Reference 13]*	Rayleigh equation suggested by Bodhaine et. al. (1999)	<0.001-0.007 change in the τ_R depending on latitude and elevation.
H_2O *[Reference 14]*	Absorption optical depth computed for channels 1020 and 1640nm using instantaneous water vapor calculation (derived from the channel 940nm).	Affects channels 1020 and 1640nm.
Earth-Sun Distance *[Reference 15]*	The effective V_o is calculated using the earth-sun distance correction.	Improved calculation of the effective V_o for each wavelength.

The corrections to the AOD retrievals, as with the water vapor retrievals, uses individual filter functions in our analysis available since 1997, prior to that batch average filter functions were applied because transmittances were not measured for all filters. Given our improved filter tracking and computational horsepower in **V2S** we are now convolving each spectral band pass to the solar spectrum, evaluating O_3 and NO_2 absorption cross sections absorption spectra at 0.1 nm resolution. Compared to the previous center wavelength analysis this makes a difference of only a few thousandths and overall is likely randomly distributed. Batch averaged filter functions are processed identically and can be raised to level 2 status.

Optical Airmasses: We have implemented optical airmasses in our algorithms for Rayleigh, H_2O, O_3 as detailed in Table A.3.

What is yet to come in V2S?

Three additional products will come on line for **V2S:**

- SeaPRiSM ocean leaving radiances driven by Giuseppe Zibordi,
- the τ_f and τ_c and eta from AOD observations developed by Norm O'Neill
- direct normal spectral irradiances

These will be released and announced over the next few weeks as we evaluate the new algorithms and determine the screening criteria for level 2 quality assurance. Also under evaluation for **V2S** will be cloud screening options and the potential for corrections from station observations.

A.5 Application of V2 to UAE

In order to assess the overall impact of the new V2S changes to a range of conditions we have compared the monthly averaged AOD in the midvisible (500 nm) and column integrated water vapor at four unique sites during the UAE^2 campaign: Sir Bu Nair Island, MAARCO (coastal site), Mezira (inland low desert), Jabal Hafeet (high elevation interior. Table A.4).

The data show that the AOD was reduced on average of less than 0.01 which is close to our theoretical expectations. The largest effect is due to air pressure for computation of Rayleigh optical depth. Expectations would have the largest

Table A.4, The September comparison of water vapor and aerosol optical depth

	V1		V2S	
Site	AOD (500 nm)	PW (cm)	AOD (500 nm)	PW (cm)
Sir Bu Nair	0.48	2.86	0.47	2.85
MAARCO	0.45	2.69	0.45	2.54
Mazira	.38	2.29	0.38	2.23
Jabal Hafeet	.33	1.65	0.32	1.61

effect on Jabal Hafeet due to more precise elevation computation of air pressure in version 2. The water vapor retrievals are closer than expectations. Non UAE comparisons indicate a 15% decrease in version 2 but during the UAE^2 campaign the decrease was from 1 to 6 %. This bears further investigation and comparison to microwave radiometers and radiosonde data taken during the campaign.

A.6 SeaPRISM-ocean leaving radiances

The SeaPRISM is a AERONET site adapted to measure the reflected energy from the ocean surface when mounted on a platform above the sea surface (Fig. 3). Abu al Bukoosh (ABK) oil platform was used as the measurement site from September through December 2004. This is a new application of the AERONET measurement program that potentially is capable of replacing very expensive ocean optics systems. Zibordi et al provided a systematic comparison between the two systems showing scientifically acceptable comparisons for ocean color research. Those and all previous comparisons were in relatively low optical depth midlatitude environments. The high aerosol regime of the Arabian Gulf provided unique opportunity to assess the SeaPRISM technique under dust and fossil fuel emissions. Figure 4 shows preliminary ocean leaving radiance observations in reflectance units from the ABK site. These values represent

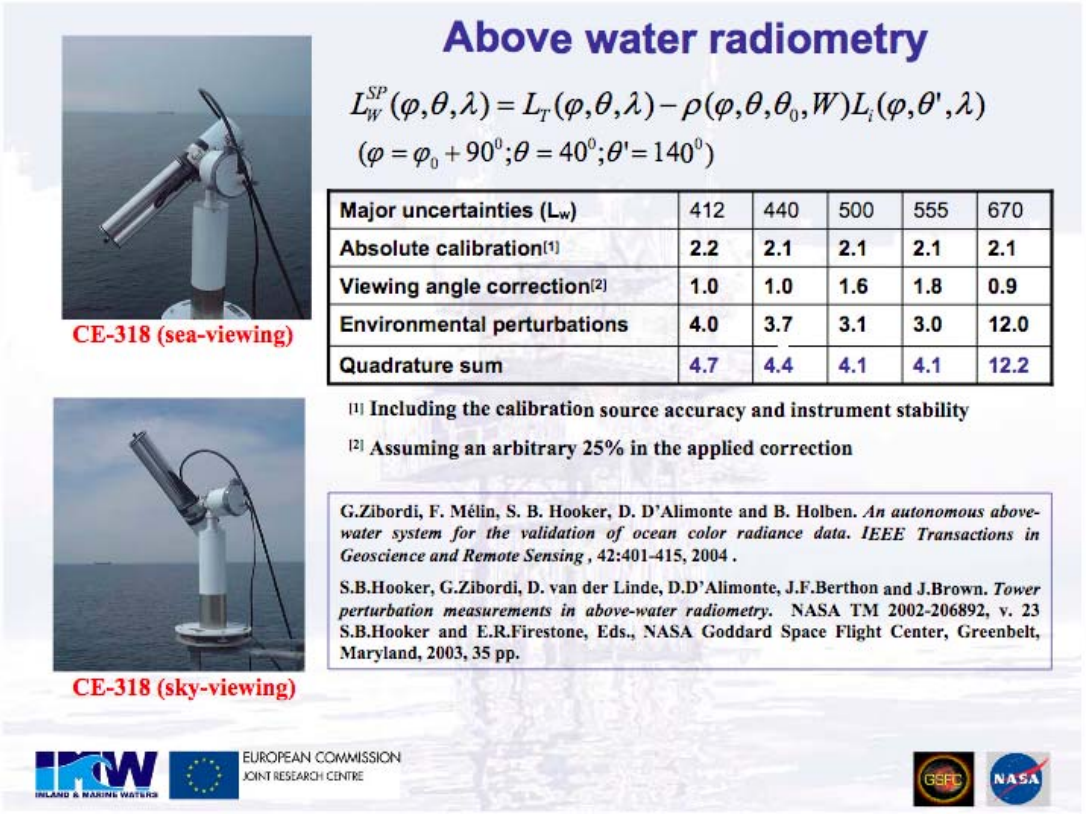

Major uncertainties (L_w)	412	440	500	555	670
Absolute calibration[1]	2.2	2.1	2.1	2.1	2.1
Viewing angle correction[2]	1.0	1.0	1.6	1.8	0.9
Environmental perturbations	4.0	3.7	3.1	3.0	12.0
Quadrature sum	4.7	4.4	4.1	4.1	12.2

Figure A.3, AERONET radiometer showing the viewing modes of the SeaPRISM.

expected deep water values and will be used to assess over water aerosol retrievals from satellites.

Further assessments of the AERONET data will be made from the collected data set including a robust assessment of the new AERONET inversion algorithms expected in September. Further synergism with lidar and hyperspectral satellite data will be pursued along with radiative forcing estimates under dust and pollution conditions. AERONET thanks the foresight of DWRS for supporting the UAE^2 campaign and particularly support for the mesoscale network established for this campaign. AERONET, NASA and the scientific community will greatly benefit from continued collaboration with DWRS.

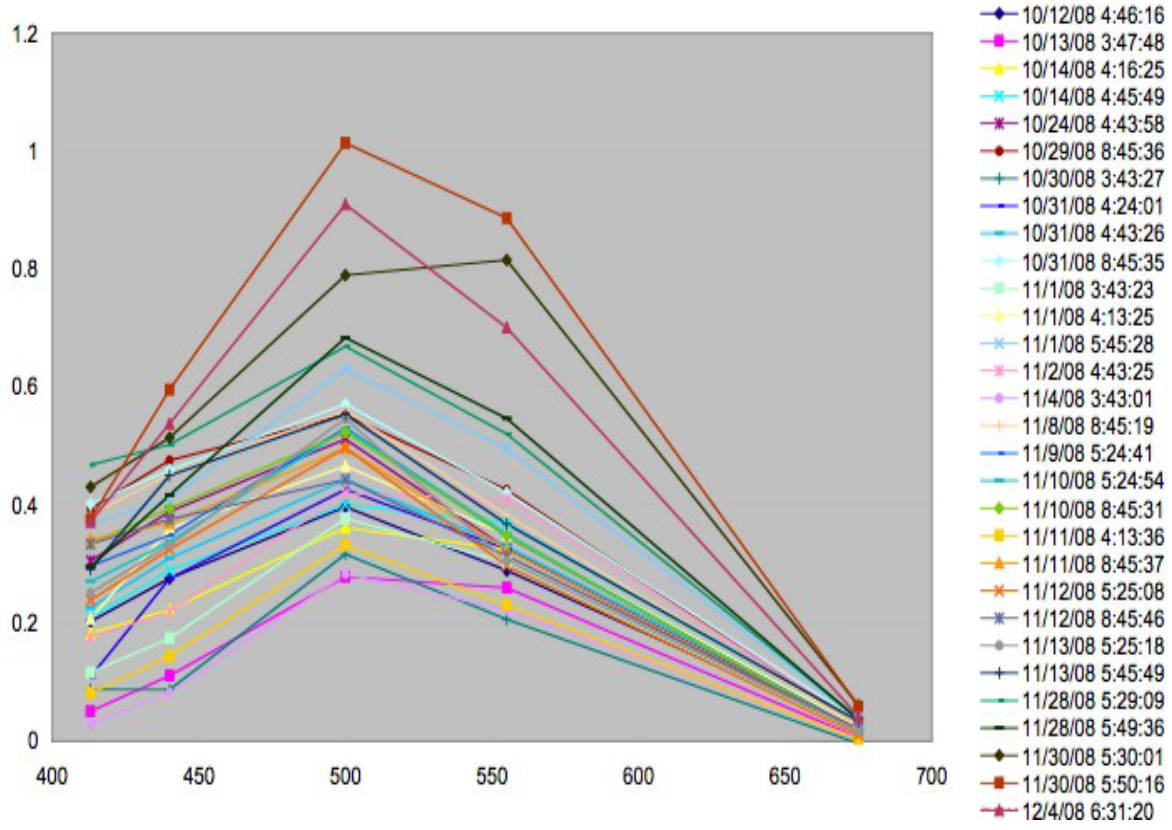

Figure A.4 The computed hemispherical reflectance vertical axis vs spectral wavelength (nm) show reasonable values for a family of ABK curves representing a variety of conditions and times of day.

Acknowledgments:

Development of **V2S** has been a time consuming effort requiring meticulous research, analysis and reanalysis by the following team members. Great kudos goes to Norm O'Neill for advocating NO_2 corrections for years and providing the initial correction efforts. Ilya Slutsker has written and implemented a battery of programs to populate a new expanded and flexible database that everyone utilizes but few appreciate the intricacies. Many thanks also to David Giles who creatively implemented the ancillary data sets with skill and insight and always managed to provide the web based solutions to keep the rest of us in the game. Alexei Lyapustin willingly provided LBLRTM modeling for our water vapor analysis. Alexander Smirnov demonstrated his masterful meticulousness in every phase of **V2S:** algorithm research, development, implementation and critical analysis. Lastly Tom Eck's great insight into the algorithms and the data combined with his broad perspective allowed a deep and thorough evaluation of the **V2S** database that we can all confidently use for our scientific research.

References:

1)
   a) TEMIS – Tropospheric NO2 from GOME and SCIAMACHY, http://www.temis.nl/airpollution/no2.html
   b) Eskes, H.J. and Boersma, K.F., 2004: Averaging kernels for DOAS total-column satellite retrievals, *Atmos. Chem. Phys.* **3**, 1285-1291, 2003.
   c) K.F. Boersma, H.J. Eskes and E.J. Brinksma, 2004: Error Analysis for Tropospheric NO2 Retrieval from Space, *J. Geophys. Res.*, **109** D04311, doi:10.1029/2003JD003962, 2004.
2) Data were obtained from the NASA/GSFC TOMS Ozone Processing Team (OPT), http://jwocky.gsfc.nasa.gov/.
3) Data were obtained from the NOAA National Weather Service NOMADS NCEP Server, http://nomad3.ncep.noaa.gov/ncep_data/index.html.
4) Burrows, J. P., Richter, A., Dehn, A., Deters, B., Himmelmann, S., Voigt, S. and Orphal J., Atmospheric remote -sensing-reference data from GOME: 2. Temperature-dependent absorption cross sections of O_3 in the 231-794 nm range, *JQSRT*, **61**, 509-517, 1999.
5) Burrows, J. P., Dehn, A., Deters, B., Himmelmann, S., Richter, A., Voigt, S. and Orphal, J., Atmospheric Remote-Sensing Reference Data from GOME: Part 1. Temperature-Dependent Absorption Cross-sections of NO_2 in the 231-794 nm Range, *JQSRT*, **60**, 1025-1031, 1998.
6) Based on computation from standard US 1976 model.
7) Based on computation from standard US 1976 model.
8) N/A
9) Kasten, F. and Young, A. T., Revised optical air mass tables and approximation formula, Appl. Opt., **28**, 4735–4738, 1989.
10) Komhyr, II'. D., Grass, K. D., and Leonard, R. K., Dobson Spectrophotometer 83: a standard for total ozone measurements, 1962-1987. J. Geophys. Res. 94:9847-9861, 1989.

11) Kasten, F., A new table and approximation formula for relative air mass. *Arch. Meteor.Geophysics. Bioklimatol*. *Ser. B*, **14**, 206-223, 1965.
12) Smirnov, A, Holben, B.N., Lyapustin A., Slutsker, I. and Eck, T.F., AERONET processing algorithms refinement, AERONET Workshop, May 10 - 14, 2004, El Arenosillo, Spain.
13) Bodhaine, B. A., Wood, N. B., Dutton, E. G., Slusser, J. R., On Rayleigh Optical Depth Calculations, J. Atmos. and Ocean. Tech., **16**, 1854-1861, 1999.
14)
    a) Schmid, B., Thome, K.J., Demoulin, P., Peter, R., Matzler, C., and Sekler, J., Comparison of modeled and empirical approaches for retrieving columnar water vapor from solar transmittance measurements in the 0.94 micron region. J. Geophys. Res., **101**, 9345-9358, 1996.
    b) Michalsky, J. J., J.C. Liljegren and Harrison, L. C: A Comparison of Sun Photometer Derivations of Total Column Water Vapor and Ozone to Standard Measures of Same at the Southern Great Plains Atmospheric Radiation Measurement Site, *J. Geophys. Res.,* **100,** 25995-26003, 1995.
15)
    a) U.S. Naval Observatory, Astronomical Applications Department: Approximate Solar Coordinates, http://aa.usno.navy.mil/faq/docs/SunApprox.html
    b) Michalsky, J., The astronomical almanac's algorithm for approximate solar position (1950-2030). Solar Energy, **40**, 227-235, 1998.

B.0 Spatial and Temporal Variability of Aerosol Optical Depth in the UAE

Principal Investigator: Thomas F. Eck, University of Maryland, Baltimore County and NASA-GSFC

Co-Investigator: Brent N. Holben, Oleg Dubovik, Alexander Smirnov, A. Sinyuk, J. S. Reid, D. Giles, J. S. Schafer

B.1 Nature of problem

In this investigation we are studying the spatial distribution of the atmospheric aerosol optical depth (AOD; integrated vertical aerosol extinction) and the temporal dynamics of AOD. The spectral dependence of the aerosol optical depth provides information on the relative optical influence of the coarse mode particles (desert dust) versus the fine mode particles from pollution sources. Information on AOD magnitude and spectral dependence is important in determining the potential climatic effects of aerosol perturbations to the radiation budget and also in making atmospheric corrections for satellite retrievals of earth surface properties. Additionally, the data provided by the ground-based Aerosol Robotic Network (AERONET) sun-sky radiometers are very important in validating satellite retrievals of AOD. The geographical location of the UAE includes strong desert dust aerosol sources from the arid lands in the region, and also strong pollution particle sources from petroleum and natural gas processing facilities. This variability of atmospheric particle type and size in conjunction with highly variable regional meteorology results in some days that are dominated by large particle desert dust, some dominated by fine particle pollution, and many days that are a mixture of the two aerosol types. This study attempts to quantify the dynamics of AOD in the late summer season in the UAE. In the near future when new retrieval products derived from sky radiance scans become available, we intend to study the dynamics of aerosol size distribution retrievals and aerosol absorption also.

B.2 Executive summary

A time series of daily average AOD at 500 nm from August 9 though October 1, 2004 for four AERONET station sites in the UAE is shown in Figure B.1a. It is noted that the 500 nm AOD is typically quite high in this season, exceeding ~0.3 on most days. The ~2 month average AOD for the island site of Sir Bu Nuair (0.50) and the coastal site of Umm Al Quwain (0.53) are approximately 25% higher than for the two inland sites in the desert, Mezaira (0.40) and SMART (0.44). The SMART site is located at the Al Ain airport. The higher AOD for sites in or bordering the Arabian Gulf may be due to the combination of very high humidity at these sites coupled with sources of fine mode particle pollution originating from petroleum industry operations at offshore platforms, on islands, and on the coast. These fine mode aerosols contain sulfates that are very hygroscopic, therefore they grow in size in high humidity environments, which thereby increases the particle scattering optical depth. The time series of the daily average Angstrom wavelength exponent (computed from 440 to 870 nm

AOD data) for the same sites and dates is shown in Figure B.1b. The Angstrom wavelength exponent is the slope of the AOD versus wavelength in logarithmic coordinates, and is a basic measure of the optically active particle size. An Angstrom wavelength exponent of near zero occurs when all aerosol particles are large (radius greater than 1 micron), while at the other extreme an Angstrom wavelength exponent of 2.0 occurs for fine mode pollution or smoke particles (radius less than 0.3 microns). At the four UAE sites in Figure B.1b, the Angstrom exponent averages 0.75 for the Gulf island site of Sir Bu Nuair, 0.63 for the coastal site of Umm Al Quwain, and 0.56 and 0.50 at the inland desert sites of Mezaira and SMART respectively. Therefore the higher Angstrom exponent values for the Gulf sites indicate that fine mode pollution particles are present in greater concentrations there than at inland sites. It is also noted in Figure B.1b that the Angstrom exponent is quite variable, ranging from ~0.2 to ~1.6, as a result of some days being dominated by strong desert dust events and some days where pollution aerosol in predominant.

We compare the AOD and Angstrom exponents at Dhadnah, located near the coast of the Gulf of Oman and at Umm Al Quwain near the Arabian Gulf coast in Figure B.2. These two sites are at the same latitude and both are located at relatively low altitude (<80 m) but are ~70 km apart in the east-west direction with a mountain range between them. Scatter plots of daily average matched AOD and Angstrom exponents in Figure B.2 show that there is relatively high correlation in AOD between the sites (~52% of the variance explained) and even higher in Angstrom exponent (~78% of the variance explained). Therefore on

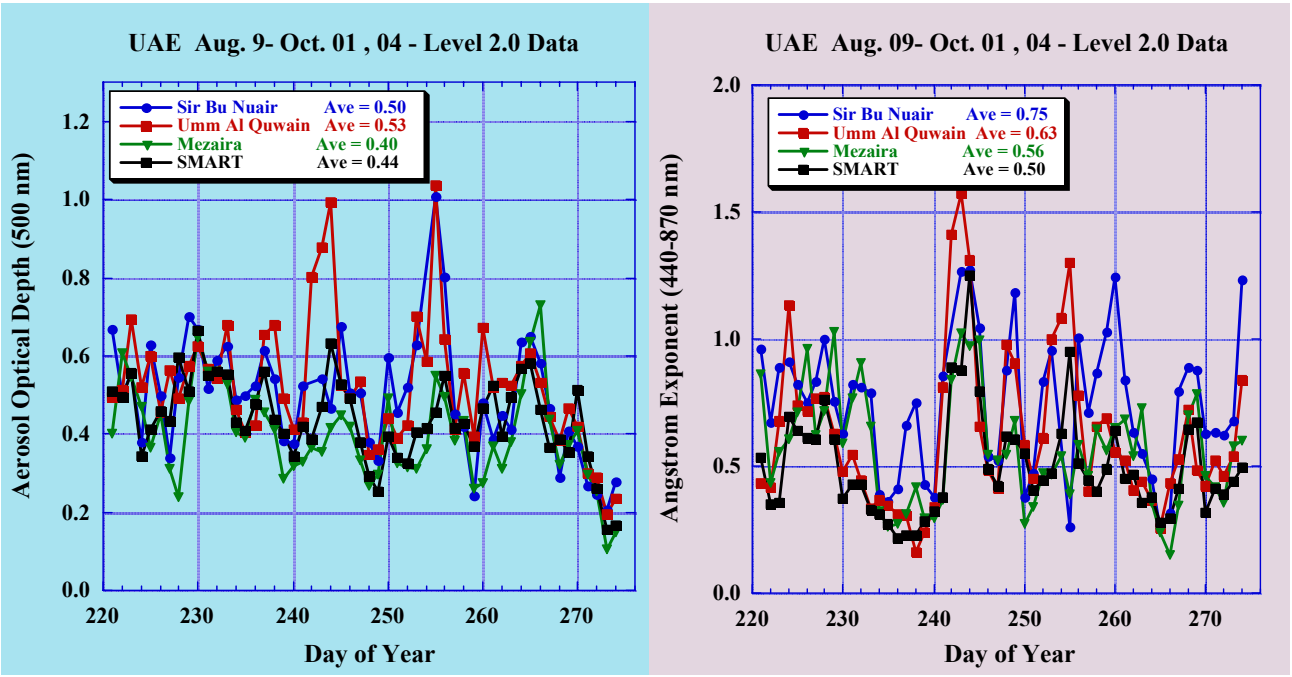

Figure B.1 Time series of AOD and Angstrom exponent at 4 AERONET sites in the UAE.

most of the days in August and September 2004 the mountain range in the northern UAE between these sites did not act as a separation barrier for aerosol type, as the aerosol size mixture was very similar on both sides of the mountains. These plots are preliminary and the correlations will increase when the data are matched in day and time rather than matched in day only as in Figure B.2.

Measurements were also made at the top of the mountain ridge at Jabal Hafeet at 1059 meters altitude were compared to measurements made at the SMART site in Al Ain at 250 meters in order to investigate the vertical partitioning of AOD in the region. The sites were only 28 km apart in horizontal distance but differed in altitude by about 800 meters. The AOD at both sites were very highly correlated as expected from their close horizontal proximity, while the AOD at Jabal Hafeet averaged 75% of the value measured at the SMART site. Therefore only ~25% of the total column aerosol AOD was attributed to the lower 800 meters above ground level. This altitude difference is similar to the altitude difference between the coast and the mountain range separating the sites of Dhadnah and Umm Al Qwain. Therefore since ~75% of the AOD occurs above the altitude of the mountain ridge this explains the high correlation between these sites separated by the mountains, as shown in Figure B.2.

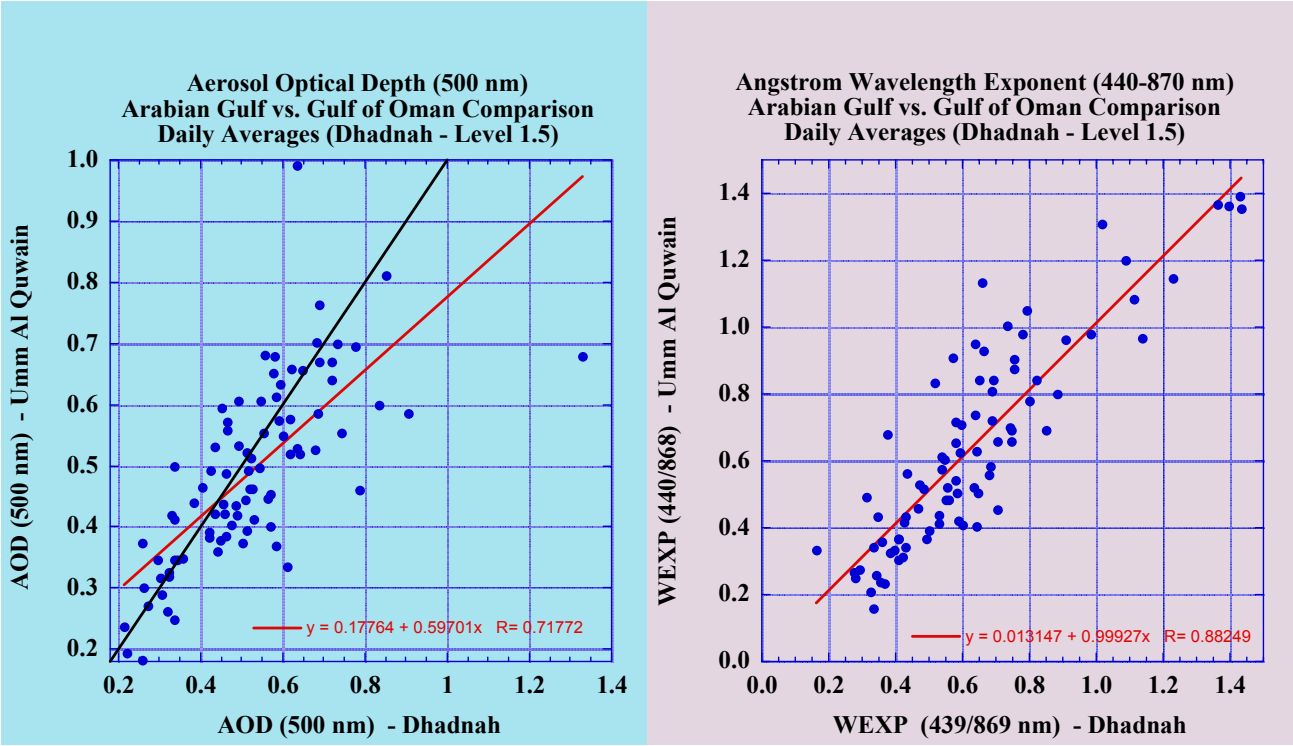

Figure B.2 Scatter-plots showing correlation of AOD and Angstrom exponent between northern UAE sites separated by a mountain range.

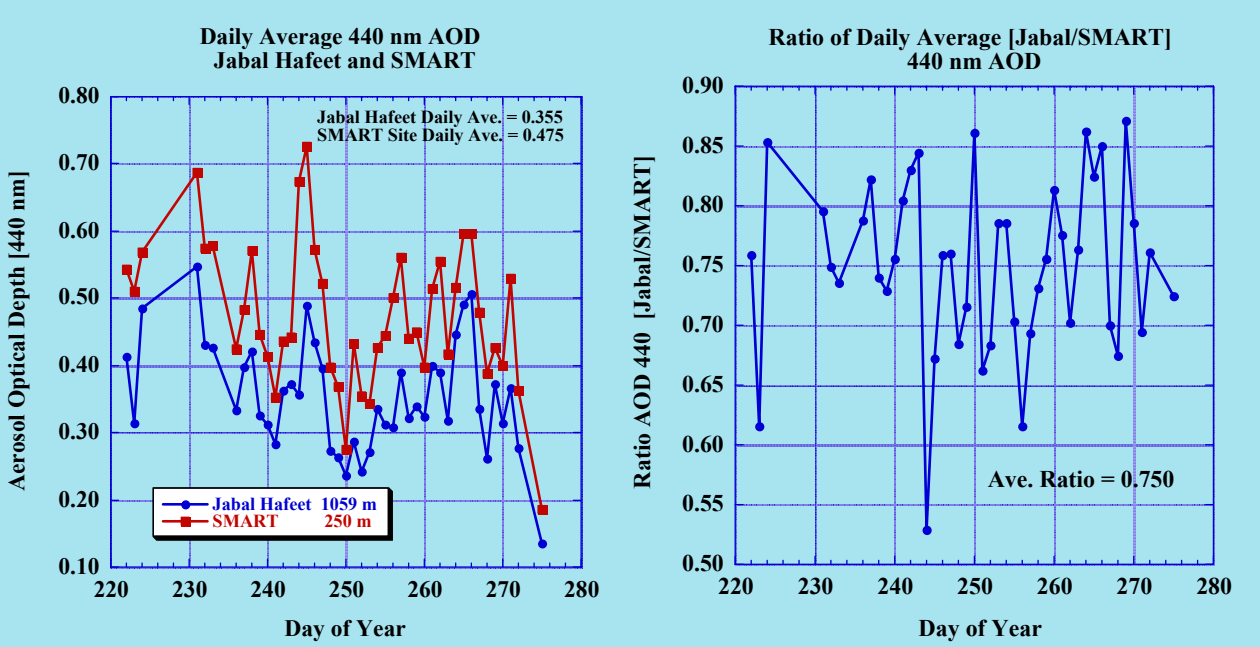

Figure B.3. AOD comparison at the Jabal Hafeet and SMART sites which are only 28 km apart in horizontal distance but differ in altitude by ~800 meters.

C.0 An Overview of MPLNET Data Collected During the UAE^2 Campaign

Principal Investigator: Ellsworth Judd Welton, NASA Goddard Space Flight Center, Greenblet, MD

The NASA Micro-pulse Lidar Network (MPLNET) [*Welton et al*., 2001] consists of micro-pulse lidar sites co-located with AERONET [*Holben et al*., 1998] sun photometers. Data sets and more information on MPLNET are available on our website, *http://mplnet.gsfc.nasa.gov*. During UAE^2, MPL systems were deployed to both the MAARCO and SMART-COMMIT sites. The micro-pulse lidar (MPL) system is a single channel (523 nm), autonomous, eye-safe lidar system that is used to determine the vertical structure of clouds and aerosols [*Spinhirne et al*., 1995]. Raw MPL data were acquired at 1-minute time resolution, and 75 m vertical resolution. The raw data were converted into uncelebrated lidar signals [*Campbell et al*., 2002; *Welton and Campbell*, 2002] and are used to infer the altitude of aerosol and cloud heights.

Figures C.1 and C.2 display MPL signals from MAARCO and SMART-COMMIT, respectively, during the entire campaign. The x-axis displays the time in UTC (day of year), and the y-axis altitude in kilometers. The colors represent aerosol and cloud layers that have backscattered laser pulses from the MPL. Hotter colors indicate more backscatter than cooler colors, deep blue shows the free troposphere where only molecular scattering occurs. Aerosols were present from the surface to 5 – 6 km at both UAE^2 sites during the experiment. The top of

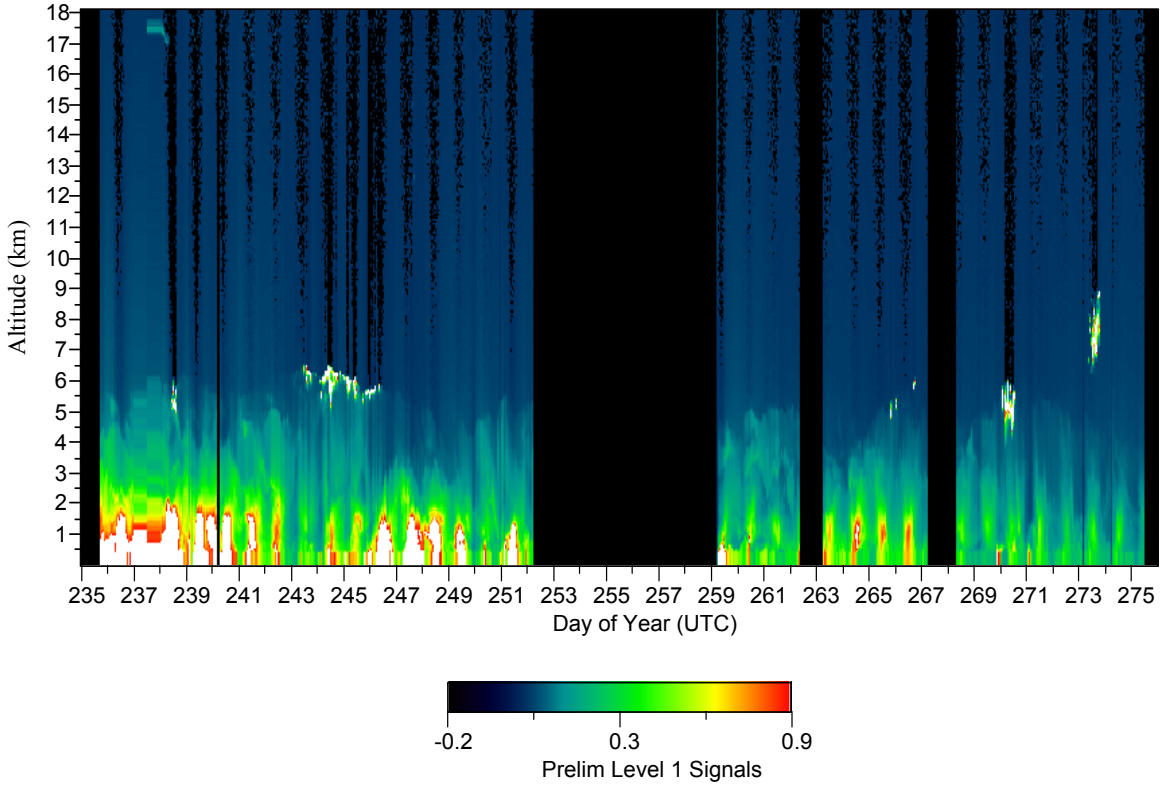

Figure C.1 MPL signals acquired at the UAE2 MAARCO site.

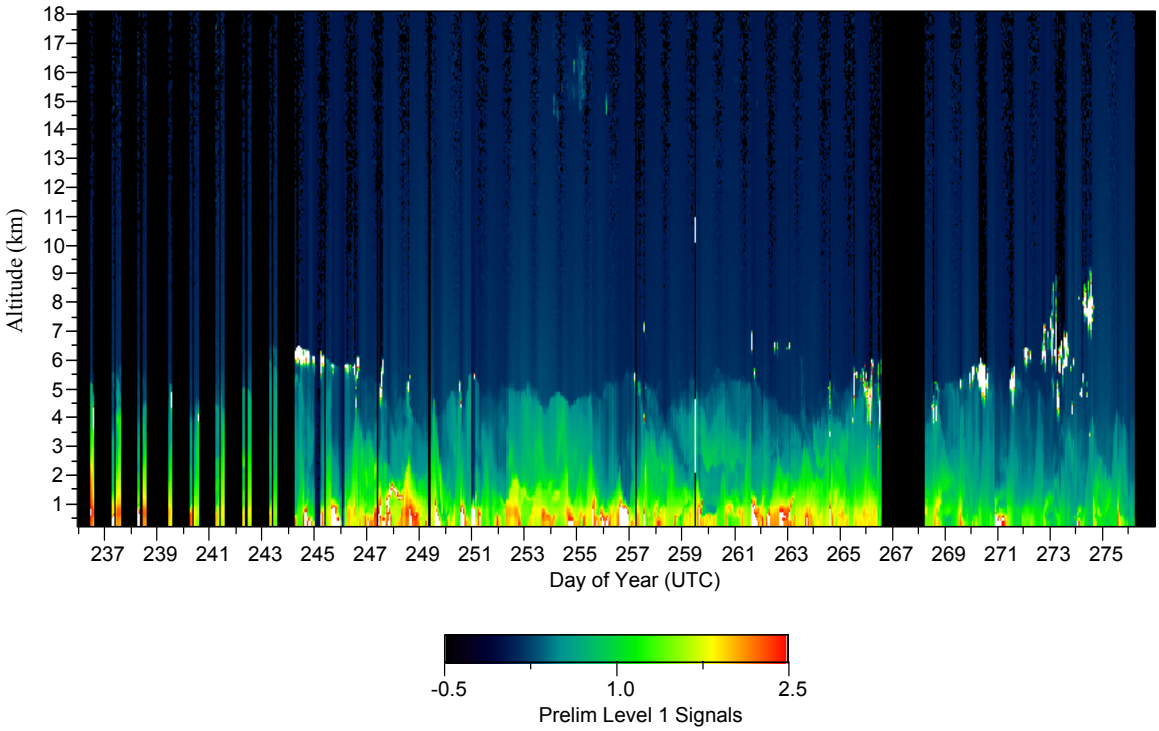

Figure C.2 MPL signals acquired at the UAE^2 SMART-COMMIT site.

the aerosol layer is visible as the pale blue-green layer bordering the free troposphere. Periods of intense apparent backscatter (red and white) appear in both MAARCO and SMART data sets, and are due to temperature fluctuations in the trailers. These effects are currently being calibrated to fix the problem, and final data will not be affected.

The MPLNET data will be used to characterize the height distribution of aerosols during UAE^2, and to study diurnal changes. The MPL also displays areas of cloud and aerosol co-location (see days 243-246, the white scattering layer at 6 km is due to clouds). Such information is helpful for studies of aerosol-cloud interaction. Finally, MPLNET data will provide information needed to help analyze satellite lidar data collected by new NASA sensors as they fly over the Arabian Gulf region. Figure C.3 shows lidar signals acquired by NASA's Geoscience Laser Altimeter System (GLAS) [*Spinhirne et al*., 2005] on the ICESat spacecraft during October 2003. The orbit track crosses the United Arab Emirates, and shows similar aerosol height characteristics as observed during UAE^2. The complex aerosol mixtures in this region present a problem for accurate satellite lidar retrievals, and MPLNET data from UAE^2 will be used to help construct algorithm look-up tables to analyze GLAS data, and results from NASA's next satellite lidar – Cloud-Aerosol Lidar and Infrared Pathfinder Satellite Observations (CALIPSO) [*Winker et al*., 2004] scheduled to launch in September 2005.

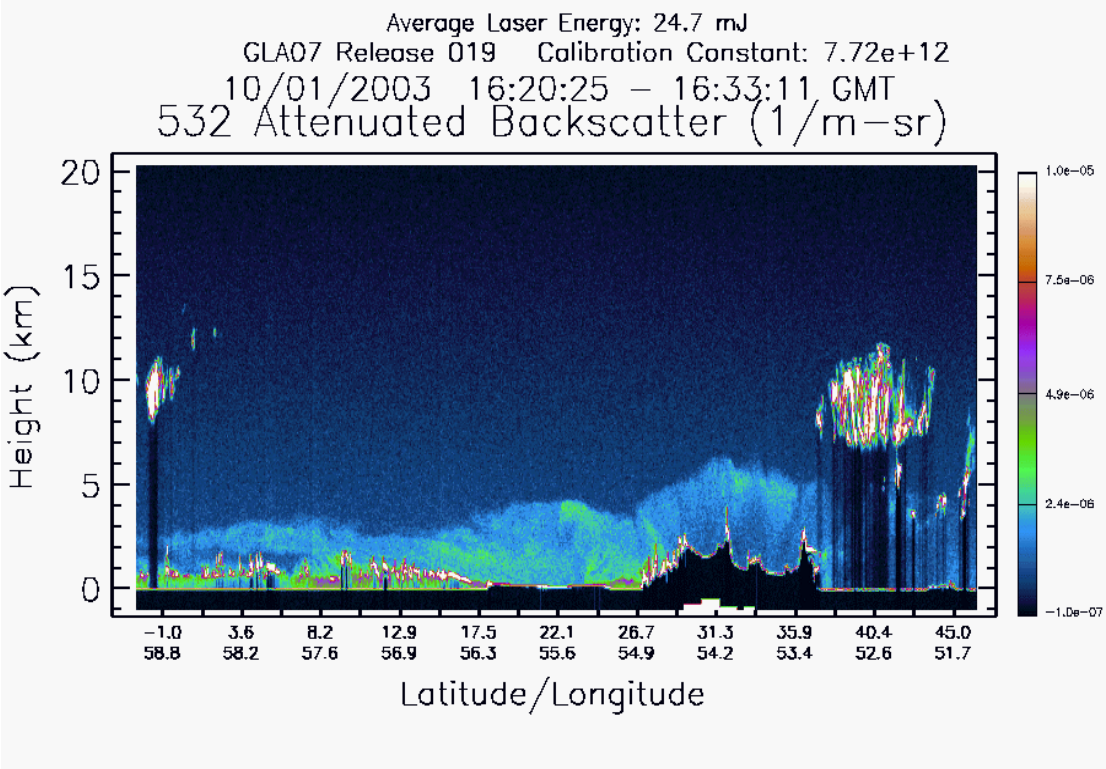

Figure C.3. GLAS satellite lidar signals during an orbit track over the UAE in October 2003.

References:

Campbell, J.R., D.L. Hlavka, E.J. Welton, C.J. Flynn, D.D. Turner, J.D. Spinhirne, V.S. Scott, and I.H. Hwang, "Full-time, Eye-Safe Cloud and Aerosol Lidar Observation at Atmospheric Radiation Measurement Program Sites: Instrument and Data Processing", *J. Atmos. Oceanic Technol.*, 19, 431-442, 2002.

Holben B.N., T.F.Eck, I.Slutsker, D.Tanre, J.P.Buis, A.Setzer, E.Vermote, J.A.Reagan, Y.Kaufman, T.Nakajima, F.Lavenu, I.Jankowiak, and A.Smirnov, "AERONET - A federated instrument network and data archive for aerosol characterization", *Rem. Sens. Environ.*, 66, 1-16, 1998.

Spinhirne, J. D., J. Rall, and V. S. Scott, "Compact eye-safe lidar systems", *Rev. Laser Eng.*, 23, 26-32, 1995.

Spinhirne, J. D., S. P. Palm, W. D. Hart, D. L. Hlavka, and E. J. Welton, Cloud and Aerosol Measurements from the GLAS Space Borne Lidar: Overview of Initial Results, *Geophys. Res. Lett.*, in-press, 2005.

Welton, E. J., J. R. Campbell, J. D. Spinhirne, and V. S. Scott, Global monitoring of clouds and aerosols using a network of micro-pulse lidar systems, in Lidar

Remote Sensing for Industry and Environmental Monitoring, U. N. Singh, T. Itabe, N. Sugimoto, (eds.), *Proc. SPIE*, *4153*, 151-158, 2001.
Welton, E.J., and J.R. Campbell, "Micro-pulse Lidar Signals: Uncertainty Analysis", *J. Atmos. Oceanic Technol*., 19, 2089-2094, 2002.
Winker, D., Hostetler, C., and Hunt, W. (2004). CALIOP: The CALIPSO Lidar. *22nd International Laser Radar Conference (ILRC 2004)*, Matera, Italy.

D.0 Aerosol Retrievals Over Land and Water using Deep Blue Algorithm from SeaWiFS and MODIS

Principal Investigator: N. Christina Hsu, NASA Goddard Space Flight Center

D.1 Nature of problem

When strong winds blow over the desert, mineral dust gets lifted from the surface and into the atmosphere. Since these airborne particles sometimes travel very far distances from their source regions, their microphysical and optical properties may change, thus creating different impacts on the environment along the transport pathway. The science questions we would like to address are:

(1) How do mineral dust aerosols interact with solar radiation not only in the downwind regions, but also over the source regions?
(2) Can we monitor the movements and track the evolutions of dust plumes from sources to sinks using satellite data?

By addressing these questions, we will obtain a better understanding of the aerosol effects on the solar heating/cooling processes. Such an understanding is crucial to improving the prediction of aerosol and climate interactions (i.e., wind and precipitation patterns). Field campaigns such as UAE^2 provide us with golden opportunities to gain a detailed and comprehensive understanding of the mineral dust and fine-mode pollution aerosol properties. Information of this kind is critical for improving the accuracy of satellite aerosol retrievals, which rely on the use of realistic libraries of aerosol characteristics. The measurements obtained by aircraft and ground based instruments help us to better interpret the results of studies that use satellite observations to determine aerosol effects on the radiation budget in the entire atmospheric column. The experiences gained in such campaigns is extremely valuable in helping scientists learn the strengths and weaknesses of satellite algorithms that use SeaWiFS and MODIS data to retrieve aerosol properties and to monitor large scale dust storms over desert and semi-desert regions.

D.2 Executive summary

During the UAE^2 field campaign, we used satellite measurements to provide a "big-picture" look at the aerosol loading distribution over the region. In particular, we provided near-real time SeaWiFS aerosol products of aerosol optical thickness and Angstrom exponent over the region of interest during August and September 2004 to support flight planning. For the post-mission analyses, we now have MODIS aerosol products of aerosol optical thickness and Angstrom exponent available from both Terra and Aqua over desert and semi-desert regions, which we derived using the recently developed Deep Blue algorithm [Hsu et al. 2004]. The ability to compare and contrast Terra (10:30 AM local time) and Aqua (1:30 PM local time) results from these products provided us with a powerful new method to track the movements and evolution of aerosol plumes that were previously hard to detect over bright-reflecting source regions such as

deserts. In Figure D., the RGB images and the retrieved aerosol optical thickness at 500 nm are shown over the Middle East for both sensors on 12 September 2004. In the Terra images, we can see a few prominent dust plumes as they began to develop over Iraq. By the time Aqua passes overhead, the dust storm had grown to cover an extensive area. We can also see the dispersal of a dust plume in southern Saudi Arabia, while the intensity and location of dust clouds over Sudan remained fairly constant.

We are currently analyzing these satellite data, in conjunction with the aircraft and ground-based measurements, to conduct research such as the following:

(1) Characterizing the temporal and spatial variability of aerosol loading over the entire region of interest, including over desert and semi-desert areas for the duration of the intensive observation period;

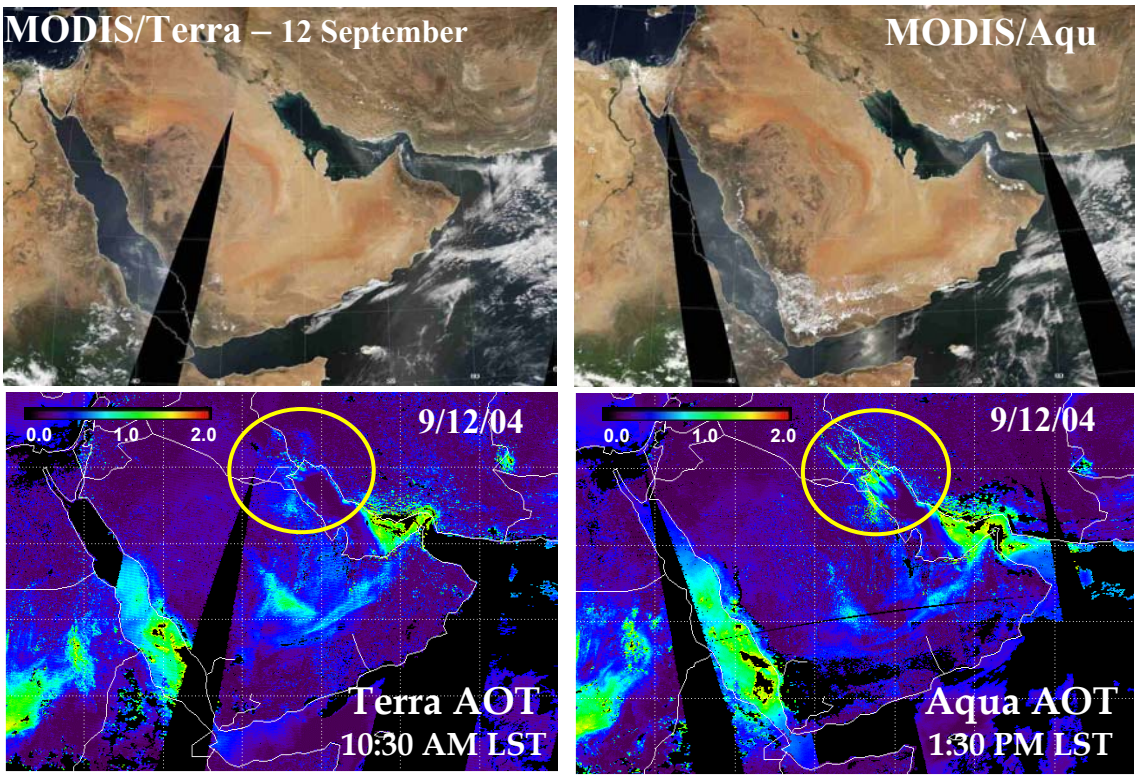

Figure D.1 Dust storms frequently occur over places like northern Africa and southwest Asia all year round. Numerous dust clouds were observed from space over Sudan, Iraq, Iran, and the southern part of the Arabian Peninsula in this September 12, 2004 satellite image from NASA's Moderate Resolution Imaging Spectroradiometer (MODIS) instruments on the Terra and Aqua satellite. The corresponding intensity of the dust plume is also depicted using a quantity called "optical thickness". The higher the dust optical thickness, the more dust.

(2) Identifying the sources of wind-blown dust to help improve the ability to forecast dust storms in the region of interest; and
(3) Characterizing the physical and optical properties of dust from different sources.

The UAE^2 field experiment has provided us invaluable information to validate the satellite derived aerosol product. This type of information was difficult to obtain before this campaign because access to this remote desert site location was difficult. The results of this work will provide a unique dataset of dust properties retrieved using MODIS and SeaWiFS data over the desert. Using this dataset, the evolution of tropospheric aerosols can be better understood by comparing their retrieved properties near the source regions with those in the downwind regions.

Measurements made by different instruments passing overhead at different times have been particularly instrumental in efforts to study the creation and evolution of dust plumes over time. A comprehensive understanding of the properties of these tiny particles as well as their temporal and spatial distribution is imperative to understanding how the Earth's atmosphere maintains its current state of equilibrium.

E.0 MISR Project/Satellite Aerosol Retrieval Validation and Regional Aerosol Mapping

Principal Investigator: Ralph Kahn, Jet Propulsion Laboratory/Caltech

Co-Investigators: Olga Kalashnikova, John Martonchik, David Diner, and Barbara Gaitley

E.1 Nature of problem

Among the strengths of the Multi-angle Imaging SpectroRadiometer (MISR) instrument, flying aboard the NASA Earth Observing System's Terra satellite [http://www-misr.jpl.nasa.gov], are its sensitivity to the shape of airborne particles [*Kahn et al., 1997*]. This means the MISR data contain some information about mineral dust micro-physical properties, that we hope to extract in the aerosol retrieval process. The MISR aerosol retrieval algorithms have demonstrated success at retrieving mineral dust mid-visible optical thickness (AOT) over both land and water, and uniquely over bright surfaces, with a sensitivity of about ±0.07 [*Martonchik et al., 2004; Kahn et al., 2005*]. We have also developed detailed models of mineral dust micro-physical properties incorporating the most recent field campaign results, with the aim of further refining the algorithm [*Kalashnikova et al., 2005*].

The biggest challenge to achieving validating MISR aerosol products is obtaining adequate ground truth. Published studies usually rely upon sun photometer data for validation, which has enormous strengths in terms of coverage and accuracy. But the sun photometer's column-averaged spectral AOT alone, and even the sky-scan size distributions, are not sufficient to constrain differences between medium and coarse mode SSA, particle shape, and vertical distribution. Prior to UAE^2, the only comprehensive field data coincident with MISR overpasses that contain dust are from the ACE-Asia campaign [*Kahn et al., 2004*], which are mixtures that include considerable pollution and background maritime aerosols as well, and from the PRIDE campaign, which turned out to be significantly cloud-contaminated.

The UAE^2 campaign was our next opportunity to collect critical field data to refine and test our algorithm. We aimed for situations where as much as possible of the aerosol vertical structure, height-resolved aerosol micro-physical properties, aerosol optical properties, and surface BRDF were observed over a few-tens-of-km region, coincident with MISR overpasses. The combination of surface-based sun photometer and lidar data, airborne sampling, optical, and physical particle characterization, and airborne remote sensing instruments promised to provide most or all the key information needed to take the next step with our algorithm.

We also aimed to contribute MISR regional aerosol retrieval results both prior to and during the campaign.

E.2 Executive summary

Table E.1 summarizes the coincidences we achieved during field operations in the UAE. The two most promising days for further study are September 01 and September 10. For these, we are working with the *in situ* measurement teams to extract key constraints on aerosol properties, atmospheric conditions, and surface reflectance. Examples of the *preliminary* MISR retrieval results are given in Figure D.1 for the September 01 event, and in Figure D.2 for the September 10 event. On September 01, two aerosol air masses are evident. Based on Version 16 results, to the north and east of the MISR swath, the mid-visible optical thickness (AOT) is 0.3 to 0.5, the single-scattering albedo (SSA) is 0.94±0.02, and the column Angstrom Exponent is between 0.5 and 1.2 (medium-to-large particles). To the west, the optical depth is lower (0.1 to 0.2), whereas the SSA and Angstrom Exponent are higher, indicating smaller, brighter particles.

Based on MISR Version 16 results, on September 10, again two aerosol air masses are evident**.** Over the Arabian Gulf, the mid-visible optical depth is 0.8 to 1.0, the SSA is 0.94±0.03, and the column Angstrom Exponent is between 0.5 and 1.2 (medium-to-large particles). These particles are predominantly spherical. Over the UAE and southward (Hamim), the optical depth is again lower (0.1 to 0.4), and the SSA (0.97±0.03) and Angstrom Exponent (0.5 to ~2.0) are higher, indicating smaller, brighter particles, a mix of spherical and non-spherical (mineral dust). MAARCO and Zakum are near the border of the two air masses.

Further analysis and inter-comparisons with field data are proceeding.

Table E.1 UAE^2 Aerocommander Flights & MISR Coordination

Sites	Date	Notes
Dalma	Sep 01	S Arabian Gulf transect, Dalma profile, MAARCO ovrflt
Land/Ocean Boundary	Sep 10	Transects + Hamim profile, MAARCO overflight
To Gulf of Oman	Sep 12	Transect to Oman, Dhadna profile, MAARCO overflight
Hamim & MAARCO profiles	Sep 28	□~0.3; Ang. 0.8; [but MISR FOV: Gulf of Oman];
Abu Al Bu Koosh	Oct 03	Heavy pollution mixed with dust; no surface BRF
Sir Bu Nuair	Oct 05	No AERONET data

BLUE = In MISR FOV

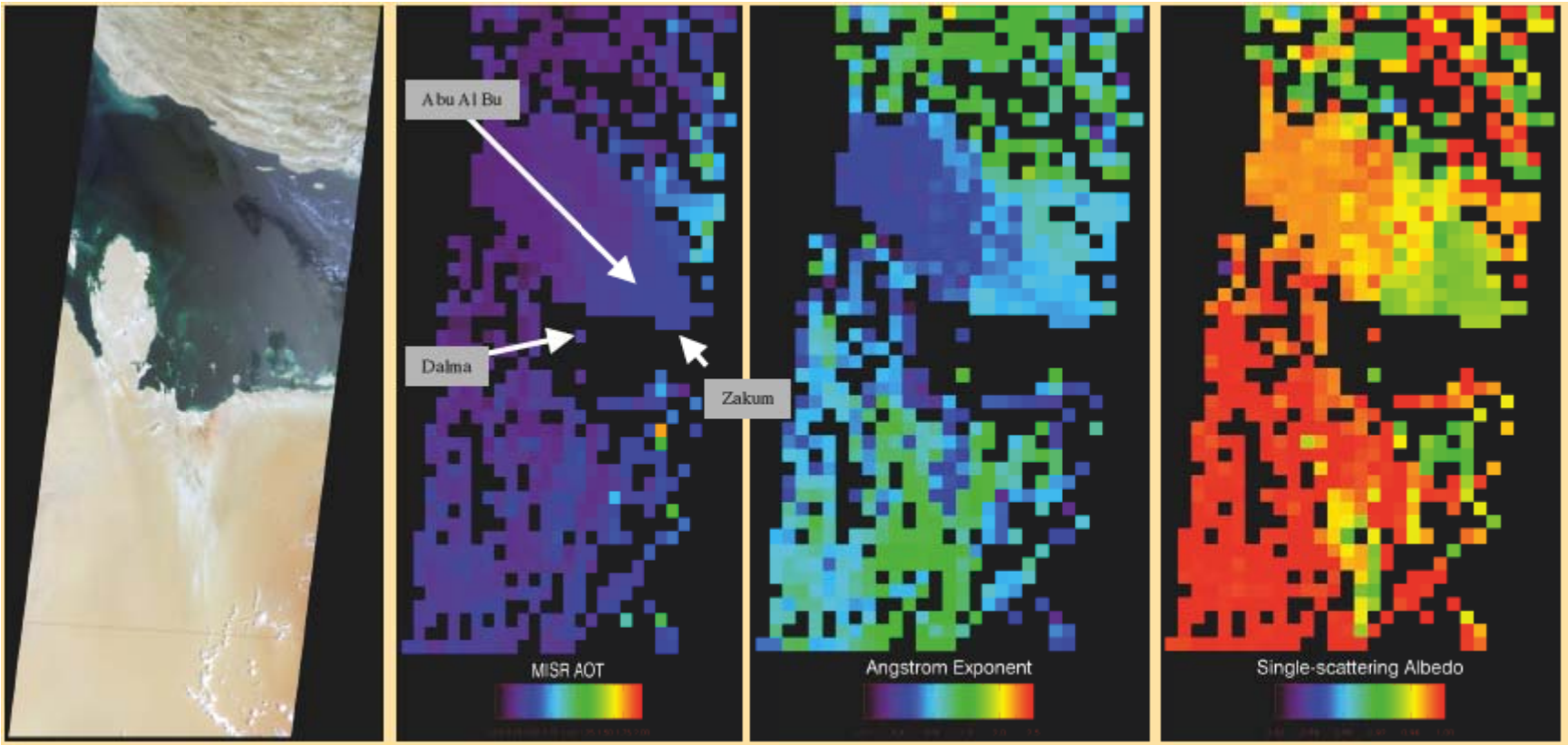

Figure E1. MISR image and Version 16 MISR Aerosol Products: Orbit 25032 **Sep 01, 2004**, Path 162, Blocks 68-73. Ground sites Abu Al Bu Koosh, Dalma, and Zakum are indicated in the AOT panel.

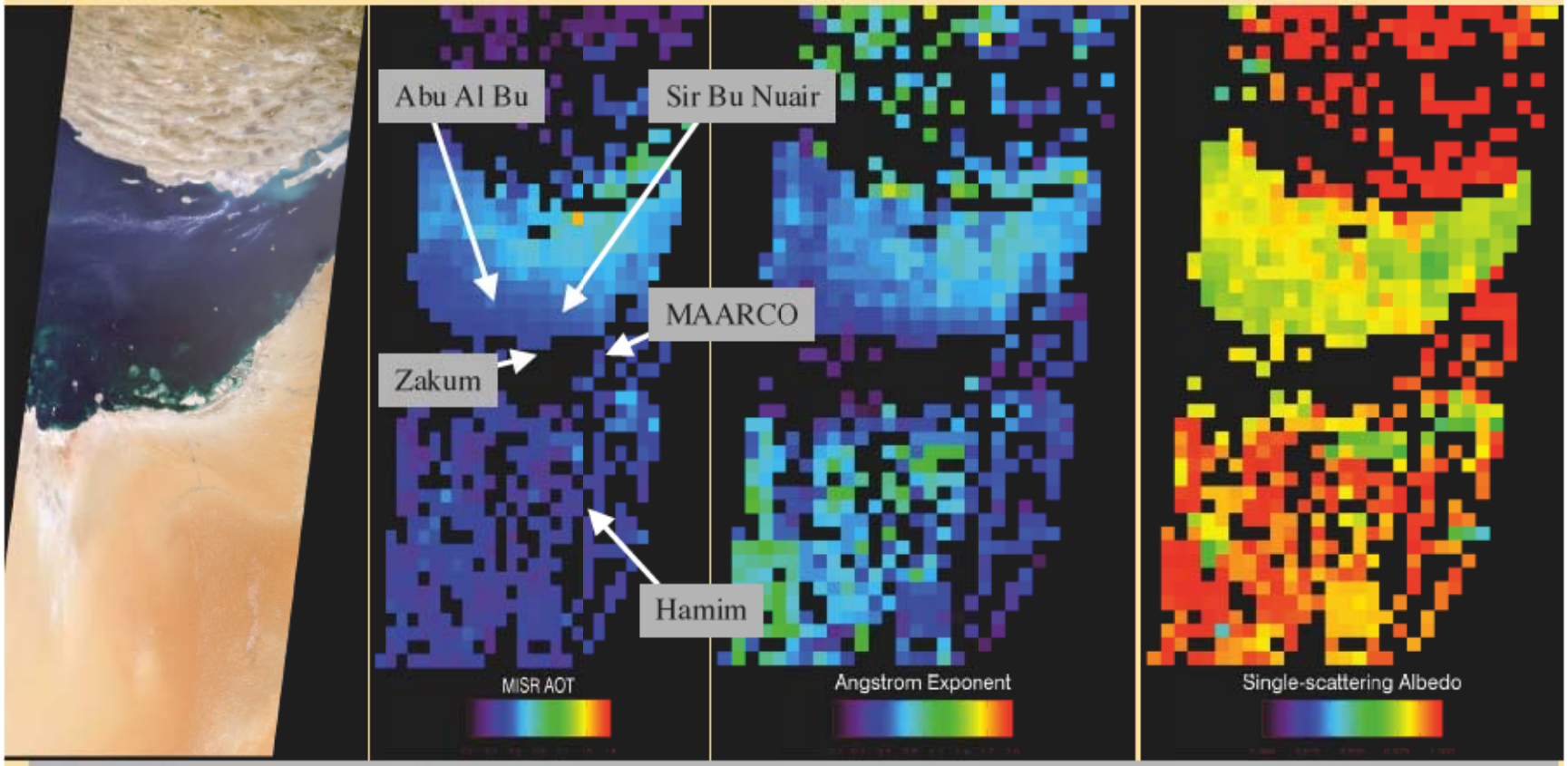

Figure E2. Orbit 25163 **Sep 10, 2004**, Path 161, Blocks 68-73. Ground sites Abu Al Bu Koosh, Sir Bu Nuair, MAARCO, and Zakum, and Hamim are indicated in the AOT panel.

References

Kahn, R., R. West, D. McDonald, B. Rheingans, and M.I. Mishchenko, (1997), Sensitivity of multi-angle remote sensing observations to aerosol sphericity, J. Geophys. Res. 102, 16861-16870.

Kahn, R., B. Gaitley, J. Martonchik, D. Diner, K. Crean, and B. Holben, 2005, MISR global aerosol optical depth validation based on two years of coincident AERONET observations, *J. Geophys. Res., doi:10:1029/2004JD004706*.

Kahn, R., J. Anderson, T.L. Anderson, T. Bates, F. Brechtel, C.M. Carrico, A. Clarke, S.J. Doherty, E. Dutton, R. Flagan, R. Frouin, H. Fukushima, B. Holben, S. Howell, B. Huebert, A. Jefferson, H. Jonsson, O. Kalashnikova, J. Kim, S-W. Kim, P. Kus, W-H. Li, J.M. Livingston, C. McNaughton, J. Merrill, S. Mukai, T. Murayama, T. Nakajima, P. Quinn, J. Redemann, M. Rood, P. Russell, I. Sano, B. Schmid, J. Seinfeld, N. Sugimoto, J. Wang, E.J. Welton, J-G. Won, S-C. Yoon, Environmental Snapshots From ACE-Asia, *J. Geophys. Res*., doi:2003jd004339, 2004.

Kalashnikova, O.V., R. Kahn, I.N. Sokolik, and W-H. Li, 2005, The ability of multi-angle remote sensing observations to identify and distinguish mineral dust types: Part 1. Optical models and retrievals of optically thick plumes, *J. Geophys. Res.,*doi: 10.1029/2004JD004550.

Martonchik, J.V., D.J. Diner, R.A. Kahn, B.J. Gaitley, and B.N. Holben, 2004, Comparison of MISR and AERONET aerosol optical depths over desert sites*, Geophys. Res. Let.,31,* doi:10.1029/2004GL019807.

F.0 United Arab Emirate Unified Aerosol Experiment (UAE^2) Near Realtime satellite support

Principal Investigators: Steven D. Miller and Arunas P. Kuciauskas
Naval Research Laboratory, Monterey, CA

F.1 Nature of the problem

The United Arab Emirates Unified Aerosol Experiment (UAE^2), conducted as an Intensive Observing Period (IOP) over August-September of 2004, has provided a rare opportunity to conduct an intensive field program in a region of central interest to aerosol research. With its distributed network of surface stations complemented by targeted flights with well-equipped research aircraft, UAE^2 has supplied an international science team with the long sought-after *in situ* data required to validate and constrain physical retrievals, evaluate aerosol model predictions, and characterize the microphysics of aerosol species from a diverse array of sources in the region. Given the complex interactions between aerosols, clouds, precipitation, and the radiation budget of the lower troposphere and surface, combined with numerous previous demonstrations of intercontinental transport of aerosols by migratory baroclinic systems and other manifestations (e.g., jet stream) of the general circulation, the outcomes of research performed on the UAE^2 dataset holds relevance not only to the immediate vicinity of data collection, but indeed to our attempts to characterize and predict global climate change.

F.2 Near real-time satellite support

The Naval Research Laboratory's Satellite Meteorological Applications Section, leveraging ongoing research programs in 6.2 (Key Parameters from Next Generation Environmental Satellites; Office of Naval Research) and 6.4 (Satellite Workstation; PMW-150 C4I&Space) provided near real-time satellite support during the active phase of the UAE^2 program. Value-added applications derived from a constellation of 10 polar orbiting satellites (including the NASA Terra/Aqua, NOAA POES, DMSP, SeaWiFS, and TRMM) and Meteosat-5 geostationary data were used in the context of mission planning, flight operations, and post-flight assessment. These products, which included MODIS and SeaWiFS dust enhancements with numerical weather prediction model surface wind overlays, aerosol optical depth, nighttime low clouds/fog/lightning, convective cloud heights, and visible/infrared/vapour/natural-colour imagery, were custom tailored to the operating domain via the same automated processing system ("Satellite Focus") employed during Operation Enduring Freedom and Operation Iraqi Freedom. Figure F.1 demonstrates the Satellite Focus interface as applied to the UAE^2 sector. Many of the satellite products shown at the first UAE^2 science team meeting drew from the Satellite Focus archives, and these products will continue to play a valuable role in providing meteorological context to the phenomena measured locally by surface stations and aircraft.

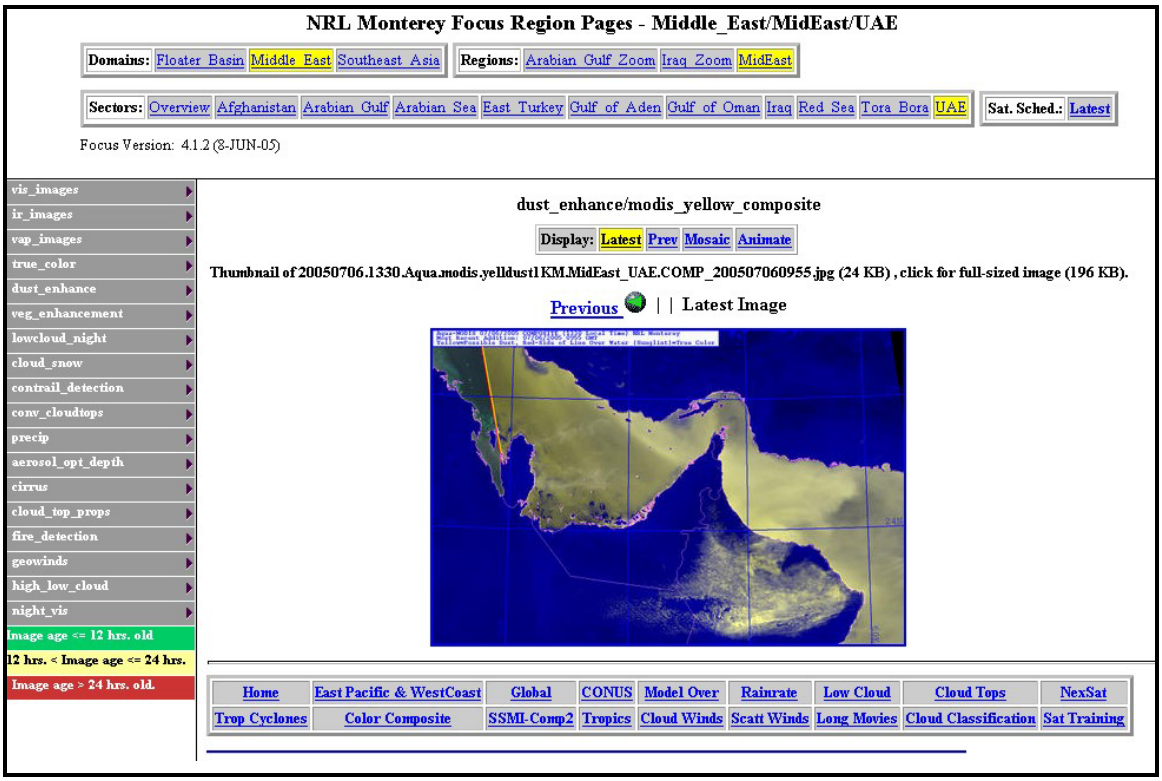

Figure F.1 The Satellite Focus Web Page interface, featuring near real-time applications from a wide assortment of environmental satellites, over the UAE^2 domain. The example shown here is a significant dust enhancement, with areas of dust highlighted in yellow.

Aerosol Optical Depth and Dust Enhancement Algorithm Evaluation

The NRL aerosol optical depth retrievals, developed in conjunction with the Naval Postgraduate School, were heretofore not validated for this region. A particularly heavy dust event crossing the southern Arabian Gulf on 12 September 2004 provided a golden opportunity to asses the algorithm's performance against both Aeronet and aircraft observations. Figure F.2 depicts the dust event, which originated from a strong Shamal in Iraq the previous day. In the left panel, the plume of significant dust concentrations has been enhanced as red. Dust is also present over land, but has not reached threshold concentrations capable of triggering the enhancement (such information is useful for quantifying the performance limitations inherent to these satellite products).

Satellite-Estimated Visibility Techniques

Estimates of horizontal visibility and slant-range visibility were also derived from these retrievals, and preliminary results show the strong dependency on the assumed dust layer geometric thickness in this calculation. Aircraft observations revealed a dual mode vertical structure, with heavier dust residing below 1 km, followed by a sharp drop off and near constant concentration up to 5 km where the air became pristine.

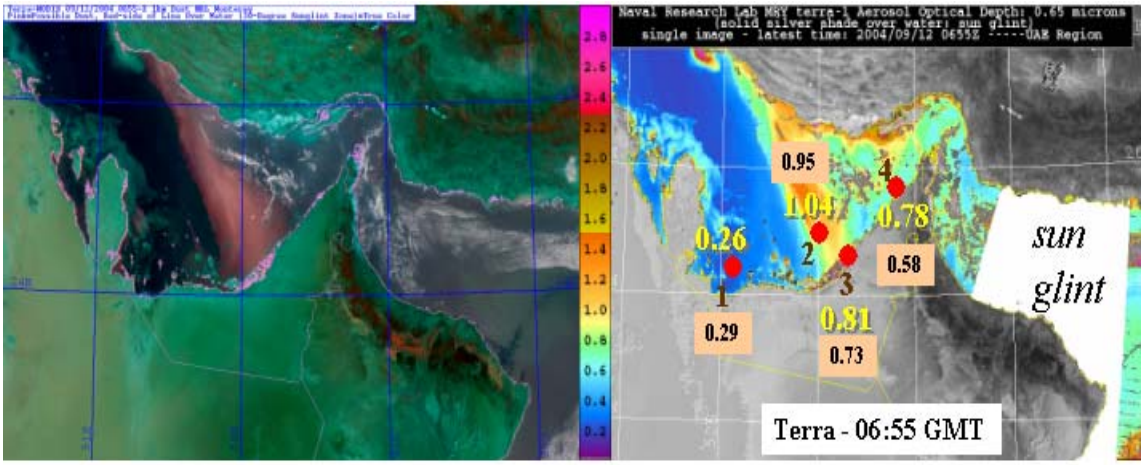

1: Dalma, 2: Sir Bu Nuair, 3: MAARCO, 4: Umm Al Quwain

Figure F.2 Left panel: the MODIS significant dust enhancement indicates the presence of a dust plume (pink) crossing the UAE^2 sector on 12 September 2004. Right panel: MODIS aerosol optical depth retrievals (colors; valid over water bodies only) with point values (yellow) corresponding to Aeronet surface observations (orange boxes), indicating generally good agreement for this case.

The horizontal visibility estimates range from less than 5 km to 15 km depending on the assumption of layer thickness. From a Navy-METOC application perspective, knowledge of the dust layer height (in this case from aircraft, but in principle also available from space lidar) and column optical depth enables the approximation of minimum sensor-to-target closing distance for a sensor embedded within the dust layer. The outcomes of this research will form the subject matter of a journal article.

Haboob Dust Storm Analysis

An unanticipated windfall of the timing of the UAE^2 field program was the frequency and regularity of thunderstorms that occurred across the domain. These storms are responsible for the ephemeral dust events known to this region as Haboobs. Derived from the Arabic word for “rushing wind,” Haboobs represent the most sudden, intense, and difficult to predict varieties of desert dust storms, forming the “walls of sand” most commonly associated with dust storms. Their difficulty to predict stems from their source—mesoscale convective systems that initiate either over local mountain topography (an elevated heat source and focus of low level convergence) but also in association with passing dynamics. Depending on the convective available potential energy and available moisture fueling the storms, the evaporation of rainfall in the dry lower atmosphere can lead to an extremely negatively buoyant air mass that imparts momentum (downbursts can easily exceed 50 kts) into the dry surface, lifting copious dust (a case study over the continental United States describes a Haboob that yielded 85 metric tons of material per square kilometer per hour) over a wide range of particle sizes. The dust propagates outward radially along the cold pool gust front.

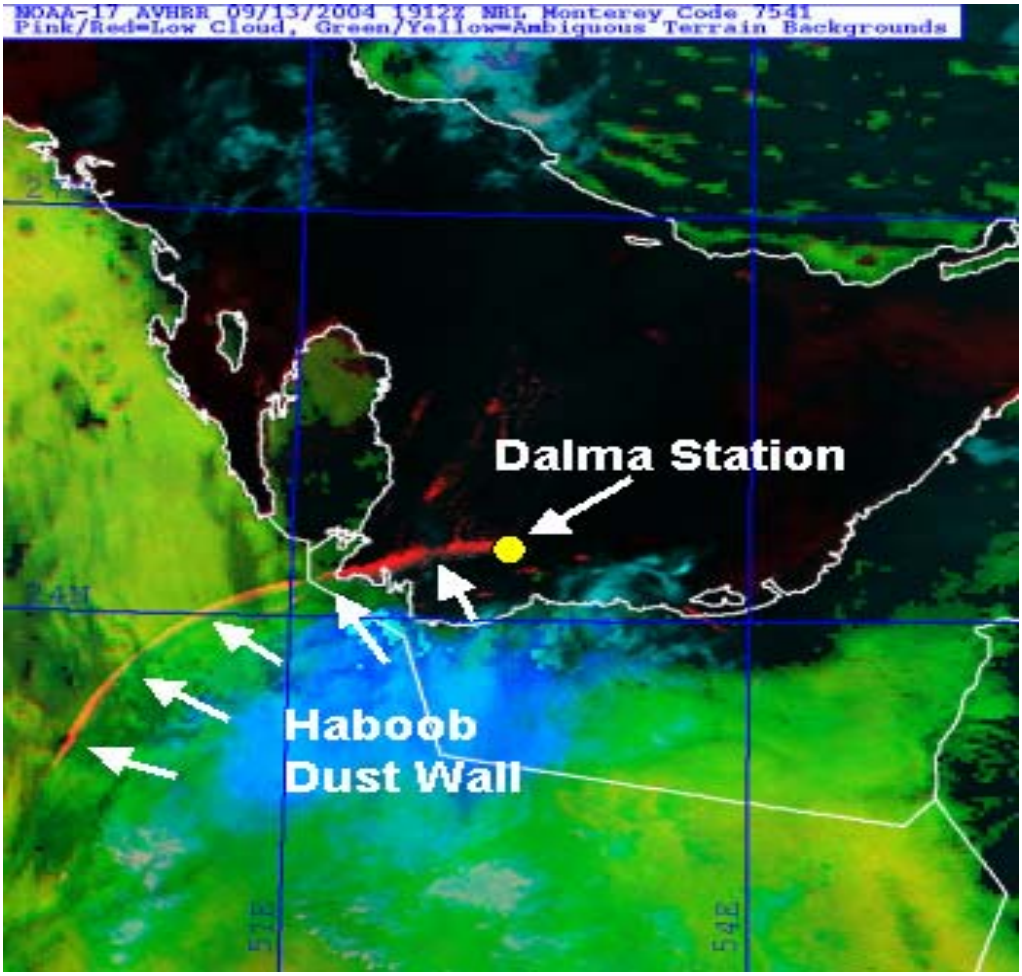

Figure F.3 The nighttime low cloud and dust product from NOAA-17 AVHRR depicts a line of dust (red) representing the leading edge of the Haboob. The deep, cold clouds associated with its parent thunderstorm complex to the south are shown in blue. Certain terrain backgrounds posing potential false alarms in this product are cast in green/yellow. The Dalma station, and estimated cross time of the Haboob, are indicated.

The opportunity to study a Haboob in situ arose on the evening of 13 September 2004, when an isolated thunderstorm developed in the early evening hours (~1400 UTC) in southeastern Saudi Arabia and tracked northwest into the eastern United Arab Emirates study region over the next 6-8 hours before dissipating. Nighttime visible data from the DMSP/OLS revealed lightning activity at 1600 UTC, with Meteosat-5 derived convective cloud top heights exceeding 17 km. By 1830 UTC, a radially propagating line of dust (inferred from the nocturnal low cloud/dust products provided by AVHRR and MODIS) had emerged from beneath the shielding anvil cirrus. Figure F.3 highlights this feature in red as observed by NOAA-17 AVHRR at 1912 UTC, and points out its current proximity to one of the UAE^2 offshore stations (Dalma). Anvil cirrus associated with the parent storm are shown in blue, and desert surfaces masked for this particular satellite application appear as green/yellow.

Figure F.4 summarizes the Dalma wind observations for a period bracketing the Haboob crossover time. The sudden decrease in prevailing northerlies and wind shift give positive indication of the thunderstorm gust front passing over the station. Unfortunately, the only measurements capable of detecting dust particles at night (nephelometer) were located at the Mobile Atmospheric Aerosol and Radiation Characterization Observatory (MAARCO) trailer a considerable distance away. While the main force of the Haboob appears to be toward the northwest (direction of storm motion), a lateral propagation of the front as observed through a finite time series of AVHRR/MODIS data raises the possibility that this dust could have reached MAARCO some hours later. We are currently examining this case study together with other documented Haboob cases recorded during the UAE^2 IOP in an attempt to quantify and statistically characterize these poorly understood events.

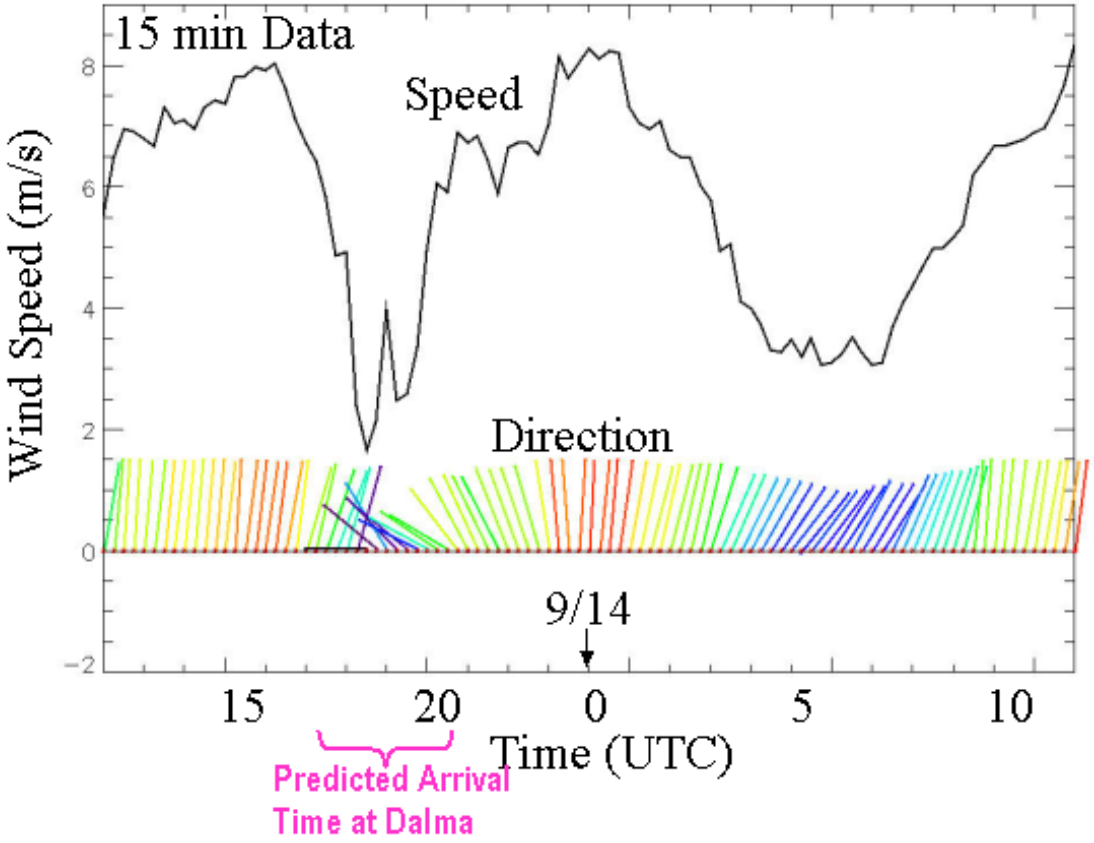

Figure F.4 Dalma station 15 min wind speed and direction observations over a period containing the possible Haboob crossing. Noted at the predicted crossover time is a breakdown in the prevailing northerlies and corresponding anomaly in the wind speed as the southern cold pool surge crosses the station.

F.3 Conclusion

Preliminary dust/aerosol-related research based on the UAE^2 dataset has yielded promising interim results. The near real-time support provided to the science team during the active IOP is now paying dividends in the context of research and case study development. We are optimistic that the outcomes of the research directions mentioned above will result in two intriguing science papers and complement the greater mission science objectives of this experiment. We are grateful to Dr. Reid and the team responsible for coordinating and executing the UAE^2 effort, and the Department of Water Resources Studies for making this study possible.

G.0 Satellite remote sensing and analysis of radiative fluxes during UAE^2

Principal Investigator: Sundar A. Christopher, Department of Atmospheric Sciences, University of Alabama, Huntsville

Co-Investigators Jianglong Zhang and Jeffrey Reid

G.1 Nature of problem

Tropospheric aerosols such as smoke from biomass burning, dust, and pollutant aerosols affect weather, climate and health by reducing visibility, altering the earth's radiative energy budget, changing cloud formation, affecting rainfall distribution, changing dynamics of circulation patterns and also by inducing respiratory diseases when sub-micron particles penetrate the lungs. One of the greatest uncertainties in our current understanding of the climate system is the effect of aerosols on the earth's radiative energy budget and the unraveling of these complex interactions of aerosols within the earth-atmosphere system continues to be a challenge since aerosols have short life times in the atmosphere and have different chemical compositions and properties that are not readily measured on global scales.

Aerosols are usually categorized as natural and anthropogenic, where dust and marine sea salt aerosols from wind driven mechanisms are called 'natural aerosols' and aerosols from biomass burning smoke, industrial and other pollution due to human-induced activities are called 'anthropogenic aerosols'. The widely used method for studying the radiative impact of aerosols is from global models where the natural and anthropogenic components are separated and the radiative effect of anthropogenic aerosols are called climate forcing of aerosols. The aerosol distributions in global models are prescribed by three dimensional chemistry transport models that compute aerosol distributions from source emissions using prescribed meteorological fields. Although these models can be used to separate the radiative effects of various aerosol fields, considerable uncertainties exist on the spatial and temporal distribution of aerosols and their associated properties.

Satellite measurements also play a major role for studying the radiative impact of aerosols although most of these studies have been confined to the oceanic regions. However most satellite data sets have limited information for precisely separating the effect of natural from anthropogenic pollution and usually only the combined effect of aerosols have been examined. However recent studies from the Polarization and Directionality of the Earth's Reflectances (POLDER) and MODIS instruments show promising results for separating the effect of anthropogenic from natural aerosols

Another technique that does not require radiative transfer calculations to convert the satellite-retrieved AOT into TOA fluxes utilizes collocated narrowband and broadband instruments from the same satellite platform although these techniques estimate the combined effect of all aerosols. In this technique aerosols are identified and their properties are obtained from multi-spectral measurements such as the MODIS and the radiative fluxes are obtained directly

from the CERES measurements therefore bypassing radiative transfer calculations. The radiative effect of aerosols can be obtained by examining TOA CERES fluxes with and without the presence of aerosols that is called SWARF.

Since aerosol climate forcing is commonly defined as the effect of *anthropogenic* aerosols (and not the combined effect of all aerosols) on the radiative energy balance there is a need to separate the retrieved AOT and consequently the SWARF into natural and anthropogenic components. It is also possible to separate dust and sea salt aerosols from fine model aerosols (a surrogate for anthropogenic aerosols) by applying thresholds to the Angstrom exponent derived from POLDER measurements to estimate aerosol absorption over cloud-free oceans. Other studies *have* distinguished dust from other aerosols by applying thresholds to the fraction of fine mode to the total AOT over the oceans (η) for studying dust transport and deposition in the Atlantic Ocean. Much like the Angstrom exponent, η is an index of particle size and aerosol type and has the potential for separating natural from anthropogenic aerosols since large η values signify larger fine mode fractions that are largely from anthropogenic aerosols. Although these methods are sensitive to the applied thresholds and are yet to be fully validated, they provide the framework for separating natural from anthropogenic aerosols from satellite observations for radiative forcing studies.

G.2 Executive summary

The UAE^2 project provides a tremendous opportunity to further improve upon existing satellite-based techniques for studying the radiative effects of aerosols. High quality data sets from insitu, ground-based and satellite platforms will be used to address the following scientific questions

1. What is the TOA and surface radiation budget of aerosols when dominated by different types dust and pollutant aerosols?
2. How can we separate the effect of anthropogenic aerosols from desert dust aerosols using combined satellite and insitu measurements?
3. What is the atmospheric radiative heating/cooling of aerosols?
4. How can we use the available measurements to study the radiation budget at the surface using radiative transfer calculations?
5. How well do CERES measurements represent radiative fluxes over bright targets?

Using combined MODIS, MISR and CERES data we examined the effect of dust aerosols on the TOA radiation budget over bright targets. Our results show that the monthly-mean LW forcing for September 2000 is 7 Wm^{-2} and the LW forcing efficiency (LW_{eff}) [Longwave forcing per unit aerosol optical thickness at 0.55 μm] is 15 Wm^{-2}. Using radiative transfer calculations, we show that simultaneous measurements of the vertical distribution of aerosols, surface temperature and water vapor are critical to the understanding of dust aerosol

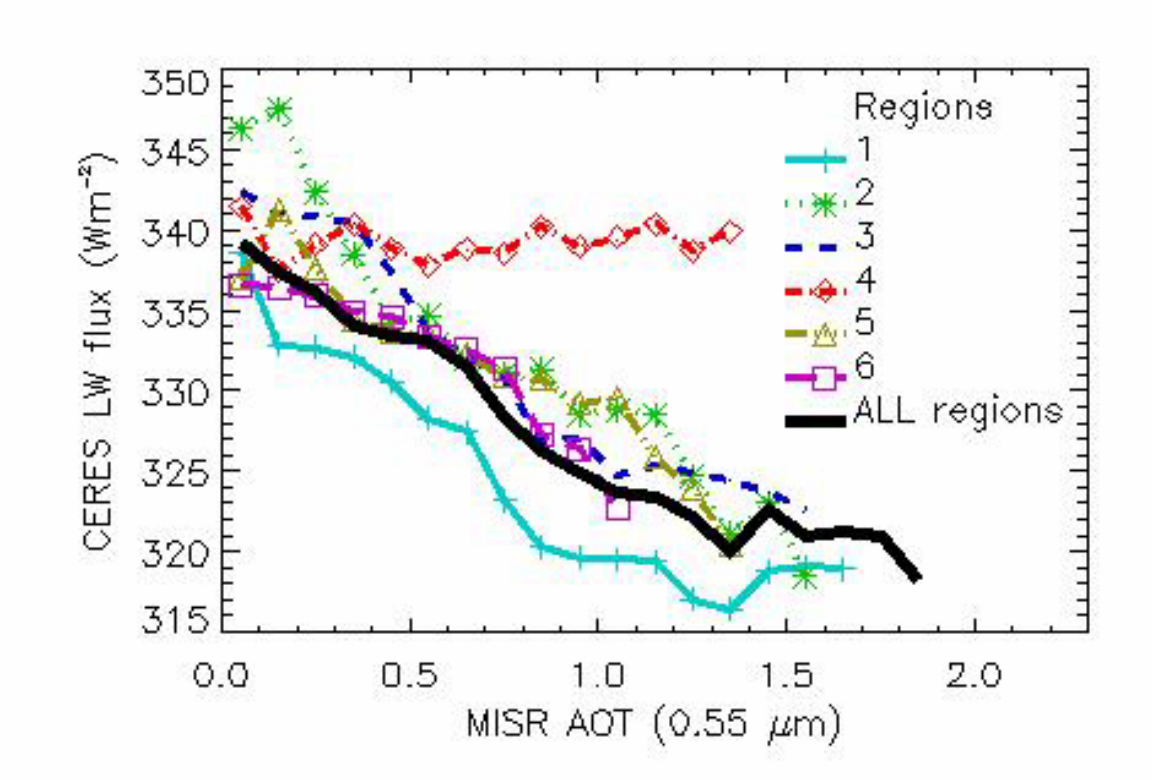

Figure G.1 MISR $\tau_{0.55\mu m}$ vs. CERES LW fluxes for six selected regions within (15°- 40°N, 20°W- 40°E). Solid black line shows the mean values for the whole region. See the following publication for more details.

forcing, and must come from other sources. Using well calibrated, spatially and temporally collocated data sets, we have combined the strengths of three sensors from the same satellite to quantify the LW forcing, and show that dust aerosols have a "warming" effect over the Saharan desert that will counteract the shortwave “cooling effect” of other aerosols. - See Figure G.1.

Zhang, J., and S.A. Christopher, Longwave Radiative Forcing of Dust Aerosols over the Saharan Desert estimated from MODIS, MISR, and CERES observations from Terra, *Geophysical Research Letters*, 30(23), doi:10.1029/2003GL018479, 2003.

H.0 Defining Infrared and Microwave Land Surface Emissivity for Improved Model Initialization of the Surface State

Principal Investigator: Benjamin Ruston Naval Research Laboratory, Monterey CA

H.1 Nature of the problem

Historically numerical weather prediction models have had a misrepresentation of the land surface temperature over desert and arid areas. Satellite retrievals of the surface temperature have indicated warmer days and colder nights over these areas than that predicted by the weather model. The excellent network of observing stations operated by the Department of Water Resource Studies provides an opportunity to do greatly needed calibration and validation work on the satellite retrieved surface temperatures. Particularly over the desert regions through the Sahara and Arabian Peninsula validation sites for land surface temperature have been scarce or non-existent, the DWRS network of land stations is a unique and incredibly valuable resource to the world weather community and is vital to providing necessary ground truth to studies in the region. Calibrated satellite land surface temperatures retrieved in this study, are provided to other researchers for use in their work as a stand-alone retrieval or as another option to the model predicted land surface temperatures. In addition, well-calibrated satellite surface temperature retrievals are incorporated into the weather models to examine forecast impacts, and will lead to a more accurate description of the land surface characteristics.

To perform a satellite retrieval of the surface temperature over land the radiating efficiency of the surface, or emissivity, must be known. The emissivity has a value between zero and one and varies across the radiometric spectra. The Naval Research Laboratory in Monterey, California has developed a retrieval system that retrieves the land emissivity simultaneously from three satellite sensors along with the a surface temperature value. These sensors span the microwave and infrared radiometric spectra. Though the land emissivity is just a boundary condition needed to retrieve the land surface temperature, continual monitoring of the land emissivity can be used to provide information about the changing health of vegetation and state of the soil.

The satellite sensors used in this research are characterized as atmospheric sounding instruments and have large ground footprints, typically between 25 and 50 kilometers. The three sensors used are the High-Resolution Infrared Radiation Sounder (HIRS), and the two Advanced Microwave Sounding Units (AMSU) labeled A and B. The sensors fly aboard the polar orbiting National Oceanic and Atmospheric Administration (NOAA) satellites 15, 16, and 17. These polar orbiting satellites are sun-synchronous meaning they ascend over the equator at the same local time each orbit. The three satellites give approximate global coverage every six hours. Mean emissivity maps for 10 surface sensitive channels from the three satellite sensors are presented in Figure H.1. These are averages from the first 15 days of overpasses from August of 2004. These emissivity means define the important boundary

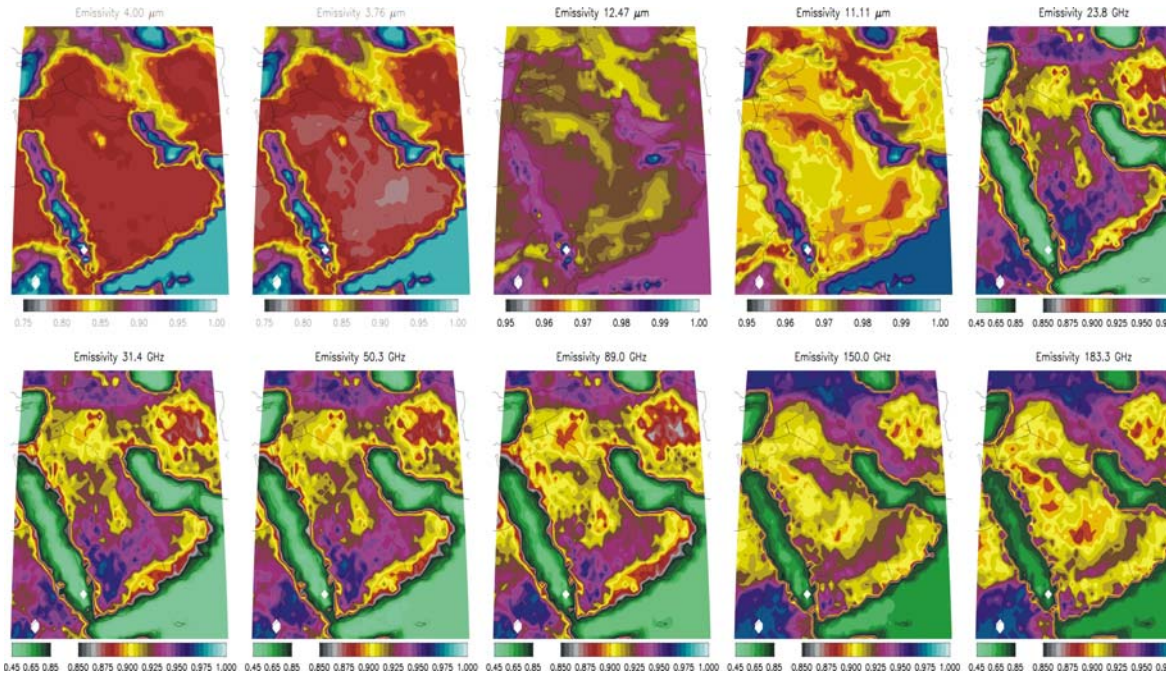

Figure H.1 Mean emissivity derived from the first 15 days of August, 2004. The ten panels correspond to surface sensitive channels on the HIRS/3, AMSU/A, and AMSU/B sensors aboard NOAA-15, 16, and 17 satellites.

condition needed to assimilate land surface temperature information into an improved forecast model. Though these sensors do not themselves resolve high-resolution features, by giving the largest model nest better information of the surface state, this can be propagated to the models finer nests.

The difference between the satellite derived land surface temperature and that in the model depends on the time of day, and location of interest. Shown in Figure H.2 are mean differences, and the range of one standard deviation for 10 sites across the United Arab Emirates. These differences of 5 degrees Celsius represent large quantities of energy in the model that drive land and sea breeze interactions. In addition, the more precise knowledge of the land surface temperature and emissivity, has shown the ability to better define the temperature and moisture in the boundary layer (approximately the lowest 1km). The additional radiosondes launched during the UAE^2 field campaign, and observations from airborne sensors have proven effective calibration and validation tools, and augment the already robust ground network of stations graciously provided by the DWRS. This researcher would like to humbly thank the participants at the DWRS for their aid in conducting an innovative field campaign of the utmost utility to the progress of weather forecasting in this region.

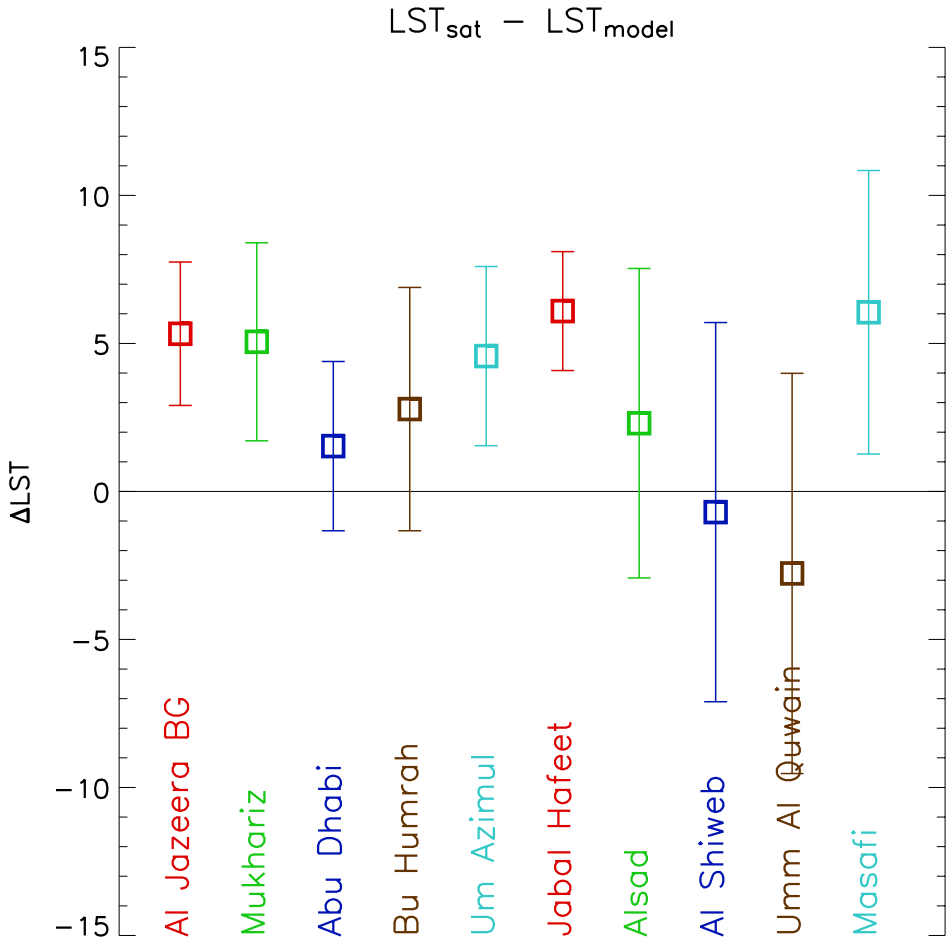

H.2: Difference (in Celsius) between the Land Surface Temperature (LST) retrieved from satellite and from the model for the first 15 day of August, 2004. The square symbol indicates the mean, and the width of the line represents one standard deviation.

I.0 The Mobile Atmospheric Aerosol and Radiation Characterization Observatory During the UAE^2 Field Campaign

Project Manager: Elizabeth A. Reid, NRL-Monterey
Cooperative Investigators: Jeffrey Reid, Kzystoff Markowicz, Marcin Witek

I.1 The MAARCO facility

The combination of surrounding desert regions and extensive oil processing and manufacturing facilities has made the Arabian Gulf's air one of the most chemically complicated in the world. Humidity, high temperatures, long-range transport of dust and aerosol particles over dry desert regions, and the Arabian Gulf nation's continuing development and growth have combined to create the current atmospheric environment. A key component of the UAE^2 mission is to interpret the aerosol particle sources, composition and processing (what are the particles, and how do they change as they move through the atmosphere), removal processes (how quickly do the particles settle out of the atmosphere), and their effect on weather and climate in the gulf region.

The Mobile Atmospheric Aerosol and Radiation Characterization Observatory (MAARCO) is a standard 20'x8' climate controlled CONEX shipping container that has been modified to function as an easily-shipped laboratory for deployment overseas, in remote areas, or on sea-going vessels. Its purpose it to perform basic research on atmospheric aerosols, gasses, and radiation (visible and IR light) in difficult to deploy regions. MAARCO will assist in validating aerosol and weather models as a ground station and often be used in conjunction with research aircraft. All MAARCO requires is input power (110, 220, or 240 3-phase), though it can utilize generators. MAARCO also has the capability to utilize telecommunications links and the Internet for real time remote displays when available.

The MAARCO container is 'mobile' in the sense that it can be easily moved it to new sites to perform research. One of the primary obstacles in performing research overseas is the difficulty in finding adequate facilities at good site locations. Most aerosol instruments prefer, if not require, climate controlled environments for stable, consistent operation. These conditions are not readily available in remote or foreign sites. Radiation instruments are for the most part less sensitive to changes in the environment, but are also much more valuable when run in conjunction with other instruments to fully characterize the local environment.

The United Arab Emirates generously hosted our research efforts, allowing us to install a mobile research laboratory, the MAARCO facility, at a remote coastal site in Al Taweela, Abu Dhabi (Figure I.1). This coastal location provided excellent opportunities to explore a region where rapid change from ocean to land conditions occurs, and to characterize aerosol particles from the sea breezes, uncontaminated by transport over local land sources. Additionally, the decision by the UAE government to allow use of lidar, Aeronet sun photometers, weather balloons, and over-flights by research aircraft at Al Taweela allowed us

Figure I.1. Overview of MAARCO container with outboard radiation and meteorology equipment with Aerocommander over-flight

to characterize the atmospheric above the site, and therefore more accurately interpret the results we collect at the surface.

I.2 Executive summary

Aerosol particles measured at the MAARCO site varied from dust to anthropogenic pollution, with many days exhibiting mixtures of both types of materials. We monitored particle concentrations and types in the atmosphere using Aeronet and MPL, and at the surface through mass, scattering, particle size, and composition measurements.

Optical depth and coarse mode mass data for the MAARCO site is presented in Figure I.2. During the months of August and September 2004, the aerosol optical thickness (AOT) measured at 500nm light (green) at the MAARCO site averaged 0.47, and varied from 0.1 (clean) to 1.2 (high concentrations of aerosol particles/poor visibility).

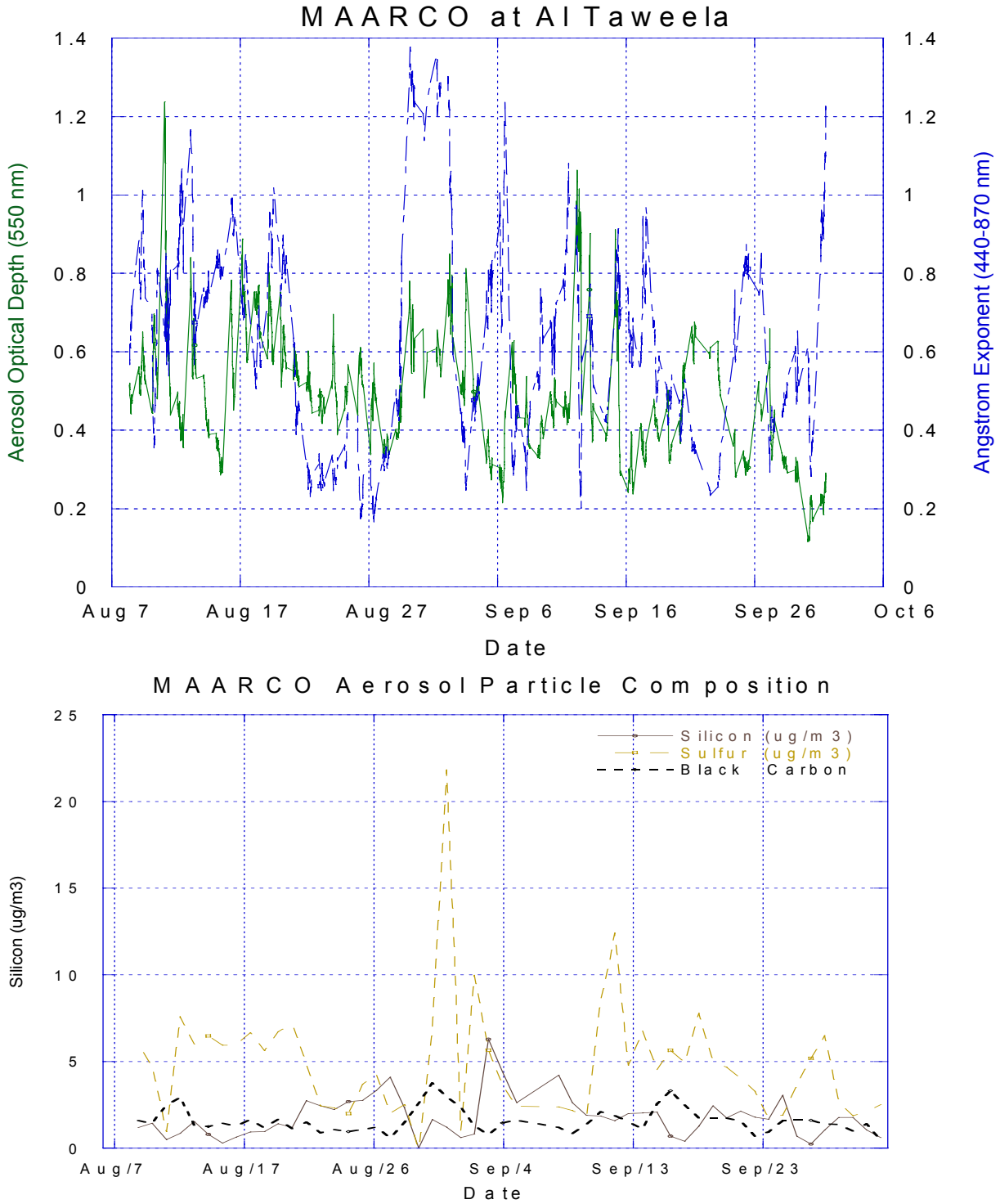

Figure I.2. (Upper) Aerosol Optical thickness and Angstrom Exponent for the MAARCO Site. (Lower) Three wavelength nephelometer data for the August 30th pollution event..

Periods of high AOT were associated with dust, anthropogenic pollution, and varying combinations of both type. The angstrom exponent gave an approximation of the type of particles – high angstrom exponents are associated with small particles (pollution events), and low values are associated with larger particles (dust events). From the MAARCO at Al Taweela plot, we can see that the period of August 29-September 1 demonstrates a classic Arabian Gulf pollution event blowing onshore in UAE (Figure I.3). This event was both preceded and followed by minor dust events. The Nephelometer and Mass plots display the change from dust to pollution particles. The bulk elemental composition data also show this change, as seen in the time series of Silicon (strongly correlated with dust) and Sulfur and Black Carbon (correlated with pollution).

We are currently in the process of performing individual particle analysis of the aerosol particles collected at the MAARCO site. This will provide statistically significant information on the elemental composition, number, shape, and size of the aerosol particles collected during at the MAARCO site. With these composition and shape data, we can begin to decode the source of these particles and understand the type of processing they have undergone during transport. With individual measurements, we will also have the necessary data to correlate light scattering measurements from surface, airborne, and satellite data, with the actual aerosol characteristics – vital information for weather and climate modeling that is often merely approximated, due to lack of physical data.

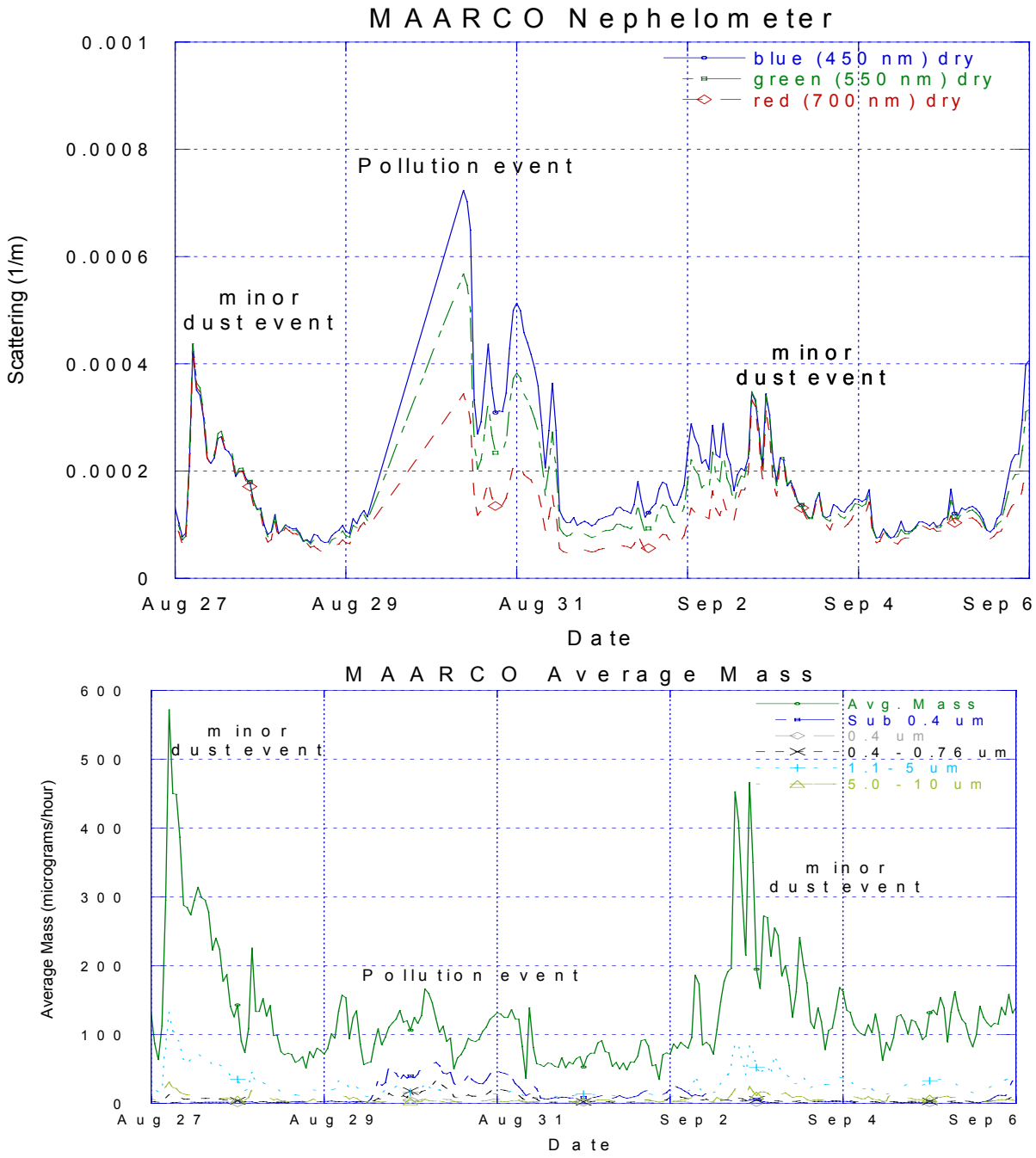

Figure I.3. Upper 3 wavelength light scattering data from the MAARCO site for the August 30 pollution and Sept 3 pollution and dust events, respectively. (Lower) Size dependant mass concentrations for the same period.

J.0 SMART Mobile Measurement Facility and UAE^2 Field Campaign

Principal Investigator: Jack Ji, ESSIC, University of Maryland

Co-Investigators: Si-Chee Tsay, Rick Hansell, Antonio Queface, and Tsung-Hsin Hsieh

J.1 Abstract

The SMART trailer from NASA Goddard Space Flight Center was deployed successfully at the meteorological observation station inside the Al Ain international airport during the UAE^2 filed campaign in August and September of 2004. The unique environment gave us a special opportunity to study the dust and the interaction between dust and manmade pollutions. The data set we collected will play an important role in assessing the impact of the aerosols in the area, especially the dust, to the local and even global climate. The studies we were involved in during the UAE^2 experiment may also help to better understand the water cycle in the region. The study results will be published with the collaborators from UAE in the refereed scientific journals. The following is a collection of example data from each sensor utilized in SMART during the UAE^2 mission. It gives a glimpse of what we can see during a scientific research with a comprehensive sensor array of remote sensing.

J.2 Selected examples of preliminary results from SMART for UAE^2

The first day we visited the meteorological station we were asked if we have UV measurement. Fortunately we do. Figure J.1 is the dose rates derived from the UV data. They are CIE erythemal dose, UVA (320~400nm), UVB (280~320nm), and PAR (400~700nm). Figure J.2 zooms in on a particular day (22-sept-2004) and throw in the cloud transmission and column ozone amount. The drop down of the dose rate and the cloud transmission in the late afternoon is due to a dusty front. As usual, to avoid overexpose to the UV radiation, stay away from the sun, especially around the noon time.

A basic measurement SMART does is the solar irradiance – the solar energy received on the ground surface. To add information about the atmosphere, the data is partitioned into three spectral bands: 0.3~3, 0.4~3, and 0.7~3 microns. The diffused radiation from the sky is measured separately. Figure J.3 shows the data from the mid August to the beginning of October. The first of October was a cloud free day with blue sky. In the diffuse irradiance plot it can be seen that most of the days during August and September were hazy, leading to the high diffuse irradiance. The similar result is also revealed by another instrument – the shadowband radiometer, as shown in Figure J4. Again, the September 22's data is used, and the sudden decrease of the irradiances in the late afternoon corresponds to the dusty front.

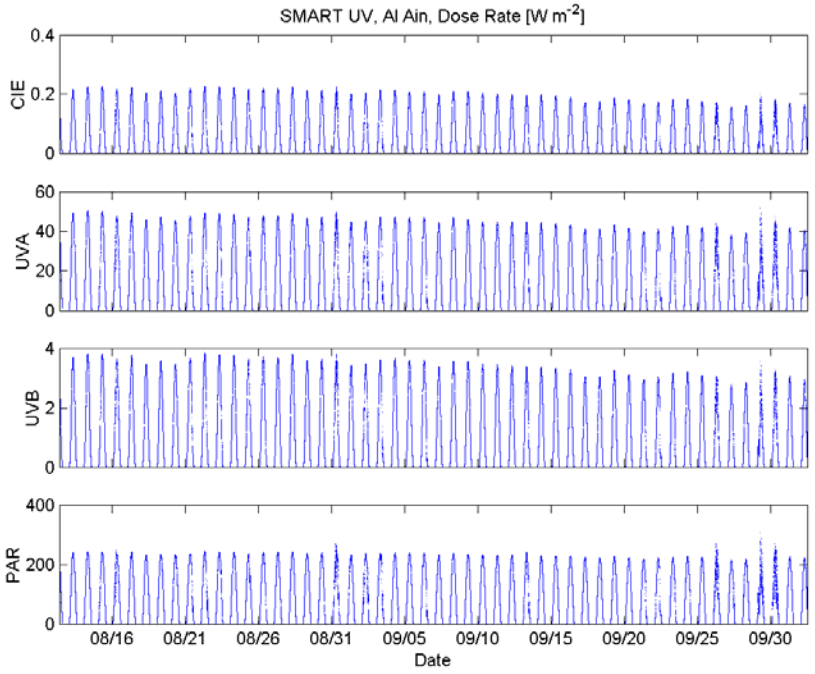

Figure J.1 Dose rate from the UV data.

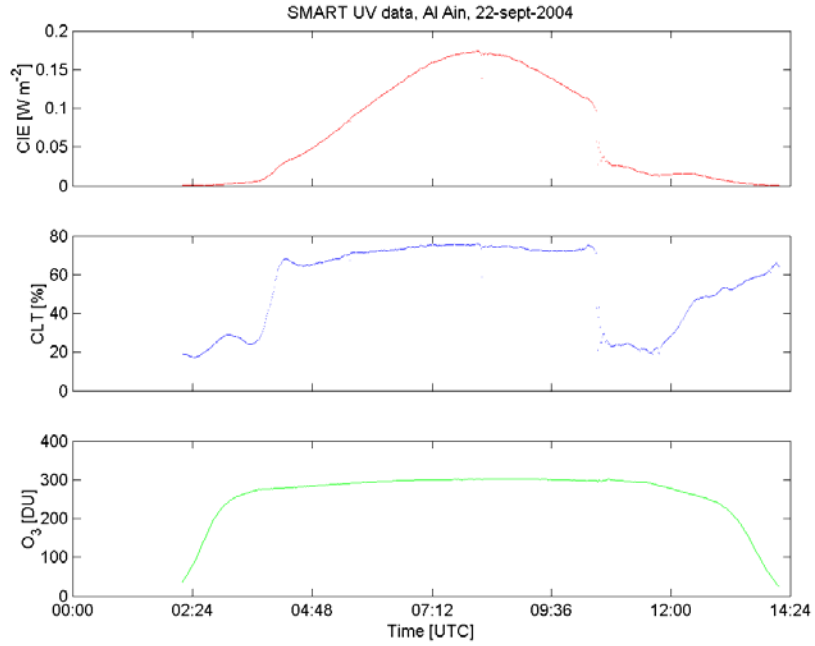

Figure J.2 CIE dose rate, cloud transmission, and ozone amount on September 22, 2004

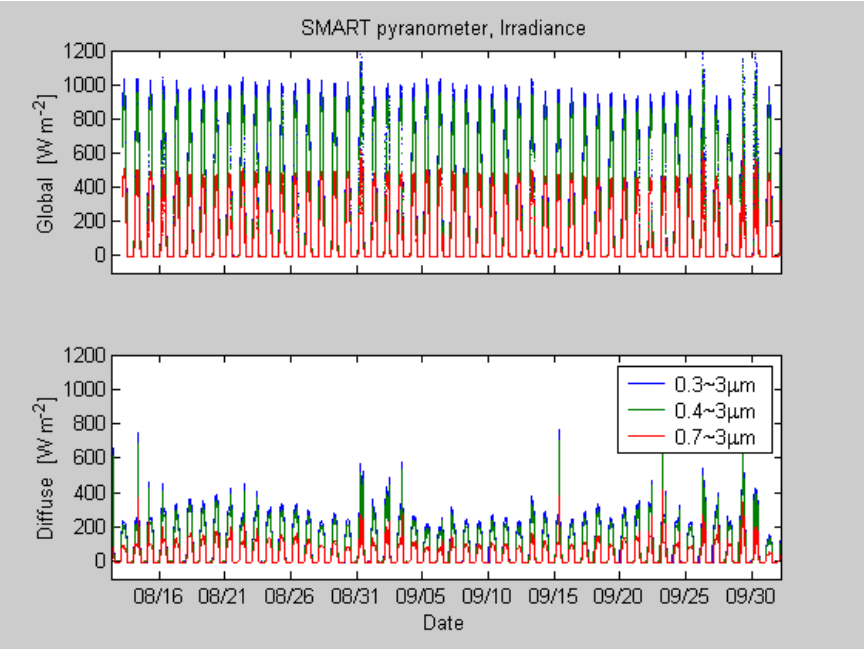

Figure J.3 Solar irradiance, global and diffuse in three spectral bands.

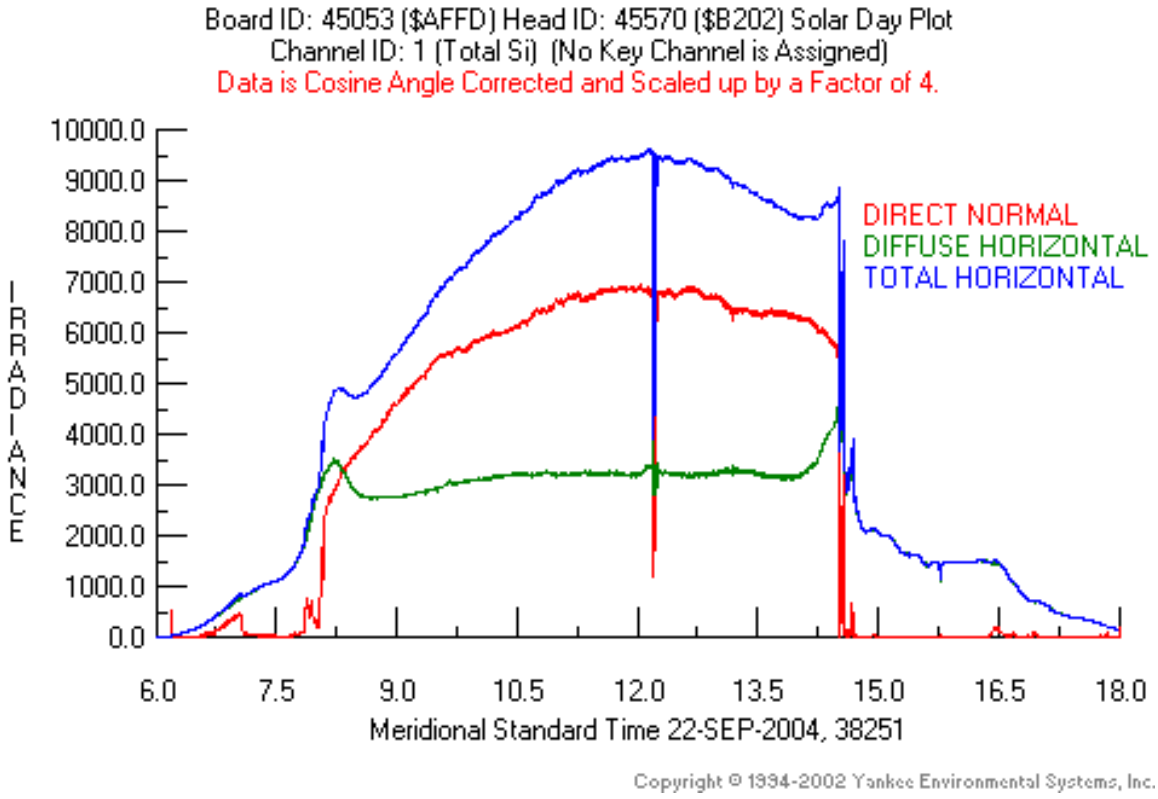

Figure J.4 An output from the shadowband radiometer.

The SMART trailer has its own meteorological sensors. The air pressure, temperature, and relative humidity were measured at a location near the surface. The results are shown in Figure J.5. They will be compared with the standard measurements from the meteorological station. Due to the change of the season, in about six weeks, the pressure shows the increasing trend, while the temperature decreases, which is consistent with the trend in the down-welling broadband infrared irradiance, as seen in Figure J.6.

The ground surface will become much hotter than the air under the sun shine. Figure J.7 is an example that on September 3, 2004, the surface temperature rose to over 60 degree Celsius while the air temperature in the shade at 30 cm above the ground reached 40 degree Celsius. When a dust storm arrived in the afternoon, the sun was blocked by the dust, and the surface temperature dropped to agree with the air temperature later of the day. The dust storm was captured by SMART's sky imager, which took dozens of snapshots of the sky every minute. Figure J.8 contains a few selected sky images.

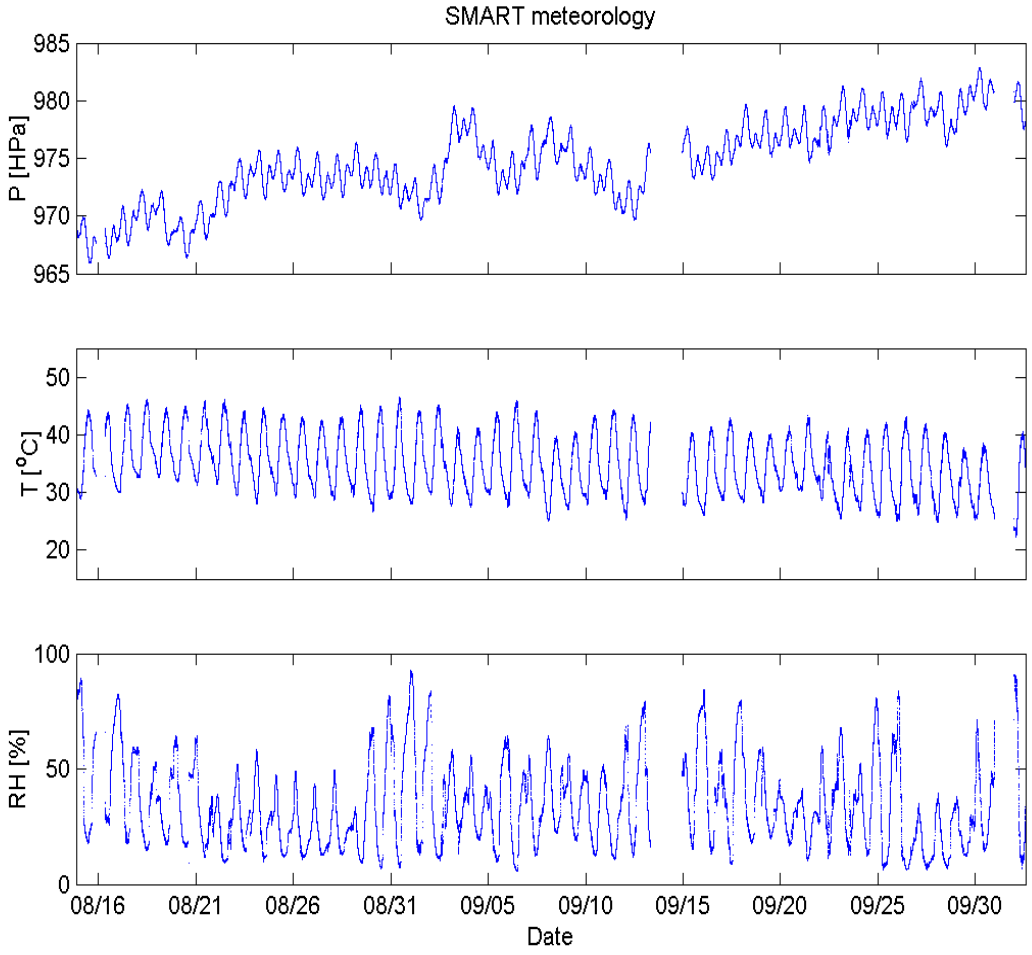

Figure J.5 Air pressure, temperature, and relative humidity measured near the ground surface

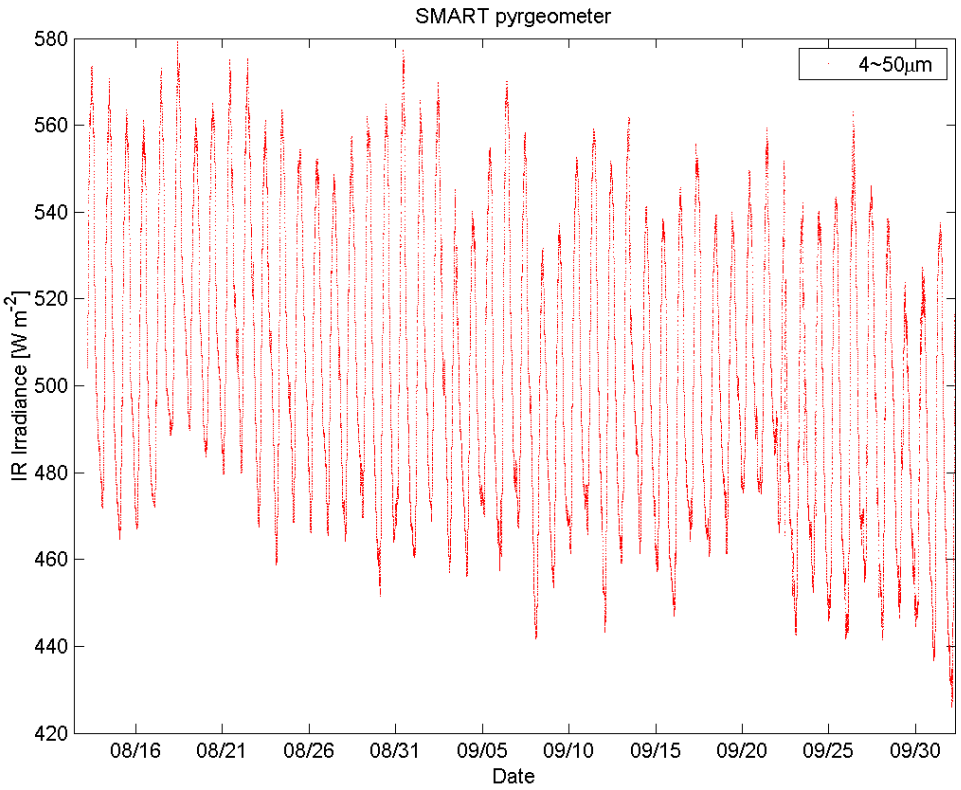

Figure J.6 Down-welling infrared irradiance.

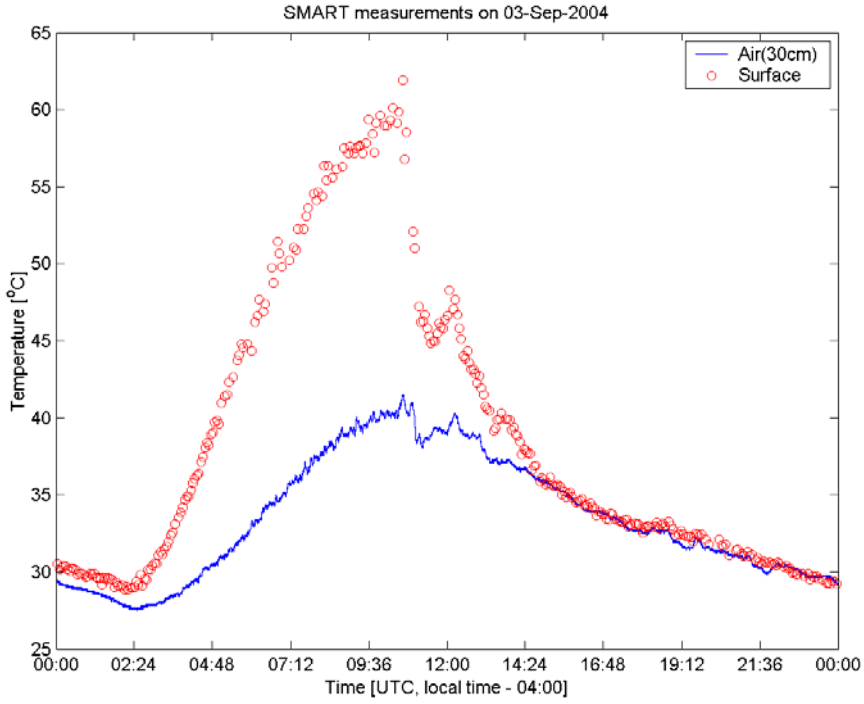

Figure J.7 Air and ground surface temperature. The drastic drop of the ground surface temperature is caused by the dust storm that blocked the sun.

Figure J.8 Selected sky images for September 3, 2004. At about 10:00 UTC, the dust front was looming at the horizon in the east. Half hours later part of the sky was blocked. The sky turns brownish during the dust storm.

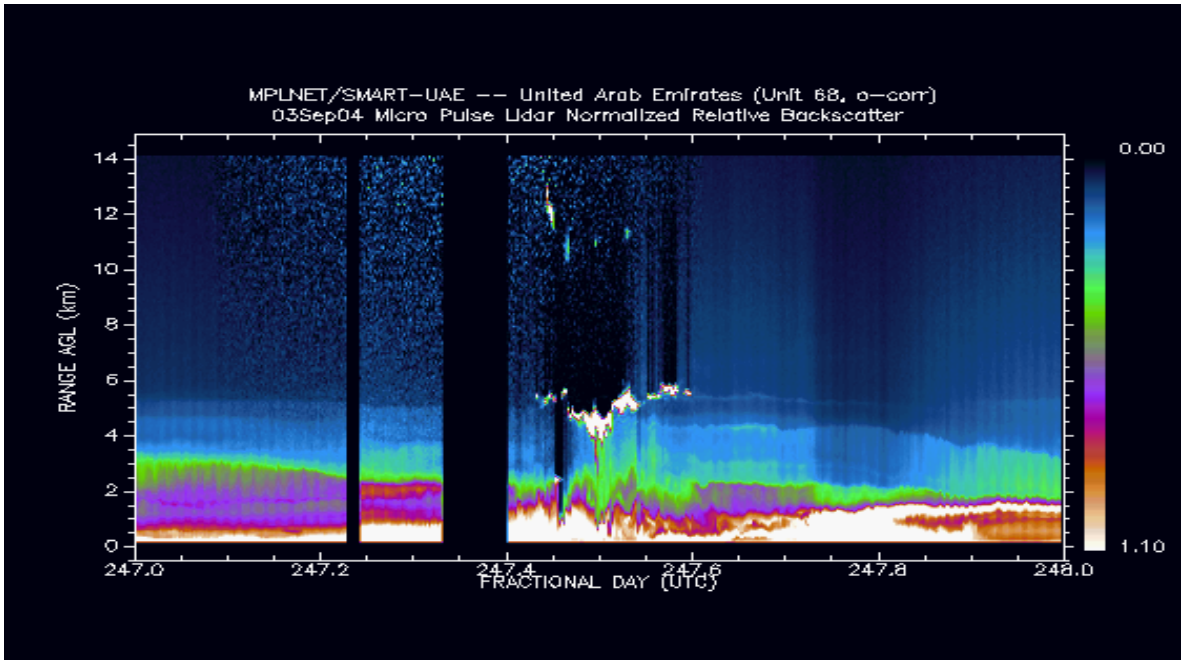

Figure J.9 Lidar image. The instrument was turned off around the solar noon to protect the detector from the sun light.
http://mplnet.gsfc.nasa.gov/Sites/Uae2/uae204.html

Although the sun was effectively blocked, the dust event on September 3 was not intense enough to block the lidar signal. Figure J.9 is from the micropulse lidar. When the dust arrived, it came with the cloud between 4 and 6 km above the ground, plus high cloud at 10 to 12 km above the ground. The lidar image also reveals a distinct boundary around 5 km above the ground. It shifted up and down daily and it was persistent.

For the September 3 dust case, the relative humidity dropped when the front arrived, indicating dryer air near the surface; while the total column water vapor in the atmosphere measured by SMART's microwave radiometer increased (Figure J.10). The SMART's AERI infrared interferometer is used to study dusty cases. Figure J.11 is an example for the September 22's case.

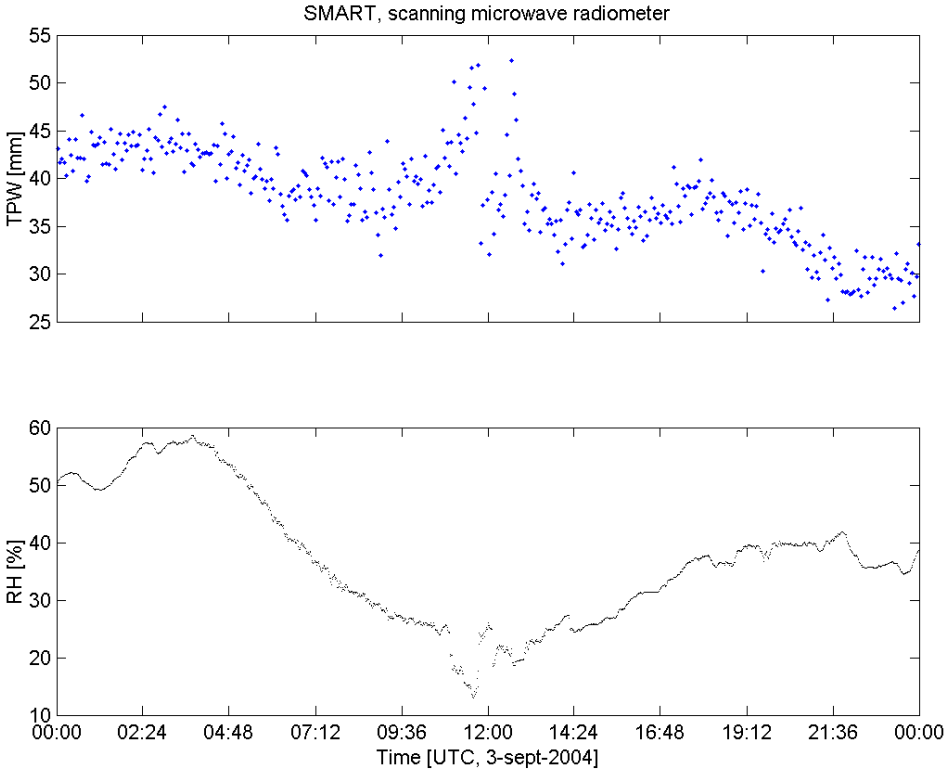

Figure J.10 Total perceptible water retrieved from a scanning microwave radiometer (SMiR). A particular case on September 3 shows while it became dryer on the surface, the column water vapor increased.

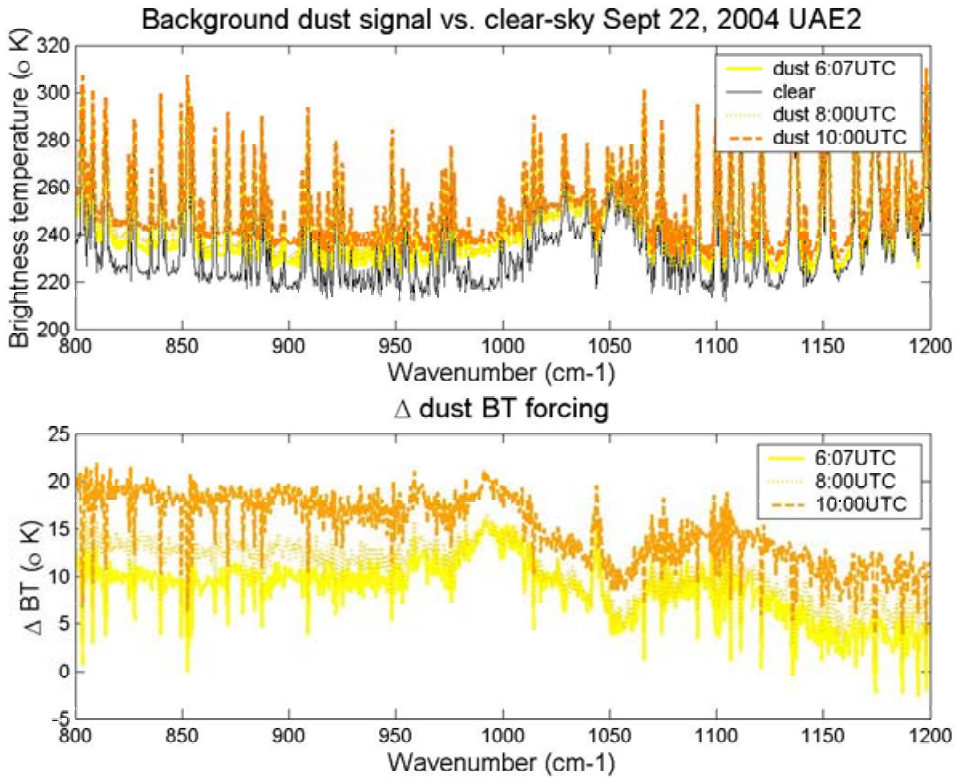

Figure J.11 Mean background dust signal – 22 September 2004, from AERI infrared interferometer.

A couple of new types of Cimel sunphotometer were mounted at the SMART site. The data can be found at the AeroNet's web site: http://aeronet.gsfc.nasa.gov/cgi-bin/uae_display?site=SMART&nachal=2&level=1&place_code=10

Another Cimel like instrument for infrared measurement was also located at the SMART site for the first half of the UAE^2 campaign. The instrument was moved to MAACRO site later to collocate with the available balloon borne sounding system there.

A special instrument that goes with SMART is an ASD spectrometer. It captured the entire solar spectrum during UAE^2. It had also been used to study the surface reflectance of the desert. An example of the results can be found in Figure J.12.

In summary, SMART survived in the harsh hot desert during the UAE^2 mission. A unique data set has been produced. Some of the results will be hard to obtain without a facility like SMART, plus all the supports and collaborations in UAE.

CLIMATE

Climate and Radiation Branch

NASA | Goddard | Lab for Atmospheres

Home
Images
News
Calendar
Personnel
Projects
Publications
Research
Reference
Search

Light through a Camel's Eyes

Image of the Week - November 28, 2004

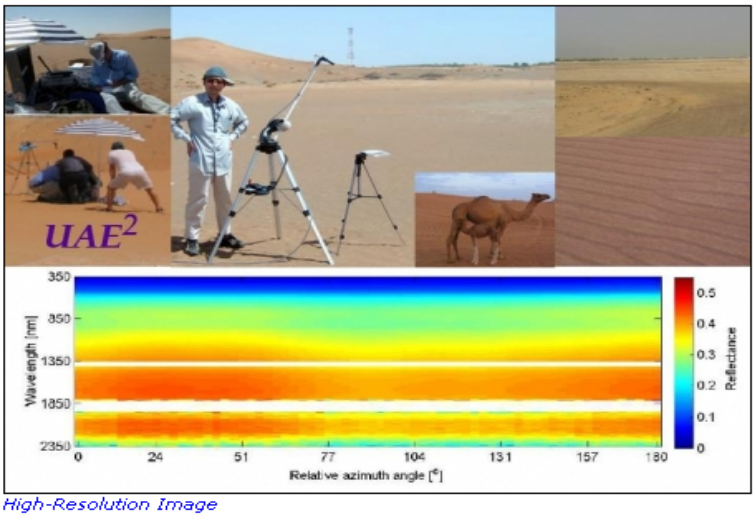

High-Resolution Image

... Encompassed by sands and dunes in a sea of deserts, it is all but irremediable for ordinary humans to maintain their sense of direction. Thus, as it is said in scriptures, the Queen of Sheba came with a caravan of camels when she sought the Wisdom of Solomon...

The differential warming/cooling effects exerted by atmospheric aerosols constitute one of the most uncertain factors in climate change related research. This is especially true over the regions of bright-reflecting surface, such as desert. What is seen in a camel's eyes through reflected sunlight by hazy desert? To assist satellite retrievals of aerosol properties over desert regions, we deployed our "camel robot" – a spectroradiometer mounted on a tripod (cf. pictures in center-panel) – during the United Arab Emirates *Unified Aerosol Experiment* to characterize the surface spectral-directional reflectance. Working under daytime dead heat of ~ 35–45°C and a wide range of relative humidity (~10% – 80%), a team of NASA/University researchers (cf. pictures in left-panel) and local authority surveyed a variety of desert sites over the Arabian Gulf. The color of the surface ranged from dull white near the coast (the remains of oceanic wash-up) to pinkish red inland (cf. pictures in right-panel), and the brightness of the surface changed depending on both the direction of sunlight illuminating and the direction of sensor viewing.

One of the key ingredients for achieving accurate aerosol retrievals from satellite observations is comprehensive understanding of surface spectral BRF's (Bidirectional Reflectance Factors), defined as a ratio of radiance measurements reflected from a targeted surface and from a spectral-angular featureless referencing plate (cf. instrument setup in center-panel). Shown in the figure is the spectral (350–2500 nm) characteristics of BRF's acquired at one of the inland sites around 13:20 local time on October 1, 2004 (Al Ain, UAE). The sun was located at 215.2° azimuth from the North and 32.9° from zenith, while the sensor scanned from 0° to 360° azimuth relative to the sun (only half of the angles shown due to near symmetry of the data) with a 45° zenith angle. Notice that the spectral BRF's varied widely from less than 5% around 350 nm to over 40% at longer wavelengths. Due to strong absorption of atmospheric water vapor around 1360–1390 nm and 1800–1950 nm, diminished sunlight reaches the surface for making meaningful measurements (replaced by white color). Also, under this particular sky condition the BRF's are weakly dependent on viewing azimuth relative to the sun – mildly peaked at the forward ("blind spot") and backward ("hot spot") direction with minimal around 90° azimuth. This figure depicts only a small slice of the spectral BRF's. To fully characterize a desert surface in the field is an important but challenging task. Stay tuned!!

Submitted by Q. Jack Ji, N. Christina Hsu, Richard A. Hansell, W. Jay Cho, Abdulla Al Mandoos and Si-Chee Tsay.

View the Image of the Week Archives

Updated:
March 14, 2005
in Glossary

Site Maintained By: *Dr. William Ridgway*
Responsible NASA Official: *Dr. Robert Cahalan*

Privacy, Security, Notices
NASA | Goddard | Atmospheres

Figure J.12. Measurement from the ASD spectrometer. Web link: http://climate.gsfc.nasa.gov/viewImage.php?id=93

K.0 Single scattering properties and radiative forcing during the UAE^2 experiment

Principal Investigator: Piotr J. Flatau, Scripps Institution of Oceanography, UCSD.

Co-Investigators: Krzysztof Markowicz, Joanna Remiszewska, Marcin Witek, Hanna Pawłowska, Warsaw University, Atmospheric Science Group

K.1 Nature of problem

The effects of sea salt, mineral dust, black carbon, and sulfates in complex environmental conditions are one of the largest sources of uncertainty in quantifying regional climate changes [Intergovernmental Panel on Climate Change, 2001]. Much recent work has been devoted to reducing these uncertainties using global circulation models, transport models, observational networks, satellite observations, and by mounting major observational campaigns (SCAR-B [Kaufman et al., 1998], TARFOX [Hobbs, 1999], ACE1 [Bates et al., 1998], ACE2 [Raes et al., 2000], INDOEX [Ramanathan et al., 2001], MINOS [Lelieveld et al., 2002]). Progress has been reported thanks to these complementary activities (Markowicz et al. 2002). Determining the radiative effects of very small particles in the atmosphere requires observations of aerosol chemistry, knowledge of the aerosol optical properties, and precise radiometric measurements at the surface and top of atmosphere. This study determines the radiative effects of aerosols during the United Arab Emirates field campaign, which took place in the summer of 2004 and was designed to study the regional effects of mineral dust and air pollution. Our instruments were located about 80km from Abu Dhabi close to the Arabian Gulf.

K.2 Instruments

During the UAE^2 field project we performed radiation measurements using total broadband (280–2800 nm) radiative fluxes obtained using Kipp and Zonen pyranometers. According to the technical specification provided by the manufacturer, this instrument has an absolute accuracy of ±9 W m^2 and the maximum flux error due to a simplified cosine response is ±10 W m^2. Several handheld Microtops II (Sun photometer and Ozonometer) [Morys et al., 2001] with spectral filters for visible and near-infrared (NIR) wavelengths were used to retrieve aerosol optical thickness (AOT), columnar water vapor, and columnar ozone. The AOT was measured by AERONET instruments (CIMEL) as well as at 380, 440, 500, 675, 870 nm by the Sun photometer and at 1020 nm by the Ozonometer. The total water column was obtained from the Sun radiance measured at 936 and 1020 nm and this information was complemented by radiosondes. Vertical profiles of the aerosol extinction coefficient at 523 nm were measured by a micropulse lidar (MPL) [see this report] and Vaisala Ceilometrers. The aerosol absorption coefficient at the surface was obtained from the Aethalometer produced by Magee Scientific Radiance Research. Measured values were corrected for a scattering artifact, the deposit spot size, the

Aethalometer flow rate, and the manufacturer's calibration. Values are reported at seven wavelengths.

Measurements of aerosol scattering and hemispheric backscattering coefficients were made with an integrating nephelometer (Model 3563, TSI Inc.) at wavelengths of 450, 550, and 700 nm at environmental relative humidity (RH) and dry RH and total suspended particles data were used. The RH was measured inside the nephelometer sensing volume. Values measured directly by the nephelometer were corrected for the angular nonidealities, including truncation errors and nonlambertian response of the nephelometer as per Anderson and Ogren [1998].

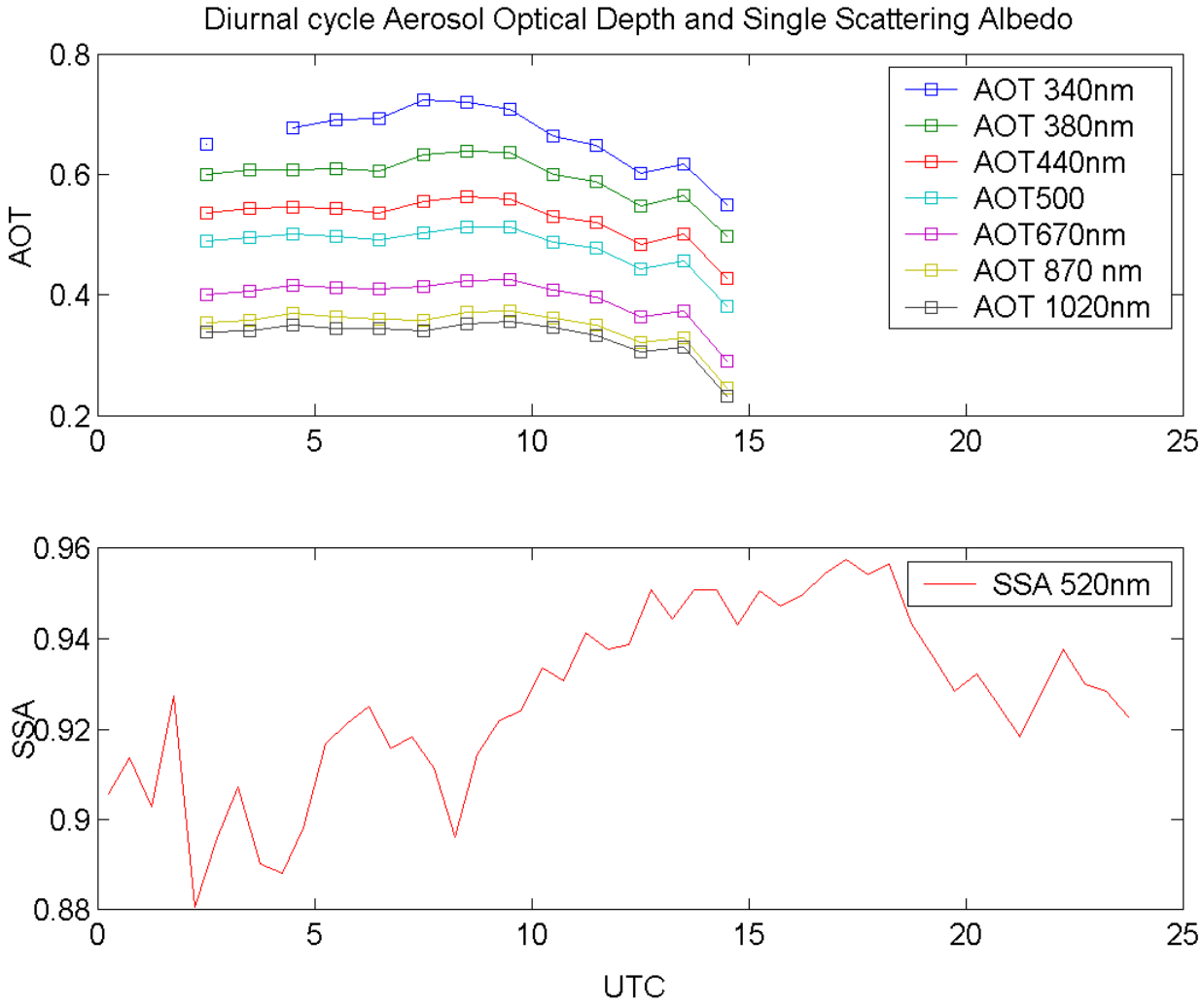

Figure K.1 Diurnal cycle of aerosol optical depths and single scattering albedo.

K.3 Preliminary results

Observations indicate that the optical depth modulation during the sea-breeze onset is fairly small (Figure K.1). This results in small average diurnal changes of aerosol optical depth (c.f. Figure K.2). We observed 7-8% change of the downwelling irradiance at the surface in agreement with observed semi-conservative optical properties of aerosols.

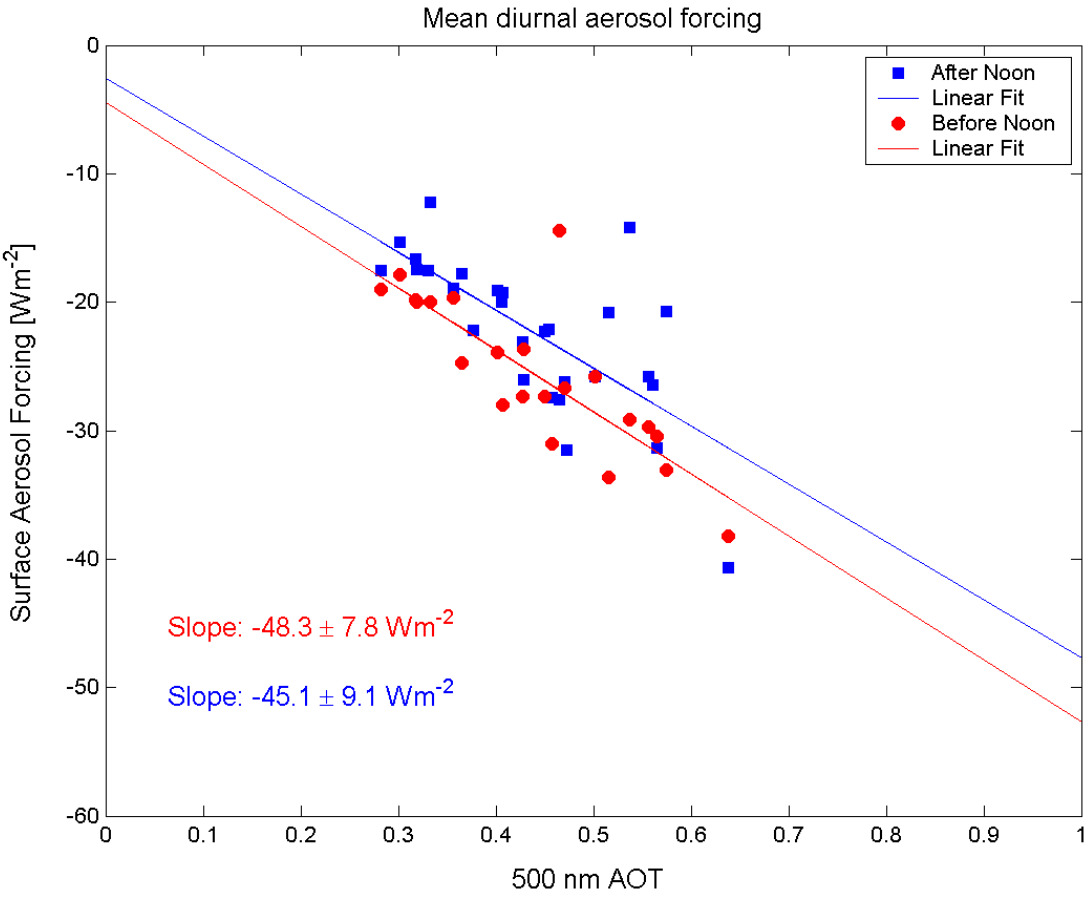

Figure K.2. Mean diurnal aerosol forcing.

References

Anderson, T. L., and J. A. Ogren, Determining aerosol radiative properties using the TSI 3563 integrating nephelometer, Aerosol Sci Tech, 29, 57–69, 1998.

Bates, T. S., B. J. Huebert, J. L. Gras, F. B. Griffiths, and P. A. Durkee, International Global Atmospheric Chemistry (IGAC) project's first aerosol characterization experiment (ACE 1): Overview, J. Geophys. Res., 103, 16,297– 16,318, 1998.

Hobbs, P. V., An overview of the University of Washington airborne measurements and results from the Tropospheric Aerosol Radiative Forcing Observational Experiment (TARFOX), J. Geophys. Res., 104, 2233–2238, 1999.

Holben, B. N., et al., An emerging ground-based aerosol climatology: Aerosol optical depth from AERONET, J. Geophys. Res., 106, 12,067– 12,097, 2001.

Intergovernmental Panel on Climate Change, Climate Change 2001: The Scientific Basis, Contribution of Working Group I to the Third Assessment Report of the Intergovernmental Panel on Climate Change, edited by J. T. Houghton et al., 881 pp., Cambridge Univ. Press, New York, 2001.

Kaufman, Y. J., et al., Smoke, Clouds, and Radiation-Brazil (SCAR-B) experiment, J. Geophys. Res., 103, 31,783–31,808, 1998.

Lelieveld, J., et al., Global air pollution crossroads over the Mediterranean, Science, 298, 794– 799, 2002.

Markowicz, K. M., P. J. Flatau, M. V. Ramana, P. J. Crutzen, and V. Ramanathan, Absorbing Mediterranean aerosols lead to a large reduction in the solar radiation at the surface, Geophys. Res. Lett., 29(20), 1968, doi:10.1029/2002GL015767, 2002.

Morys, M., F. M. Mims, S. Hagerup, S. E. Anderson, A. Baker, J. Kia, and T. Walkup, Design, calibration, and performance of MICROTOPS II handheld ozone monitor and Sun photometer, J. Geophys. Res., 106, 14,573– 14,582, 2001.

Raes, F., T. Bates, F. McGovern, and M. Van Liedekerke, The 2nd Aerosol Characterization Experiment (ACE-2): General overview and main results, Tellus, Ser. B, 52, 111 –125, 2000.

Ramanathan, V., et al., Indian Ocean Experiment: An integrated analysis of the climate forcing and effects of the great Indo-Asian haze, J. Geophys. Res., 106, 28,371– 28,398, 2001.

L.0 Polarization instrument at the MAARCO site

Principal Investigator: Alexander Smirnov, GEST/NASA Goddard Space Flight Center, Greenbelt, MD.

Co-Investigators: B.N.Holben, M.Sorokin, I.Slutsker, T.F.Eck

L.0 Nature of problem

The UAE^2 experiment gave a unique opportunity not only to deploy well-known reliable instrumentation but also to test newly designed innovative equipment. Deployment of the two-filter wheel polarization instrument significantly enhanced our knowledge on the dust aerosol optical properties. Also, it enriched the capabilities of other science team members using this additional dataset in their research. Despite a preliminary character of the results presented below we would like to emphasize the uniqueness of the multi-spectral sun and polarized sky measurements in the tough desert environment.

L.0 Executive summary

Figure L.1 (a and b) presents temporal variations of aerosol optical depth at a wavelength 500 nm and Angstrom parameter during the Intensive Field Campaign of UAE^2 (August-September 2004). Certain days with predominantly dust aerosol, pollution or mixture of both clearly can be identified.

Spectral dependence of the degree of linear polarization is shown on Figure L.2. Atmospheric conditions can be characterized as turbid with the predominance of dust aerosol. As expected, maximum of linear polarization is located in the blue spectral range at a scattering angle of ~90º. Strong depolarization exists comparing to the ideal case of pure molecular atmosphere.

Angular and spectral dependence of the degree of linear polarization can be observed in Fig. 3 for a variety of cases when dust aerosol prevails (smaller Angstrom parameters). For the urban/industrial (pollution) aerosol degree of polarization is higher (Figure L.4) because particles of the pollution type aerosol are smaller than dust particles, which are not only bigger by size but also non-spherical. Angular dependence for various aerosol conditions is presented on Figure L.5. It shows a fairly complex pattern, however, two major features can be seen, i.e. for all optical conditions considered the maximum of the degree of polarization was at about scattering angle 90º and when aerosol load increases then polarization decreases.

It is very appealing to study the relationship between aerosol optical depth and degree of polarization. Figure L.6 shows very good correlation for the channel 500 nm. However we cannot uniquely characterize optical conditions having only optical depth measurements at hand even for known aerosol type. Angstrom parameter is very well correlated with the degree of polarization at 1020 nm (Figure L.7) but also in that case a significant scatter does not allow uniquely defining aerosol optical state.

Further analysis and new measurements will significantly improve our understanding of the processes involved in aerosol formation, evolution and transport.

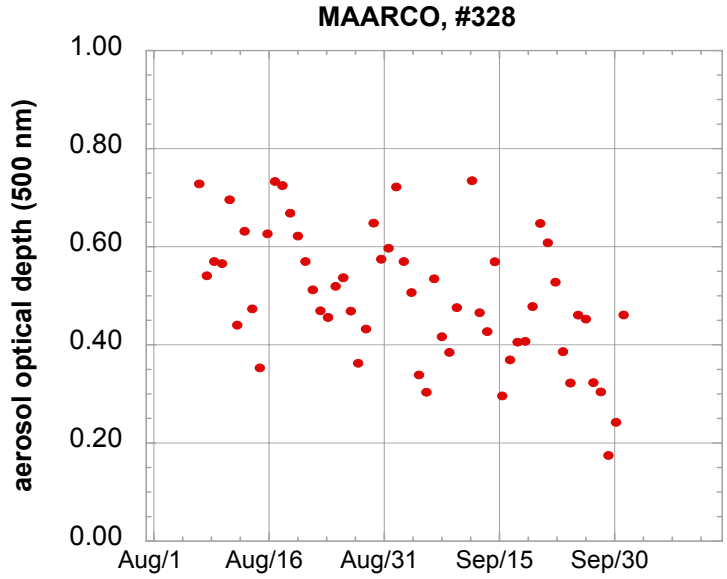

Figure L.1a

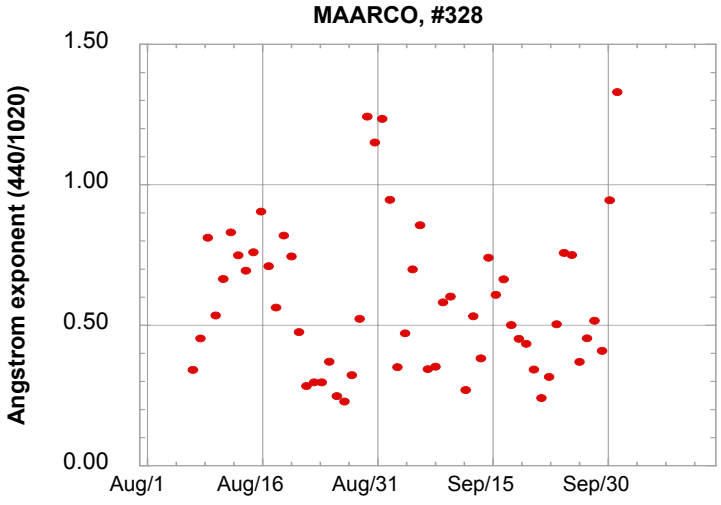

Figure L.1b

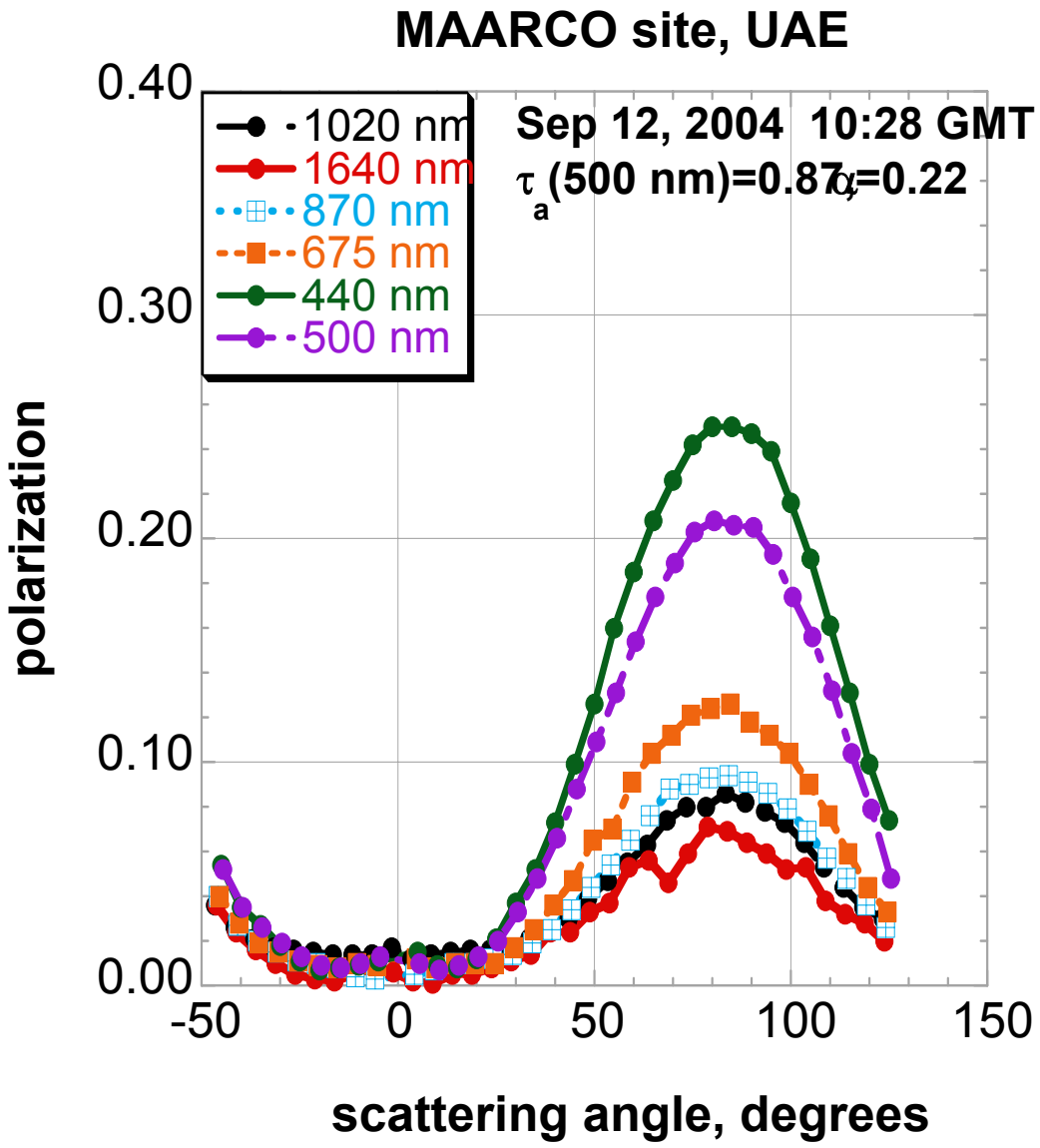

Figure L.2. Sky polarization as a function of scattering angle for the Sept. 12 , 2004 dust event at the MAARCO site.

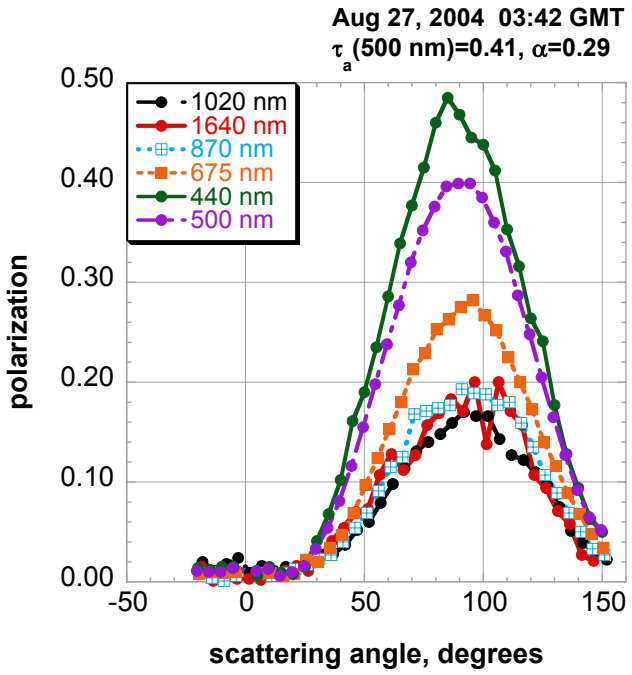

Figure L.3a

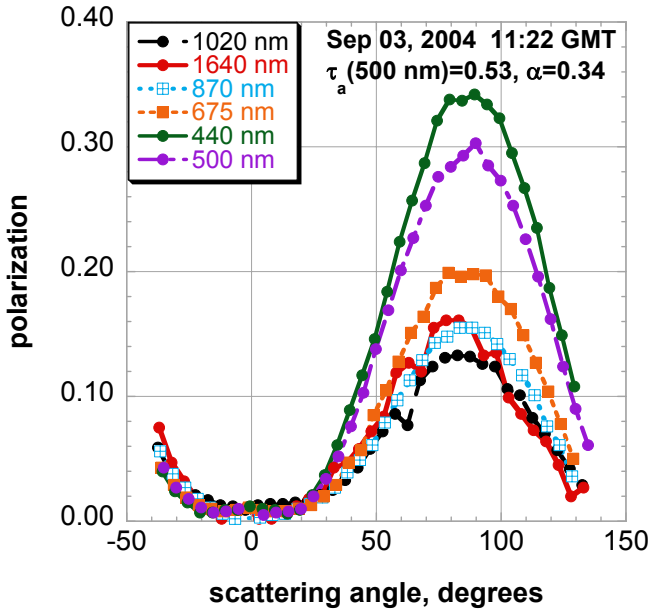

Figure L.3b

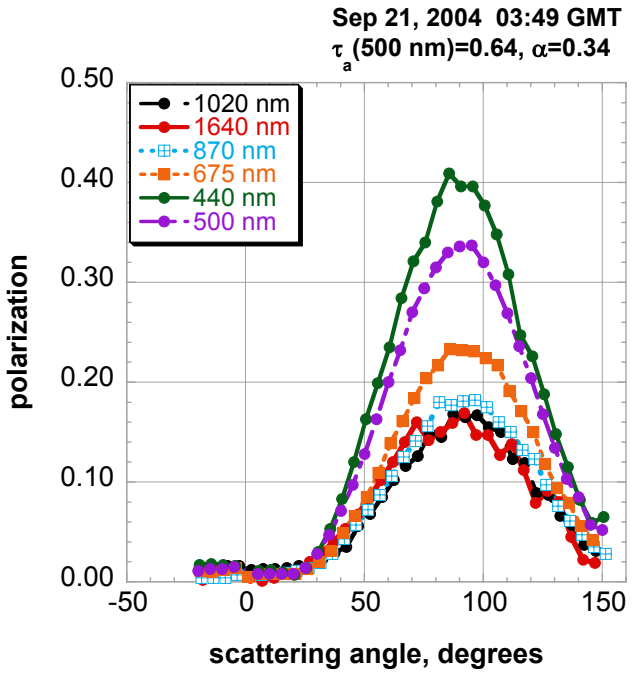

Figure L.3c

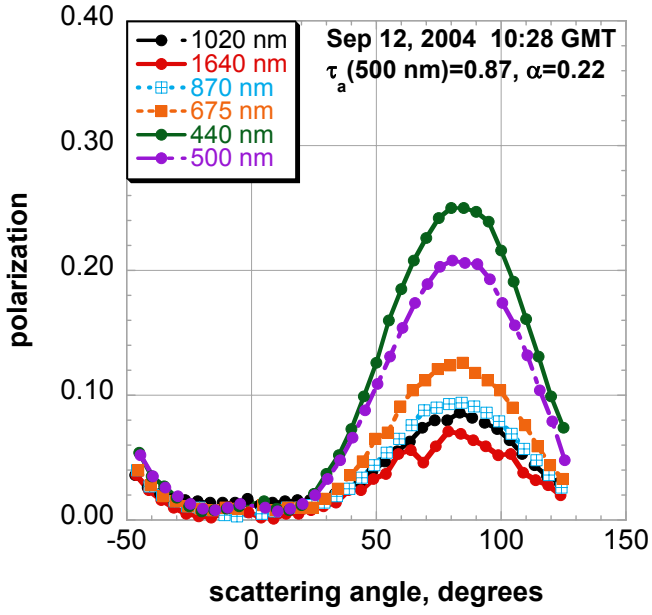

Figure L.3d

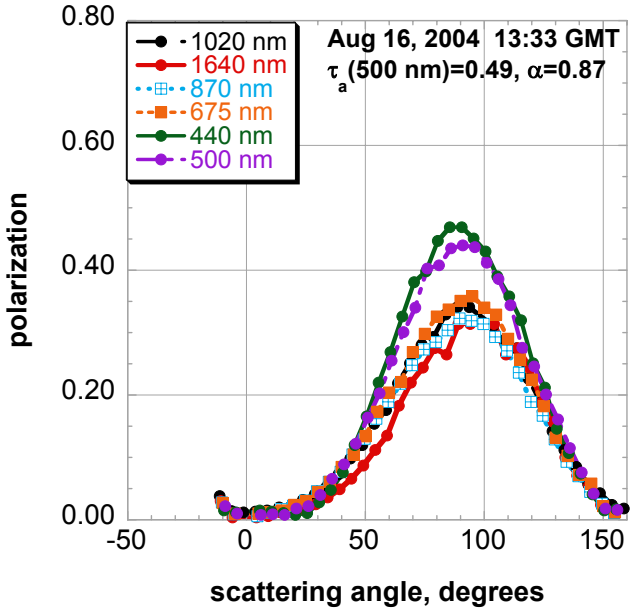

Figure L.4a

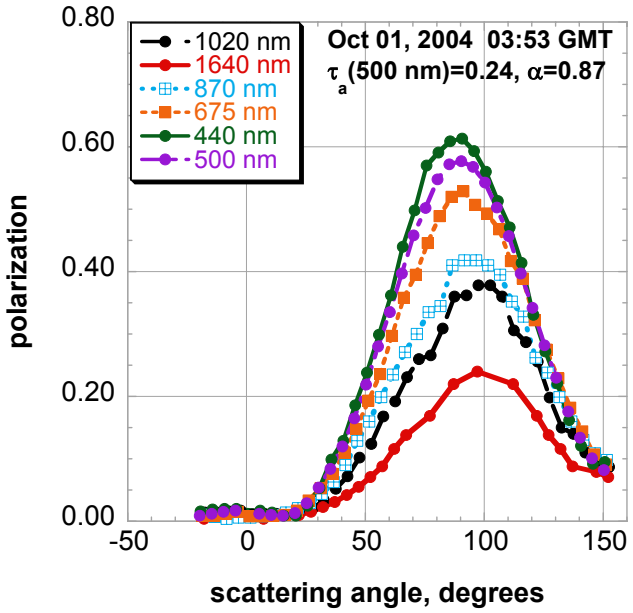

Figure L.4b

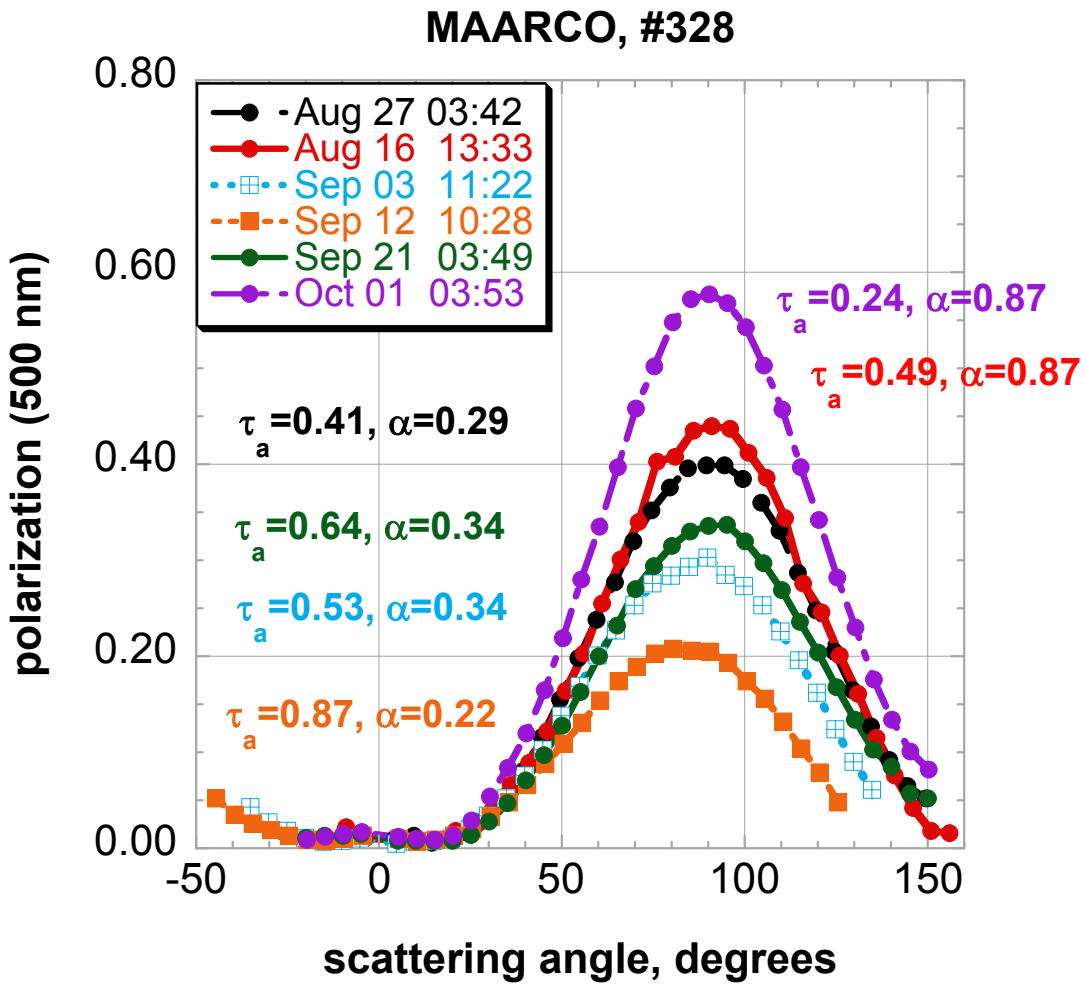
MAARCO, #328
Aug 27 03:42
Aug 16 13:33
Sep 03 11:22
Sep 12 10:28
Sep 21 03:49
Oct 01 03:53
τa =0.24, α=0.87
τa =0.49, α=0.87
τa =0.41, α=0.29
τa =0.64, α=0.34
τa =0.53, α=0.34
τa =0.87, α=0.22
polarization (500 nm)
0.80
0.60
0.40
0.20
0.00
-50
0
50
100
150
scattering angle, degrees

Figure L.5

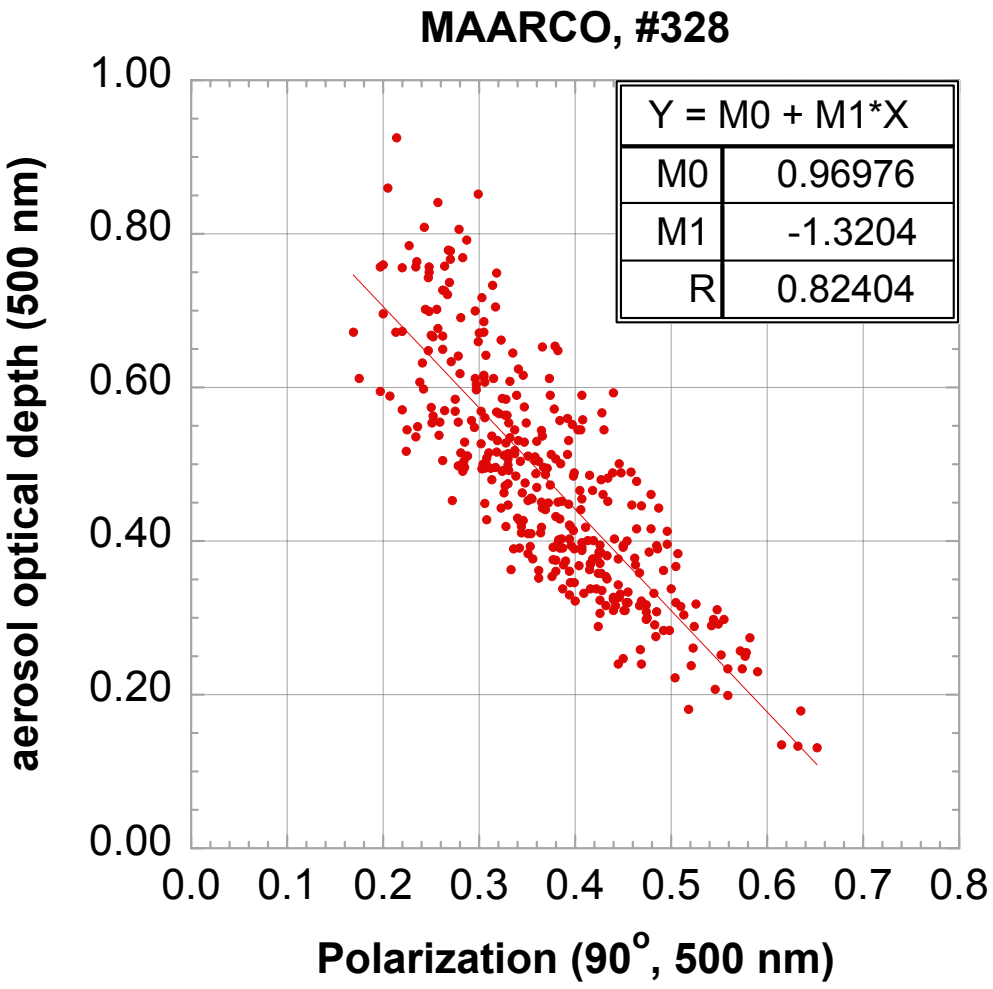

Figure L.6. Optical depth versus 90 degree polarization for all data at the MAARCO site.

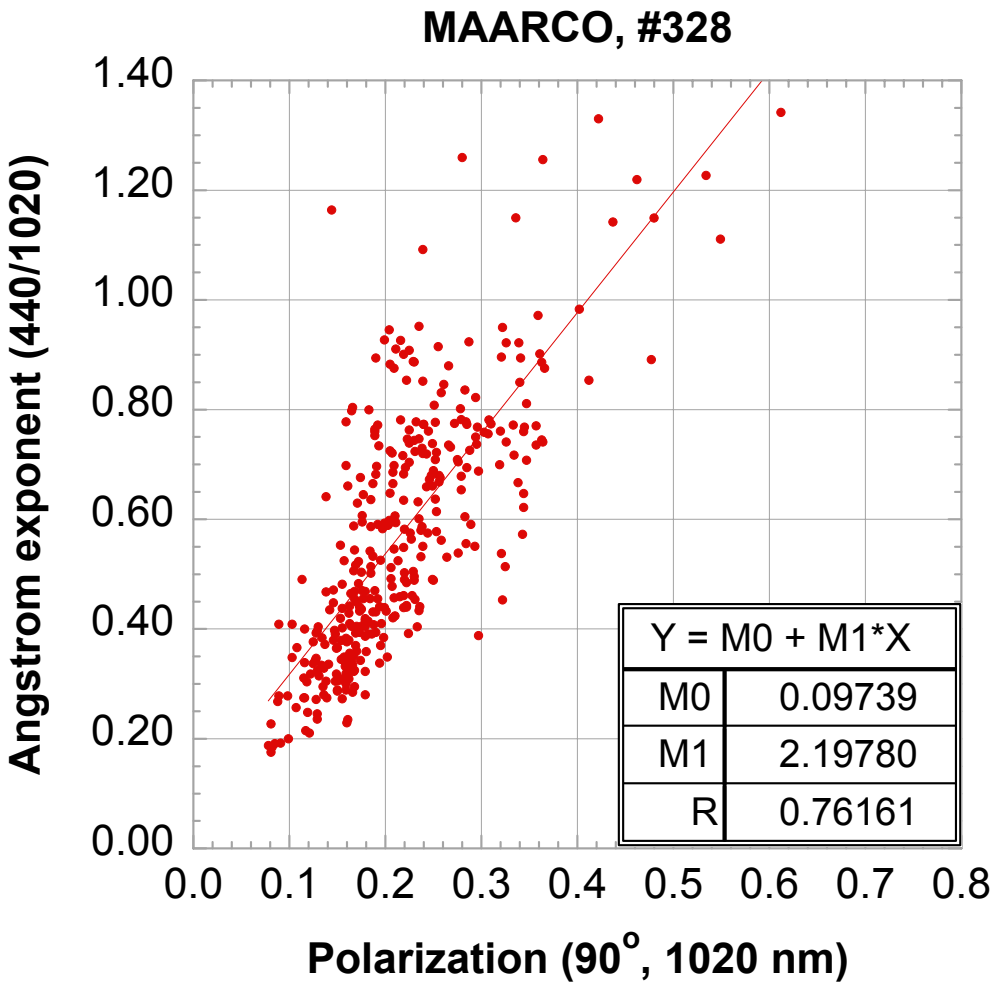

Figure L.7 Angstrom Exponent versus 90 degree polarization for all data at the MAARCO site.

M.O Radiomatery in the thermal infrared with *CLIMAT* in the UAE

Principal Investigators : Michel Legrand & Bahaiddin Damiri
Laboratoire d'Optique Atmosphérique, Université de Lille-1
59655 Villeneuve d'Ascq cedex, France, *legrand@loa.univ-lille1.fr*

M.1 Abstract

In this report we describe the 4-channel ground-based thermal infrared (TIR) radiometer CLIMAT. The various possible applications of the instrument are then reviewed, focusing especially on the remote sensing of mineral dust, the purpose of the instrument presence in the UAE. Some results of a previous campaign in the Sahel are presented to illustrate the information content on mineral dust included in the radiometric measurements. A spectral signature of desert dust is derived, which is shown to be strongly dependent on dust composition. The signature is in good agreement with simulations based on independent determinations of dust properties. A similar study is planed using the measurements of CLIMAT in UAE in August and September 2004, in order to assess the radiative properties and the mineral composition of the Arabian dust.

M.2 The radiometer *CLIMAT*

The radiometer CLIMAT (Conveyable Low-noise Infrared radiometer for Measurements of Atmosphere and ground surface Targets) is designed to perform measurements in the thermal infrared (TIR). It is dedicated to ground-based observations, but a similar airborne model has been developed for operation from an aircraft or from any vehicle. These instruments were developed in the 90's at the Laboratoire d'Optique Atmosphérique (LOA), in collaboration with other research laboratories and institutes and with the manufacturer CIMEL.

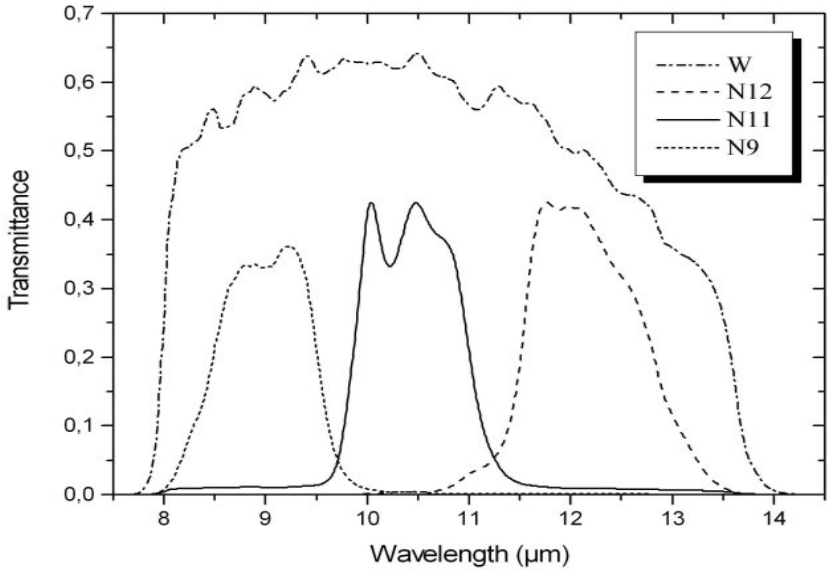

Figure M.1 Spectral transmittance of the channels of the radiometer CLIMAT (from Legrand and Pancrati, in press).

Figure M.2 Road surface temperature monitoring with CLIMAT (North of France, 2000).

The instrument uses a thermopile as radiation sensor. The thermopile output voltage and cold junction temperature are measured and used to derive the radiance or brightness temperature of viewed targets. The instrument contains a wheel equipped with three narrowband interference filters labeled N9 (8.2-9.2 μm), N11 (10.0-11.0 μm) and N12 (11.5-12.5 μm). A broadband channel labeled W (8-14 μm) can be selected using a position of the wheel without filter. The spectral transmittance functions are shown in Figure M.1 for the four channels of the instrument. The radiometric calibration of the instrument is performed using the radiance of a blackbody at temperatures accurately measured with a platinum probe. The instrument showed a satisfactory stability of its calibration coefficients with a maximum change of 1.4% over 7 months. Typically, the radiometric noise (NEDT) is in the order of 50 mK. A supplement of description and performances of the radiometer CLIMAT can be found in Legrand et al. (2000).

The instrument is made up with an optical head connected to an electronic unit. In the field the optical head is aimed by a robot towards its target. A field blackbody allows the calibration of the instrument to be controlled and corrected if necessary. The measurement protocol is driven from the electronic unit. The data are collected into a local PC (they can also be transmitted via a telephone line through a modem or via a satellite). Figure M.2 shows the instrument in operation for the monitoring of surface temperature of a road tarmac (for study of icing detection). One can see the optical head mounted at the top of a mast with its blackbody. The electronic unit is in the case fastened to the mast close to the ground. More informations relevant to in situ use of the instrument for field measurements can be found in Brogniez et al. (2003).

M.3 Remote sensing of mineral dust in the thermal infrared

The applications for which the radiometer CLIMAT was initialy developed are the calibration, validation and analysis of data supplied by the Earth observing satellites. However, the instrument proves also very useful by means of its own measurements, independently of the presence of a satellite. In addition to the previously mentioned ground surface temperature measurements, the instrument can be used to measure sea surface temperature (Brogniez et al.). The surface measurements can be used also to emittance determination. Several studies with economic interest are possible such as rock composition analysis and monitoring of vegetation growth and health. For atmospheric applications, the measurements of CLIMAT can be dedicated to the remote sensing of clouds (Brogniez et al., 2004) and of aerosols (Legrand and Pancrati, 2005).

When looking at the sky, the instrument is able to detect the desert dust by means of the radiation emitted in the TIR. The size distribution of dust includes a significant fraction of large particles (>1 μm) which can be "seen" by the instrument, and its mineral components are characterized by peaks of absorption at wavelengths around 10 μm. Figure M.3 describes the spectral location of the narrow channels N9, N11 and N12 with respect to the peaks of the extinction coefficients of quartz and clay species (illite and kaolinite), the major mineral components of Saharan dust. We can see that the measurement sensitivity for dust made up as a mixture of the previous species, is maximum for N9 and minimum for N12. Figure M.4 depicts the spectral signature obtained with the radiometer CLIMAT for desert dust at Banizoumbou nearby Niamey, Niger, in agreement with the predicted results from Figure M.3. Figure M.4 compares also the measured spectral signatures with simulations calculated using the measured size distribution from AERONET and the measured mineral composition of dust. Such results let predict the possibility to retrieve dust mineral composition from its remote sensing with CLIMAT.

M.4 *CLIMAT* measurements during the UAE^2 campaign

During the UAE2 campaign, the radiometer CLIMAT has been used at the SMART site inland in August, then at the MAARCO site on the coast, North of Abu Dhabi City, in September 2004. Figure M.5 shows the brightness temperature of the UAE sky derived from CLIMAT at the SMART station, throughout the period 24 to 31 of August. The oscillations depict the diurnal cycle (the air in the lower atmosphere is warmer during daylight that during night, and perhaps also more dusty). The scattered high values reveal cloud occurrence, in agreement with the level-1 AOT time series (from AERONET, SMART data, PI B. Holben). The smooth variations are those of cloudless sky. The analysis of the respective levels of each channels will supply information on desert dust particle size and mineral composition. It is to be carried out in the coming months.

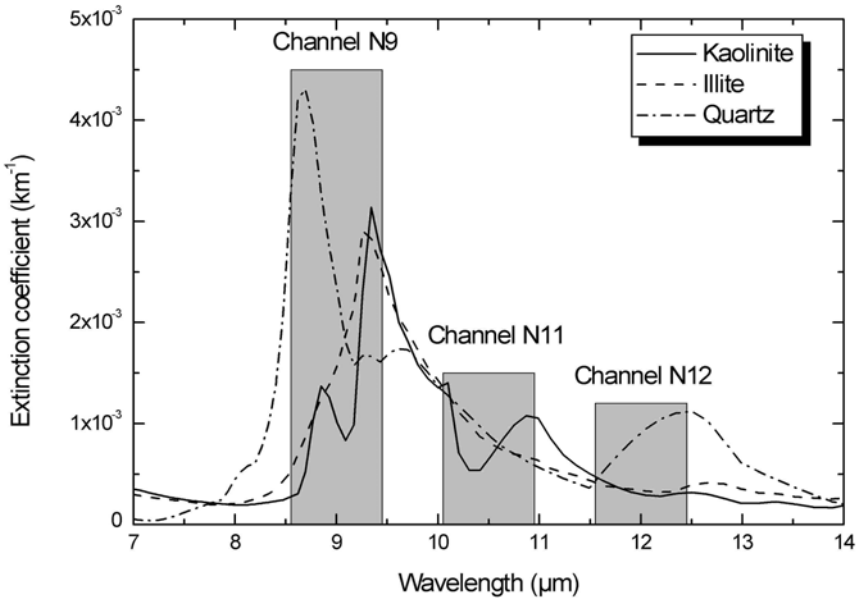

Figure M.3 Spectral variations of the extinction coefficient of quartz, illite and kaolinite, along with the location of the narrow channels (from Legrand and Pancrati, in press).

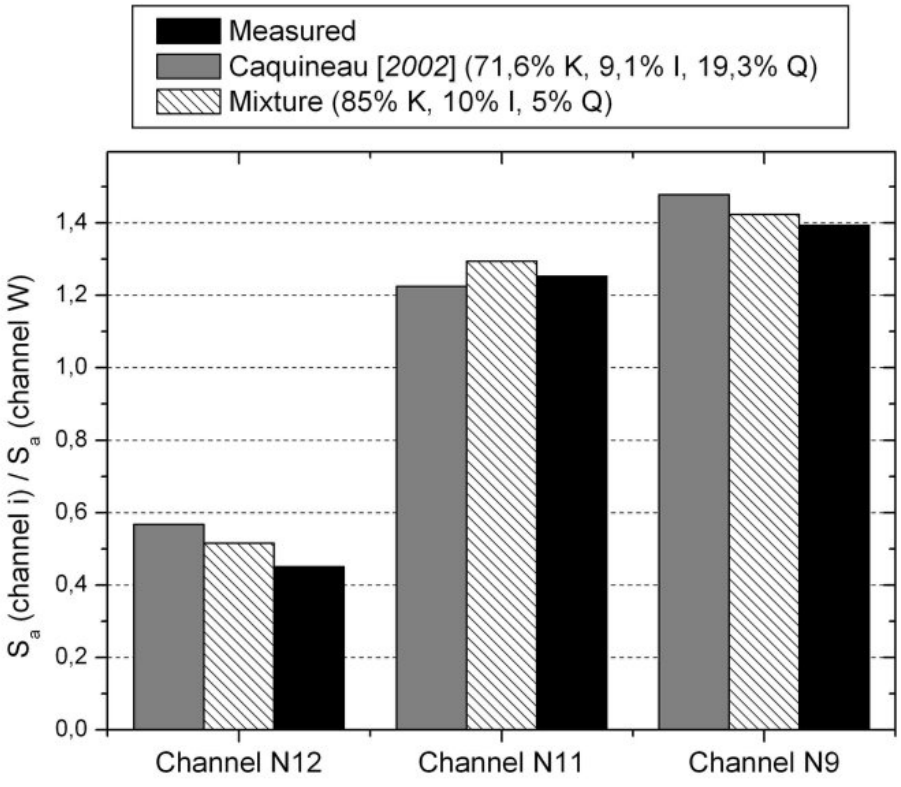

Figure M.4 Simulated spectral signatures of Sahelian mineral dust compared to the CLIMAT-measured signature (from Legrand and Pancrati, in press).

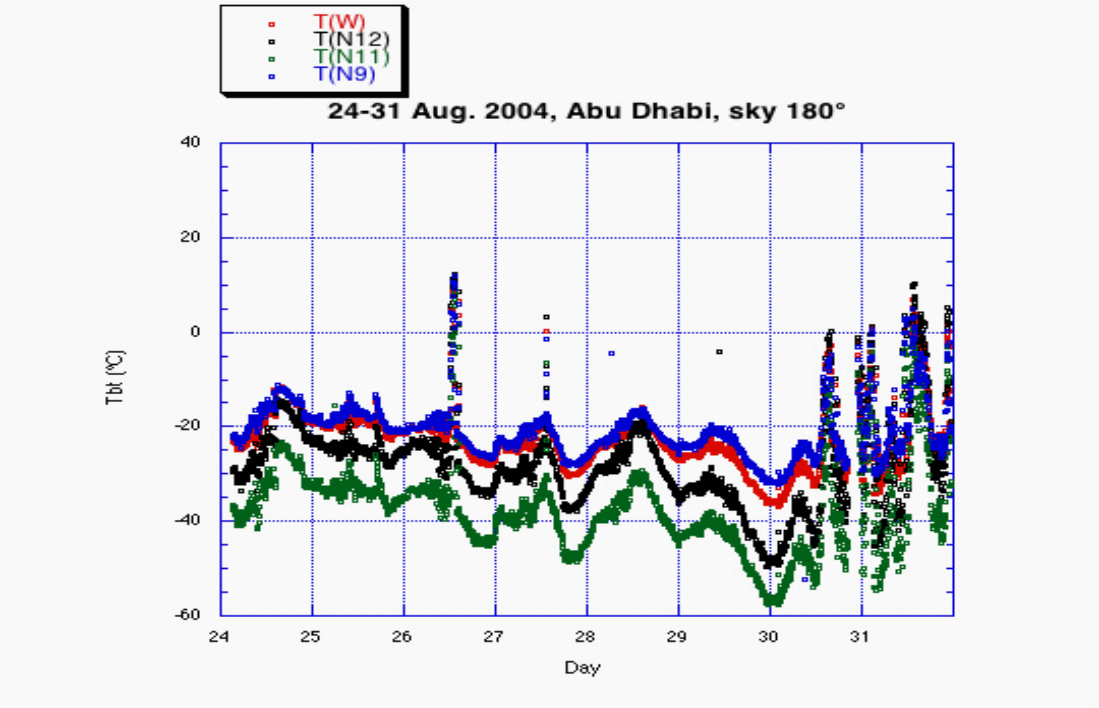

Figure M.5 Brightness temperatures at zenith in the four CLIMAT channels (UAE, SMART station, August 2004).

***Acknowledgements*.**

This study was made possible thanks to the invitation to participate of Brent Holben. We thank Si-Chee Tsay and Jeff Reid for their hosting of our instruments at their SMART and MAARCO stations. We are also indebted with all those who participated to the transport, deployment, dismounting and operation control of the instruments, who did measurements files copies and mails and kept us informed of the experiment progress, including Jack Ji, Rick Hansell, Piotr Flatau, and Elizabeth Reid. We thank the DWRS for their invaluable logistical help, with the receipt, storing and return of our instruments.

References

Legrand, M., C. Pietras, G. Brogniez, M. Haeffelin, N.K. Abuhassan, M. Sicard, 2000: A high-accuracy multiwavelength radiometer for in situ measurements in the thermal infrared. Part I: characterization of the instrument. *J. Atmos. Oceanic Technol.,* **17,** 1203-1214.

Brogniez, G., C. Pietras, M. Legrand, P. Dubuisson, M. Haeffelin, 2003: A high-accuracy multiwavelength radiometer for in situ measurements in the thermal infrared. Part II: behavior in field experiments. *J. Atmos. Oceanic Technol.,* **20,** 1023-1033.

Brogniez, G., F. Parol, L. Bécu, J. Pelon, O. Jourdan, J.-F. Gayet, F. Auriol, C. Verwaerde, J.-Y. Balois, Bahaiddin Damiri, 2004: Determination of cirrus radiative parameters from combination between active and passive remote sensing measurements during FRENCH/DIRAC 2001. *Atmos. Res.,* **72,** 425-452.

Legrand, M., O. Pancrati, 2005: Thermal infrared radiometry, microphysical properties and geochemical nature of mineral dust. in *IRS'2004: Current Problems in Atmospheric Radiation*, W.L. Smith and Yu. M. Timofeyev (Eds), A. Deepak Publishing, Hampton, Virginia, *in press*.

N.0 Fine Mode Aerosol Pollution over the United Arab Emirates

Principal Investigator: Kristy E. Ross, Climatology Research Group, University of the Witwatersrand, Johannesburg, South Africa

Co-Investigators Stuart J. Piketh, Jeffrey S. Reid and Elizabeth A. Reid

N.1 Abstract

The aerosol loading of the atmosphere over the United Arab Emirates is composed not only of dust, but also of pollution that is largely derived from oil-related activities. Fine mode aerosols with diameter less than 2.5 μm are most efficient at scattering incoming solar radiation, and have implications for climate change. The smaller aerosols may also pose a health hazard if present in high concentrations, and are responsible for visibility reduction. The composition of the fine mode aerosol has been obtained from filters that were collected over a 24-hour period at the MAARCO site on the coast of the United Arab Emirates between Abu Dhabi and Dubai from 9 August to 30 September 2004 during the United Arab Emirates Unified Aerosol Experiment (UAE^2). Ammonium sulphate is the most prevalent constituent of the fine mode aerosol in the region (57% of the mass), followed by organic matter (13%), alumino-silicates (11%), calcium carbonate (9%) and black carbon (4%). Source apportionment indicates that most of the fine aerosol mass is derived from fossil fuel combustion (72%), while mineral dust (20%) and local vehicle emissions (9%) also contribute to the fine aerosol loading. The organic carbon to total carbon ratio of the aerosol is 0.65, which is typical of fossil fuel combustion. A case study from 12 September 2004 is used to illustrate how the Passive Cavity Aerosol Spectrometer Probe (PCASP) on the aircraft gives information about the size distribution of the fine mode aerosol in the different layers in the atmosphere. In this case at least three distinct aerosol layers were present, separated by temperature inversions. The size distribution became broader and skewed towards larger sizes with height, indicating a more aged aerosol higher in the atmosphere.

N.2 Nature of the problem

Measurements collected during past cloud seeding projects have indicated that pollution levels over the United Arab Emirates are elevated well above background levels, mainly due to the oil-related activities conducted in the region. In particular, the concentration of fine mode aerosols is high close to major industrial areas and over the offshore oilfields (Figure N.1). Fine mode aerosols are particulate matter with diameter less than 2.5 μm, also called PM2.5. Elevated concentrations of fine mode aerosols can have negative impacts on human health and the environment. High PM2.5 concentrations are associated with health problems, especially respiratory illnesses; they cause haze that reduces visibility; and they can change the nutrient balance when deposited. Submicron particles are also very efficient at scattering incoming solar radiation, and thus may affect climate by disturbing the radiation balance.

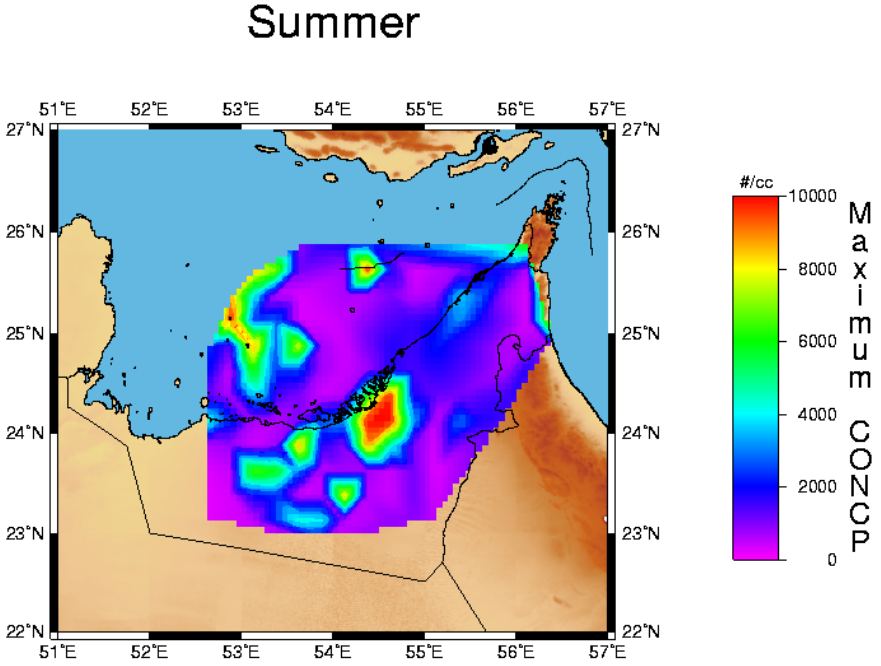

Figure N.1: Maximum fine mode aerosol concentrations (diameter between 0.1 and 3 μm) recorded over the United Arab Emirates from the aircraft during the summer (R.P. Burger)

The characterization of fine mode aerosols was one of the main objectives of the United Arab Emirates Unified Aerosol Experiment (UAE^2), an international scientific project which was conducted in the United Arab Emirates in the summer of 2004. Both the composition and size of the fine mode aerosol were investigated. The preliminary results are presented in this report.

N.3 Data and methods

In order to see how significant the contribution of pollution is to the total aerosol loading over the UAE and to identify the main constituents of the pollution, Teflon, quartz and nucleopore filter samples were collected at the Mobile Atmospheric Aerosol and Radiation Characterization Observatory (MAARCO) site on the coast between Abu Dhabi and Dubai from 9 August to 31 September 2004 (Figure N.2). Filters were changed every day at around 09:00 local time. The Teflon filters were used for gravimetric mass and analyzed via X-ray efflorescence for 40 elements from iron to lead. The quartz filter was analyzed via the thermal optical reflectance method that divides carbon into four organic carbon fractions, pyrolyzed organic carbon and three elemental carbon fractions.

Figure N.2: The Mobile Atmospheric Aerosol and Radiation Characterization Observatory (MAARCO) site, located on the coast between Abu Dhabi and Dubai for August and September 2004 (photo on the right courtesy D. Westphal).

Both the health impacts and climatic implications of aerosol particles are determined by their size distribution i.e. the concentration of particles of different sizes. Fine mode aerosols were measured using a Passive Cavity Aerosol Spectrometer Probe (PCASP), flown on board the Aerocommander during UAE^2 (Figure N.3). The PCASP measures aerosols with diameter between 0.1 and 3 μm and classifies the aerosol particles into 20 size bins based on the scattering of light. Measurements are collected every second which, based on an airspeed of 100 m s-1, corresponds to a horizontal resolution of 100 m.

Figure N.3: Left: The Passive Cavity Aerosol Spectrometer Probe (PCASP), mounted on the nose of the Aerocommander during UAE^2. Right: A close-up of the PCASP (mounted on the wing in this case)

N.4 Aerosol chemical composition and source apportionment

Sulphates, which are assumed to occur as ammonium sulphate, are the dominant constituent of the fine aerosol loading and account for 58% of the aerosol mass. Dust comprises about 20% of the fine aerosol and is fairly evenly partitioned between alumino-silicates and calcium carbonates. The alumino-silicate mass was calculated by scaling up the aluminum mass using the

composition of typical crustal material (Mason, 1966), and the calcium carbonate mass was calculated by assuming that all calcium over and above that which could be accounted for by the alumino-silicates was in the form of calcium carbonate. Total particulate organic matter was calculated by scaling up the organic carbon mass by 1.7 (Mayol-Bracero *et al.*, 2002). Sea salt was negligible as it mainly occurs in the coarse mode. Sea salt mass was calculated by scaling up chlorine in order to be conservative, but may account for up to 1.5% of the mass if Na is used as the tracer. The residual is less than 5%, and can probably be mainly accounted for by nitrates which we have not measured yet.

The chemical composition of the aerosol particles over the Negev Desert in Israel (Formenti *et al.*, 2001) and over the Indian Ocean in an airmass originating over the Arabian Peninsula (Gabriel *et al.*, 2002) have been included for comparison (Figure N.4 right). Aerosol composition over the UAE and over Israel is remarkably similar, especially if most of the residual over Israel is organic matter. In both locations, the aerosol is dominated by sulphates. However, the mass concentration over the UAE (36 $\mu g.m^{-3}$) is twice as high as that over Israel (20 $\mu g.m^{-3}$), which is indicative of higher levels of combustion or greater accumulation of pollution. Well-aged airmasses from the Arabian Peninsula sampled over the Indian Ocean have a much lower aerosol mass concentration (7 $\mu g.m^{-3}$) and differ in aerosol composition – carbonaceous compounds are much more prevalent than over the land (Gabriel *et al.*, 2002).

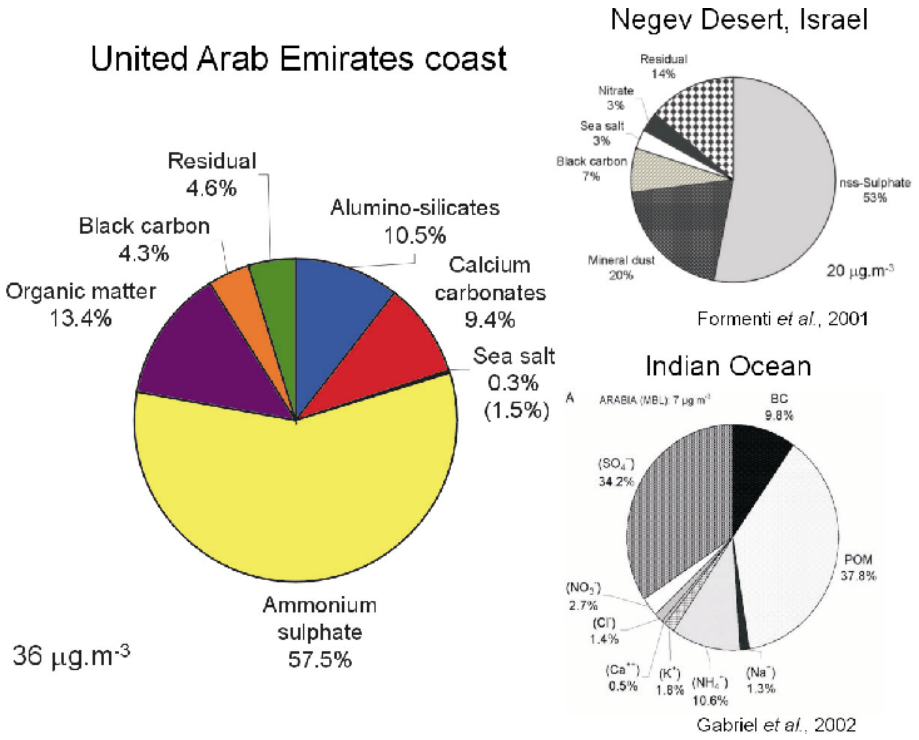

Figure N.4: Left: Fine mode aerosol chemical composition, as measured on the coast of the United Arab Emirates in summer 2004. Right: Aerosol chemical composition in the Negev Desert, Israel (Formenti *et al.*, 2001) and over the Indian Ocean (Gabriel *et al.*, 2002) for comparison.

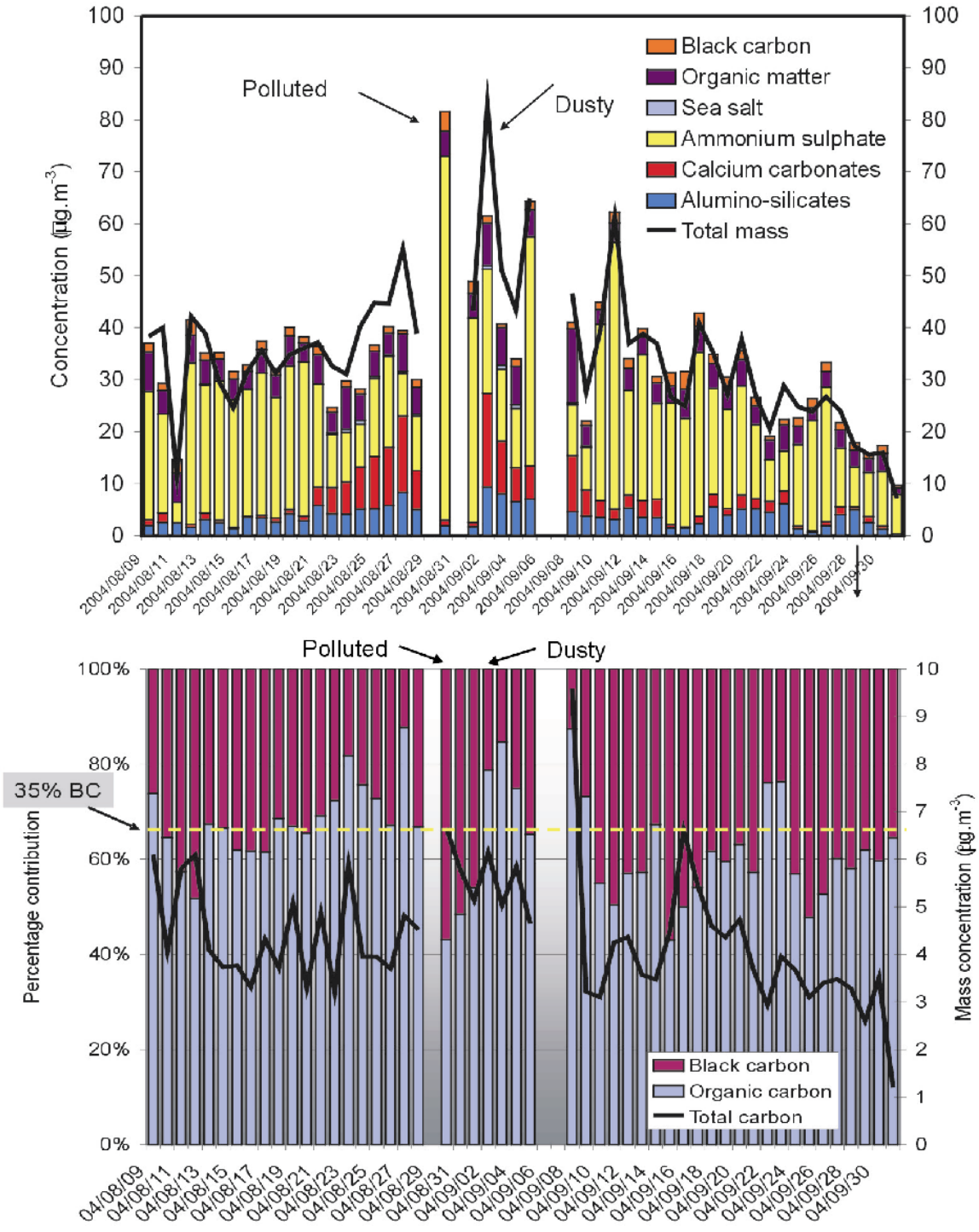

Figure N.5: Daily fine mode aerosol chemical composition (upper) and partitioning of total carbon between black carbon and organic carbon (lower), as sampled on the UAE coast from 9 August to 30 September 2004

The composition of the aerosol varies from day to day (Figure N.5 upper). The contribution of dust (alumino-silicates and calcium carbonates) to the total mass that has been accounted for, varies from 3% to 58%. Dust and pollution episodes can be identified. The fine aerosol was initially dominated by ammonium sulphate. From 21 August to 9 September, dust constituted a much larger component of the fine aerosol loading (more than 25% on most occasions), with the exception of 30 August and 1 September, when dust contributed less than 6% of the fine mass loading. Dust concentrations were lower in the latter part of the project, except for 18-23 September and 27-29 September, when dust generally contributed more than 20% of the fine aerosol mass.

The partitioning of carbonaceous aerosols is determined in part by the temperature and conditions during combustion and subsequent aging of the aerosol, and has radiative implications as black carbon is the light-absorbing fraction of the aerosol. Partitioning stays relatively constant from day to day, and on average the organic carbon to total carbon ratio is 0.65 (Figure N.5 lower), which is fairly close to that of typical diesel emissions and fossil fuel combustion. Biomass burning, for example, has a much lower black carbon fraction (5-10%). Dust episodes tend to be correlated with greater organic carbon content, which may indicate a crustal source for some of the organic carbon.

The origin of the pollution and dust for the episodes on 30 August and 2 September 2004 respectively have been identified using three day backward trajectories calculated using the online National Oceanic and Atmospheric Administration (NOAA) HYbrid Single-Particle Lagrangian Integrated Trajectory (HYPLIT) model (http://www.arl.noaa.gov/ready/hysplit4.html; Draxler and Hess, 1997; 1998). On 30 August the surface flow, shown in red, stagnated over the Gulf for at least 3 days before flowing onshore. The pollution is therefore of local

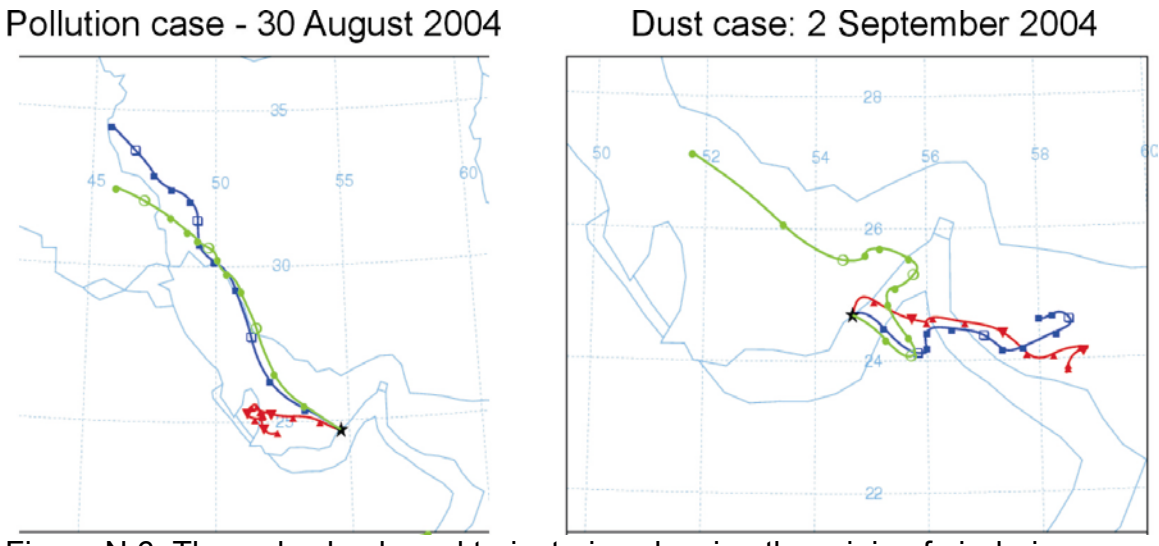

Figure N.6: Three-day backward trajectories showing the origin of air during a pollution episode on 30 August 2004 and during a dust episode on 2 September 2004

origin. Prior to the dust episode on 2 September 2004, the surface airmass was advected over the peninsula east of MAARCO. The signature thus reflects local dust.

A simple source apportionment shows that most of the fine aerosol mass over the UAE is composed of fossil fuel combustion products (72%) (Figure N.7). Mineral dust comprises 20% of the fine mode aerosol. Emissions from local vehicular activity account for 9% of the total mass, and sea salt for only 0.3%. It should be noted that most dust and sea salt particles are in coarse mode (diameter greater than 2.5 μm), which is why their contribution to the fine mode is so small.

Source apportionment was attained by attributing all the lead to vehicle emissions, and assuming that it constitutes 0.3% of the PM2.5 mass derived from vehicle exhausts. All chlorine which was not accounted for by crustal material (assuming typical ratios) was considered to be from sea salt, and to occur as sodium chloride. Mineral dust is the sum of the alumino-silicates and calcium carbonates. The remainder is assumed to be products of fossil fuel combustion.

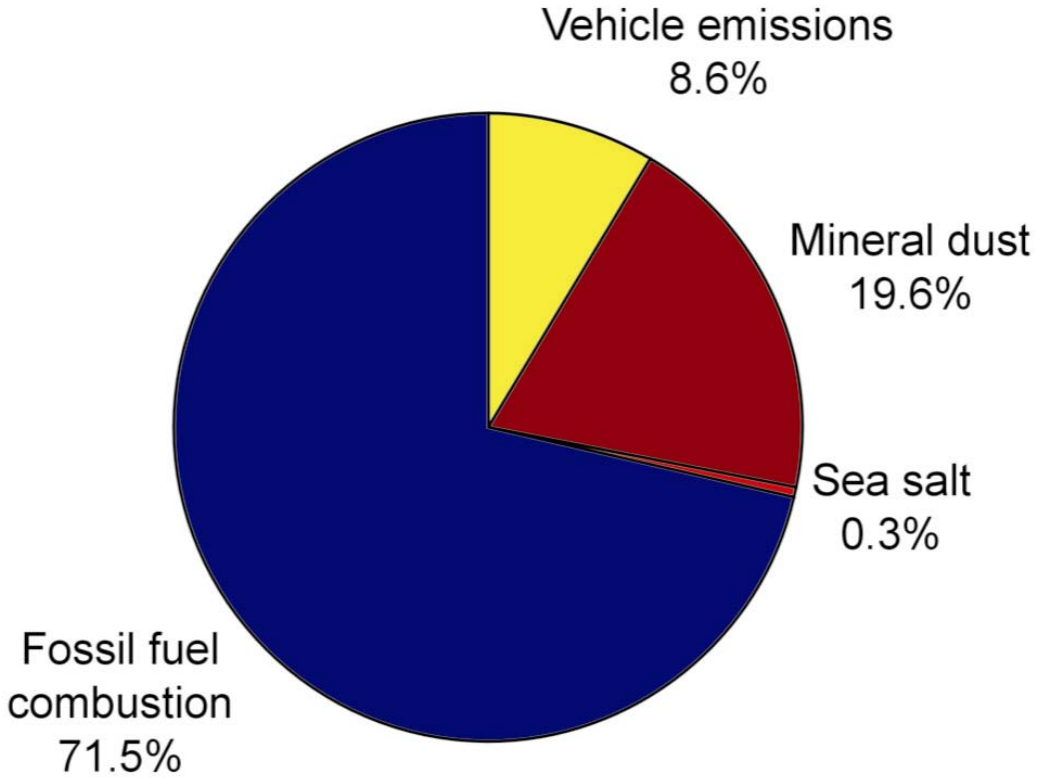

Figure N.7: Source apportionment for fine mode aerosols over the UAE coast

N.5 Aerosol size distribution

Information about the size of aerosols with height in the atmosphere is obtained from the PCASP. This enables us to investigate the optical properties of the aerosols at different levels in the atmosphere, and gives us an indication of the source of the aerosols. To illustrate the value of the PCASP, results from a flight conducted over the MAARCO site on 12 September 2004 are presented.

The profile over MAARCO was conducted during a dust episode when AOT was very high (around 0.9) and Angström Exponent was low (less than 0.3), indicating that the aerosol loading was dominated by coarse aerosols (Figure N.8 right). The profile was conducted between Dubai and the MAARCO site (Figure N.8 left), and started at an altitude of 4000 m at 10:32 UTC and ended at around 150 m at 10:46 UTC.

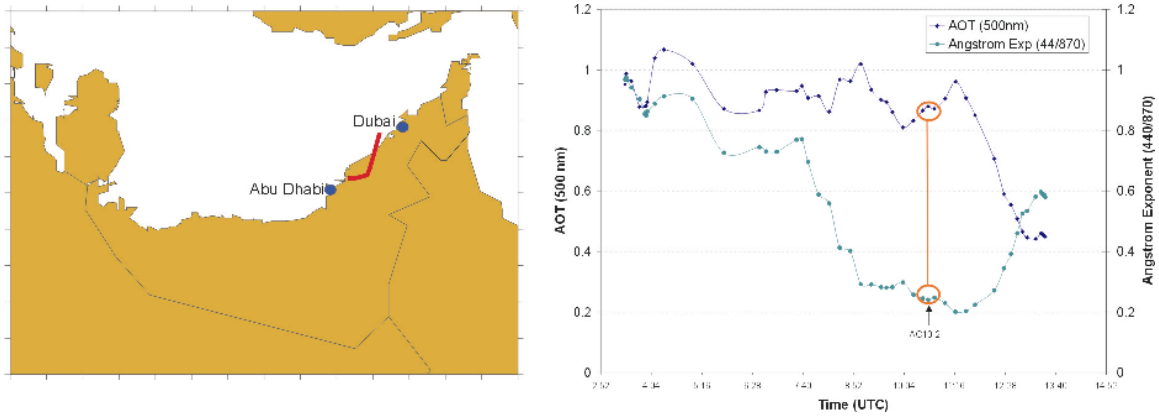

Figure N.8: Left: The location of the vertical profile from 10:32 to 10:46 UTC on 12 September 2004; Right: The aerosol optical thickness and Angstrom Exponent on 12 September 2004. The time of the vertical profile is indicated in red.

On this occasion the boundary layer was capped at around 1500 m by a temperature inversion with magnitude 2.5ºC (Figure N.9). Relative humidity dropped off at the top of the boundary layer to less than 10%. The atmosphere was extremely stable in the boundary layer, and there were numerous inversion layers. These inversions prevent the upward dispersion of aerosol particles, and so effectively trap pollution.

The normalised aerosol size distributions show that there were at least three different airmasses present on 12 September (Figure N.10). The aerosol closest to the surface (size distribution 1) had the narrowest size distribution and was dominated by small particles, indicating recently emitted pollution. Size distributions 2, 3 and 4, higher up in the boundary layer, are broader and skewed towards larger particles, indicating a more aged aerosol. The size distribution of the aerosol above the boundary layer (size distributions 5 and 6) is even more skewed towards larger particles, which were probably formed due to coagulation.

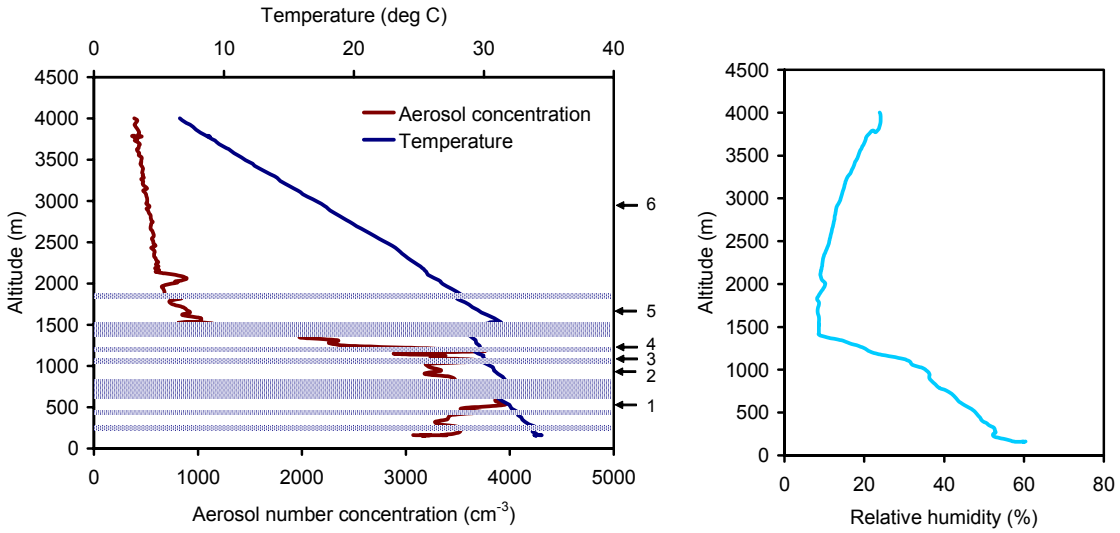

Figure N.9: Left: Vertical profiles of accumulation mode aerosol concentration and temperature over the UAE coast on 12 September 2004. Temperature inversions are indicated with stippled lines; layers for which the size distributions are shown are labeled on the right. Right: Vertical profile of relative humidity

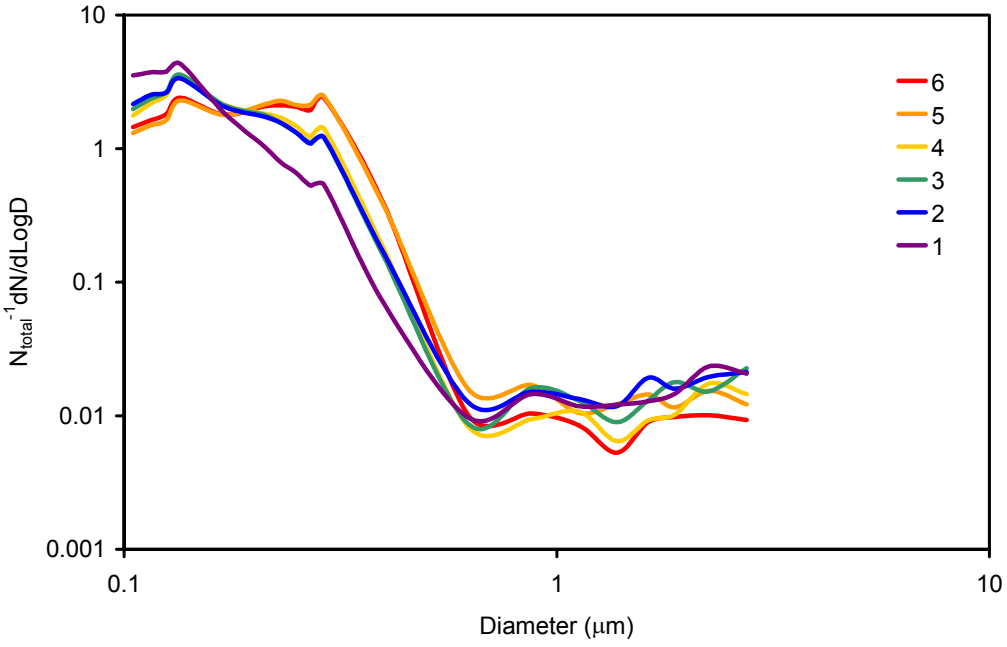

Figure N.10: Normalised aerosol size distribution for the six layers identified on the profile conducted over the UAE coast on 12 September 2004.

The PCASP can also be used to check the accuracy of the fine mode size distribution that is derived from the sun photometer measurements, and see how the size distribution of the integrated atmospheric column, as retrieved by the sun photometer, compares to the size distribution in the various layers in the atmosphere. For the case of 12 September 2004, there is a poor correlation between the size distribution derived from the sun photometer and that measured in-situ by the PCASP (

Figure N.11). This is probably due to the high dust loading on this occasion, which dominated the optical properties of the atmosphere, and made the retrieval of the fine mode difficult.

The correlation between the PCASP measurements and the AERONET retrieval is much better for the case of 3 September (Figure N.12) when the total aerosol loading was much lower. The spheroidal retrieval is better than the spherical retrieval, in that the radius with maximum volume concentration is correct, although the volume concentration is too low at that radius.

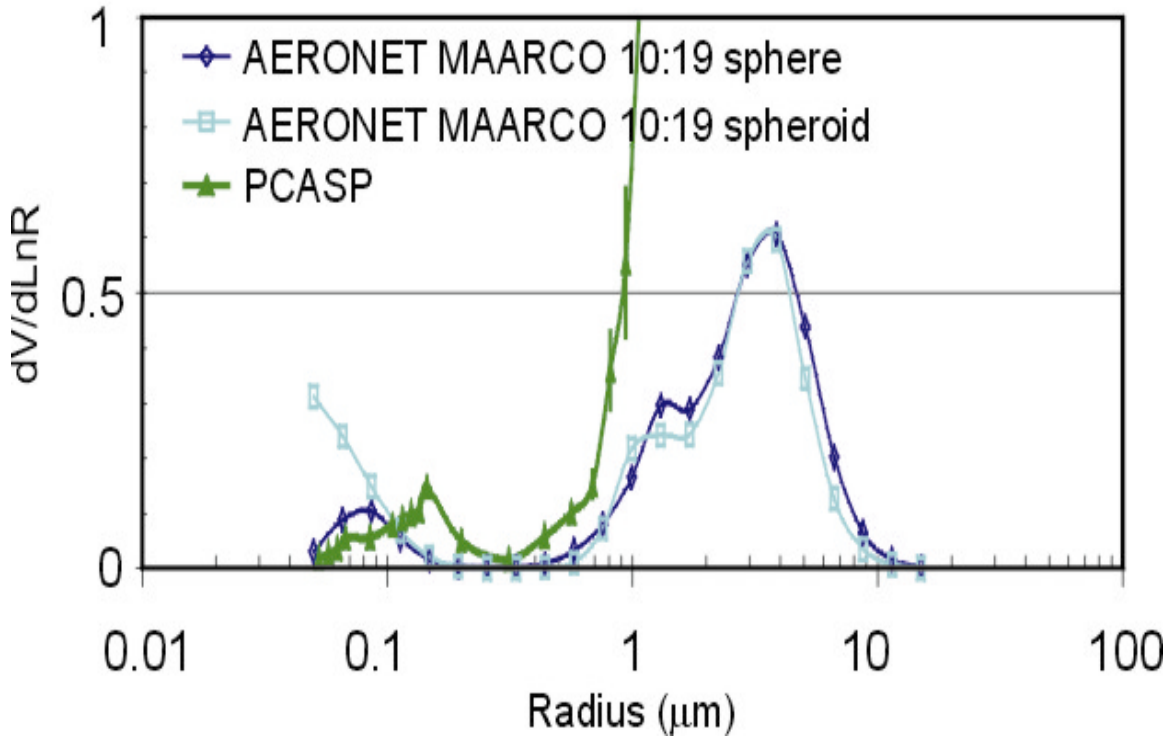

Figure N.11: Size distribution derived from the AERONET sun photometer and that recorded by the PCASP on 12 September 2004

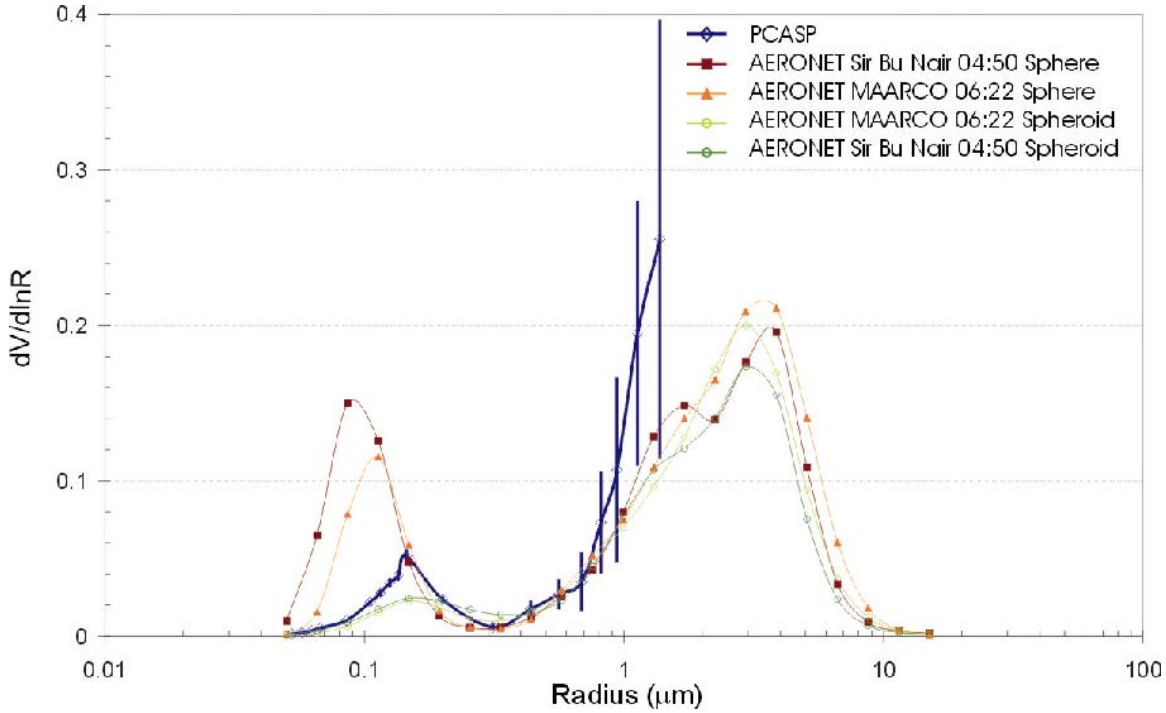

Figure N.12: Size distribution derived from the AERONET sun photometer and that recorded by the PCASP on 3 September 2004

N.6 Conclusion

The chemical composition and size distribution of fine mode aerosols (diameter less than 2.5 μm) were investigated during the UAE^2 project conducted in the UAE during the summer of 2004. The fine mass loading was dominated by ammonium sulphate (on average 58%), with dust (alumino-silicates and calcium carbonate), organic matter and black carbon being the other major constituents. A simple source apportionment indicates that most of the fine aerosol was derived from fossil fuel combustion (72%), probably from oil-related activities in the region.

As has been found previously, the atmosphere over the UAE is highly stratified, several layers with differing aerosol characteristics can be identified. During the dust episode on 12 September 2004, at least three different aerosol layers were present. The accumulation mode size distribution was skewed towards larger sizes at higher altitudes, indicating that the airmasses higher up were more aged than those closer to the surface.

The high concentrations of fine mode aerosols over the region are expected to have implications for cloud formation and direct radiative forcing over the region, especially given the fact that the bulk of the fine mode is comprised of ammonium sulphate, which acts as cloud condensation nuclei and is an efficient scatterer of incoming solar radiation.

References

Draxler, R.R. and Hess, G.D., 1997: Description of the Hysplit_4 modeling system, NOAA Technical Memorandum, ERL ARL-224, December, 24p.

Draxler, R.R. and Hess, G.D., 1998: An overview of the Hysplit_4 modeling system for trajectories, dispersion, and deposition, *Australian Meteorological Magazine*, 47, 295-308.

Formenti, P., Andreae, M.O., Andreae, T.W., Ichoku, C., Schebeske, G., Kettle, J., Maenhaut, W., Cafmeyer, J., Ptasinsky, J., Karnieli, A. and Lelieveld, J., 2001: Physical and chemical characteristics of aerosols over the Negev Desert (Israel) during summer 1996, *Journal of Geophysical Research*, 106 (D5), 4871-4890.

Gabriel, R., Mayol-Bracero, O.L. and Andreae, M.O., 2002: Chemical composition of submicron aerosol particles collected over the Indian Ocean, *Journal of Geophysical Research*, 107 (D19), 8005, 10.1029/2000JD000034.

Mason, B., 1966: *Principles of Geochemistry*, John Wiley, New York.

Mayol-Bracero, O.L., Kirchstetter, T.W., Gabriel, R., Novakov, T., Streets, D.G. and Andreae, M.O., 2002: Carbonaceous aerosols over the Indian Ocean during INDOEX: Chemical characterization, optical properties and probable sources, *Journal of Geophysical Research*, 107, 10.1029/2000JD000039.

O.0 Establishment of the Mass Scattering Efficiency of Dust

PI: Jeffrey S. Reid, Naval Research Laboratory, Monterey CA
Co-Investigators: Elizabeth A. Reid, Jainglong Zhang

O.1 Nature of problem

At some point during the aerosol modeling process one must link the relative amount of aerosol particles to the amount of light that is scattered or absorbed. The mass extinction efficiency (α_e), mass scattering efficiency (α_s) is the most commonly used parameter for this purpose. Its units ($m^2\ g^{-1}$) are a simple ratio of the optical cross section (in m^2) to the total mass in g. If α_s is reasonably well known, then measurements of aerosol optical depth (via AERONET Sun photometers or satellites), can be linked directly to the atmospheric mass loading of pollution or dust.

While conceptually simple, the complexity of various aerosol species makes the mass light efficiencies a fairly uncertain parameter-especially in regions impacted by both small pollution particles and larger dust. At the heart of the problem is that the mass scattering efficiency is strongly dependant on the ratio of particle size to the wavelength of light scattered.

An example of the wavelength dependant mass extinction efficiency for various aerosol species is presented in Figure O.1. Here we normalize by density

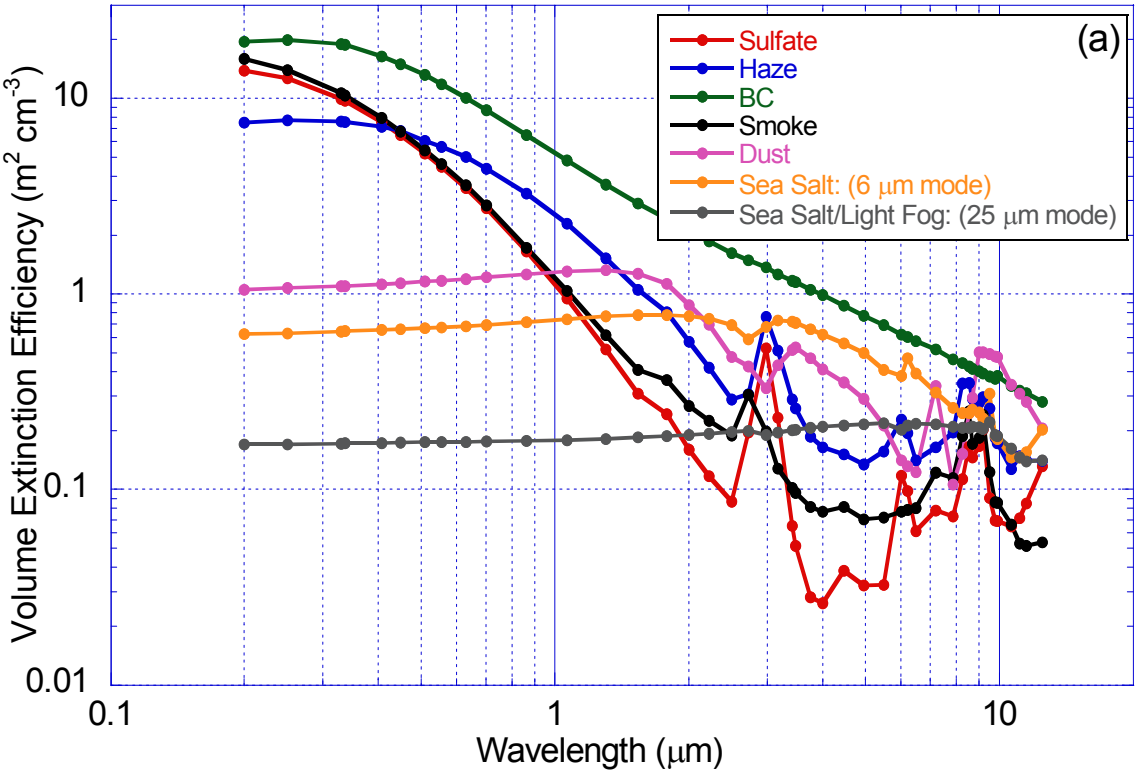

Figure O.1 The volume extinction efficiency for a variety of aerosol species. To convert to mass extinction efficiency, simply divide by the particle density

to compute a "volume scattering efficiency." We include most of the species found in the atmosphere including sea salt, dust, pollution, black carbon (BC), and smoke.

Examination of this figure demonstrates the findings of a multitude of sensitivity studies for short-wave radiative forcing (visible 0.3-0.8 μm), variations in particle size can have a dramatic impact in α_e. Large particles such as dust and sea salt are essentially spectrally flat up into the near infrared. In the mid to long wave infrared, only dust, sea salt, and fog are active.

In a region such as the Arabian Gulf all of these species are present. In order to use satellite or Sun photometer to infer particle mass concentrations, very specific estimates of the mass scattering and extinction need to be determined. In this work unit, we will analyze UAE^2 data to provide such parameterizations.

O.2 Executive summary

To determine the mass scattering efficiency of aerosol particles in the UAE^2 campaign, we deployed a complete set of aerosol instrumentation into the Mobile Atmospheric Aerosols and Radiation Characterization Observatory (MAARCO). This included filters for gravimetric and chemical analysis, nephelometers for measuring light scattering, and a variety of spectrometers for measuring particle size distributions.

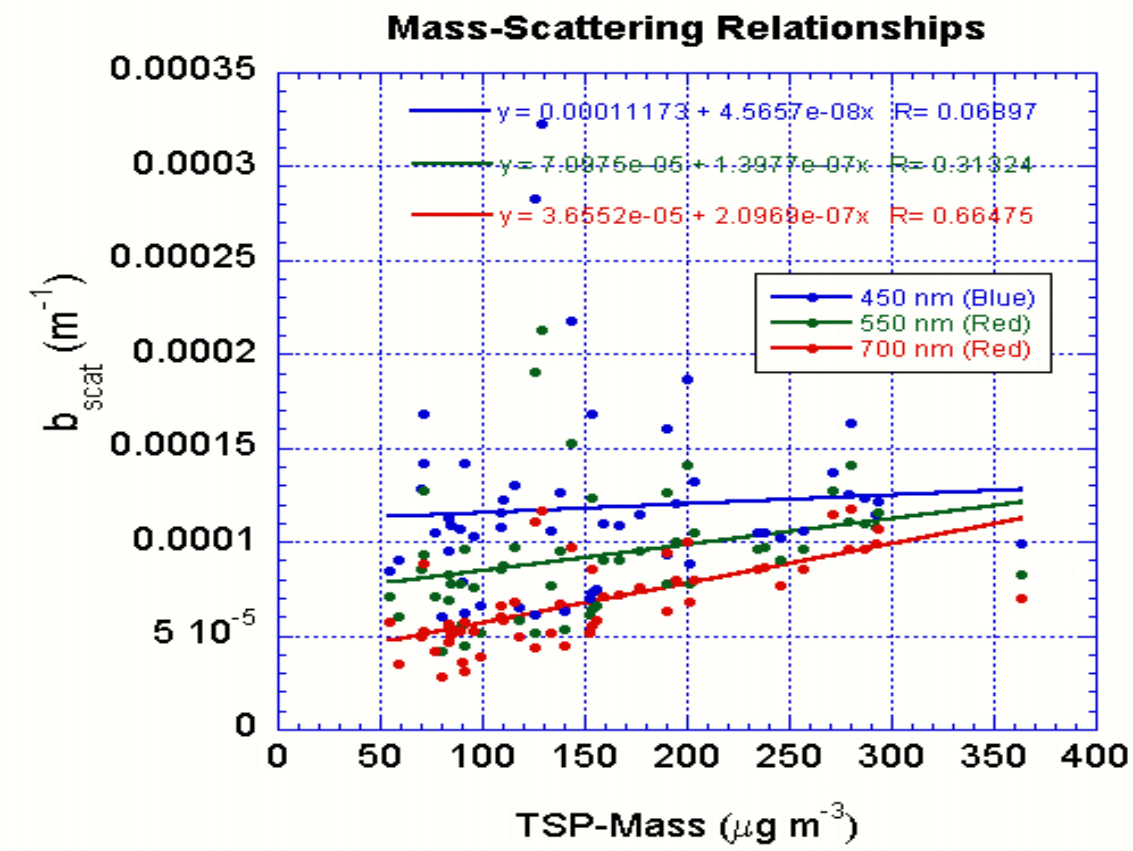

Figure O.2. Regression of the total dry light scattering coefficient (b_{scat}) versus total aerosol mass measured on a filter.

A plot of total dry light scattering versus suspended particulate matter mass (TSP, particles <15 mm in diameter) fro the entire UAE^2 study period is presented in Figure O.2. On a whole, we find not bulk relationship between particles mass and light scattering. This is due to the complicated nature of the atmosphere and the relative amounts of high scattering efficiency pollution particles and low efficiency dust.

Despite the lack of order in Figure O.2, only moderate amounts of analysis reveals that the mass scattering efficiency can be broken down easily into its fine and coarse mode components. We begin by examining the wavelength dependant light scattering in the Angstrom exponent. The Angstrom exponent α is defined as the slope of light scattering versus wavelength on a log-log plot, and is frequently utilized for discrete wavelengths through:

$$\alpha = \frac{\ln(bscat_{\lambda 1} / bscat_{\lambda 2})}{\ln(\lambda_1 / \lambda_2)}$$

We can guess from Figure O.1 that Angstrom exponents on the order of 0-0.5 (i.e., flat) are dominated by coarse mode particles such as dust and sea salt. Conversely, Angstrom exponents above 1 tend to be dominated by fine mode particles such as pollution or smoke. We computed the mass scattering efficiency for each data point in Figure O.2 and plot the result versus the Angstrom exponent in Figure O.3. Here we find much more order than in Figure O.2 and have determined that the average mass scattering efficiency for dust in the UAE is 0.4 $m^2\ g^{-1}$. For fine mode particles (say when the Angstrom exponent is near 2), the raw value is 1.5 $m^2\ g^{-1}$. However, this does not account for the presence of large coarse mode particles which contribute to the total mass but not the light scattering. If we correct for this, we derive a value of 3 $m^2\ g^{-1}$ for the background pollution.

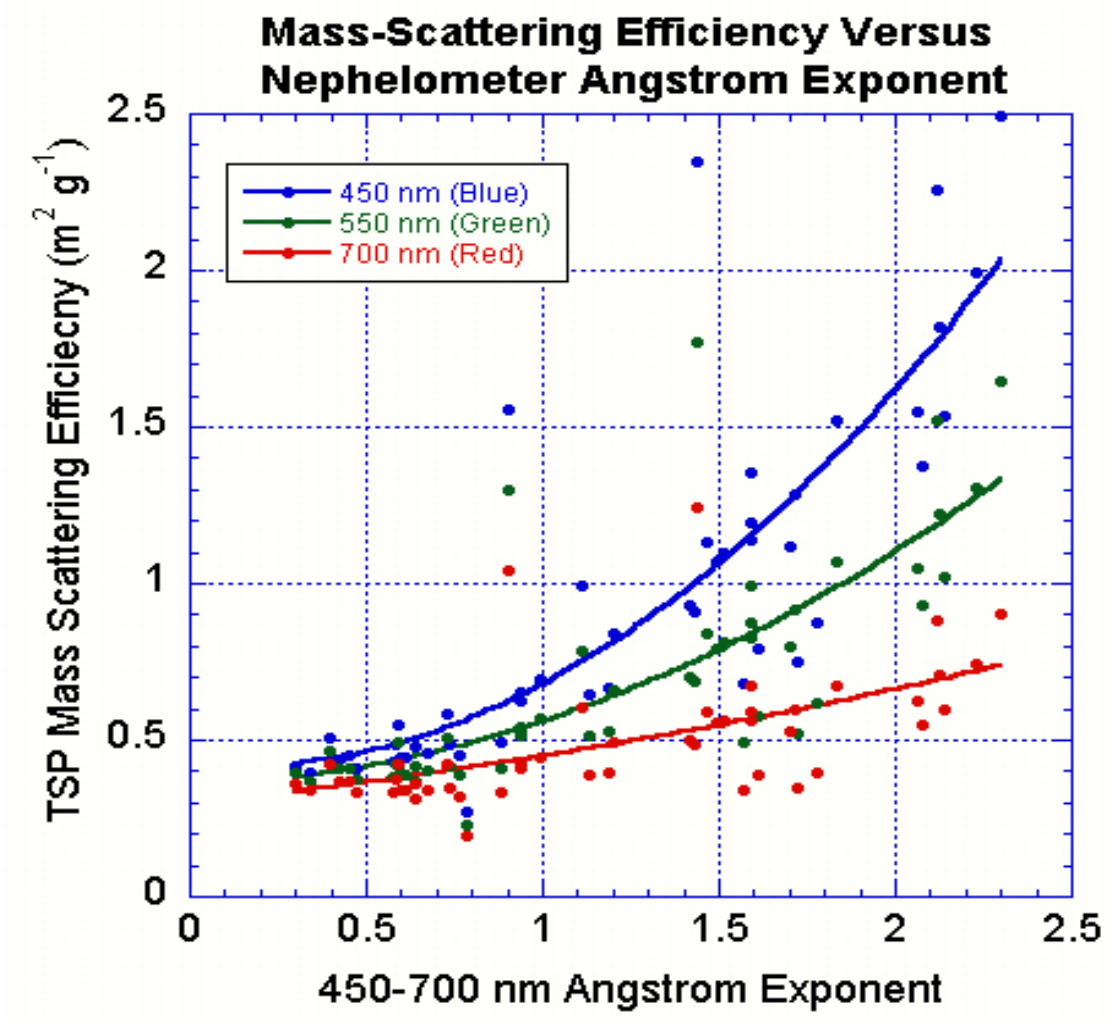

Figure O.3 Particle mass scattering efficiency versus Angstrom exponent. Larger Angstrom values indicate smaller particles.

P.0 Particle Hygroscopicity in the Polluted Arabian Gulf Marine Boundary Layer

Principal Investigator: Jeffrey S. Reid, NRL Monterey CA
Co-Investigators: Elizabeth A. Reid, Kristy Ross, Jainglong Zhang

P.0 Nature of the problem

Soluble compounds within aerosol particles result in water condensing onto their surface. At higher relative humidity, aerosol particles can grow in diameter from 100 to 250%. This process, called hygroscopic growth, is one of the most fundamental properties of aerosol particles. Indeed, at 80% relative humidity, fine mode pollution can increase its total scattering by a factor of two. One of the principal goals of the UAE^2 mission is to determine of the hygroscopic growth properties of aerosol particles in the UAE^2 are similar to other regions of the world.

P.1 Executive summary.

During the United Arab Emirates Unified Aerosol Experiment, a pair of dried and quasi-ambient nephelometers were placed inside the Mobile Atmospheric Aerosol And Radiation Characterization Observatory (MAARCO) at a coastal site to study the impact of particle hygroscopicity on ambient light scattering. By allowing the quasi ambient nephelometer to freely adjust, the ratio of dried to quasi-ambient would give the information regarding the upper "return half" of the hygroscopicity curve. We also examined the mass scattering efficiency of fine mode pollution particles. By combining data with AERONET and lidar data we parsed the contribution of condensed water on regional light scattering and aerosol optical thickness. As expected, particle hygroscopicity varied significantly as a function of coarse/fine partition. For time periods without significant dust, dry mass scattering efficiencies of fine mode particles were on the order of 3.3 $m^2 g^{-1}$ at 550 nm-typical for sulfate based pollution.

Figure P.1 presents the ratio of ambient light scattering to light scattering at humidity less than 35% as a function of ambient humidity. At 80% RH (fairly common over the Arabian Gulf), more than half of light scattering is due to hygroscopic processes. We also did not encounter a significant difference in particle hygroscopicity with wavelength. This particle hygroscopic curves looked very similar to the measurements of *Carrico et al.,* [2003], with *f*(80%) equal to 2.2. This was somewhat surprising given that the Arabian Gulf fine mode aerosol particles have a larger sulfate mass fraction than its other Asian counterparts. Despite being a relatively shallow feature, the impact of hygroscopicity on regional optical depth was found to be ~20%. We compared AERONET retrievals of fine mode particle size to our hygroscopic and did not see any shift in retrieved size distribution.

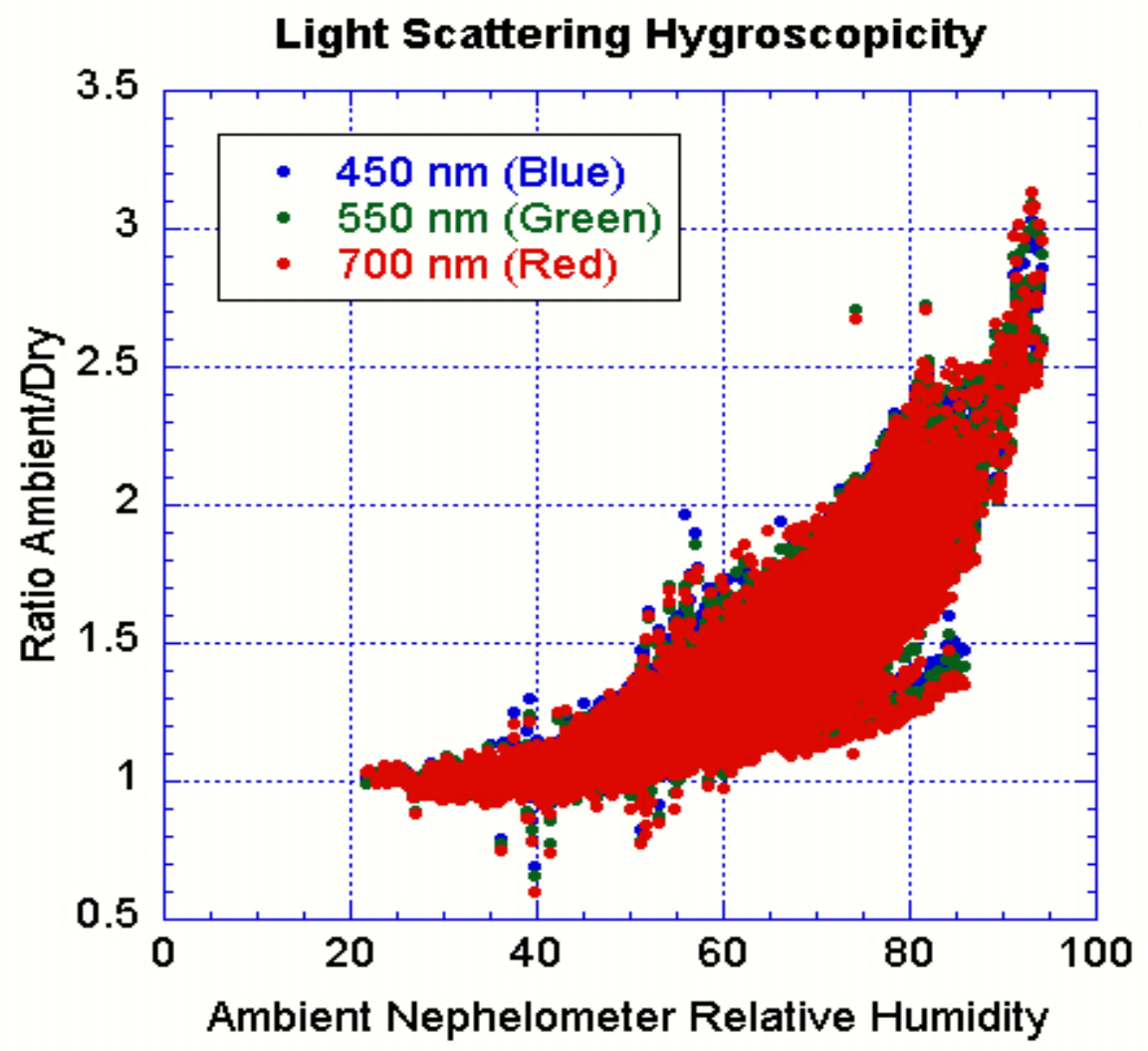

Figure P.1 Ratio of Ambient to dry light scattering as a function of ambient relative humidity.

Q.0 Measurements of Aerosol Phase Functions With A Polar Nephelometer

Principal Investigator: John N. Porter University of Hawaii, HIGP, SOEST, Honolulu, HI

Q.1 Nature of the Problem

In order to derive aerosol properties from remote measurements (satellite, lidar, sky radiance, etc) we need knowledge of the aerosol scattering properties. Of particular importance is the angular distribution of scattered light (the aerosol phase function). For example small particles scatter more light in side directions while large particles scatter more in forward directions. If the aerosol size distribution is known then Mie theory can be used to calculate the aerosol phase function. Assuming a set of aerosol models, this approach is often used for satellite aerosol retrievals. When dust aerosols are present then Mie theory is not valid and more complex algorithms are needed to derive the aerosol phase function. Direct measurements of the aerosol phase function are therefore useful to validate aerosol models and obtain quantitative knowledge of aerosol scatter.

Q.2 Executive Summary

During the UAE experiment we operated a custom aerosol polar nephelometers to measure aerosol phase functions. The basic design of the system is shown in Figure Q.1. The system can measure scattered light from 1-179 degrees scattering angles. This system is often mounted on the back of a small truck and transported to field locations (Figure Q.2). The ground polar nephelometer collects scattered light from both scanning and fixed locations (Figure Q.1). During the scan, the aerosol concentrations and laser intensity can vary. In order to normalize out these variations, scattered light is also collected at a fixed location (~45 ° scattering angle). Dividing the scanning measurements by the fixed angle measurements normalizes out the variations due to aerosol concentration and laser intensity.

Figure Q.3 shows an example of an aerosol phase function collected at the MAARCO site in the United Arab Emirates (UAE) during the 2004 experiment. The parallel-polarized light is shown in red and the perpendicular polarization scattered light is shown in blue. We are currently processing the data and carrying out quality checks on the data. When completed these will be submitted to the UAE data set. We are also in the process of testing different aerosol scatter codes, which will allow comparing the aerosol optical properties with the *in situ* aerosol measurements carried out at the MAARCO site.

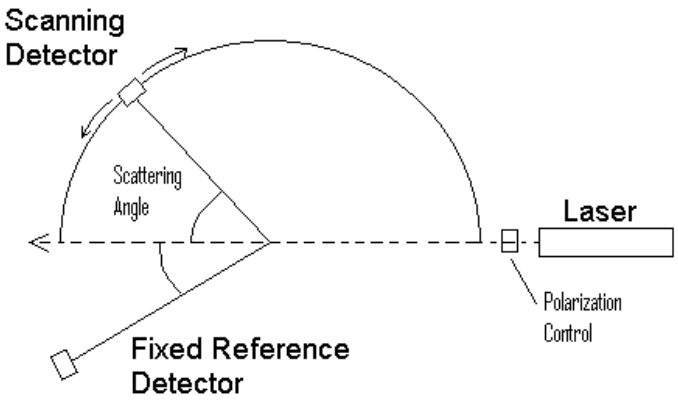

Figure Q.1 Basic design of polar nephelometer. Aerosol scattered light is collected at a fixed angle and from a scanning arm.

FigureQ. 2. Ground polar nephelometer mounted on the back of pickup

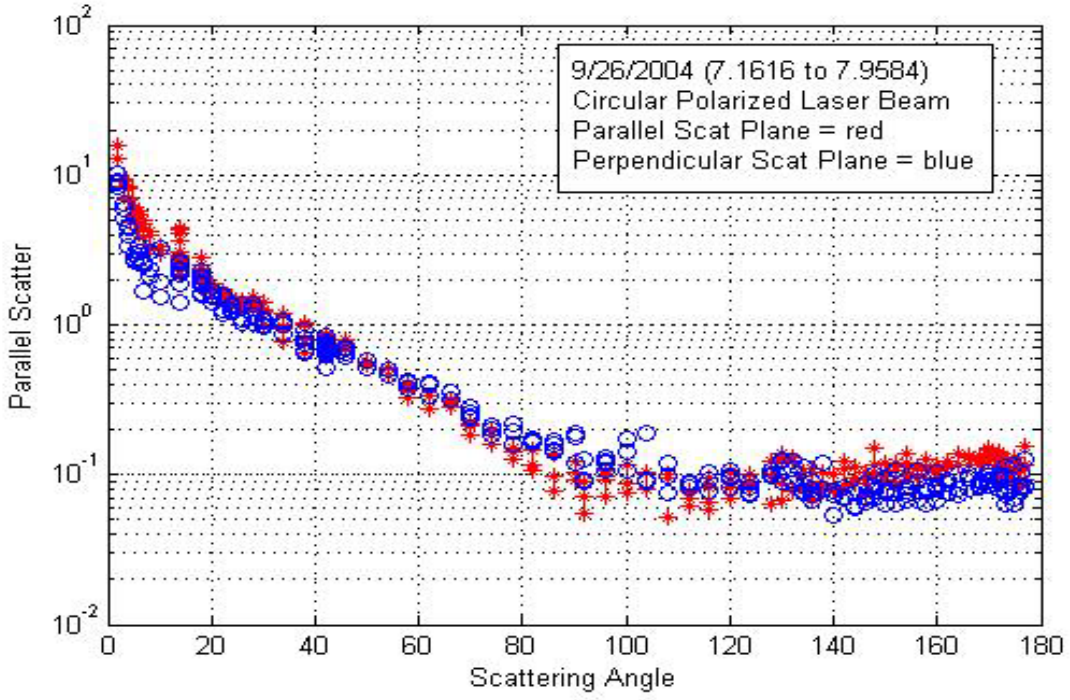

Figure Q.3 Aerosol phase function measured of 9/26/2004 in the United Arab Emirates at the Marco site.

R.0 Aerosol Retrieval Using Transmission and Multispectral AATSR Data

Principal Investigator: Gerrit de Leeuw, TNO, The Hague, The Netherlands

Co-Investigators: Arie N. de Jong, Jolanta Kusmierczyk-Michulec, Robin Schoemaker, Marcel Moerman, Peter Fritz, Jeff Reid, Brent Holben

R.1 Nature of the problem

The retrieval of aerosol properties from spectral information requires a basic understanding of the aerosol optical properties of the various aerosol types that may occur in the area of interest. Furthermore, information needs to be available on the response of the aerosol properties to meteorological conditions, in particular relative humidity and vertical mixing. Usually such information is only approximately available and often *a priori* information is used based on climatology.

The United Arab Emirates Unified Aerosol Experiment (UAE^2) provided a comprehensive data base including aerosol and meteorological information which allows for the development of retrieval algorithms. Part of the data is used for algorithm development, the rest for testing and evaluation of the results. The TNO team works on the retrieval of aerosol information from data collected along a horizontal path using a transmissometer with 7 wave bands from the UV to the Thermal Infrared and from data from the Advanced Along-Track Scanning Radiometer (AATSR) aboard the ESA Environmental satellite ENVISAT. The data serve to explore the retrieval of the most abundant aerosol types in the UAE area (dust and fossil fuel burning), whereas the specific purpose of the transmissometer is the exploration of infrared wave bands for this purpose.

R.2 Executive summary

TNO participated to the UAE^2 campaign with the retrieval of aerosol properties using AATSR, and its multi-band optical/IR transmissometer (de Jong and Fritz, 2005) providing horizontal, path-integrated transmission data. The transmissometer emitter and receiver were both installed close to MAARCO site, with a retro-reflector at a distance of 890 m across the harbor that provided a total transmission path of 1780 m. The wave bands were roughly centered at 0.45. 0.6, 0.9, 1.5, 2.3, 4 and 10 μm.

The transmission T at each wavelength is given by:

$$T = \frac{I}{Io} = \int_{r=0}^{r=R} \exp(-\alpha r) dr \,,$$

where I_o is the intensity of the radiation emitted by the source, I is the radiation received after passing through the atmosphere over a range R, α is the atmospheric extinction coefficient at each point r in the atmosphere. α is the sum of molecular and aerosol extinction, each of which has an absorption and a scattering component: $\alpha_{tot} = \alpha_{mol}^{abs} + \alpha_{mol}^{scat} + \alpha_{aer}^{abs} + \alpha_{aer}^{scat}$. Each term is a function of wavelength and depends on the nature of the gaseous and aerosol species in the transmission path. In general each of these terms may vary with r, in the

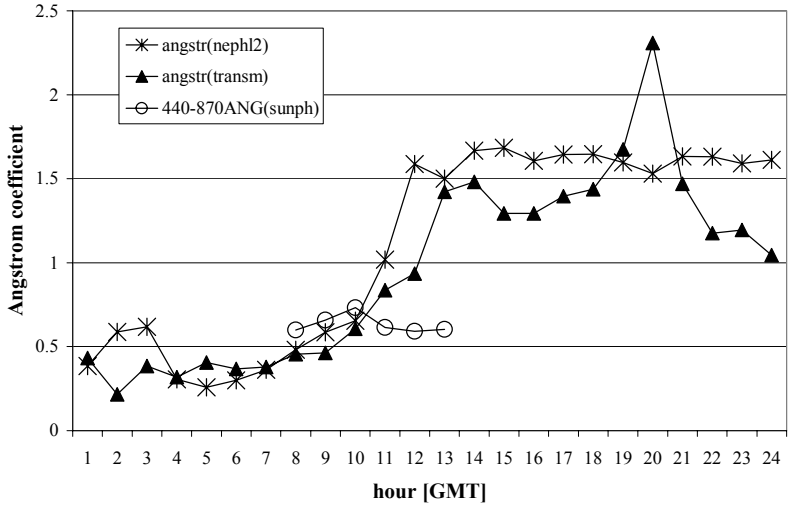

Figure R.1 Preliminary comparison of Ångström coefficients derived from data from the nephelometer, the sun photometer and the transmissometer, for 24 September 2004. See text for further explanation.

following horizontal homogeneity along the 890 m transmission path was assumed.

The molecular extinction depends on meteorological parameters such as relative humidity, air temperature and atmospheric pressure. The molecular contribution to the extinction was calculated with the MODTRAN model using input from the TNO meteorological station. After subtraction of the results from the total extinction the aerosol contribution was retained.

This was done for each wave band because the variation of the aerosol extinction coefficient with the wavelength contains information on the particle size distribution and, because most aerosol types occur in certain size bands, this information relates to the aerosol species. This property is used in the retrieval process when multispectral data are available, such as from AATSR and the TNO transmissometer. Therefore, we concentrate here on the Ångström relation: $\alpha_A(\lambda) = C\lambda^{-a}$, where λ is the wavelength and α is the Ångström coefficient.

Figure R.1 shows a preliminary comparison of Ångström coefficients calculated from the transmissometer data in the visible range, with those calculated from 'wet' nephelometer data measured in MAARCO and with those obtained from the MAARCO sun photometer aerosol optical depth (AOD), for 24 September, 2004. Figure R.1 shows that until about 10:30 GMT, the transmissometer and nephelometer Ångström coefficients are similar and trace each other very well. This was expected because both were obtained from measurements at the MAARCO site. On the other hand, the nephelometer provides a local point measurement as opposed to the transmissometer which integrated over an 1780 m over water path, which may explain differences

observed later that day (i.e. over water different conditions may have occurred than at MAARCO). At about 10:30 the sea breeze kicked in, with a wind speed of about 3-4 m/s which was too low to generate significant sea spray. At the same time the extinctions dropped significantly at all visible and NIR wavelengths whereas Figure R.1 shows that the transmissometer and nephelometer Ångström coefficients increased from about 0.5 to about 1.6. All this information indicates that the aerosol size distribution changed. The decrease in extinction indicates that the number of submicron particles decreased, whereas the increase in Ångström coefficients indicates that the number of larger particles decreases even more.

This happens near the surface. However, the sun photometer derived Ångström coefficients in Figure R.1 show that for the vertical column there is not such a drastic change. Apparently, for this particular day (24 September), in off-shore winds the column data were representative for ground observations, but in on-shore wind the mixing is insufficient and the retrieved aerosol parameters were different from those observed at the surface at the coastal MAARCO site. This needs to be further elaborated by comparison with vertical structure observations (lidar, aircraft).

The sun photometer derived aerosol properties were the starting point for comparison with the transmissometer data. It appears that extinctions calculated from the sun photometer derived aerosol parameters compare favorably with the transmission measurements at the very shortest wavelengths. However, at

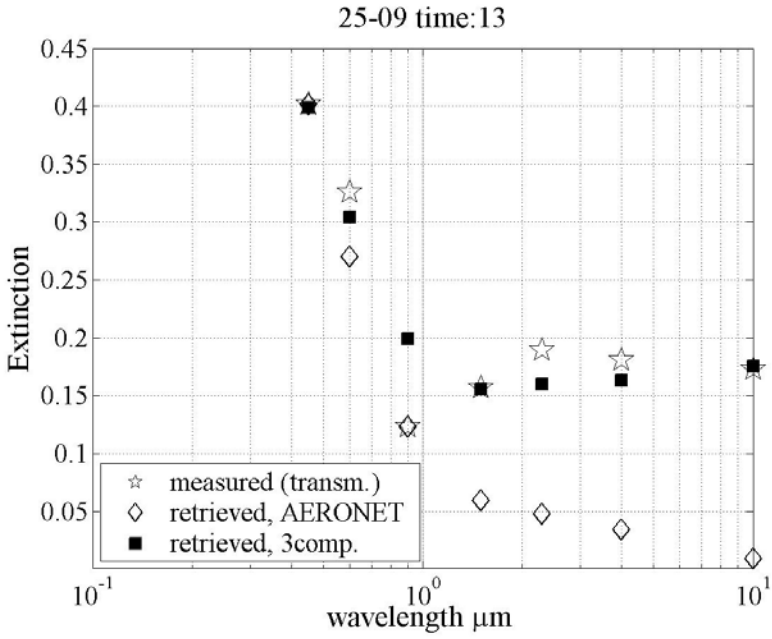

Figure R.2 Comparison of extinction coefficients calculated from the transmissometer data, and from aerosol size distributions (see legend). The 'retrieved, AERONET' data were obtained with the aerosol properties retrieved from the MAARCO sun photometer data, for the 'retrieved, 3 comp.' extinction coefficients a third mode was added.

longer wavelengths there is a large discrepancy, as show in Figure R.2. However, the addition of a third mode, describing the contribution of larger particles, significantly increases the extinction coefficients at the longer wavelengths. Based on these results, a three mode aerosol model is proposed for the retrieval of aerosol information from the transmissometer data, including the IR wavelengths. This approach is currently tested for other days for which data are available from UAE^2.

A major challenge for the retrieval of aerosol information from satellite data is to distinguish the reflectance from aerosols and from the underlying surface. AATSR has the special feature of two viewing angles, one in nadir and one in the forward direction. This feature has been used for retrieval over land (Veefkind et al., 1998). However, over bright surfaces and over turbid coastal water (case 2 water) the performance of the algorithm had not been tested. Also the retrieval in the presence of desert dust and industrial pollution had not been tested before. Hence UAE^2, with its suite of data from a variety of sources, offered an excellent opportunity to test and improve the AATSR algorithm.

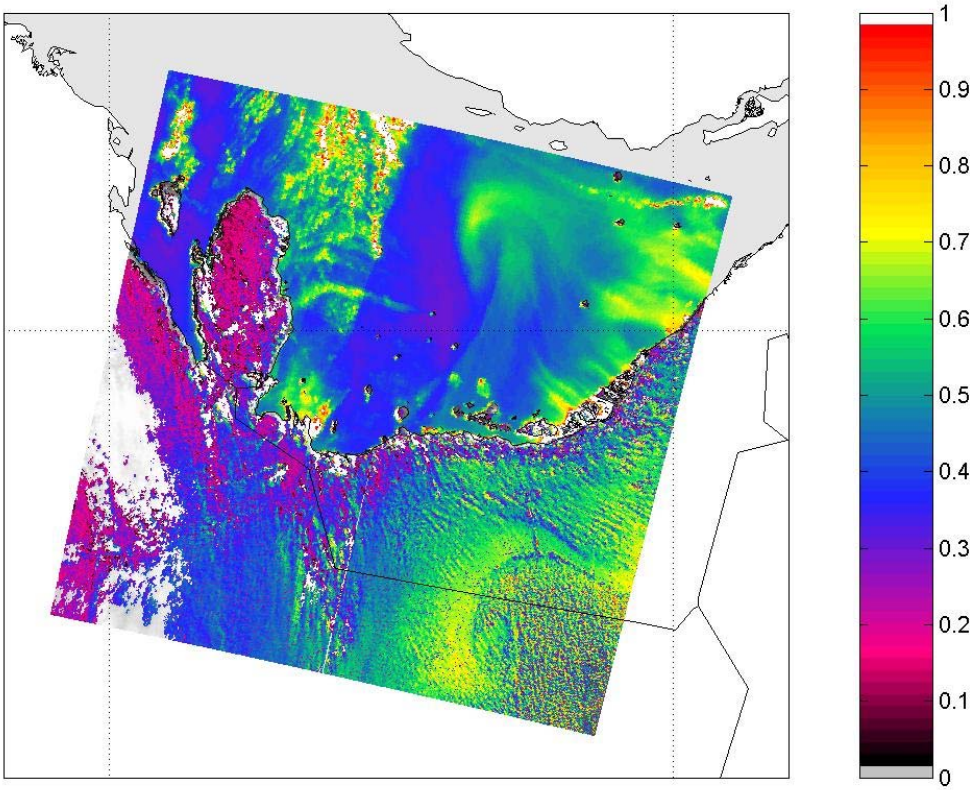

Figure R.3 AOD at 0.67 μm over part of the UAE^2 area retrieved from AATSR data on 7 September 2004.

Preliminary results are shown in Figures R.3 and R.4. Figure R.3 shows the AOD at 0.67 µm over the UAE^2 area retrieved from AATSR data on 7 September 2004. Clearly visible are the aerosol plumes advected off the UAE coast and in the stagnant air over the Gulf. There seems to be a discontinuity in the AOD distribution over land along the coast, which has to be further investigated. However, apart from this, the AOD over land, away from the coast, and over water, are quite similar.

The available AATSR frames over the area have been used to retrieve the aerosol properties with the current algorithm and the results were compared with the UAE^2 AERONET sun photometer data. Results are presented in Figure R.4. All comparisons were made with AERONET data obtained within 10 minutes from the time of overpass. Figure R.4a shows the comparison for all water sites, i.e. all sites for which sun photometers were at an island. Here we have an excellent comparison with a regression coefficient of 0.78 (22 data points). There seems to be a very small bias with the AATSR derived AOD slightly higher, but mostly within one standard deviation. For the retrieval over land (Figure R.4b) the comparison is less favorable, with a regression coefficient of 0.57 (53 data points) and a slight bias to underestimating the AATSR derived AOD. However, in view of the bright surface, and most AOD within 0.1 of the AERONET AOD, this is a satisfactory result.

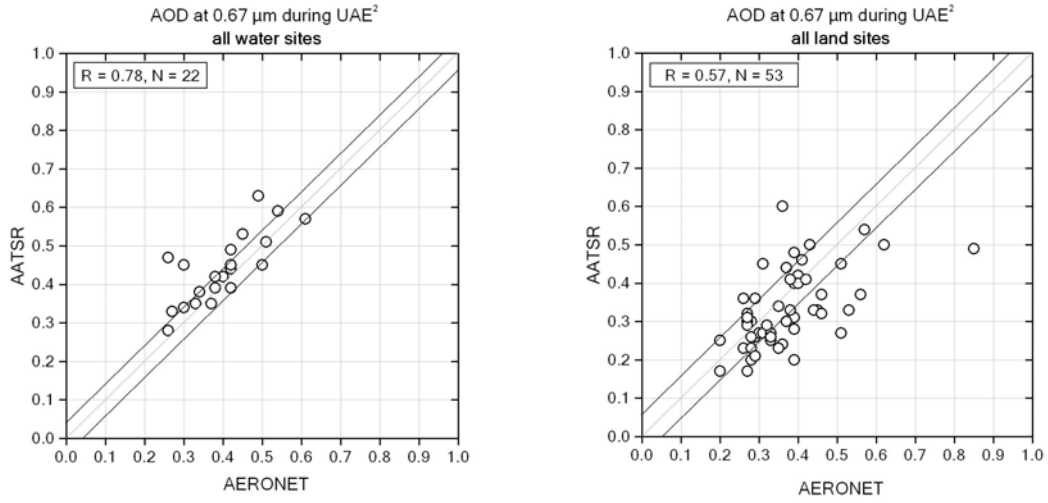

(a) (b)

Figure R.4 Comparison of AOD derived from AATSR data during UAE^2 with AERONET sun photometer data, for all water sites (a) and for all land sites (b)

Acknowledgements:
The contribution of TNO to UAE^2 was financially supported by the Netherlands Ministry of Defense.

References

De Jong, A.N. and P.J. Fritz, 2005: Two-way multi-band optical/IR transmission measurements in the Persian Gulf-Coastal Region, Proceedings SPIE, September 2005, Brugge (Belgium), in preparation.

Veefkind, J.P., G. de Leeuw and P.A. Durkee, Retrieval of aerosol optical depth over land using two-angle view satellite radiometry during TARFOX. Geophys. Res. Letters. 25(16), 3135-3138, 1998.

S.0 An Investigation of the Coastal Circulations and Aerosol Transport in the Arabian Gulf Region

Principal Investigators: Rebecca E. Eager and Sethu Raman, Department of Marine, Earth, and Atmospheric Sciences, North Carolina State University State Climate Office of North Carolina

An observational and modeling study was performed over the Arabian Gulf region to investigate the coastal circulations and aerosol transport in the area. Climatological data and observations from the United Arab Emirates – Unified Aerosol Experiment (UAE^2) were used to develop a better understanding of the complex meteorological processes in the Arabian Gulf region. The geography of this region is unique because it can cause land-sea-air-land interactions that will modify the overlying air masses and affect local meteorology significantly.

During the summer months, the UAE is influenced by the southwest Indian monsoon. This causes light northwesterly winds over the Arabian Gulf. Superimposed on the northwesterly winds are the sea and land breeze circulations. Climatological data suggests that sea breezes occur on more than 77% of days in all months of the year and land breezes occur on more than 71% of the days. The occurrence of the sea and land breeze circulations are higher (90-99%) during the summer months when large-scale weather patterns are quiescent. Observed mean sea and land breeze frequencies at Abu Dhabi for different months are shown in Table S.1.

A selection of the wind roses of the daily distribution of the wind direction is shown in Figure S.1. Wind roses are shown for Abu Dhabi, Al Heben, Alkhazna,

Table S.1 Percentages of days per month when sea breeze and land breeze circulations develop.

Sea Breeze and Land Breeze Frequency: Abu Dhabi, 1995-2002

Month	Sea Breeze Frequency	Land Breeze Frequency
January	82	81
February	77	71
March	81	71
April	93	84
May	96	95
June	99	94
July	99	96
August	96	97
September	99	99
October	98	100
November	92	93
December	90	91

Dalma, Das Island, and Wadi Al Bih. The winds are most frequently from the northwest at Das Island, Dalma, and Abu Dhabi. Further north along the UAE coastline, at Wadi Al Bih the wind direction is most frequently from the north. At Al Heben near the Gulf of Oman coast, the winds are typically from the southeast. Alkhazna is located inland and has winds most commonly from the north.

The timing and horizontal extents of the sea breeze circulation, both onshore and offshore were determined by a network of surface meteorological stations throughout the UAE. The sea breeze timing and horizontal extent inland and offshore varies daily. Sea breezes typically form along the southern Arabian Gulf coast between 1300 and 1600 LT. Further inland and offshore, the sea breeze circulation forms between 1600 and 1900 LT. The sea breeze ends around sunset, and onshore synoptic winds continue until the land breeze forms. The land breeze forms once land surface cools to a temperature cooler than the sea surface temperature and continues until the sea breeze reforms on the following day. An example of timing and horizontal extent of the sea breeze is shown for 9-11 September 2004 in Figure S.2 for the stations of Das Island, Qarnen, Dalma, Sir Bani Yas, Alqlaa, Owtaid, and Mukhariz. The coastline at these stations is oriented east to west. Sea breeze winds are therefore northerly (270° to 90° with respect to north), and land breeze winds are southerly (90° to 270°).

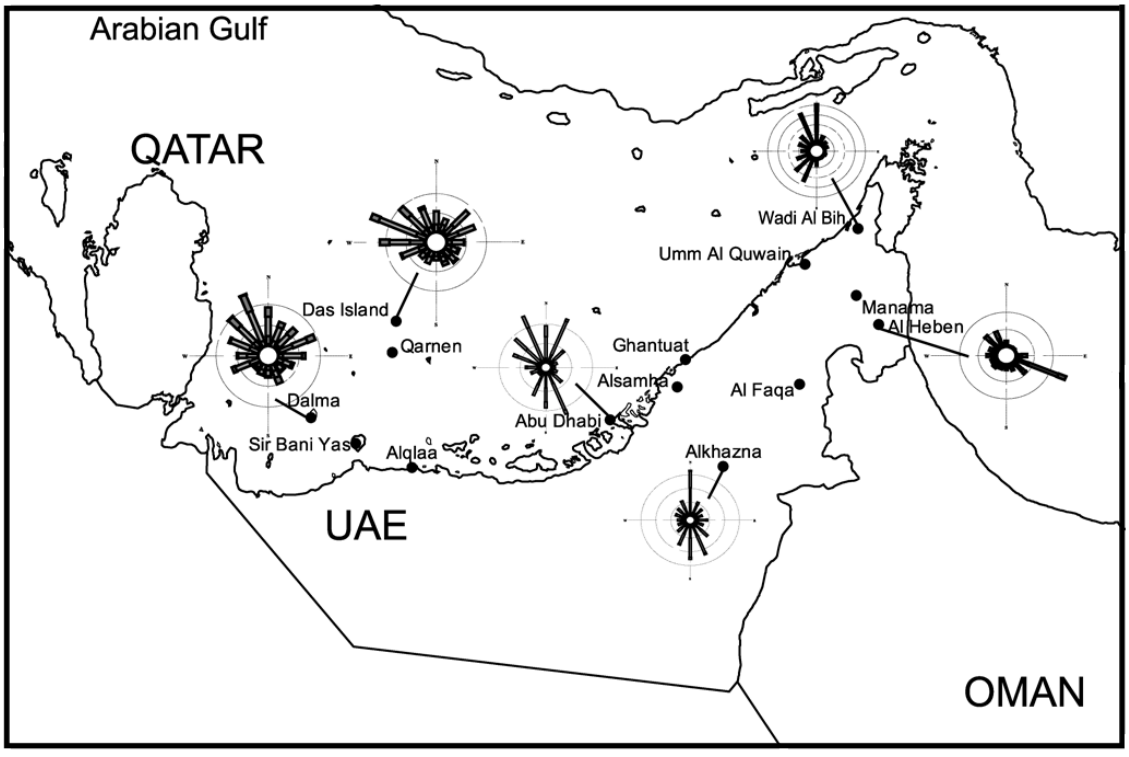

Figure S.1 Frequency of daily winds at Das Island, Dalma, Abu Dhabi, Alkhazna, Al Heben, and Wadi Al Bih stations for July 2004. Circles are drawn at 5% intervals at all stations except Al Heben, at which circles are drawn at 10% interval.

On 9 September, the sea breeze is first evident at 1300 LT at Alqlaa, on the coast. It penetrates inland to Mukhariz (130 km inland) by 1500 LT, and extends offshore to Das Island (115 km offshore) by 2100 LT. On 10 September, the sea breeze is again first evident at the coast at 1300 LT. The sea breeze reaches the island stations earlier in the afternoon than on 9 September, and only extends inland to Owtaid (80 km inland).

The vertical extent of the sea breeze circulation was determined using radiosonde observations taken at 1200 UTC (1600 LT) at Abu Dhabi. The vertical extent of the onshore winds varies daily and ranges between 750 and 1468 m. The soundings also show the depth of the return offshore current above the onshore sea breeze winds, as shown for Abu Dhabi on 4 September 2004 in Figure S.3. On 4 September, the boundary layer height was estimated to be about 1500 m at Abu Dhabi at 1200 UTC. Onshore winds occur near the surface to a height of about 750 m, with a return offshore flow from 750 m to 1100 m. The sea breeze circulation is comprised of both the onshore flow and the return offshore flow; therefore the total height of the sea breeze circulation on 4 September 2004 was 1100 m.

Measurements of aerosol concentration taken during the UAE^2 experiment were used to investigate aerosols, namely dust, transported in the Arabian Gulf region. Vertical profiles of dust concentration along with vertical profiles of potential temperature and wind are used to determine the source region, transport distance, and height of the dust layer. The aircraft aerosol vertical profiles suggest highest dust concentrations occur near the surface. The wind direction in the layer of the highest dust concentration varies diurnally, and

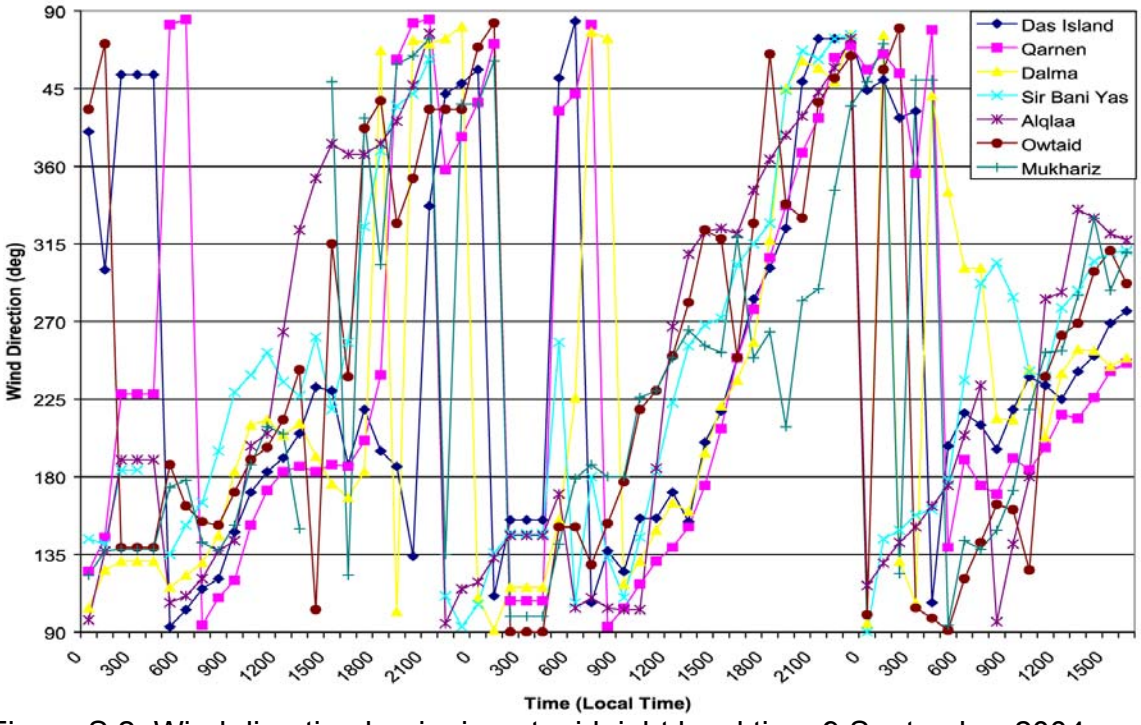

Figure S.2 Wind direction beginning at midnight local time 9 September 2004 through 1600 LT 11 September 2004 at Das Island, Qarnen, Dalma, Sir Bani Yas, Alqlaa, Owtaid, and Mukhariz. Time is in local time (UTC+4 hours).

indicates dust being transported to the UAE from all areas surrounding the Arabian Gulf.

An example of the aircraft vertical profiles is given in Figure S.4 for 13 September 2004. The aircraft vertical profile was performed near the Mobile Atmospheric Aerosol and Radiation Characterization Observatory (MAARCO) site, located near Alsamha, between 0650 and 0754 UTC (1050-1154 LT). The top of the boundary layer was located at 750 m, and the highest concentration of dust aerosols was below this inversion. The wind direction at the surface near MAARCO was southeasterly, suggesting the source region for this dust is within the UAE.

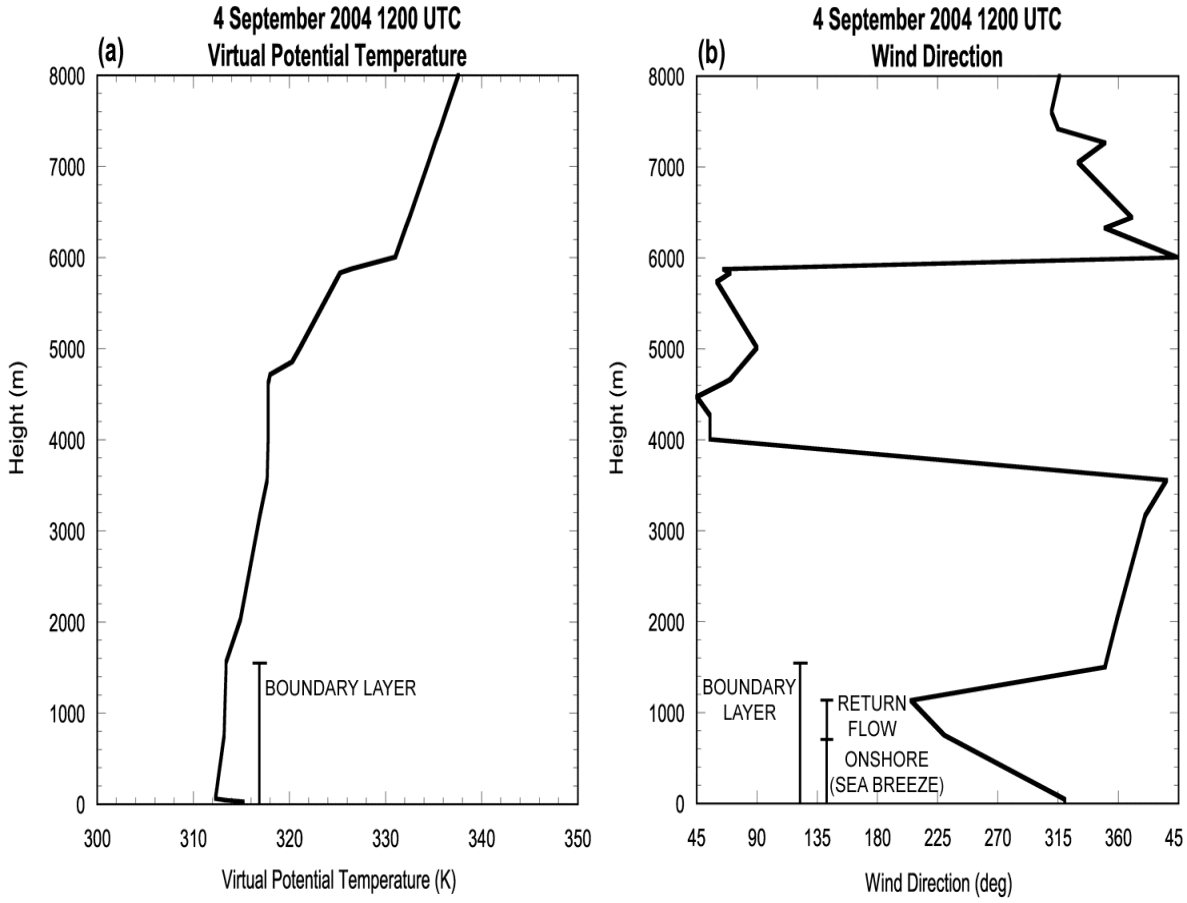

Figure S.3 (a) Virtual potential temperature and (b) wind direction profiles at 1200 UTC (1600 LT) on 4 September 2004. The height of the boundary layer, the onshore sea breeze flow, and the return flow are indicated.

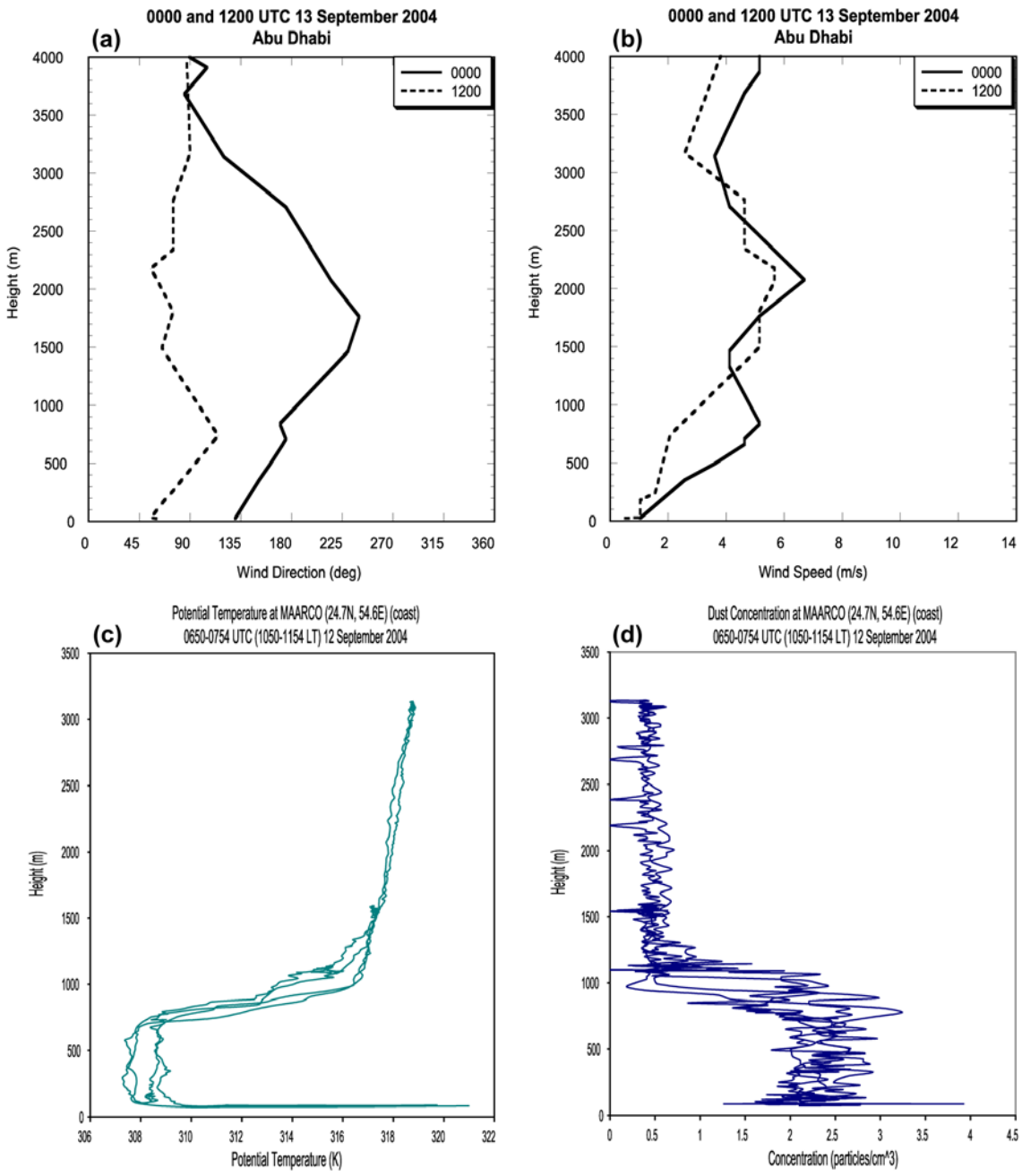

Figure S.4 (a) Wind direction and (b) wind speed vertical profiles at 0000 and 1200 UTC (0400 and 1600 LT) 13 September 2004 at Abu Dhabi. (c) Aircraft potential temperature and (d) dust concentration profiles at MAARCO (24.7°N, 54.6°E) at 0650-0754 UTC (1050-1154 LT) 13 September 2004.

Numerical simulations of two periods during the summer of 2004 were performed to test the ability of the Coupled Ocean/Atmosphere Mesoscale Prediction System (COAMPS®) to resolve the sea breeze circulation. The first time period selected was 9-11 September 2004, when observations indicated the development of a well-defined sea breeze on all three days. Figure S.5 shows the vertical velocity, potential temperature, and north-south wind vectors for 1500 UTC (1900 LT) 10 September 2004. At this time, the sea breeze extended inland to 23.9°N (33 km inland). At the southern edge of the sea breeze was the sea breeze front with a maximum upward motion of 0.18 m s^{-1} (18 cm s^{-1}).

The second case study was performed for 28-30 September 2004. During this time period, no sea breeze was noted in the observations for 28 September; however, a sea breeze did form on 29 September. The model predicts the formation of a sea breeze on both days. The boundary layer height can be estimated by the model predicted turbulent kinetic energy (TKE). As shown in Figure S.6 for 1200 UTC (1600 LT) 28 September 2004, TKE values over the

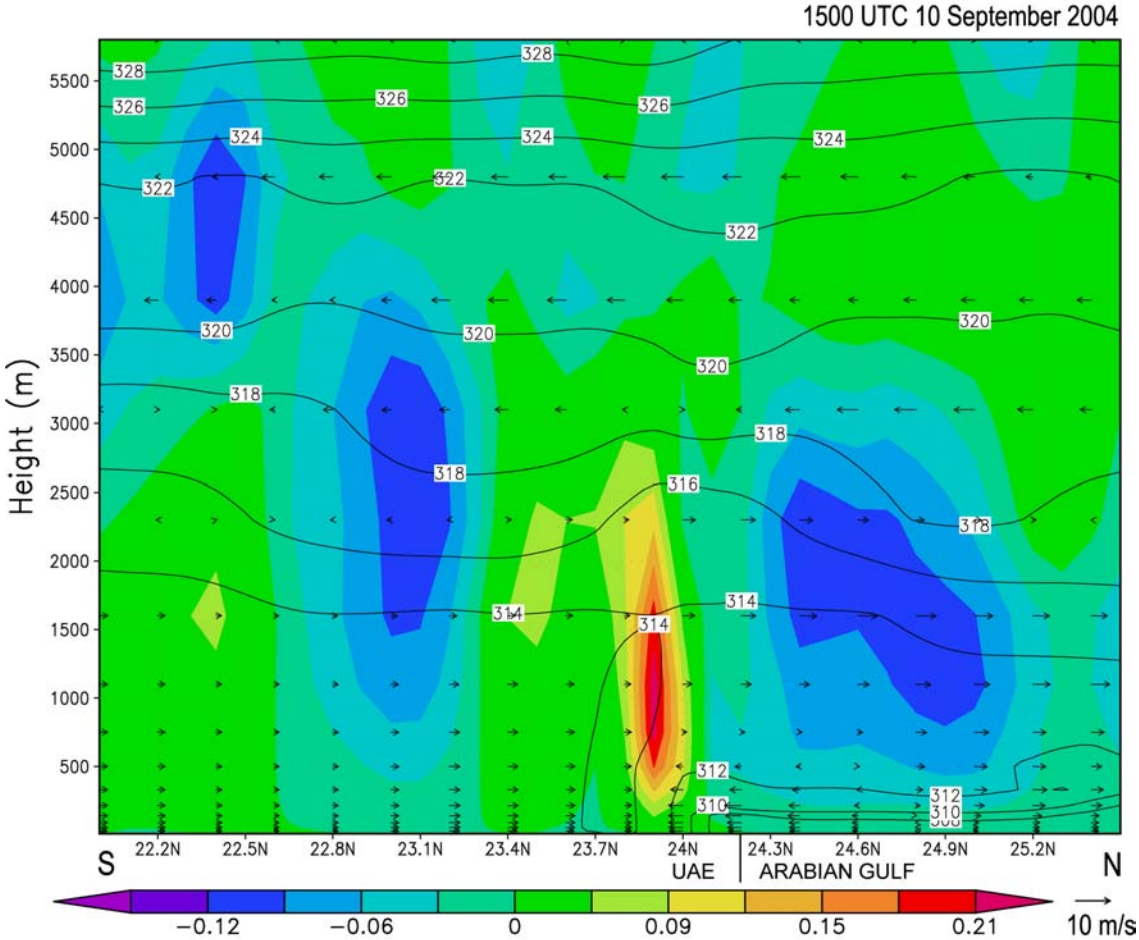

Figure S.5. Vertical velocity (shaded, m s^{-1}), potential temperature (contoured, K), and V-W wind vectors for 1500 UTC (1900 LT) 10 September 2004 along 53.02°E from 22°N to 26°N.

UAE were 2.4-2.7 m^2 s^{-2}. After sunset, the TKE over the land decreases to near zero. Figure S.7 shows the vertical velocity, potential temperature, and north-south wind vectors for 1500 UTC (1900 LT) 29 September 2004. A region of convergence and upward motion is predicted at the sea breeze front, with vertical velocities of 0.18 m s^{-1} (18 cm s^{-1}). The sea breeze extended inland 189 km and 233 km offshore, with onshore winds extending to a height of 500 m with a return offshore current from 750 to 1100 m.

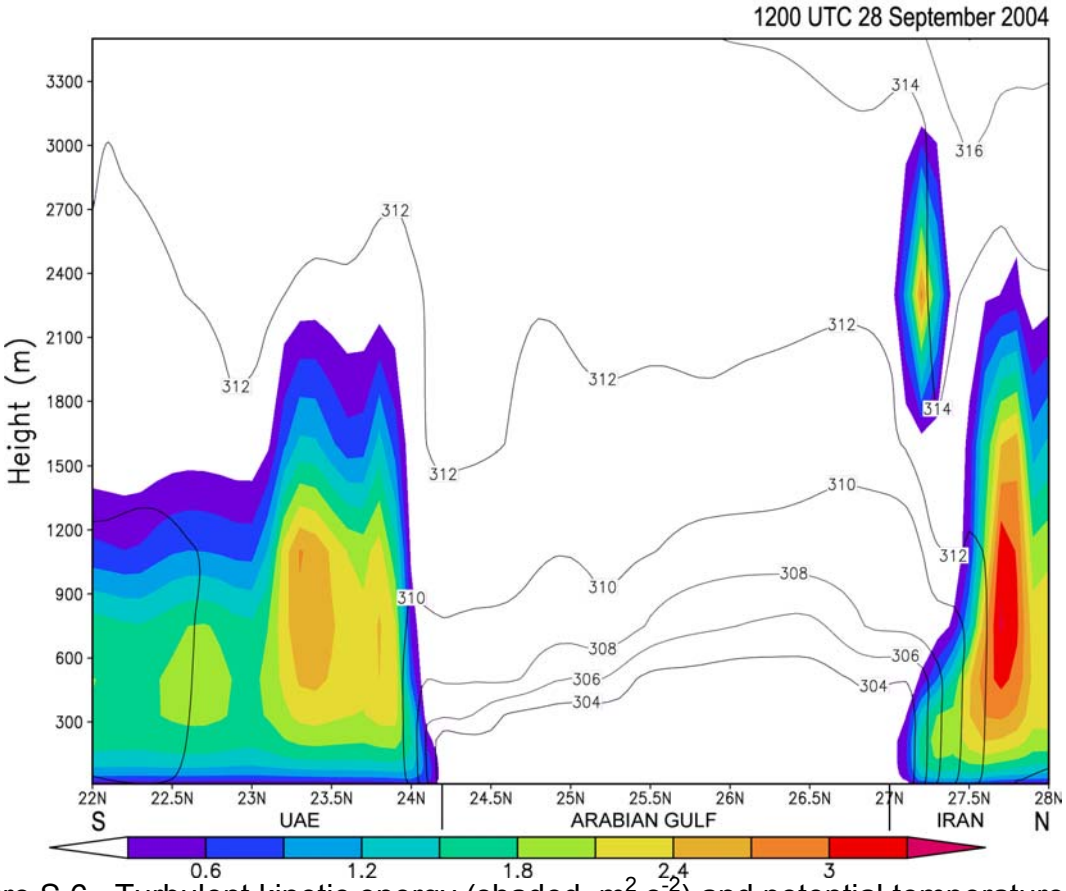

Figure S.6. Turbulent kinetic energy (shaded, m^2 s^{-2}) and potential temperature (contoured, K) for 1200 UTC (1600 LT) 28 September 2004 along 53.02°E from 22°N to 28°N.

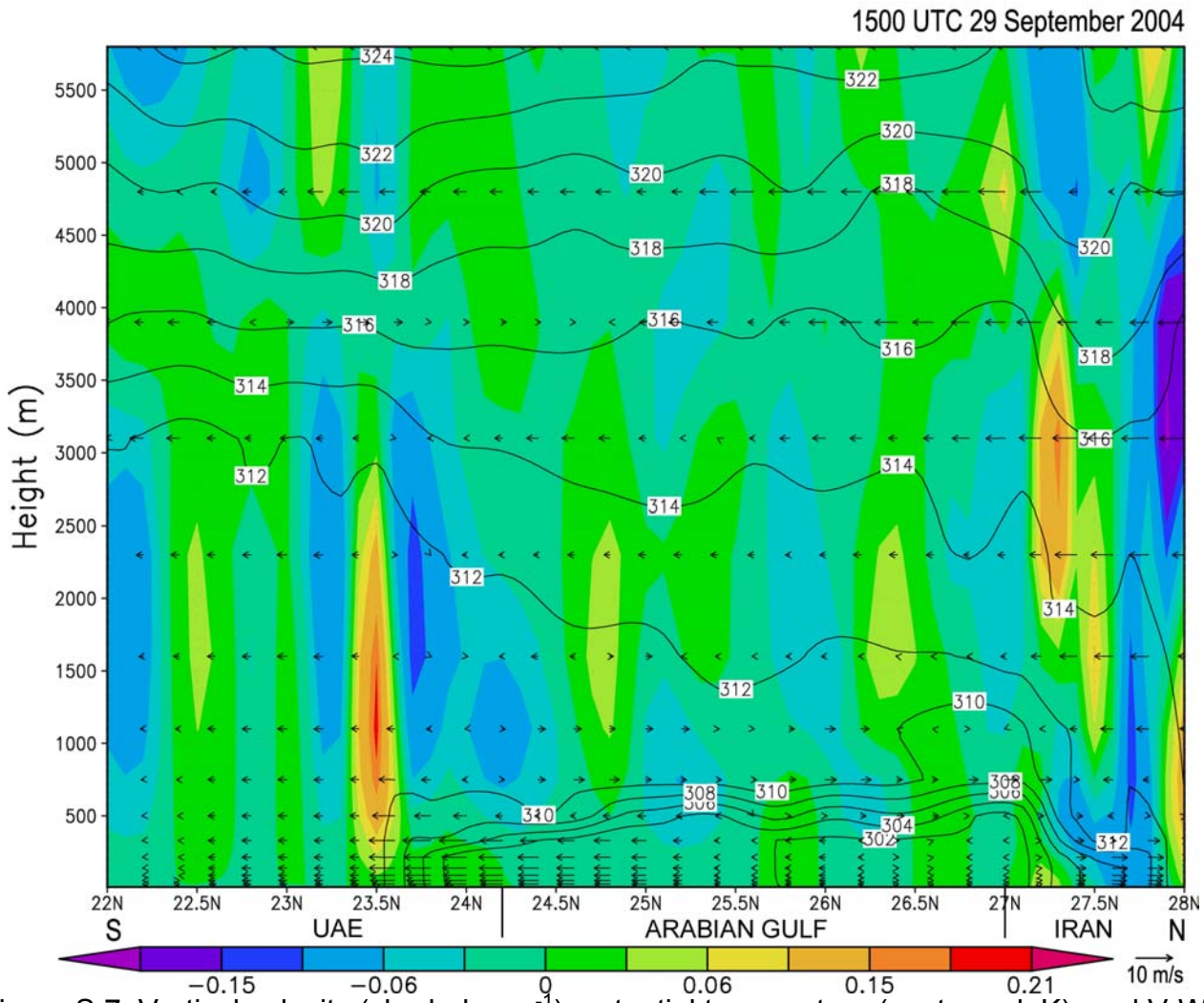

Figure S.7 Vertical velocity (shaded, m s^{-1}), potential temperature (contoured, K), and V-W wind vectors for 1500 UTC (1900 LT) 29 September 2004 along 53.02°E from 22°N to 28°N.

Appendix A. Mission Team Members

Airborne Deployment Team (Piketh and Reid)
Anthony Bucholtz (NRL Monterey): Airborne radiometers.
Dan Breed (NCAR): Cloud microphysics
Roelof Burger (SAWS/U. Witwatersrand): Cloud microphysics
Piotr Flatau (Scripps/UCSD): Airborne radiometers.
Charles Gatebe (GEST)/GSFC: CAR radiometer
Michael King (GSFC): CAR radiometer
Vanderlei Martins (GEST/GSFC): Aerosol particle absorption
Tara Jensen (NCAR): Cloud microphyscis
Stuart Piketh (U. Witwatersrand): Cloud microphysics.
John Porter (University of Hawaii): Airborne lidar
Jeffrey Reid (NRL Monterey): Aerosol microphysics, land-sea meteorology
Kristy Ross (U. Witwatersrand): Aerosol chemistry

Ground Deployment Team (Holben)
Steve Cliff (UC Davis): DRUM impactor
Arie de Jong (TNO): IR differential radiance spectroscopy, transmissometry
Gerrit de Leeuw (TNO): Transmissometry
Thomas Eck (GEST/GSFC): AERONET retrievals
Piotr Flatau (Scripps/UCSD): Surface radiative properties
Brent Holben (GSFC): AERONET Sun photometer
Jack Ji (GEST/GSFC): SMART/COMMIT
Krzysztof Markowicz (U of Warsaw): Aerosol radiative forcing
Vanderlei Martins (GEST/GSFC): Aerosol particle absorption
Norm O'Neill (Univ. of Sherbrooke): Aerosol optical properties.
Antonio Queface, (U Witwatersrand): Radiaition
Elizabeth Reid (NRL Monterey): Single particle analysis, MPL lidar
Jeffrey Reid (NRL Monterey): Aerosol Chemistry & microphysics.
Joanna Remiszewska (Univ. of Warsaw): Aerosol forcing, data assimilation
Joel Schafer (GEST/GSFC): AERONET retrievals
Alexander Smirnov (GEST/GSFC): AERONET retrievals
Si-Chee Tsay (GSFC): SMART, surface radiation.
Ellsworth Judd Welton (GSFC): Micropulse lidar
Nicola Walton (U. Witwatersrand): Atmospheric chemistry
Marcin Witek (U of Warsaw): Radiative forcing

Remote Sensing Team (Kahn, Hsu, Gatebe)
Robert Arnone (NRL Stennis): SeaWiFS & MODIS ocean products
Sundar Christopher (Univ. of Alabama): CERES & MODIS integration
Gerrit de Leeuw (TNO): AATSR
Phil Durkee (NPS): High-resolution AOT retrievals
Charles Gatebe (GEST/GSFC): Surface almucantar/CAR Fusion, BRDF
Hashem Al Hashemi (DWRS): Regional remote sensing/GIS
Christina Hsu (GEST/GSFC): AOT retrievals over bright surfaces

Ralph Kahn (JPL): MISR aerosol retrievals
Olga Kalashnikova (JPL): MISR aerosol retrievals
Jolanta T. Kusmierczyk (TNO): ATSR dust retrievals
Michel Legrand (Univ of Lille): Infrared properties of dust
Steve Miller (NRL Monterey): Dust products
Ben Ruston (NRL Monterey): Microwave radiance temperature inversions
Nazmi Saleous (GEST/GSFC): MODIS aerosol retrievals
Robin Schoemaker (TNO): ATSR aerosol retrievals
Adnan Sharaf (DWRS): Regional remote sensing/GIS
Dominick Vincent (NPS) High-resolution AOT retrievals

Meteorology Team (Westphal)
Hamid Brashdi (Dir. Gen. of Civil Aviation and Meteor., Oman): Regional meteorology
Mian Chin (GSFC): GOCART aerosol modeling
Rebecca Eager (NC State): COAMPS, land-sea flow processes
Suffian Farrah (DWRS): Regional forecasting
Tracy Haack (NRL Monterey): near surface temperature/humidity profiles
Ahmed Ibrahim (DWRS): Regional forecasting
Ming Liu (NRL Monterey): COAMPS dust forecasting
Sethu Raman (NC State): COAMPS, land-sea flow processes
Annette Walker (NRL Monterey): Dust forecasting and source functions
Douglas Westphal (NRL Monterey): NAAPS dust forecasting

South African Aerocommander Crew (Piketh)
Steve Broccardo (Orsmond Aviation): South African project manager
Steve Edwards (Orsmond Aviation): Electrical engineer
Hans Kruger (Orsmond Aviation): Cloud seeding pilot
Steve Mandel (Orsmond Aviation): Aerocommander cloud seeding chief pilot
Harry McGarry (Orsmond Aviatian): Chief mechanic
Gary Willis (Orsmond Aviation): Aerocommander UAE^2 chief pilot

Appendix B. Aerocommander Flight Tracks

This appendix contains the flight tracks of the South African Aerocommander aircraft utilized in the UAE^2 campaign. The South African Weather Services are the sole owners of the aircraft although it is operated in the United Arab Emirates under the lease to Orsmond Aerial Spray (PTY) Ltd The aircraft is twin turbo prop aircraft with Garret turbine engines. The aircraft are pressurized and are able to operate between sea level and approximately 28 000ft. Over the past year one of the aircraft, ZS-JRB, has been utilized in the United Arab Emirates for both atmospheric chemistry and weather modification experiments.

The airplane operates with standard aircraft avionic equipment. It is equipped with a GARMIN GNS430 Global Positioning System. The Aircraft has several atmospheric measurement capabilities that have been added over the past five years. The aircraft measures all atmospheric state parameters. These include temperature, pressure, humidity, dew point temperature and liquid water content

In addition, the airplane is equipped to carry six PMS aerosol and water droplet probes. Two probes are mounted on the front nose of the aircraft and two probes are hung under each wing. Several PMS probes are available for use on the aircraft. These include a Forward Scattering Spectrometer Probe (FSSP 100), a Optical Array Probe (OAP2DP or OAP2D2P), a Two Dimensional Cloud Probe (2DC or 2D2C) and a Passive Cavity Aerosol Spectrometer Probe (PCASP 100x).

A series of other equipment can be mounted in the interior of the airplane. In general the equipment is housed in 19 " rack mounts. All data collected on the aircraft can be logged on a dedicated Airborne Data Acquisition System (ADAS). The ADAS is capable of storing data at 10 Hz on a flash card. The data is converted into NetCDF and ASCII format during post-processing. Depending on the configuration of the equipment mounted in the aircraft, it is possible for two scientists in addition to the pilot to fly on board the aircraft during a research flight.

Additional equipment installed on the Aerocommander for the mission included and airborne lidar. a three wavelength nephelometer, an aerodynamic particle sizer, and filter samplers

Flight tracks are color coded by a relative scale of coarse mode particle mass concentration.

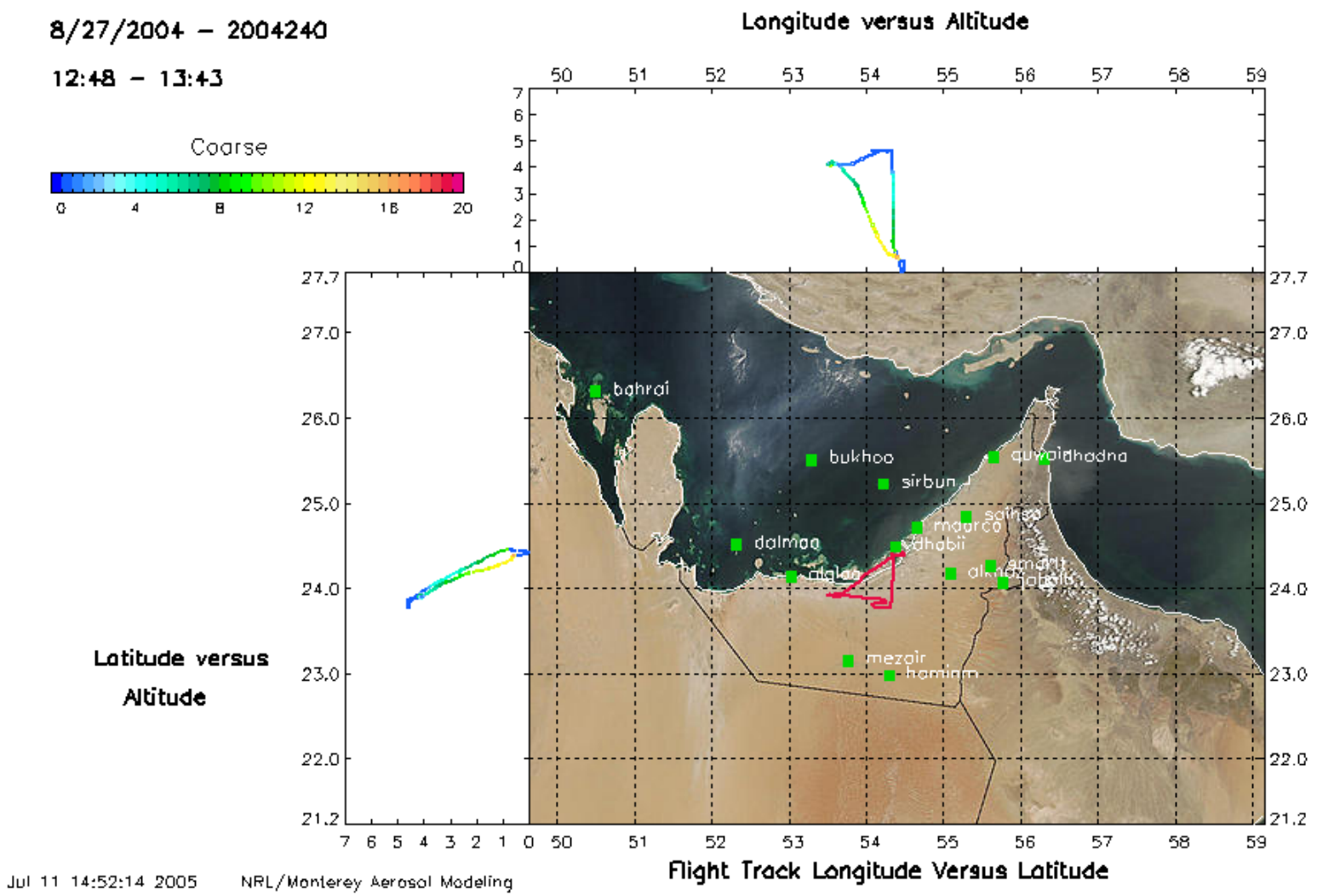
JRAUAE2-20040827A
8/27/2004 - 2004240
12:48 - 13:43
Coarse
0 4 8 12 16 20
Longitude versus Altitude
Latitude versus Altitude
Flight Track Longitude Versus Latitude
bahrai
bukhoo
sirbun
dalmaa
mezair
hamim
Jul 11 14:52:14 2005
NRL/Monterey Aerosol Modeling

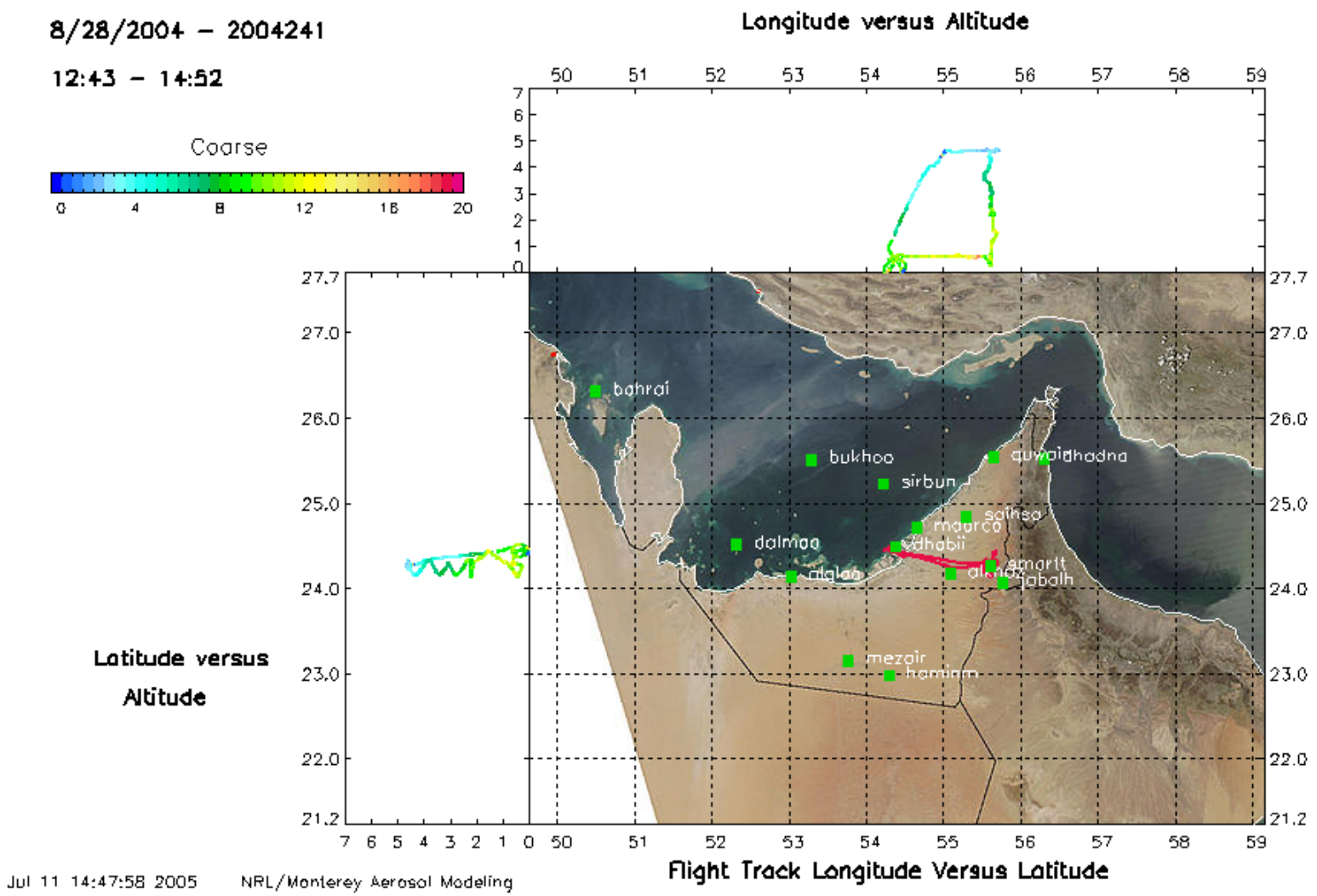
JRAUAE2-20040828A
8/28/2004 - 2004241
12:43 - 14:52
Coarse
0 4 8 12 16 20
Longitude versus Altitude
Latitude versus Altitude
bahrai
bukhoo
sirbun
quwaidhaena
saihsa
maurco
dalmaa
abudhabi
alqlaa
alkhaz
jabalh
mezair
hamiam
Flight Track Longitude Versus Latitude
Jul 11 14:47:58 2005
NRL/Monterey Aerosol Modeling

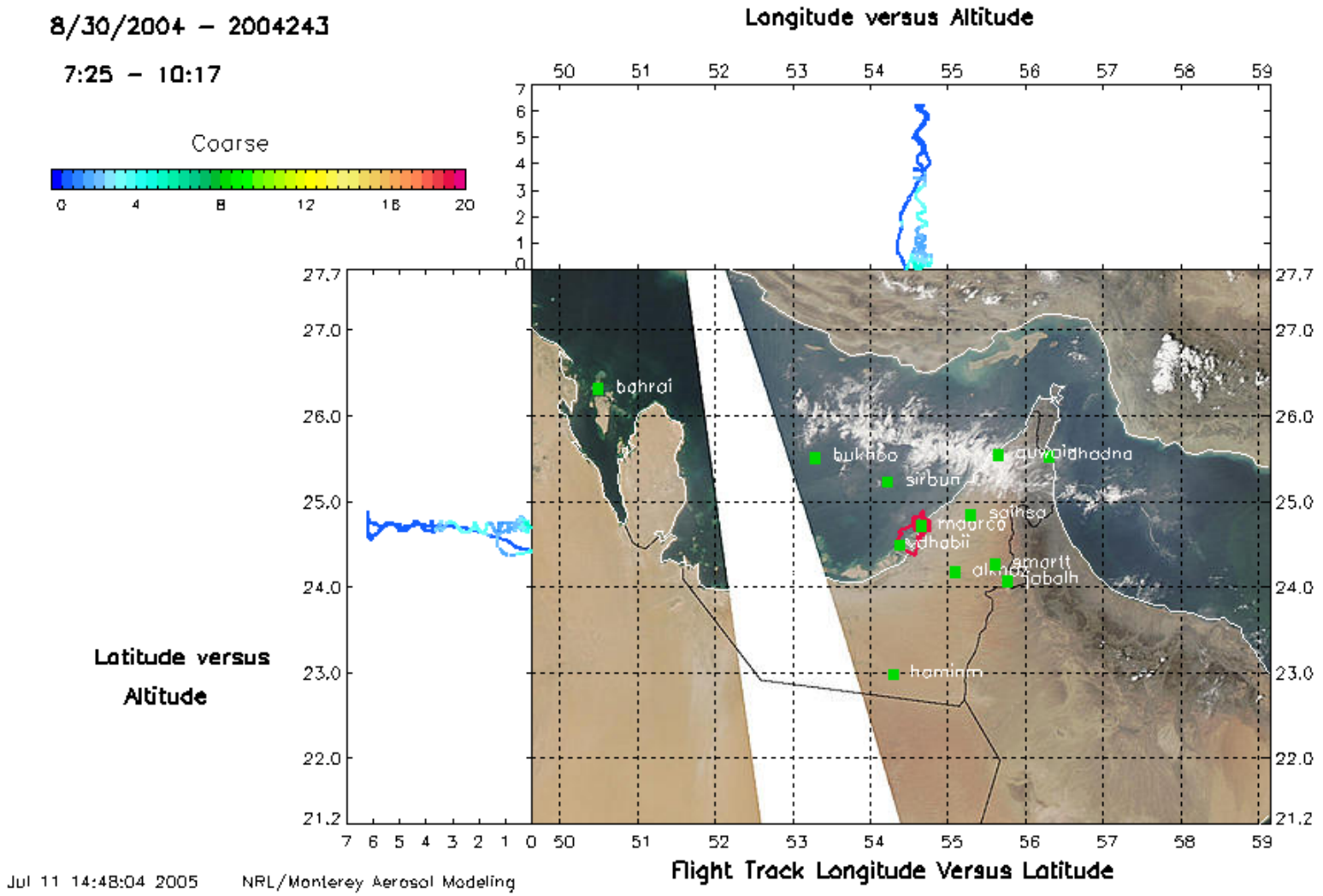
JRAUAE2-20040830A
8/30/2004 - 2004243
7:25 - 10:17
Coarse
0
4
8
12
16
20
Longitude versus Altitude
50
51
52
53
54
55
56
57
58
59
27.7
27.0
26.0
25.0
24.0
23.0
22.0
21.2
bahrai
bukhbo
sirbun
saihsa
maurco
abdhabii
amarit
jabalh
hamimm
Latitude versus Altitude
Flight Track Longitude Versus Latitude
Jul 11 14:48:04 2005
NRL/Monterey Aerosol Modeling

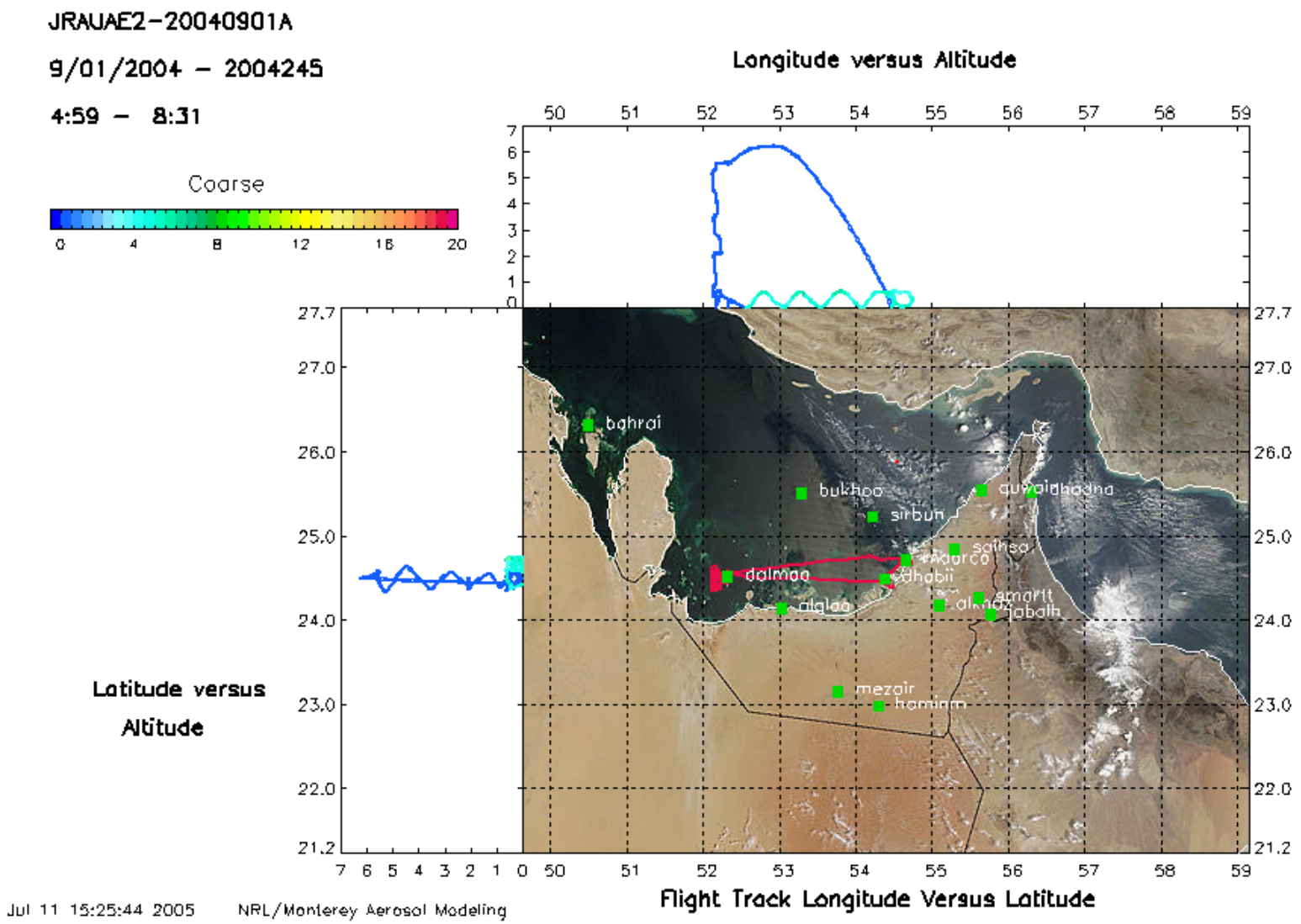
JRAUAE2-20040901A
9/01/2004 – 2004245
4:59 – 8:31
Coarse
0 4 8 12 16 20
Longitude versus Altitude
Latitude versus Altitude
Flight Track Longitude Versus Latitude
Jul 11 15:25:44 2005
NRL/Monterey Aerosol Modeling
bahrai
bukhoo
sirbun
quweidhana
saihsa
madrca
dalmaa
abuDhabii
alqlaa
alkhaz
smarit
jabalh
mezair
hamim

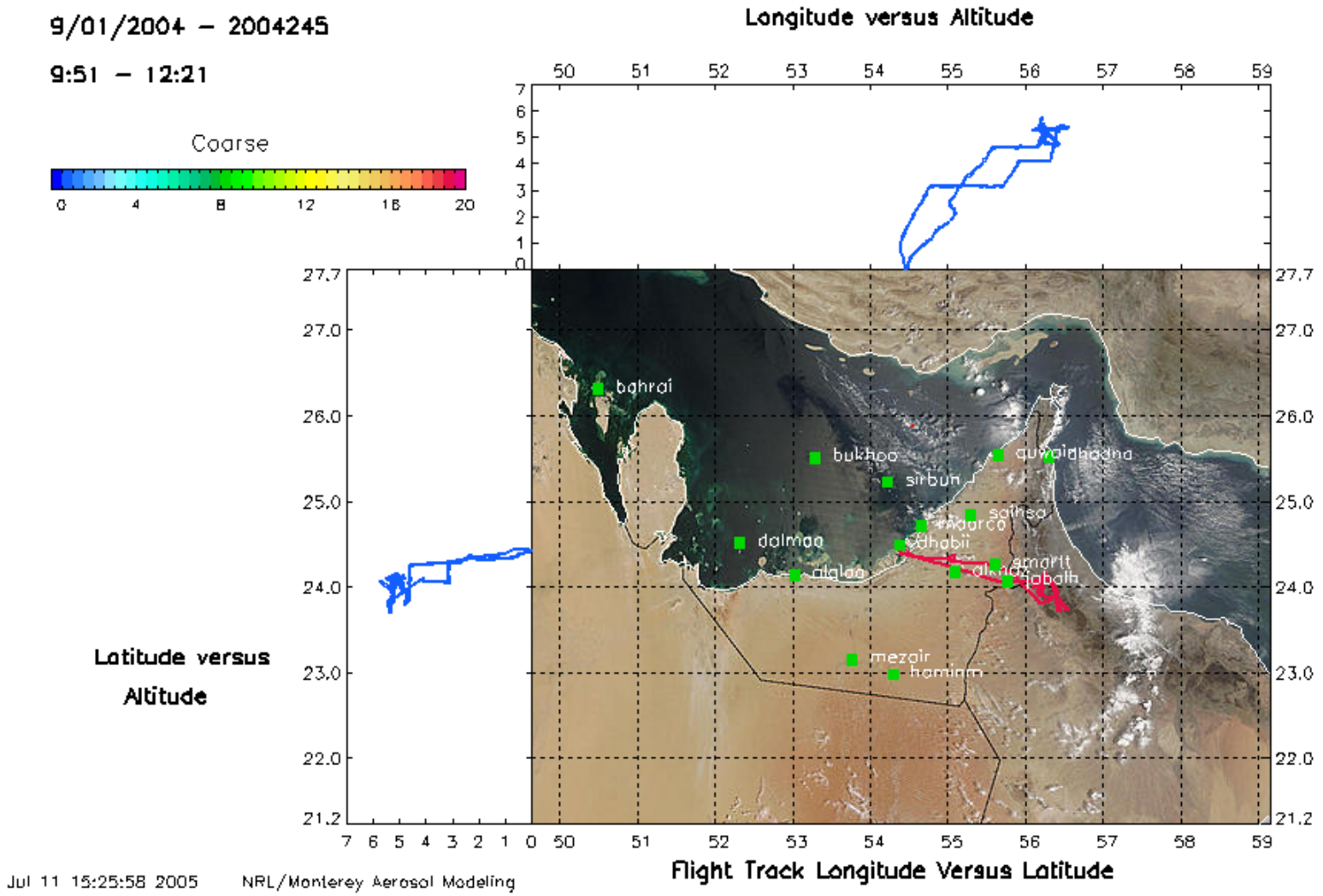
JRANCAR-20040901A
9/01/2004 - 2004245
9:51 - 12:21
Coarse
0
4
8
12
16
20
Longitude versus Altitude
Latitude versus Altitude
bahrai
bukhoo
sirbun
qurqaidhadna
saihsa
madrca
dalmaa
abhabi
smarit
jabalh
alqlaa
mezair
hamimm
Jul 11 15:25:58 2005
NRL/Monterey Aerosol Modeling
Flight Track Longitude Versus Latitude

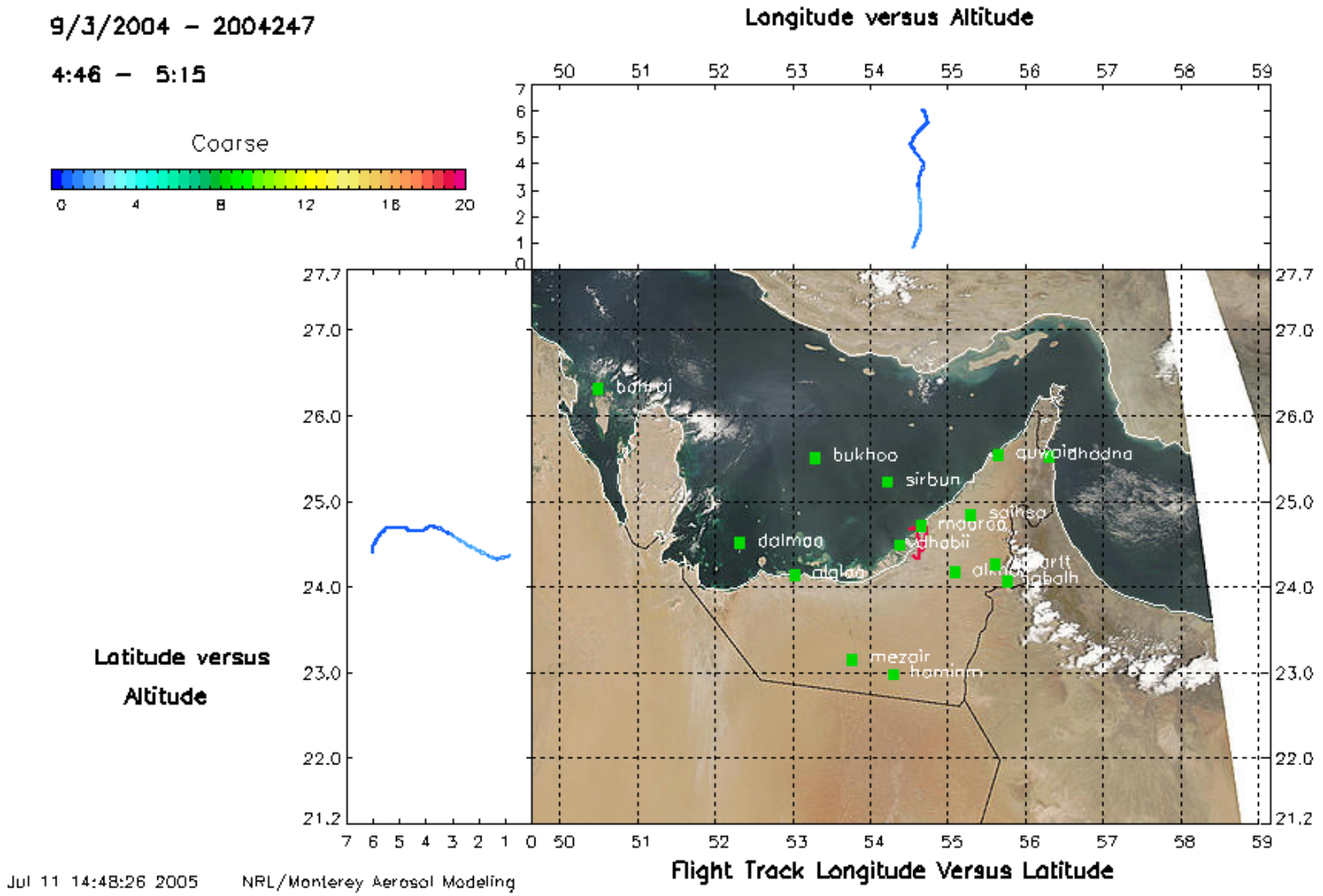
JRAUAE2-20040903A
9/3/2004 - 2004247
4:46 - 5:15
Coarse
0 4 8 12 16 20
Longitude versus Altitude
Latitude versus Altitude
Flight Track Longitude Versus Latitude
Jul 11 14:48:26 2005
NRL/Monterey Aerosol Modeling
bahrai
bukhoo
sirbun
quwaidhaina
saihsa
maqraa
dalmaa
abhabii
mezair
hamiam

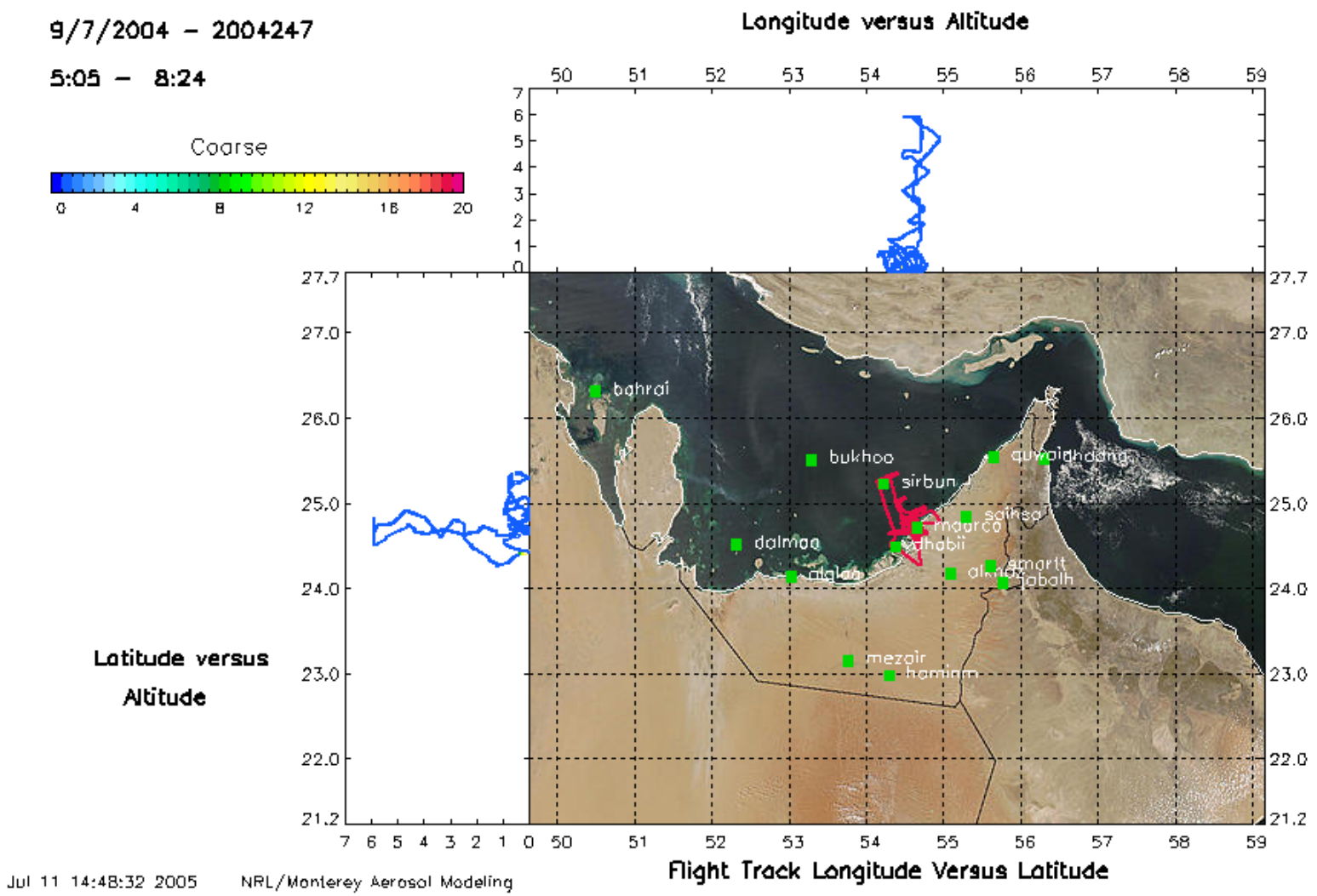
JRAUAE2-20040907A
9/7/2004 - 2004247
5:05 - 8:24
Coarse
0 4 8 12 16 20
Longitude versus Altitude
Latitude versus Altitude
Flight Track Longitude Versus Latitude
Jul 11 14:48:32 2005
NRL/Monterey Aerosol Modeling
bahrai
bukhoo
sirbun
dalmaa
mezair
hamim
jabalh

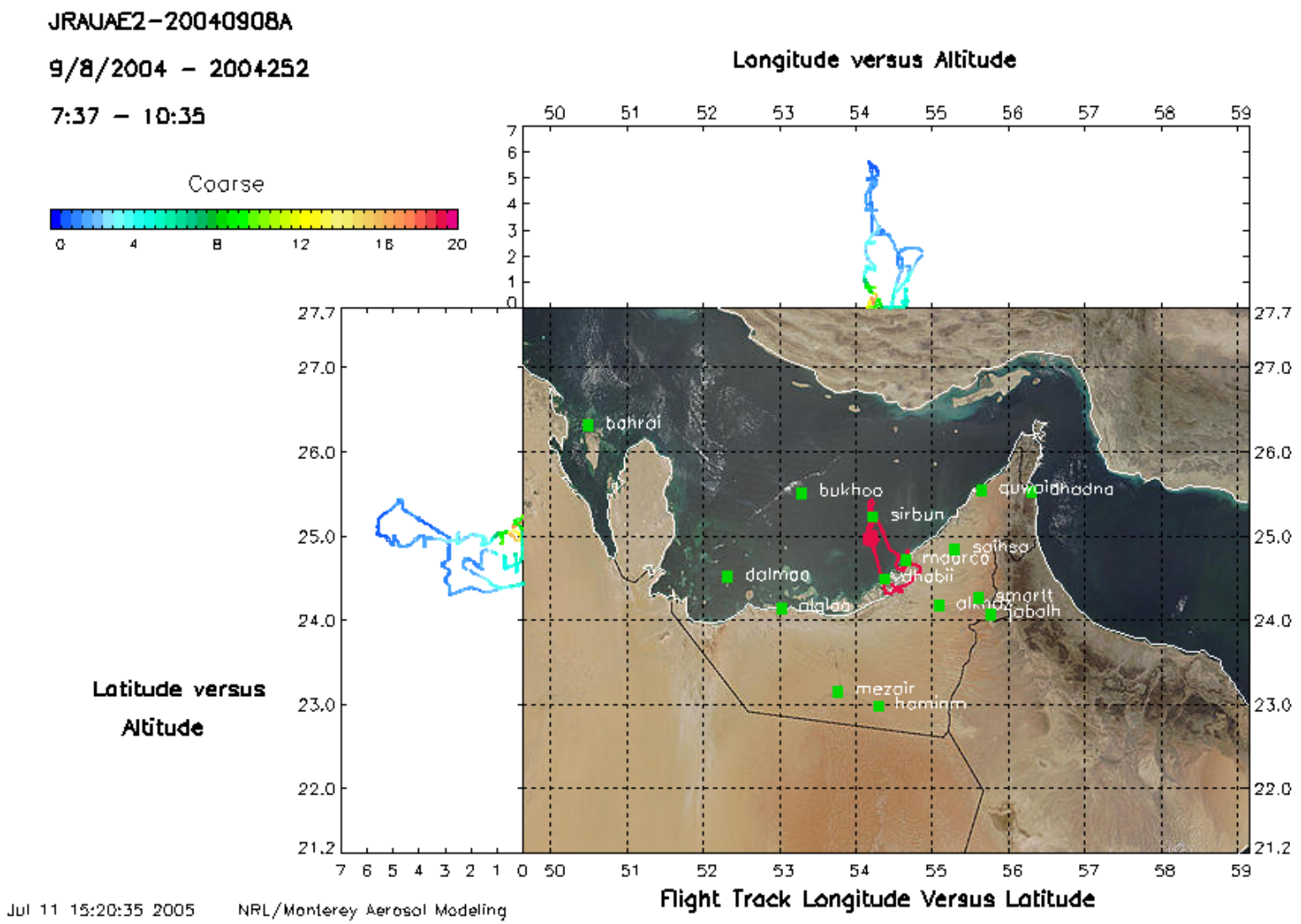
JRAUAE2-20040908A
9/8/2004 - 2004252
7:37 - 10:35
Coarse
0
4
8
12
16
20
Longitude versus Altitude
Latitude versus Altitude
Flight Track Longitude Versus Latitude
bahrai
bukhoo
sirbun
quwaidhadna
saihsa
maurco
dalmaa
abdabii
alglaa
smarit
jabalh
mezair
hamiam
Jul 11 15:20:35 2005
NRL/Monterey Aerosol Modeling

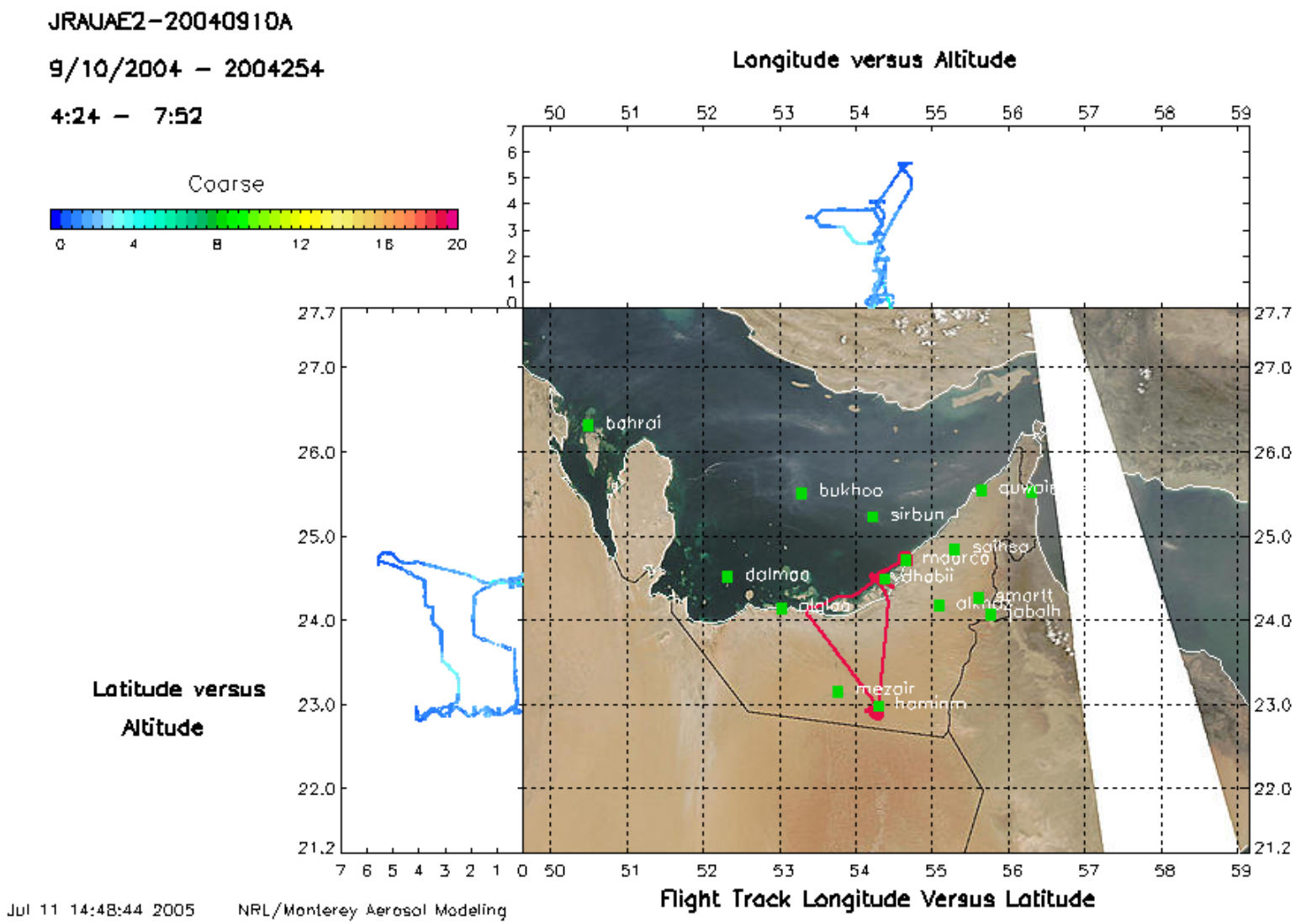
JRAUAE2-20040910A
9/10/2004 – 2004254
4:24 – 7:52
Coarse
0 4 8 12 16 20
Longitude versus Altitude
Latitude versus Altitude
Flight Track Longitude Versus Latitude
bahrai
bukhoo
sirbun
dalmaa
mezair
hamim
Jul 11 14:48:44 2005
NRL/Monterey Aerosol Modeling

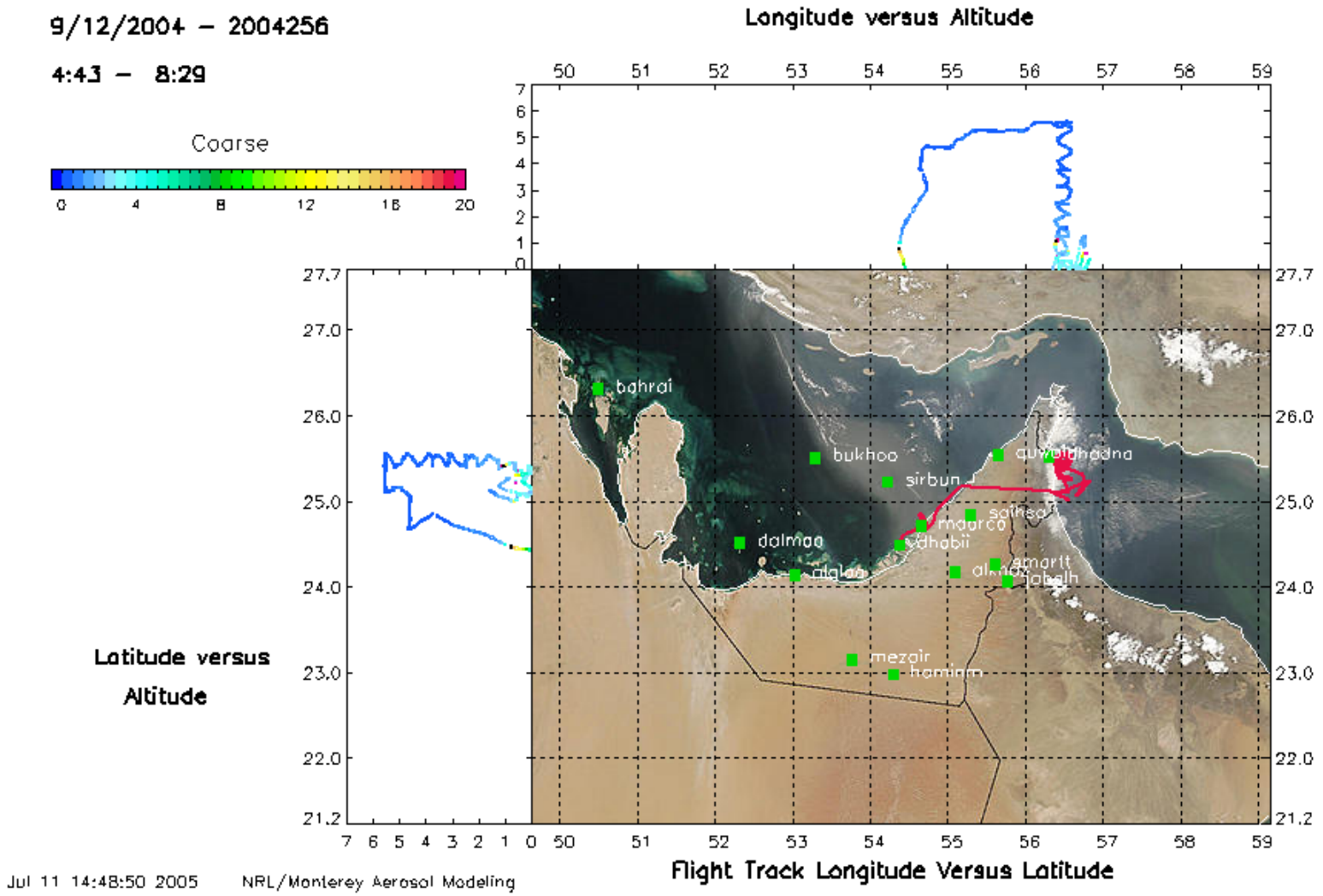
JRAUAE2-20040912A
9/12/2004 – 2004256
4:43 – 8:29
Coarse
0 4 8 12 16 20
Longitude versus Altitude
Latitude versus Altitude
bahrai
bukhoo
sirbun
dalmaa
mezair
hamiam
Flight Track Longitude Versus Latitude
Jul 11 14:48:50 2005
NRL/Monterey Aerosol Modeling

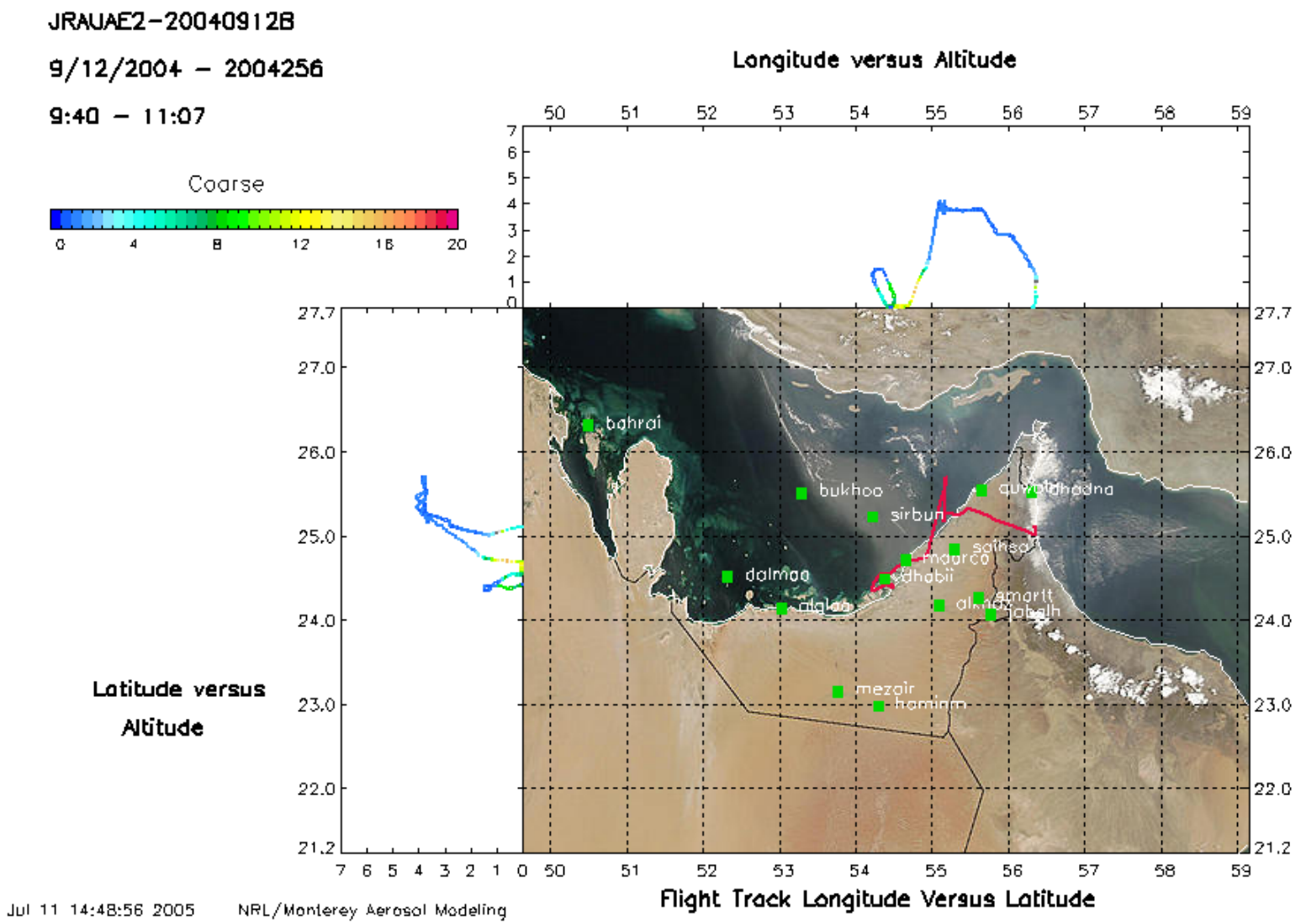
JRAUAE2-20040912B
9/12/2004 – 2004256
9:40 – 11:07
Coarse
0 4 8 12 16 20
Longitude versus Altitude
Latitude versus Altitude
bahrai
bukhoo
sirbun
dalmaa
mezair
hamiam
Jul 11 14:48:56 2005
NRL/Monterey Aerosol Modeling
Flight Track Longitude Versus Latitude

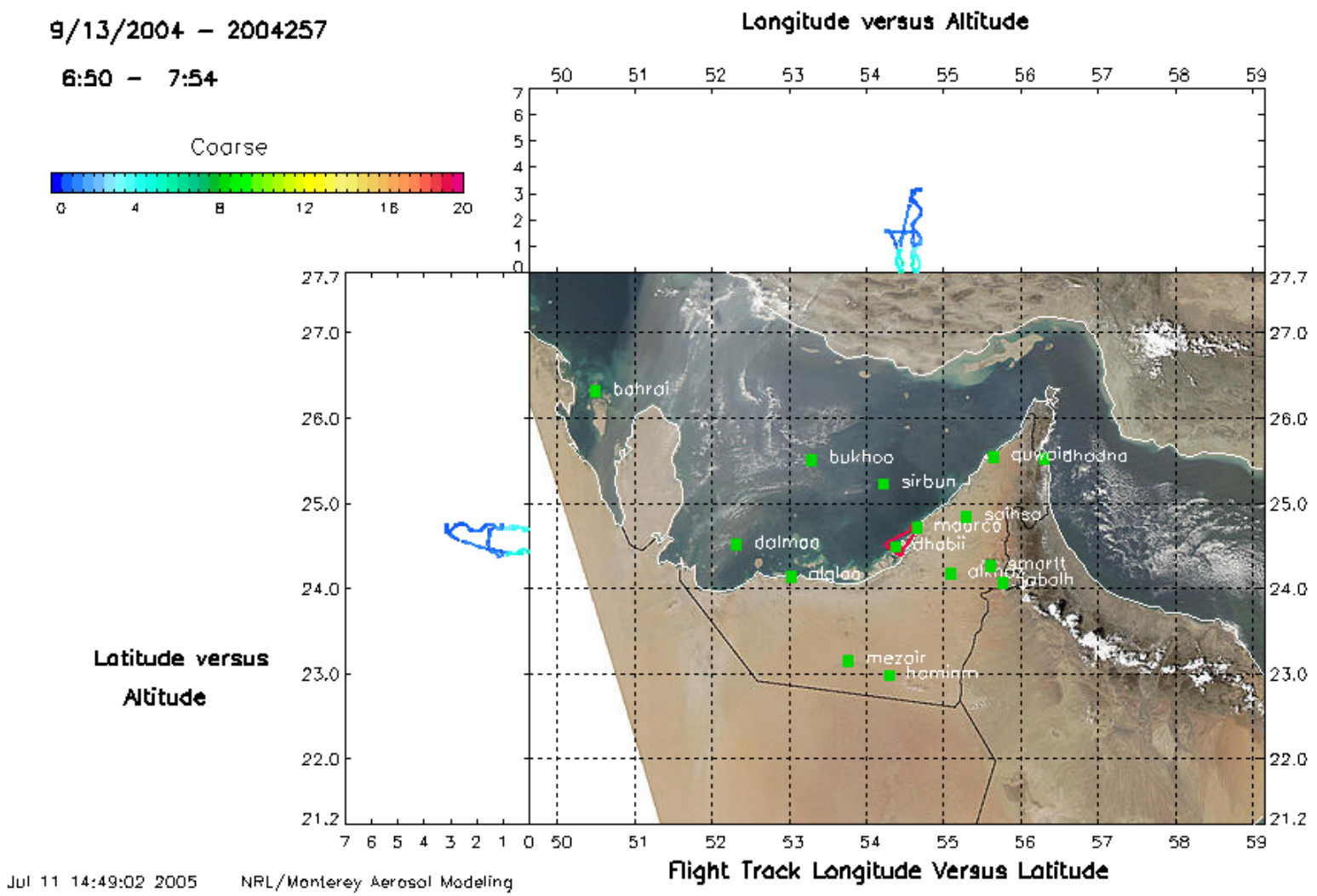
JRAUAE2-20040913A
9/13/2004 - 2004257
6:50 - 7:54
Coarse
0 4 8 12 16 20
Longitude versus Altitude
Latitude versus Altitude
Flight Track Longitude Versus Latitude
bahrai
bukhoo
sirbun
quwaidhaena
saihsa
maurco
dhabii
dalmaa
alqlaa
almarft
jabalh
mezair
hamiam
Jul 11 14:49:02 2005
NRL/Monterey Aerosol Modeling

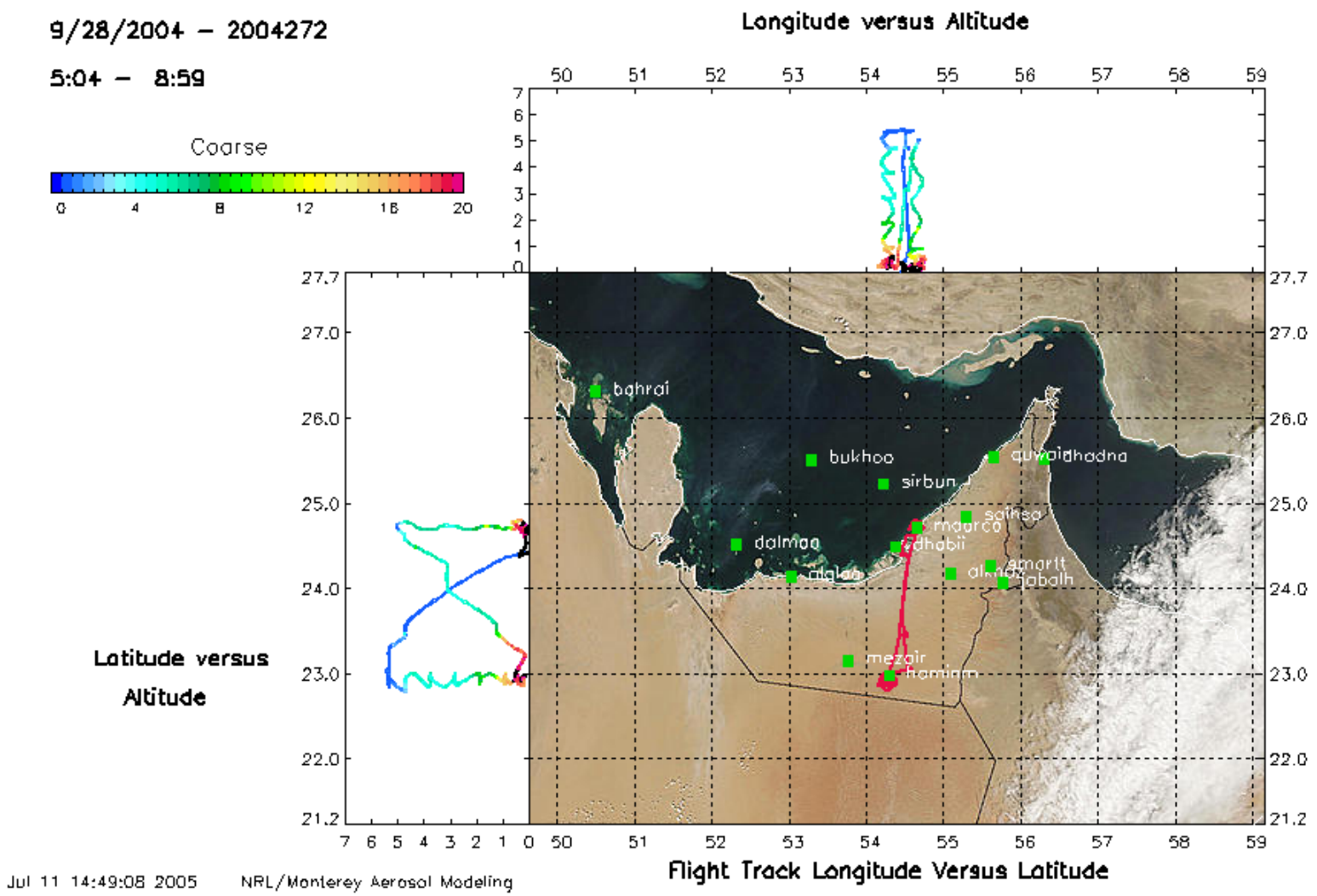
JRAUAE2-20040928A
9/28/2004 – 2004272
5:04 – 8:59
Coarse
0 4 8 12 16 20
Longitude versus Altitude
Latitude versus Altitude
bahrai
bukhoo
sirbun
dalmaa
mezair
hamiam
Jul 11 14:49:08 2005
NRL/Monterey Aerosol Modeling
Flight Track Longitude Versus Latitude

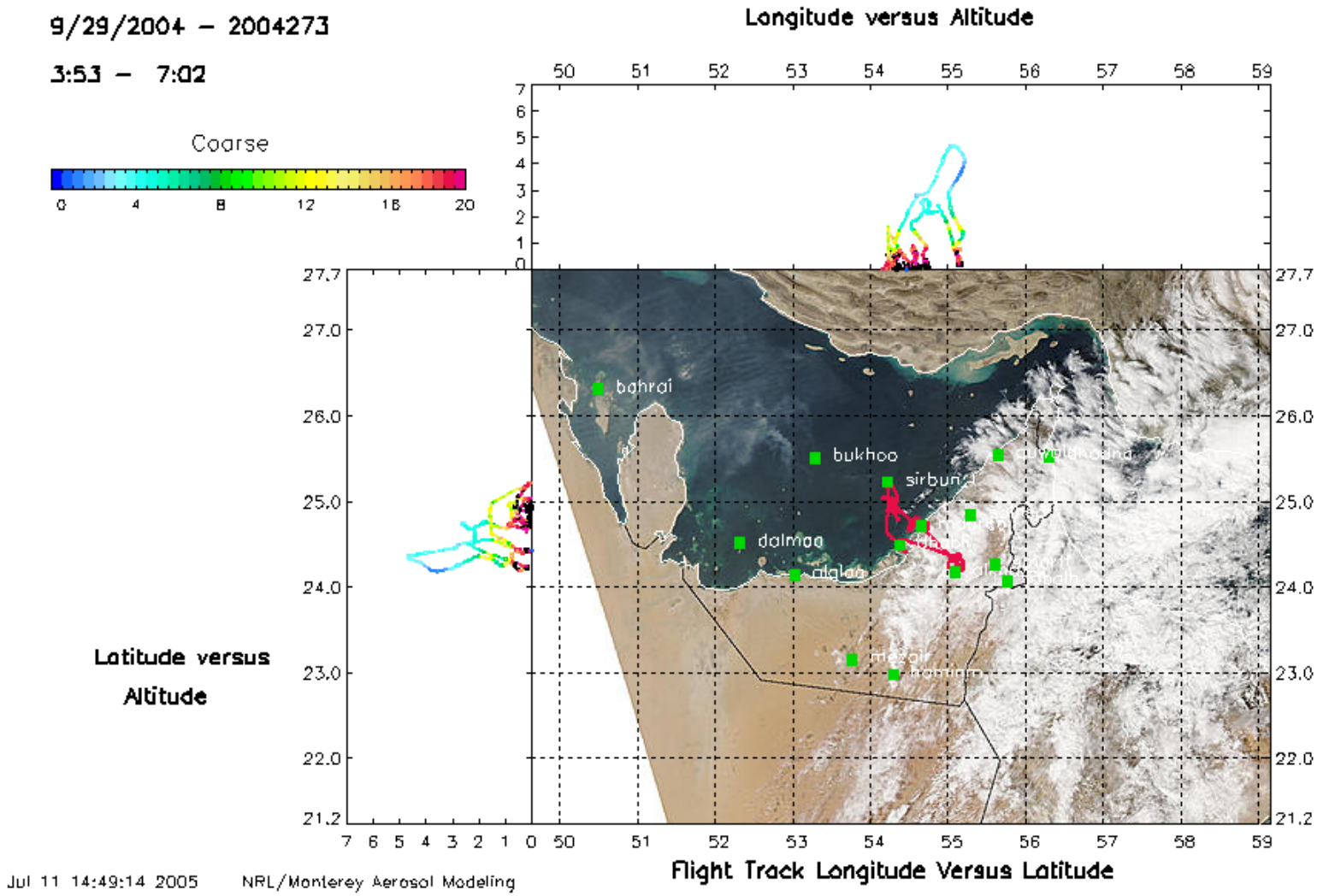
JRAUAE2-20040929A
9/29/2004 – 2004273
3:53 – 7:02
Coarse
0 4 8 12 16 20
Longitude versus Altitude
Latitude versus Altitude
bahrai
bukhoo
sirbuni
dalmaa
Flight Track Longitude Versus Latitude
Jul 11 14:49:14 2005
NRL/Monterey Aerosol Modeling

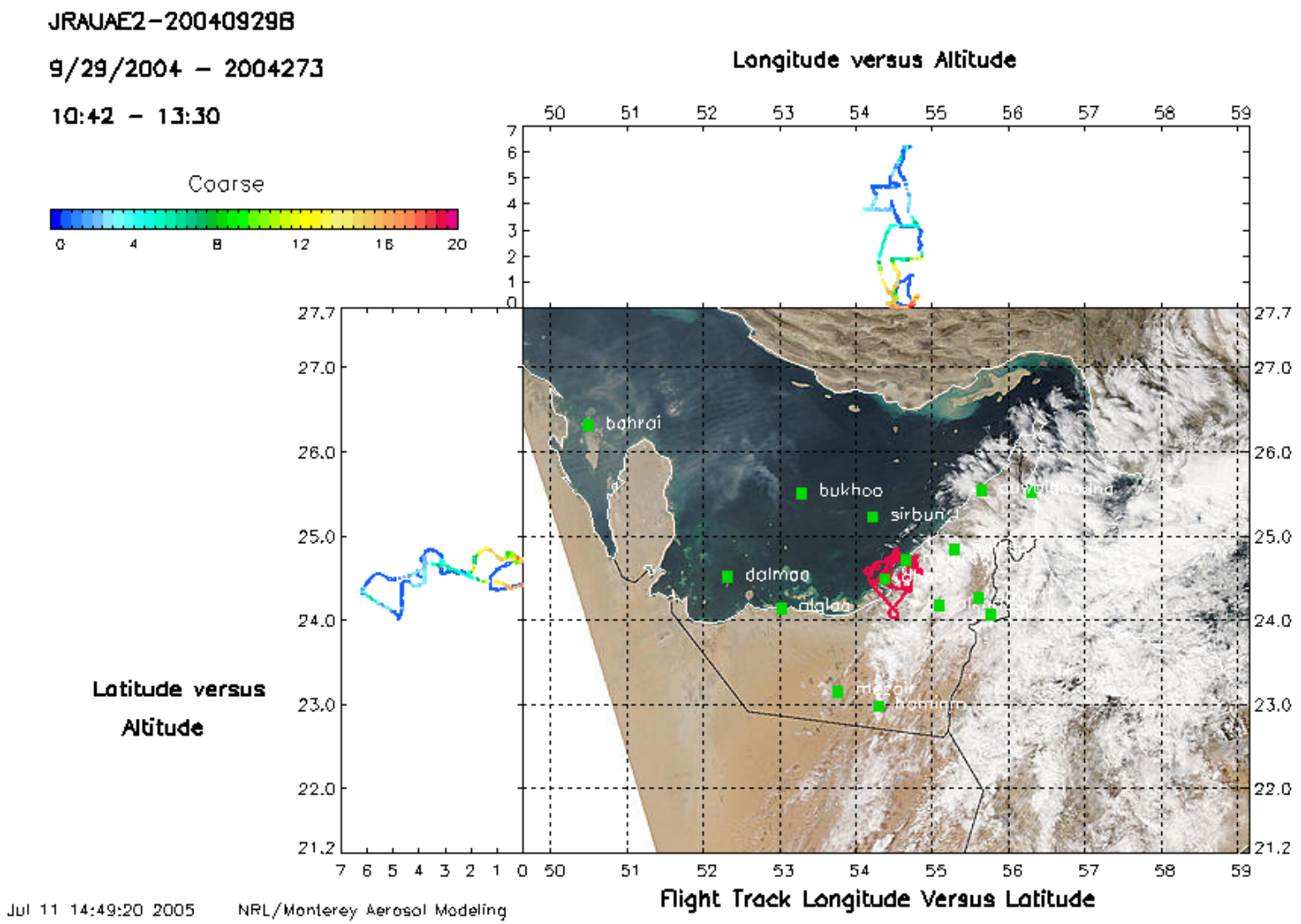
JRAUAE2-20040929B
9/29/2004 – 2004273
10:42 – 13:30
Coarse
0 4 8 12 16 20
Longitude versus Altitude
Latitude versus Altitude
bahrai
bukhoo
sirbuni
dalmaa
mezai
Jul 11 14:49:20 2005
NRL/Monterey Aerosol Modeling
Flight Track Longitude Versus Latitude

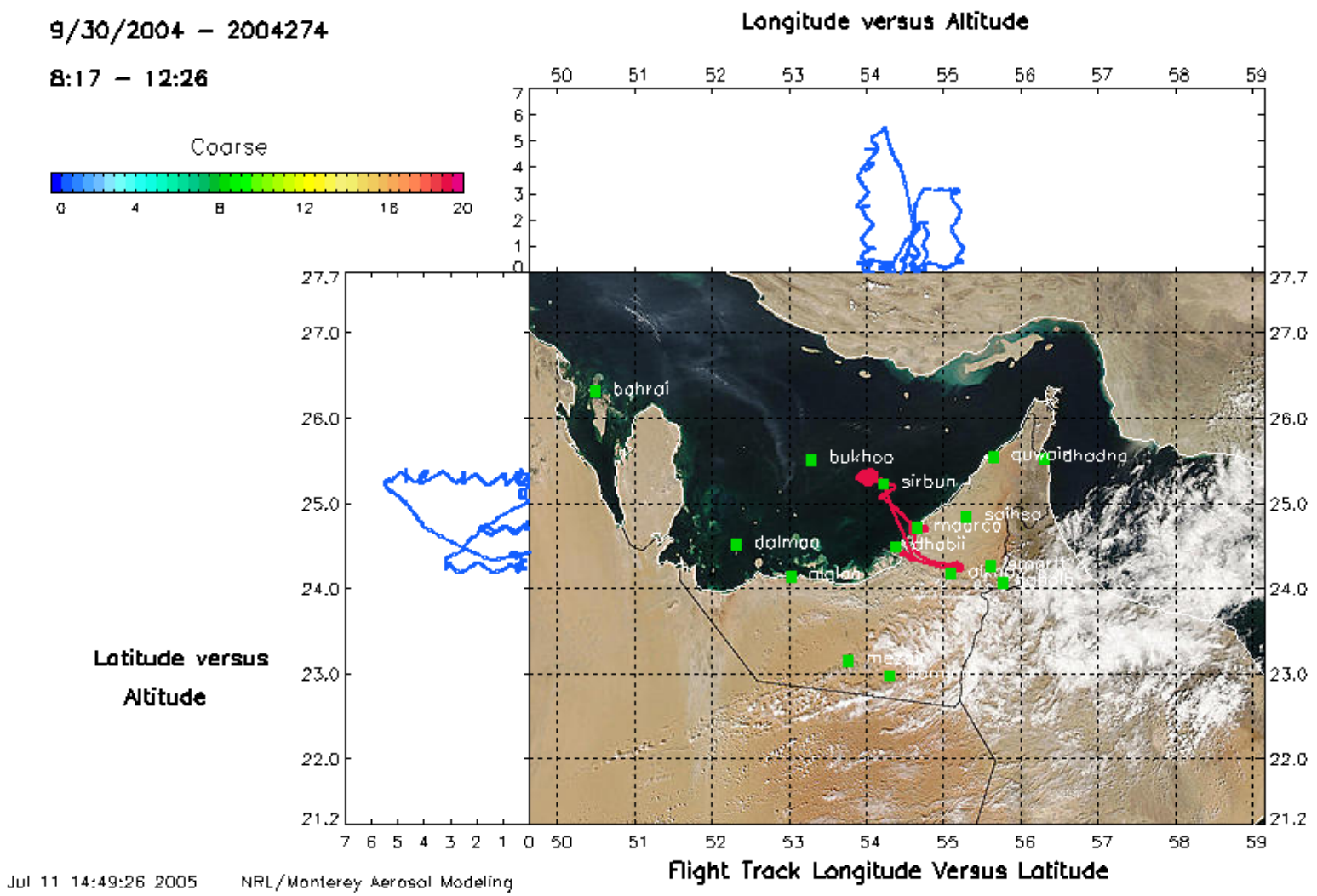
JRAUAE2-20040930A
9/30/2004 - 2004274
8:17 - 12:26
Coarse
0
4
8
12
16
20
Longitude versus Altitude
Latitude versus Altitude
bahrai
bukhoo
sirbun
dalmaa
Flight Track Longitude Versus Latitude
Jul 11 14:49:26 2005
NRL/Monterey Aerosol Modeling

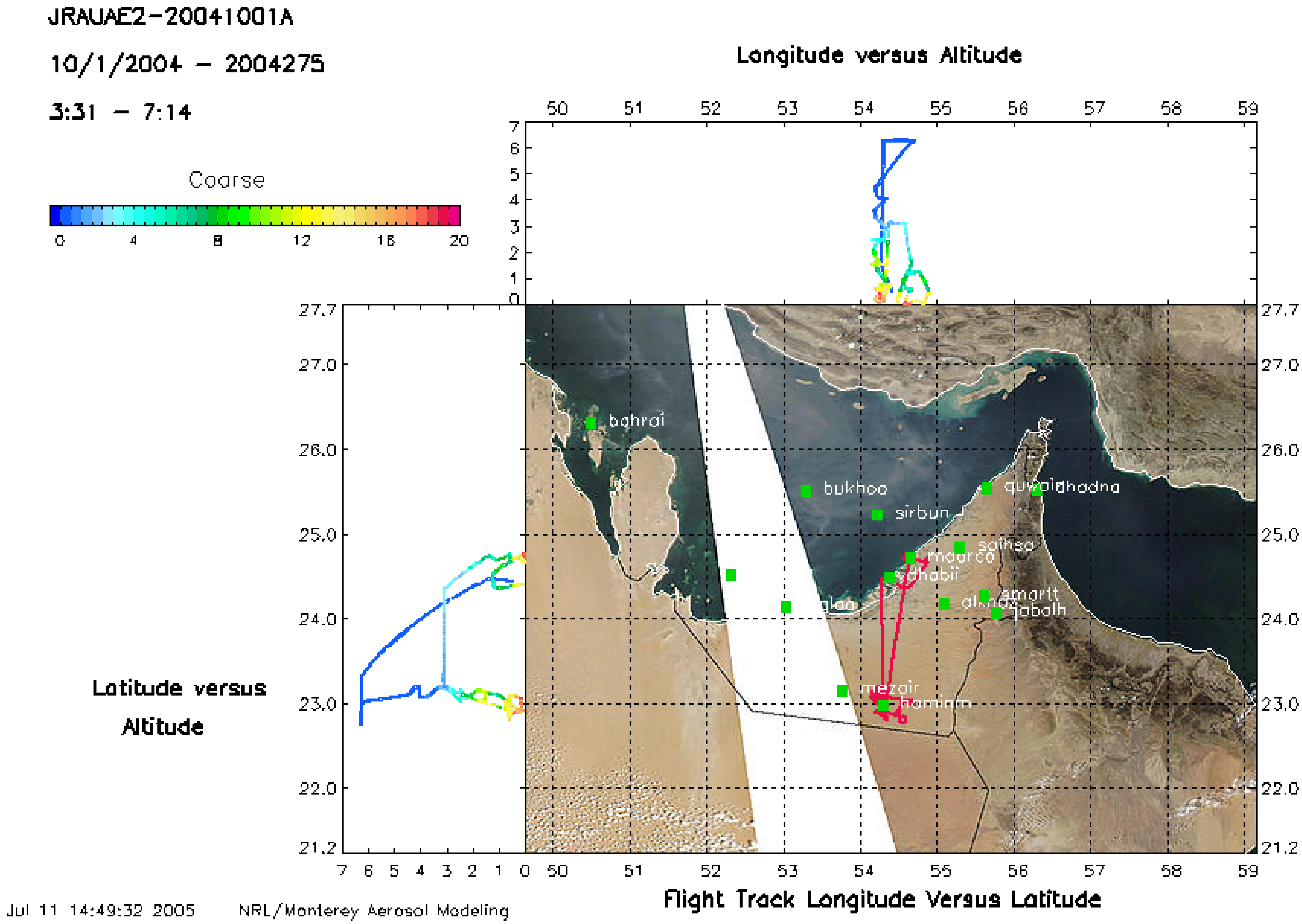
JRAUAE2-20041001A
10/1/2004 - 2004275
3:31 - 7:14
Coarse
0 4 8 12 16 20
Longitude versus Altitude
Latitude versus Altitude
Flight Track Longitude Versus Latitude
bahrai
bukhoo
sirbun
quwaidhadna
saihsa
maqrca
dhabii
amarit
jabalh
mezair
hamim
Jul 11 14:49:32 2005
NRL/Monterey Aerosol Modeling

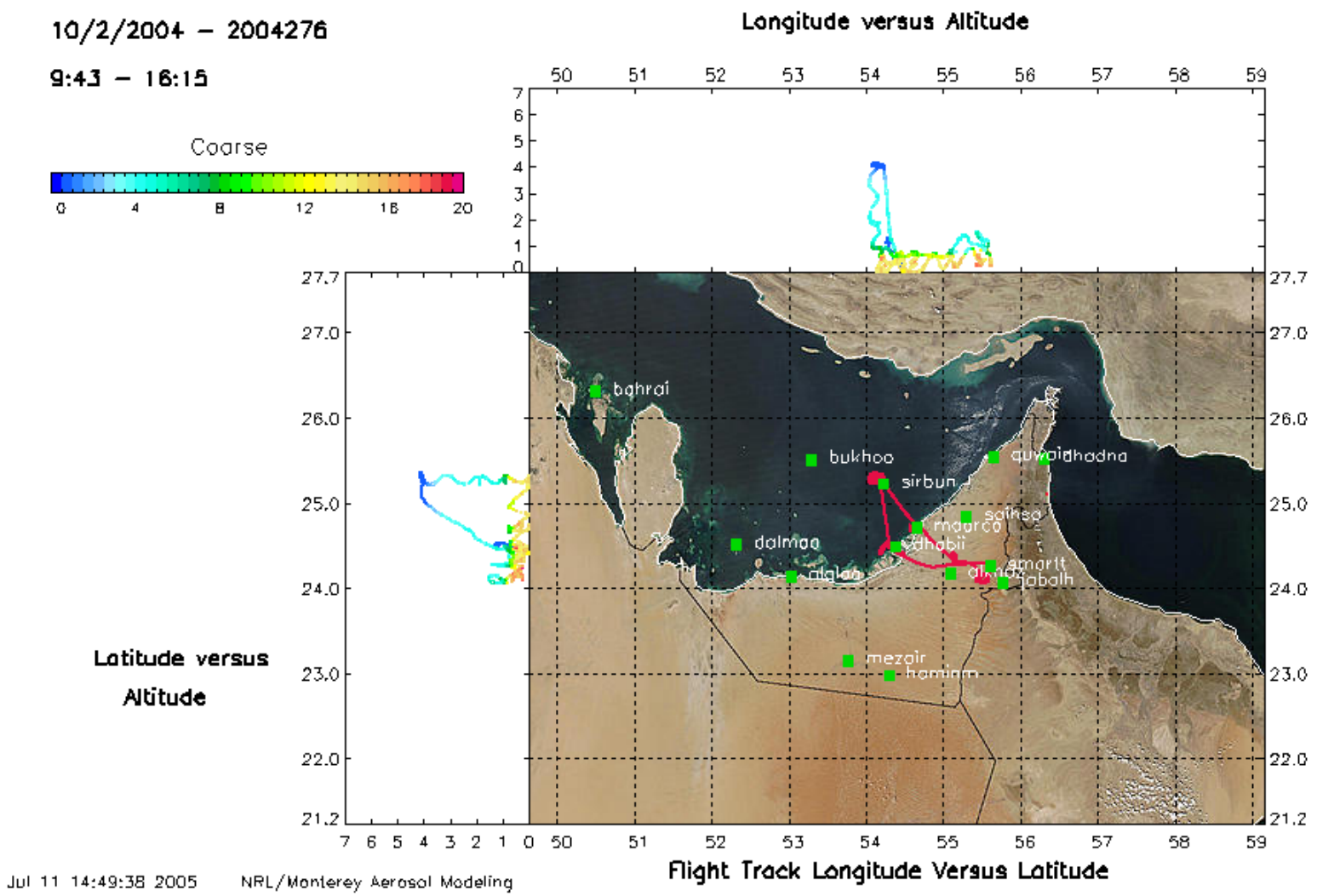
JRAUAE2-20041002A
10/2/2004 – 2004276
9:43 – 16:15
Coarse
0
4
8
12
16
20
Longitude versus Altitude
Latitude versus Altitude
Flight Track Longitude Versus Latitude
Jul 11 14:49:38 2005
NRL/Monterey Aerosol Modeling
bahrai
bukhoo
sirbun
quwaidhadna
saihsa
maurco
dalmaa
dhabii
amarit
jabalh
mezair
haminm

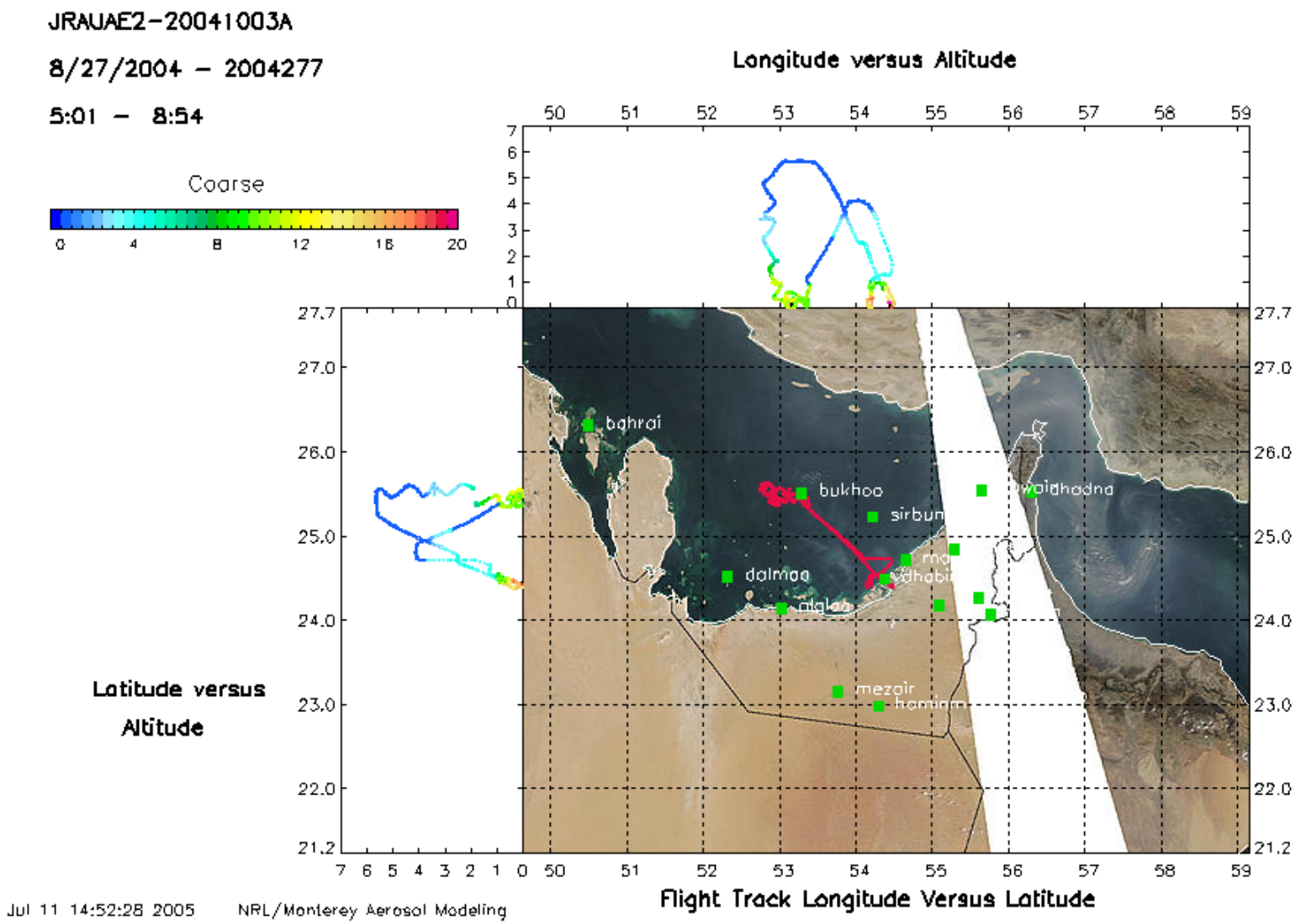
JRAUAE2-20041003A
8/27/2004 - 2004277
5:01 - 8:54
Coarse
0
4
8
12
16
20
Longitude versus Altitude
Latitude versus Altitude
bahrai
bukhoo
sirbun
dalmaa
mezair
Flight Track Longitude Versus Latitude
Jul 11 14:52:28 2005
NRL/Monterey Aerosol Modeling

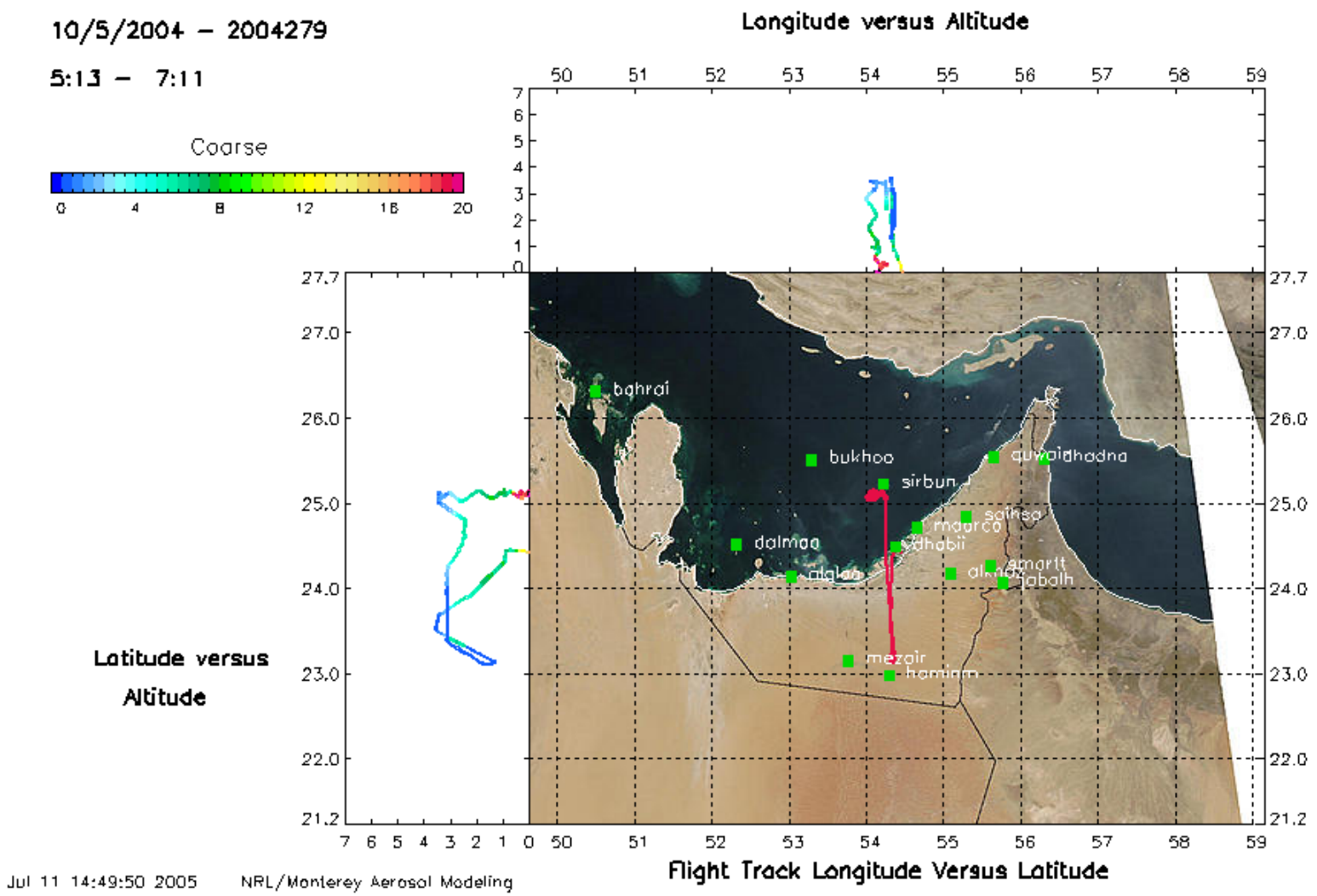
JRAUAE2-20041005A
10/5/2004 – 2004279
5:13 – 7:11
Coarse
0 4 8 12 16 20
Longitude versus Altitude
Latitude versus Altitude
Flight Track Longitude Versus Latitude
bahrai
bukhoo
sirbun
quwaidhaena
saihsa
maurco
dalmaa
abudhabi
alqlaa
amarit
jabalh
mezair
hamiam
Jul 11 14:49:50 2005
NRL/Monterey Aerosol Modeling

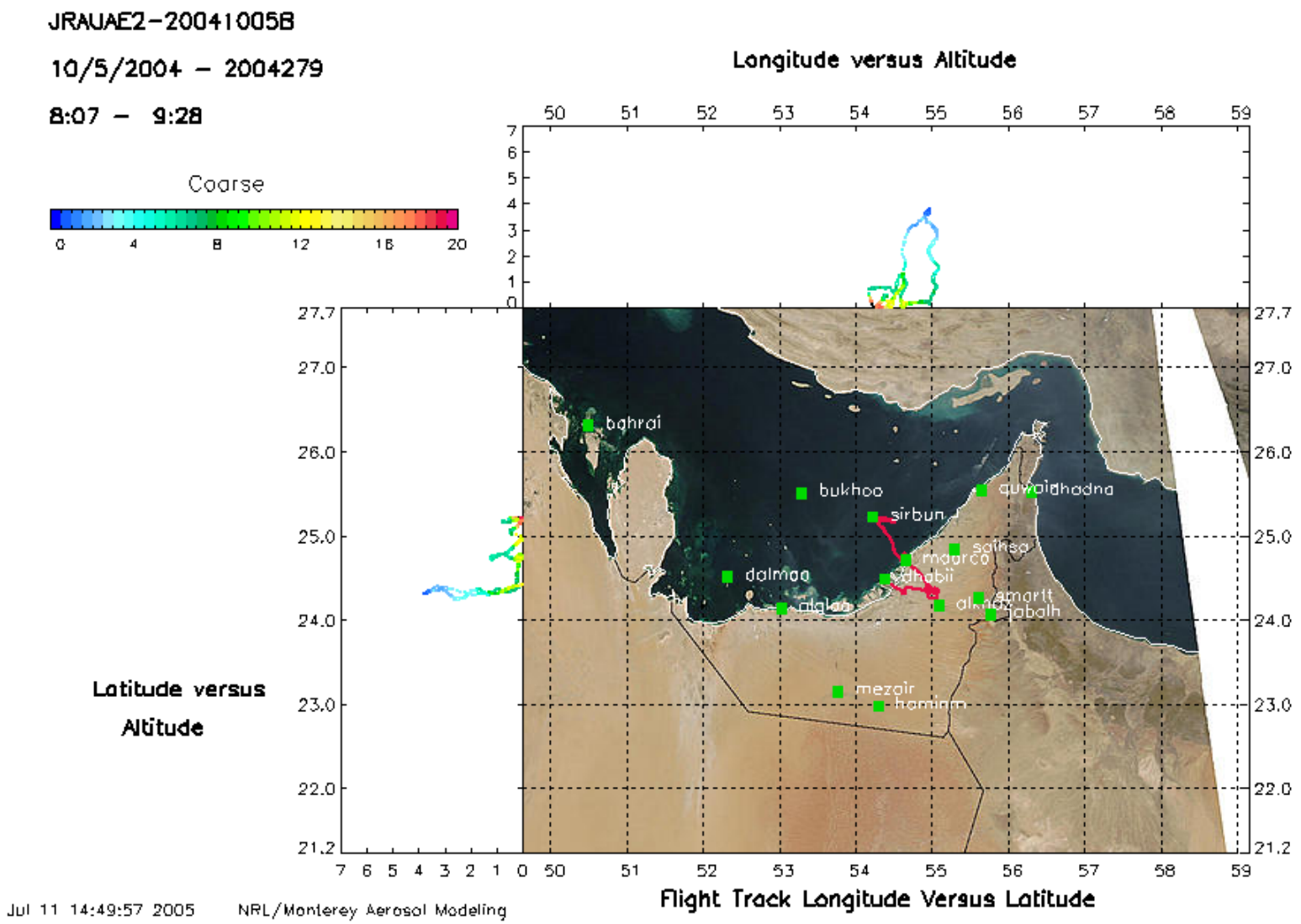
JRAUAE2-20041005B
10/5/2004 – 2004279
8:07 – 9:28
Coarse
0 4 8 12 16 20
Longitude versus Altitude
Latitude versus Altitude
bahrai
bukhoo
sirbun
quwaidhaana
saihsa
maurco
dalmaa
abudhabi
alqlaa
alkhaz
jabalh
mezair
hamiam
Jul 11 14:49:57 2005
NRL/Monterey Aerosol Modeling
Flight Track Longitude Versus Latitude